Elucidation of the structure based mechanism of the sterol-dependent membrane disrupting activity of the marine sponge derived peptide Theonellamide A

（海綿由来ペプチド・セオネラミドAの

構造に基づくステロール依存的膜攪乱活性の機構解明）

By

Kimberly Borromeo Cornelio

Department of Chemistry
Graduate School of Science
Osaka University
2017

Elucidation of the structure based mechanism of the sterol-dependent membrane disrupting activity of the marine sponge derived peptide Theonellamide A

（海綿由来ペプチド・セオネラミドAの

構造に基づくステロール依存的膜攪乱活性の機構解明）

A Thesis Submitted to the
Graduate School of Science
Osaka University

In Partial Fulfillment of the Requirements for the Degree of
Doctor of Philosophy (Ph.D.) in Chemistry

By

Kimberly Borromeo Cornelio

Department of Chemistry
Graduate School of Science
Osaka University
2017

Abstract

Sponges comprise of a large and diverse group of invertebrates under the phylum Porifera which are considered functionally important members of the marine benthic communities. Marine sponges have been an abundant source of new, diverse, and highly potent bioactive compounds, appealing as a target for isolation studies. The structural diversity of compounds isolated from marine sponges provide novel leads against bacterial, viral, fungal, parasitic and cancer diseases which prove to be difficult targets for current pharmaceuticals. Bioactive metabolites isolated from sponges include terpenoids, alkaloids, macrolides, polyethers, nucleoside derivatives, and peptides to name a few.

Theonellamide-A (TNM-A) is a member of the family of antifungal bicyclic dodecapeptides known as theonellamides, isolated from the marine sponge *Theonella* sp. Although the detailed mechanism of action of TNMs is still unclear, it was recently revealed that it has preferential interaction to 3β-hydroxysterols more than to any other components of the plasma membrane. Moreover, surface plasmon resonance measurements indicated that its affinity to POPC liposomes was greatly enhanced in the presence of 3β-hydroxysterols and this preferential binding was revealed to be due to the peptide's direct interaction with 3β-hydroxysterols based on ^{2}H solid state NMR studies. ^{31}P solid state NMR measurements also revealed that TNM-A can disrupt membrane bilayers in the presence or absence of cholesterol (Chol). In order to formulate a mechanism to explain TNM-A's membrane disrupting activity, several aspects that could affect its membrane action were examined in this study such as its behavior in solution, interaction with 3β-hydroxysterols, and interaction with sterol-free and sterol-containing membranes.

The affinity and interaction of TNM-A with 3β-hydroxysterols was assessed by solution ^{1}H NMR titration measurements. However, due to the poor solubility of Chol in the NMR solvent of TNM-A (4:1 DMSO-d_6/H_2O), a Chol derivative 25-hydroxycholesterol (25-HC) was used for peptide/3β-hydroxysterol interaction studies. Before proceeding with the titration measurements, the suitability of 25-HC as a Chol derivative was initially examined using solid state NMR techniques. Through ^{2}H solid state NMR measurements, it was confirmed that TNM-A also exhibits direct interaction with 3*d*-25-HC, similarly to 3*d*-Chol and 3*d*-ergosterol. Moreover, results from ^{31}P solid state NMR indicated that TNM-A's interaction with 25-HC-containing POPC membranes also resulted to similar membrane perturbations as it did with chol-containing membranes evidenced by the appearance of an isotropic peak within the powder pattern spectra characteristic of lamellar membranes upon incorporation of TNM-A to POPC/25-HC membranes. Altogether, these results indicate that 25-HC can be used as a Chol derivative in the examination of TNM-A/3β-hydroxysterol interactions. Results from ^{1}H NMR titration measurements indicated that TNM-A has weak interactions with 3β-hydroxysterols in solution with K_d values of about 37 μM-49 μM. Moreover, majority of the peptide protons only incurred very minor chemical shift changes (Δδ) upon addition of 25-HC suggesting that the electronic environment of the peptide protons remained relatively unchanged during the peptide/sterol interaction. Interestingly, most of the TNM-A protons incurring the greatest Δδ after addition of 25-HC were confined in one region of TNM-A's sequence involving residues Iser, β-MeBrPhe, OHAsn, Asn, Apoa and sAla which points to a possible sterol interaction site of the peptide. However, no intermolecular NOEs between 25-HC and TNM-A

protons in the speculated site of interaction, or in the entire peptide structure. It is highly possible that this is a consequence of the fast association and dissociation of the TNM-A/25-HC, beyond the timescale of NOESY NMR detection limits.

The propensity of TNM-A to form self-aggregates in aqueous environment was also assessed through diffusion ordered spectroscopy (DOSY NMR). Results indicate that TNM-A has the propensity to form oligomeric structures in aqueous environment, with an approximate aggregation number of 2 and 9, based on peptide concentration. The tendency of TNM-A to form micellar aggregates in solution and in the presence of 25-HC was also examined by the pyrene 1:3 ratio method. Results indicated that TNM-A forms micelle-like assemblies in aqueous media above peptide concentrations of ~186 μM. However, in the presence of 25-HC in solution, the formation of micelle-like assemblies by TNM-A is delayed to a higher peptide concentration of ~ 299 μM. This result not only confirms the interaction of TNM-A with 25-HC but also suggest that the interaction of TNM-A/3β-hydroxysterols interaction in solution is stronger than TNM-A/TNM-A interactions.

The effect of TNM-A in the membrane morphology of artificial membranes were also assessed through differential interference and confocal fluorescence microscopy using POPC or POPC/Cho GUVs with pure TNM-A or with 10 mol% of the fluorescent TNM derivative TNM-DCCH. Microscopy images indicate that TNM-A binds faster to Cho-containing GUVs than to sterol-free ones. More importantly, images revealed that TNM-A can disrupt membrane bilayers by altering membrane curvature but only to Cho-containing liposomes. Aside from binding slower to Cho-free GUVs, TNM-A did not induce significant membrane deformations to this type of liposome. In addition TNM-A's membrane association and localization were also assessed through ^{1}H NMR paramagnetic quenching measurements using model membranes such as SDS-d_{25} micelles and Cho-free and Cho-containing DMPC-d_{54}/DHPC-d_{22} bicelles (q=0.5). Data suggest that TNM-A binds more to Cho-containing membranes and inefficiently associates with Cho-free ones as mostly remain in the aqueous environment probably as aggregates. Results also indicate that when TNM-A interacts with model membranes it remains surface bound and does not insert, regardless of the presence or absence of Cho. However, it should be noted that when TNM-A binds Cho-containing membranes, it resides in a relatively deeper region close to the lipid-water interface. On the other hand, when TNM-A associates with Cho-free membranes, it resides mostly near the most hydrated region of the membrane near the polar headgroup of phospholipids. A mechanism was proposed to explain the membrane action of TNM-A.

Table of Contents

List of Abbreviations

AMPs	antimicrobial peptides
TNMs	Theonellamides
TNM-A	Theonellamide A
TNM-DCCH	Theonellamide 7-diethylaminocoumarin-3-carboxylic acid hydrazide
3β-OH	3β-hydroxysterols
DMSO	dimethyl sulfoxide
DMSO-d_6	deuterated dimethyl sulfoxide
D_2O	deuterium oxide
POPC	1-palmitoyl-2-oleoyl-sn-glycero-3-phosphocholine
Chol	cholesterol
25-HC	25-hydroxycholesterol
3*d*-cholesterol	3-*d*-cholesterol
3*d*-25-HC	3-*d*-25-hydroxycholesterol
3*d*-ergosterol	3-*d*-ergosterol
17α-HP	17α-hydroxypregnenolone
DMPC-d_{54}	1,2-dimyristoyl-d_{54}-*sn*-glycero-3-phosphocholine
DHPC-d_{22}	1,2-dihexanoyl-d_{22}-*sn*-glycero-3-phosphocholine
SDS-d_{25}	Sodium dodecyl sulfate-d_{25}
GUV	giant unilamellar vesicles
MLV	multilamellar vesicles
SUV	small unilamellar vesicles
PL	phospholipids
NMR	Nuclear Magnetic Resonance Spectroscopy
ssNMR	solid-state Nuclear Magnetic Resonance Spectroscopy
NOESY	Nuclear Overhausser Effect Spectroscopy
DOSY	Diffusion Ordered Spectroscopy
HPLC	High Pressure/Performance Liquid Chromatography
MS	Mass Spectrometry
SPR	Surface Plasmon Resonance
CSA	chemical shift anisotropy
Δδ	chemical shift change
K_d	dissociation constant
PBS	phosphate buffered saline
L_o/L_d	liquid ordered/liquid disordered phases
[L]/[P]	ligand (25-HC)/peptide (TNM-A) ratio
I/I_o	Relative ^{1}H signal intensities
I_1/I_3	Pyrene fluorescence intensity at λ_1 (374 nm) over fluorescence intensity λ_3 (383 nm)
PyPC	Pyrene-labelled phosphatidyl choline
AM	Amphidinol
amB	Amphotericin B

List of Figures

List of Tables

List of Schemes

Chapter 1

General Introduction –Mechanism of Action of Membrane Active Compounds and Marine Sponge-Derived Natural Products

1.1 Biological Membrane and Membrane Active Compounds

Biological membranes are essential cellular structures that act as a selectively permeable barrier which encloses the cell (or intra-cellular organelles), defines its boundaries, and maintains the differences between the systems' components from its external environment.[1–4] It is composed of a phospholipid bilayer containing integral and peripheral proteins and carbohydrates which are attached to either lipids (glycolipid) or proteins (glycoprotein).[5,2] Considered as dynamic structures, biological membranes change composition throughout the life of a cell and more importantly, have its lipid bilayer diffusing in lateral or even transverse directions.[2,5] This model of the biological membrane is known as the Fluid Mosaic Model proposed by Singer and Nicolson back in 1972.

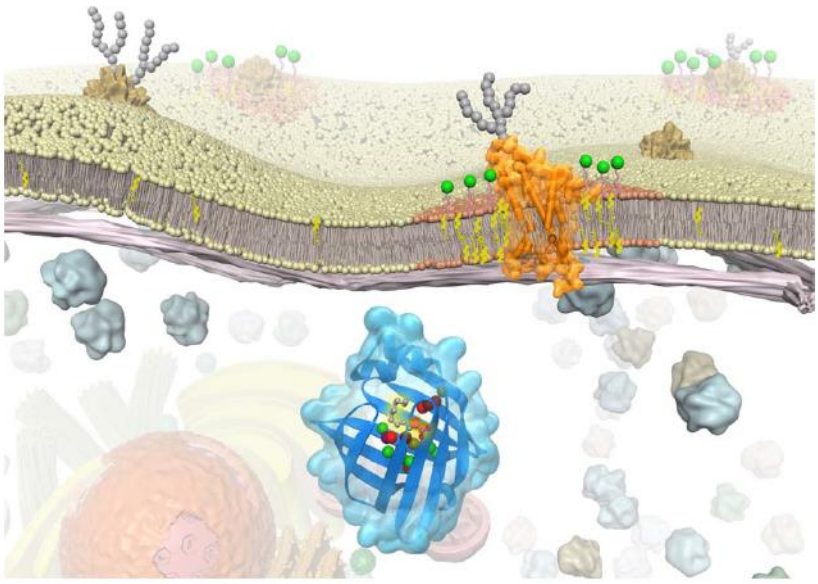

Figure 1-1. A recent illustration of a cellular membrane. Reprinted with permission from Figure 1 of *Chem. Rec.* **2015,** *00*, 1-16.[5] Copyright © (2015) Wiley Online Library: The Chemical Society of Japan & Wiley-VCH Verlag GmbH & Co. KGaA, Weinheim.

In the fluid mosaic model, the bilayer is pictured as a dynamic two-dimensional oriented viscous solution wherein hydrophobic and hydrophilic interactions contribute most to the formation of the lipid bilayer. As presented in Figure 1-1, the fluid mosaic model describes the bilayer having the nonpolar fatty acid chains of the phospholipids sequestered together away from contact with water while its ionic/zwitterionic groups are in direct contact with the aqueous phase of the exterior surface of the bilayer.

Coined as “Mosaic”, the membranes are said to be composed of various components such as phospholipids (*i.e.* glycerophospholipids and sphingolipids), cholesterol, proteins, and oligosaccharides - proteins being the most predominant. Also, in this model, a clear distinction between peripheral and integral proteins was acknowledged. Peripheral proteins were defined as loosely associated proteins that dissociate from the membrane, free of lipids by only mild treatments (*i.e.*, increase in ionic strength of the medium or addition of chelating agent). On the other hand, integral proteins are a set of heterogeneous globular proteins embedded in the membrane forming an amphipathic structure, with its ionic and highly polar regions protruding from the membrane into the aqueous phase and the nonpolar regions buried in the hydrophobic interior of the membrane. [5,2]

The hydrophobic interior of biological membranes generally have a fluid-like rather than gel-like consistency and maintenance of this bilayer fluidity is considered essential for normal cell growth and reproduction. The fluidity of biological membranes are influenced by temperature and membrane composition.[2–4] Over a narrow temperature range, membranes can undergo changes to its fluidity because of the packing, differing lengths, and degree of unsaturation of the fatty acyl chains within the center of the phospholipid bilayer which influences the extent of van der Waals interactions present in the system. Presence of cholesterol in the mammalian cell membrane (or ergosterol in the case of fungal cell membranes) not only can reduce permeability of the membrane to hydrophilic/water soluble molecules but also affect the fluidity of the membrane bilayer.[2]

Cholesterol is intercalated within the phospholipids of the membrane bilayer with its polar hydroxyl group located near the polar head groups of the phospholipids and its hydrophobic steroid tail portion interacting with the acyl chains somehow restricting movement.[6, 7] Cholesterol’s interaction with other lipids are a consequence of its structure. For instance, the small hydroxyl headgroup of cholesterol is not enough to shield its hydrophobic sterol ring from water so it is proposed that neighboring lipids that have larger headgroup can favorably interact with cholesterol to fulfill this role which is known as the umbrella effect.[8,9] Through hydrogen bonding, cholesterol may also associate with other lipids with saturated acyl chains to form complexes that could lower the chemical potential of the sterol. This could lead to a lower availability of cholesterol for enzymatic reactions or making it less extractable from the membrane. Such modes of interaction of cholesterol with other lipids are described in Figure 1-2.[9] The puckered 4-ring structure of cholesterol gives it special biophysical properties that gives ordering to lipids surrounding it.[9] However, the net effect of cholesterol in membrane fluidity is rather complicated. Presence of cholesterol restricts random movement of polar head groups of the fatty acyl chains that reside near the surface of the outer membrane leaflet through hydrogen bonding. But at the same time, cholesterol can either disrupt packing of the membrane by separating and dispersing the fatty acyl chains of the phospholipids causing the inner regions of the bilayer to become slightly more fluid or as mentioned previously, complexing with other phospholipids reducing membrane fluidity.[10] In eukaryotic plasma membranes where sterol content is high, cholesterol makes the bilayer less fluid at temperatures near 37 ^{o}C but it can also keep the membrane fluid at temperatures below phase transition temperature by preventing the acyl chains from binding to each other.[11] Nevertheless, all cell membranes, though containing various phospholipids and differing sterol content, are fluid at the temperature at which the cell is grown.[2, 11]

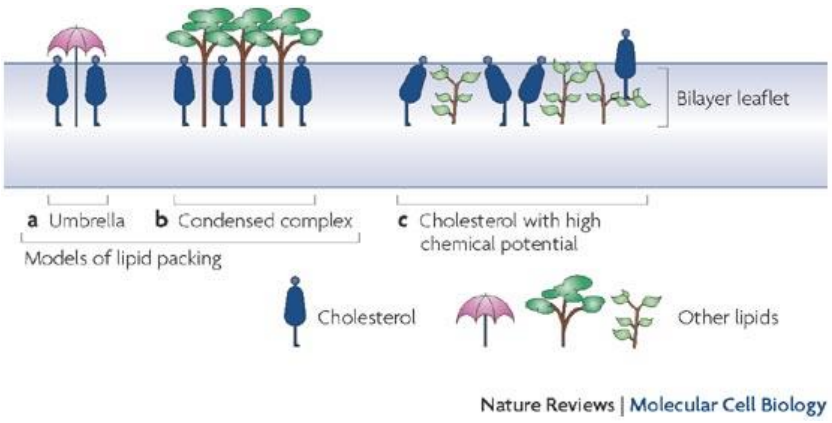

Figure 1-2 Illustration showing the models of cholesterol interaction with other lipids. Reprinted with permission from Box 1 of *Nat. Rev. Mol. Cell Biol.* **2008,** *9*, 125-138. Copyright © (2008) Nature Publishing Group.[9]

The importance of biological membranes cannot be emphasized more. Aside from providing a semi-permeable enclosure to cells and intracellular organelles, bounding their internal components from the external environment, biological membranes also serve as a platform for several significant processes. Biological membranes act as scaffolds holding various kinds of proteins and glycolipids needed for specialized cellular functions essential for growth and development such as ligand recognition, vesicle fusion and endocytosis, signal transduction, ion conductivity, and ATP synthesis to name a few.[12] For this reason, biological membranes, and its components, prove to be important targets in the field of drug development.

Antimicrobial peptides and membrane-active compounds are being recognized as a possible source for novel therapeutic agents for the treatment of antibiotic-resistant bacterial infections.[13,14] As a matter of fact, numerous drugs that target the cell membrane are now being sold as commercial drugs as antimicrobial, antiviral, and antifungal agents, among others. Well-known examples of these said drugs come from antimicrobial peptides such as Daptomycin and Polymyxin B. Antimicrobial peptides (AMPs) are considered as an essential part of the host's innate resistance and serves as the first line of defense against infection. Since numerous studies have emphasized that the mechanism of action of AMPs are different from clinically-used antibiotics, hopes for developing potent drugs for the treatment of multi-drug resistant infections from AMPs are high.[15]

Daptomycin is a lipopeptide antibiotic produced by *Streptomyces roseosporus* (Figue 1-3, A).[16] Sold under the trade name Cubicin, it is prescribed to patients suffering from systemic infections caused by gram positive pathogens, including methicillin and vancomycin resistant *Staphylococcus aureus*. Daptomycin exhibits its antibacterial activity via a calcium-dependent insertion of its lipid tail to the target membrane followed by formation of ion-conductance channels that cause efflux of cations and membrane potential dissipation, eventually leading to cell death without causing cell lysis. [17–20]

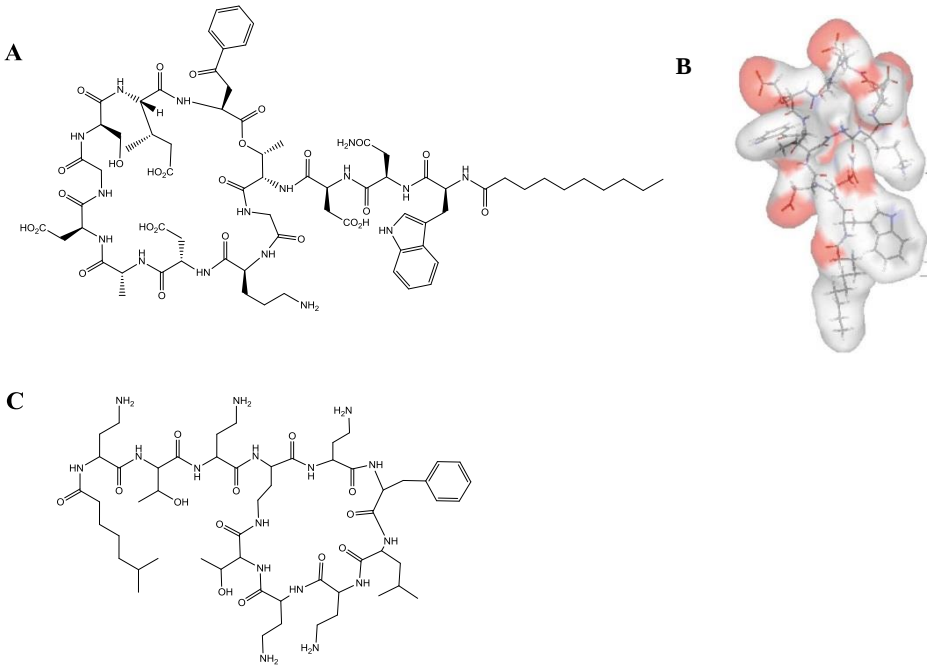

Figure 1-3. Structures of antimicrobial peptides (A&B) Daptomycin[16,17], and (C) Polymyxin B[21]. Figure 1-3B is reprinted with permission from Figure 3 of *Org. Biomol. Chem.* **2004**, *2*, 1872-1878, Copyright © (2004) The Royal Society of Chemistry.

Polymyxin B, on the other hand, is a membrane active cyclic lipopeptide produced by the gram-positive bacterium *Bacillus polymyxa* (Figure 1-3, B).[21–24] It potently permeabilizes the outer and cytoplasmic membranes of multi-drug resistant gram-negative bacteria such as *Acinetobacter baumannii*, *Pseudomonas aeruginosa*, and *Klebsiella pneumoniae.* In contrast to daptomycin, the bactericidal activity of polymyxins stem from its ability to bind lipid A of the lipopolysaccharide (LPS) in the bacterial membrane, leading to membrane disintegration.[21–24] In order to do this, initial electrostatic interaction occurs between the cationic Dab side-chains of polymyxins and the anionic phosphate moiety of the lipid A component of LPS causing the displacement of divalent cations (Ca^{2+} and Mg^{2+}) that bridge LPS molecules.[23] Furthermore, the *N*-terminal fatty acyl tail of the polymyxin also interacts with the fatty acyl chains of lipid A. This hydrophobic interaction proves to be crucial for antibacterial activity as polymyxin nonapeptide, a polymyxin derivative without the fatty acyl moiety, is devoid of antibacterial activity.[24] After interaction with lipid A, polymyxin neutralizes LPS and prevent pathophysiologic effects of endotoxin.

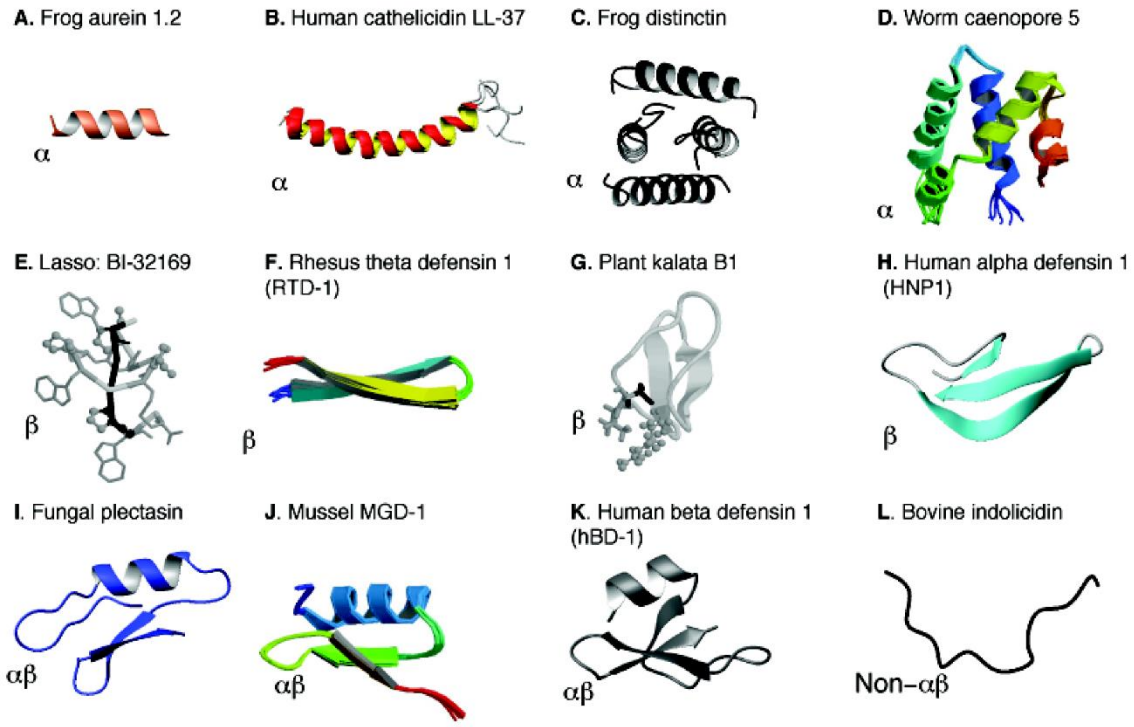

Figure 1-4. 3D structures of other known antimicrobial peptides with their structural family (α, β, αβ, and non-αβ) indicated in the lower left hand corner of each structure. Structural coordinates were obtained from the RCSB Protein Data Bank (PDB). Reprinted with permission from Figure 4 of *Pharmaceuticals*, **2013**, *6(6)*, 728-758.[25] Copyright © (2013) MDPI AG.

From decades of research, it already became obvious that membrane active compounds have varying ways of targeting the membrane, like Daptomycin and Polymyxin B among other examples. But in general, the integrity of the biological membrane of the target organisms are compromised by initially permeabilizing the bilayer.

1.2 Mechanisms of Membrane Permeabilization

To date, a number of mechanisms of membrane permeabilization are already known and these mechanisms permeabilize the membrane either by creating pores traversing the bilayer, which usually result to ion conductance altering transmembrane potential, or by non-pore forming mechanisms that compromise membrane integrity. A common feature of these membrane permeabilization mechanisms is that, initial binding of the membrane active molecule to the target membrane surface occurs usually through electrostatic interactions or preferential binding to specific components or regions in the membrane.[15,26] Nonetheless, from the action of membrane-active compounds, target organisms lose membrane permeability barrier and integrity and more often than not, lead to malfunction of critical cellular functions essential for survival.

1.2.1 Pore-Forming Mechanisms

The pore formation mechanism of membrane permeabilization was first suggested by Baumann and Mueller in their study of Alamethicin back in 1974, which accounted for the single-channel conductance it induced in black lipid membranes.[27] From then on, the barrel-stave pore model, became the archetype of how AMPs and other membrane active compounds form transmembrane pores. But currently, there are two pore-forming mechanisms recognized: the barrel-stave and toroidal pore mechanisms.

In a ***barrel stave pore***, the AMPs associate as dimers or complexes aligned vertically and parallel to each other after binding and inserting to negatively charged bacterial membranes. The resulting pore structure formed is a barrel-like channel assembly with a central lumen spanning the entire length of the membrane with the peptide as staves, similar to the pore structure formed by alamethicin.[15,27–29] To optimize peptide-lipid interactions, the hydrophobic peptide regions align with the lipid core region of the bilayer and the hydrophilic peptide regions form the lining of the water-filled pore lumen as seen in Figure 1-5. In the case of alamethicin, about 3-11 parallel helices can comprise the pore assembly with an inner and outer diameters of about ~18 Å and ~40 Å, respectively.[30,31] Similarly, Ceratotoxin A, a cationic alpha-helical AMP produced by the Miditerranean fruit fly *Ceratitis capitata*, is also known to permeabilize the membrane through the barrel-stave mechanism forming voltage-dependent ion channels comprising of 5-6 peptide helices.[32,33] A well-defined and favorable assembly is formed by the AMPs and the lipids in the bilayer in this model and the driving force for peptide penetration is largely from hydrophobic interactions.[32]

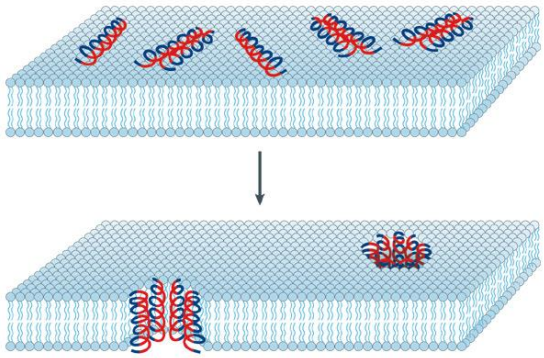

Figure 1-5. Carton representation of the barrel-stave pore formation mechanism by antimicrobial peptides. The blue and red regions of the alpha-helices indicate the hydrophobic and hydrophilic portions of the AMPs. Reprinted with permission from Figure 3 of *Nat. Rev. Microbiol.*, **2005**, *3*, 238-250.[11] and Figure 1 of *Biopolymers*, **1998**, *47*, 451-463.[29] Copyright © (2005) Macmillan Publishers Ltd. and (1998) John Wiley & Sons, Inc.

On the other hand, in the ***toroidal pore model***, AMPs penetrate the membrane to induce the lipid monolayer to bend continuously forming a highly curved transmembrane pore having both the inserted peptides and lipid headgroups lining the water core. This pore-formation mechanism was first proposed

for the 23-residue cationic AMP Magainin back in 1995[33,34], but several other AMPs were already recognized to induce toroidal pore formation such as protegrin-1[35], melittin[36], and MSI-78[37], to name a few. Magainin- induced toroidal pore is comprised of ~4-7 magainin monomers and ~90 lipid molecules with an approximate inner and outer diameter of ~30-50 nm and ~70-84 nm, respectively. Initially, AMPs bind parallel to the membrane surface by virtue of electrostatic interactions. After a threshold concentration of AMP is reached, formation of a toroidal pore starts with the polar face of the peptides associating with the phospholipid headgroups and the lipids starting to tilt from the lamellar normal. The continuous bend of the phospholipids connects the outer leaflet to the inner leaflet creating a pore similar to a toroidal hole as seen in Figure 1-6. In the formation of a toroidal pore, membrane thinning occurs as a result of the positive curvature strain caused by the embedding of the AMPs to the lipid head-group region, which facilitates toroidal pore formation. However, if the lipids forming the bilayer have a polar head group cross-sectional area smaller than that of its tail, like phosphatidylethanolamine (PE), pore formation will be inhibited because the insertion of AMPs will lead to a negative curvature in the membrane forming a concave shape of the lipid-peptide aggregate.[32]

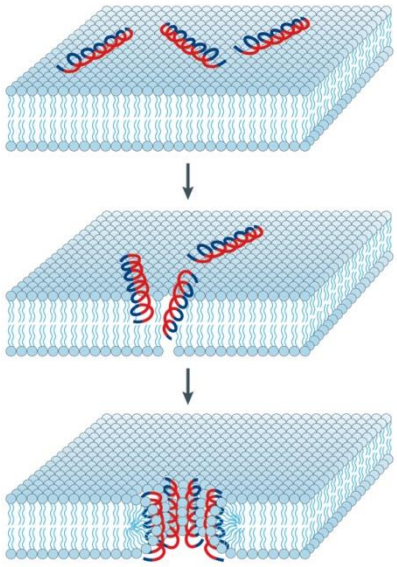

Figure 1-6. Carton representation of the toroidal pore formation mechanism by antimicrobial peptides. The blue and red regions of the alpha-helices indicate the hydrophobic and hydrophilic portions of the AMPs. Reprinted with permission from Figure 5 of *Nat. Rev. Microbiol.*, **2005**, *3*, 238-250.[13] and Figure 1 *Biopolymers*, **1998**, *47*, 451-463.[29] Copyright © (2005) Macmillan Publishers Ltd. And (1998) John Wiley & Sons, Inc.

1.2.2 Non-Pore Forming Mechanisms

Pore formation mechanisms for membrane permeabilization have long been scrutinized and various experiments are being carried out in hopes of completely characterizing these processes. However, until now no conclusive data can attest if the formation of transmembrane pores or channels indeed happens, even transiently in cells or synthetic bilayer systems.[38,39] In a paper written by W. Wimley, the inconsistency of vesicle-based leakage experiment results with the idea of the discrete pore formation was

pointed out to present quantitative data refuting the notion of pore formation as a mechanism of membrane permeabilization by AMPs.[34] Simulation experiments were carried out using small molecule probes entrapped in large unilamellar vesicles (LUVs) to examine its diffusion through single pore in the form of a water filled channel of 10 Å diameter. Results from simulation predicted a 50,000 ions per second per pore rate of release. But these results are incompatible with usual vesicle leakage experiment results that use LUVs containing about 100,000 lipids and a peptide to lipid (P:L) ratio of about 1:100. The internal volume of an LUV used in such experiments is about 10^{-19} L, capable of entrapping about 2500 probe molecules. If a single pore is present, all these probe molecules could be released in a fraction of a second at most. But in reality, where the vesicles in leakage experiments usually have about 1000 bound peptides constituting more than 100 pores (based on a 1:100 P:L rato) , rates of release for ions only range from 0.1 to 100 ions per second per vesicle. Another compelling fact is that, leakage induced by AMPs are often incomplete further strengthening the notion that discrete pores are actually never formed.[38] For these reasons, analyses suggest that AMP-induced leakage results from the general disruption of membrane integrity, and not because of the formation of true pores. Most AMPs are not potent membrane-permeabilizing peptides strong enough to induce formation of equilibrium pores in membranes, even in anionic membranes. This may be a result of their need to be selective to bacterial versus eukaryotic membranes.

The most recognized non-pore forming mechanism of membrane permeabilization is the detergent or carpet model but several other non-pore forming mechanisms have already been proposed namely sinking raft model, charge cluster model, leaky slit model, and the interfacial activity model.

1.2.2.1 Detergent or Carpet Model

In the ***detergent or carpet model***, peptides accumulate in the membrane surface of the target organism covering it (or a portion of it) in a way similar to a carpet.[13,15] After a threshold concentration of the peptide monomer is reached, peptides permeate and disrupts the bilayer in a detergent-like manner eventually leading to the formation of micelles. This mechanism of membrane permeabilization was first suggested for the AMP cecropin A based on the observation of Steiner et al. that at the concentration needed to obtain 50% cell killing, cecropin A was present in sufficient amounts to completely cover the bacterial surface.[40] It may be noted that in the detergent or carpet model, toroidal transient holes form enabling more peptides to access the membrane as can be seen from Figure 1-7. The pore-forming models and the detergent or carpet model share common characteristics as both initialize by the AMPs' parallel association to the membrane surface, followed by peptide accumulation to reach a threshold concentration. However, a notable difference of the detergent or carpet model to the barrel-stave mechanism is that AMPs do not insert into the hydrophobic region of the bilayer but remain in the surface interacting with the polar head groups of the phospholipids throughout the disruption of the membrane. As a matter of fact, results from ATR-FTIR spectroscopy indicated that cecropin P1, an AMP also considered to disrupt the membrane through the detergent or carpet mechanism, incorporated parallel to the membrane surface without altering the order parameter of the acyl chains, suggesting that it did not traverse the hydrophobic core. [41]

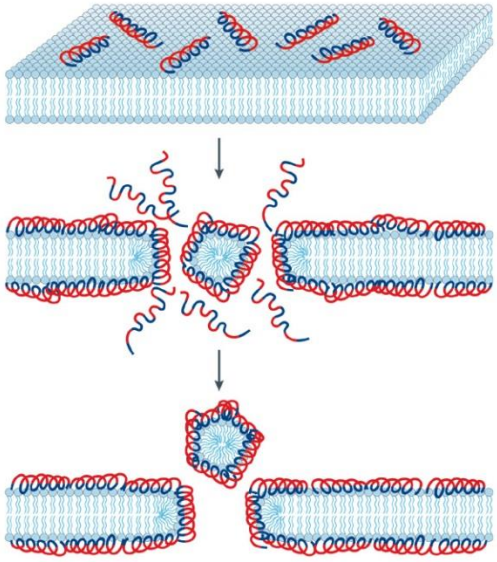

Figure 1-7. Carton representation of the detergent or carpet mechanism by antimicrobial peptides. The blue and red regions of the alpha-helices indicate the hydrophobic and hydrophilic portions of the AMPs. Reprinted with permission from Figure 4 of *Nat. Rev. Microbiol.*, **2005**, *3*, 238-250.[13] and Figure 1 of *Biopolymers*, **1998**, *47*, 451-463.[29] Copyright © (2005) Macmillan Publishers Ltd. And (1998) John Wiley & Sons, Inc.

1.2.2.2 Sinking-Raft Model

In the ***sinking raft model***, peptides are thought to aggregate side-by-side, parallel to the membrane surface, forming an assembly similar to a "raft" and sink into the outer bilayer leaflet of the membrane as seen in Figure 1-8.[42–45] This mechanism was first proposed by Almeida et al. in 2002, to account for the kinetics of transient pore formation, graded dye efflux, and peptide translocation resulting from the interaction δ-Lysin, a 26 amino acid hemolytic peptide produced by *Staphylococcus aureus*, with phospholipid vesicles.[42] It was suggested that a possible driving force of this mechanism is the presence of a mass imbalance caused by peptide binding to the outer leaflet of the membrane resulting to a local curvature strain. In the case of δ-Lysin, an antiparallel dimer and a monomer of the peptide associate forming a trimer on the membrane surface. Simultaneous with the sinking of the raft-like assembly formed from the peptide trimer, slight bending of the helices occur as it penetrates to the middle of the bilayer so that its hydrophilic regions remain in contact with water. At this point, penetration of the helices happens by a combination of rotational and downward movement. During this movement, the hydrophobic regions of the helices continue to be associated with the lipid acyl chains and the hydrophilic regions line a transient cavity, from which dye efflux is thought to occur. Peptide translocation comes to a completion when the trimer reaches the inner leaflet of the bilayer, mass imbalance relieved, and the transient cavity closes. When the sinking raft model was introduced, trimer peptide assembly was proposed but was noted that the model can also be applied to other aggregate sizes such as dimers or tetramers.[41-43] Few years after this model was proposed, Almeida et al. again used this mechanism to partly account for the permeation and the graded dye release induced by transportan 10 (tp10), a 21 residue peptide derived from the AMP mastoparan produced by wasp *Vespula lewisii*.[42]

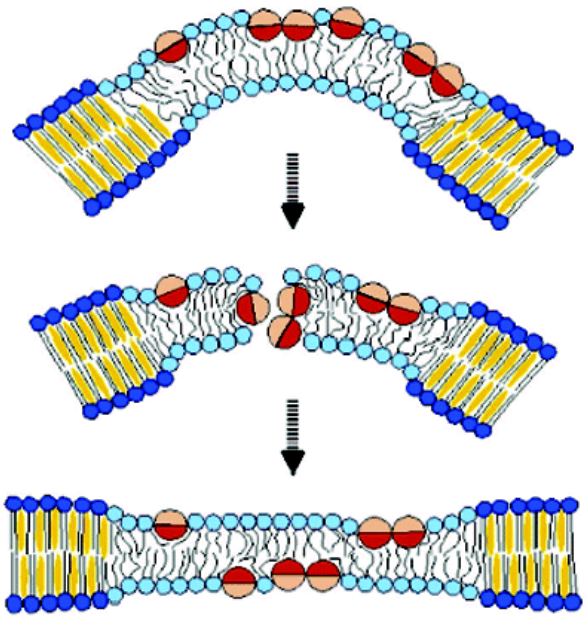

Figure 1-8. Carton representation of the Sinking-raft model by antimicrobial peptides. The peptides are represented as circles with the red and peach regions signifying the hydrophobic and hydrophilic portions. Reprinted with permission from Figure 8 of *Biochemistry,* **2004**, *43*, 8846-8857.[43] and Figure 6 of *Biochemistry*, **2005**, *44*, 9538-9544.[44] Copyright © (2004 and 2005) American Chemical Society.

1.2.2.3 Charge Cluster Model

More recent mechanisms of membrane permeabilization have emerged and one of them is the charge cluster model. This mechanism is rooted from the fact that many cationic amphipathic AMPs can segregate anionic lipids from zwitterionic ones and are able to pass through the cell wall, given that a sufficient positive charge density is present in their sequence.[46–48] feio wadwhani In the ***charge cluster model,*** the highly cationic AMPs' (+6 to +10 charge) interaction with the outer leaflet of the cytoplasmic membrane causes clustering of anionic lipids away from zwitterionic lipids resulting to a large reorganization of the membrane and consequently, an increase in the concentration of anionic lipids and cationic peptides in certain domains of the membrane (Figure 1-9).[47] This reorganization may lead to small defects in the bilayer or to large membrane permeabilization, and even functional impairment of the proteins that lose the anionic lipids recruited by the AMPs.[46–48] As a matter of fact, the increased toxicity of numerous antimicrobial agents to Gram-negative bacteria is increasingly being correlated to such mechanism of lipid segregation.[47]

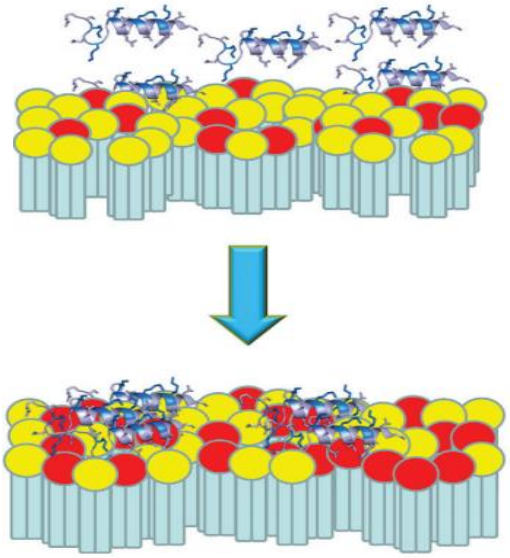

Figure 1-9. Illustration showing the clustering of anionic lipids (red) by cationic amphipathic AMPs resulting to the formation of domains separately containing zwitterionic lipids (yellow) and anionic lipid-peptides. Reprinted with permission from *Prog. Lipid Res.*, **2012**, *51*, 149-177.[47] Copyright © (2012) Elsevier.

1.2.2.4 Leaky Slit Model

The ***leaky slit model*** is also non-pore forming model of membrane permeabilization recently suggested to explain the membrane damage that can be induced by amphipathic fiber forming proteins and peptides that can span the membrane like that of Plantaricin A (plA), an antimicrobial 26-residue peptide pheromone produced by *Lactobacillus plantarum*.[49] Kinnunen et al. based the leaky slit model on how fibrous proteins can arrange itself in the membrane while causing the membrane to be highly "leaky". In this model, it was suggested that lipid-bound fibrous peptides can arrange into a linear amphipathic array with its hydrophobic face in contact with the hydrophobic acyl chains of the bilayer as can be seen from Figure 1-10 (left).[49] Since the hydrophilic face of the fibrous peptides cannot interact with the hydrophobic lipid acyl chains from the opposing contacting bilayer to seal the opening, lipids from the other side are forced to adopt a highly positive curvature. Toxicity would then be a consequence of the resulting arrangement as it would be highly permeable to solutes and would be difficult for the cell to repair.[47,49]

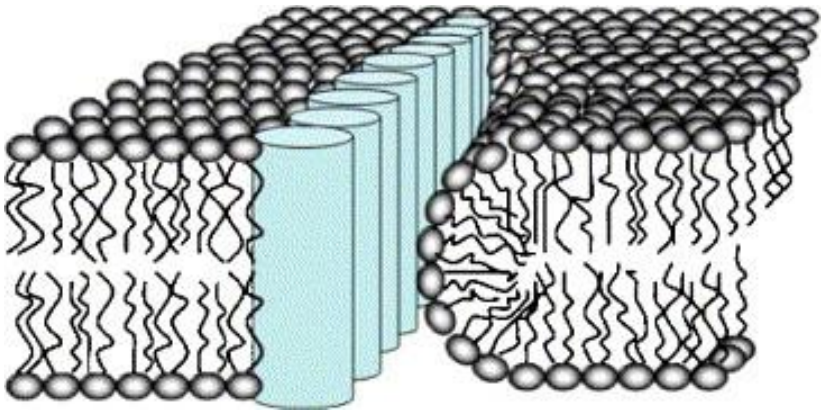

Figure 1-10. Illustration showing the leaky-slit mechanism induced by fiber-forming peptides represented as blue cylinders. Reprinted with permission from Figure 13 of *Biochimica et Biophysica Acta*, **2006**, *1758,* 1461–1474.[49] Copyright © (2006) Elsevier.

1.2.2.5 Interfacial Activity Model

Another recently proposed non-pore forming membrane permeabilization mechanism highlighted the ability of a peptide to perturb the permeation barrier imparted by the thick hydrocarbon core of the lipid bilayer.[38,50,51.] Wiener and White described the lipid bilayer as having a 25-30 Å thick hydrocarbon core that presents a strict barrier for polar or charged solutes to permeate through. This highly hydrophobic core is sandwiched between two bilayer interfacial zones that are about 10-15 Å thick and contains lipid polar groups, water, solution counterions, and small amounts of hydrocarbon.[38,50]

In the ***interfacial activity model***, the peptide is able to perturb the permeability barrier by partitioning into the interfacial regions of the bilayer and consequently, altering the vertical lipid packing of the hydrocarbon core and disrupting the segregation of the hydrophobic core and the interfacial zone.[38,50] Peptides that are amphipathic, but have imperfect segregation of polar and non-polar groups, can be considered to have interfacial activity. These prerequisites are necessary for the peptide to exhibit interfacial activity in order to deform the bilayer in a way that the hydrocarbons are intermingled with the polar lipid headgroups. When these peptides insert into the bilayer through hydrophobic residues, the presence of one or two nearby polar residues also allows the movement of the lipid polar headgroups, together with the polar residues of the peptide, deeper into the membrane. The outcome of the interfacial activity model is the bilayer translocation of the peptide at low peptide concentrations and a cooperative transbilayer movement of peptide, lipids, and solutes at higher peptide concentrations. An illustration showing a molecular dynamics simulation performed by Sengupta and Marrink that embodies an interfacial activity mechanism is shown in Figure 1-11.[51]

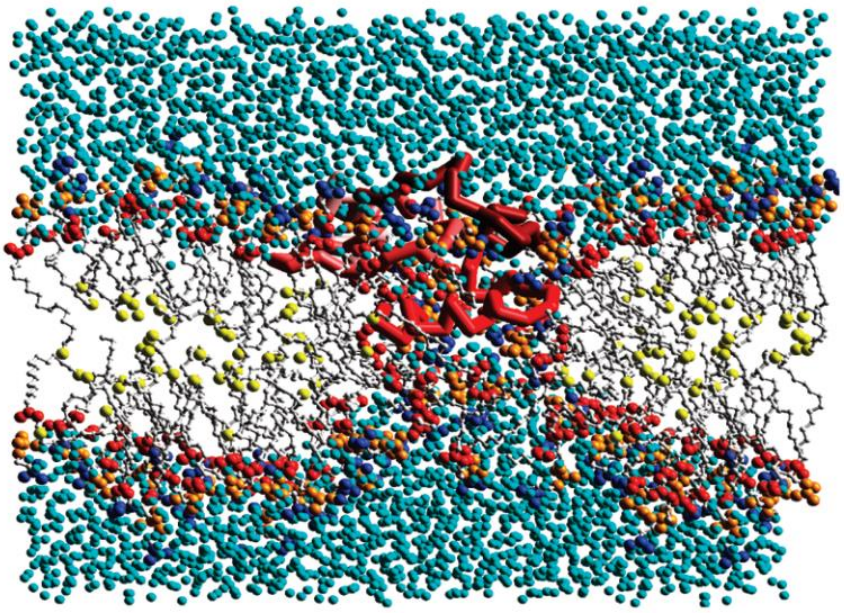

Figure 1-11. Molecular dynamics simulations that illustrate the interfacial activity mechanism of membrane permeabilization. Reprinted with permission from Figure 6 of *ACS Chem. Biol.*, **2010**, *5*, 905-917.[38] and Figure 2 of *Biochim. Biophys. Acta, **2008**, 1778,* 2308-2317.[51] Copyright © (2010) American Chemical Society and (2008) Elsevier.

1.3 Methods for Examining Membrane Interactions and Membrane Permeabilization

The interaction of AMPs and other membrane active compounds with the phospholipid bilayer is recognized as a key determinant for understanding how they elicit their biological activity.[52] Despite the numerous mechanisms describing the interaction and membrane permeabilization of such compounds, the consensus about biological membranes is that it is either (1) the main target of membrane active compounds or AMPs *or* (2) it is a barrier that must be crossed to target core metabolic pathways to elicit biological activity.[47] Thus, the importance of examining membrane interactions and elucidating the mechanism of membrane permeabilization cannot be overstated.

1.3.1 Examining Membrane changes and Intermolecular Interactions by Solid-State Nuclear Magnetic Resonance (ssNMR) and solution state NMR

In the past, the methods for examining membrane interactions have been impeded mainly due to technology limitations but have greatly progressed in recent years. For example, NMR methods to study lipid-peptide interactions have significantly developed through the emergence of solid state NMR techniques and the use of synthetic phospholipid membrane models such as micelles, bicelles, and liposomes.[53] The most commonly used nuclei in the study of lipids is the ^{31}P as biological membranes are mainly comprised of high proportions of lipids containing a phosphate moiety in their polar headgroup providing a sensitive NMR probe.[53,54,55] Solid state ^{31}P NMR studies can be employed to examine structural or dynamic response of phospholipid headgroups upon interaction with AMPs or membrane active compounds. Since the ^{31}P spectra reflects a large chemical shift anisotropy (CSA) range and exhibit

characteristic line shapes for various lipid phases (*i.e.*, lamellar, hexagonal arrangement, micelles, Figure 1-12)[53], it can be utilized to examine induction of non-lamellar phases by AMPs and membrane active compounds as these are indications of membrane disruption.[54,55] When it is possible to prepare samples with deuterium labeling, ^{2}H NMR methods can also be utilized to examine membrane interactions. Synthetic membrane systems containing deuterated phospholipids, either in the head group or in the acyl chains can be used. For instance, if membrane active compounds or AMPs interact with the lipid polar headgroups, it can be observed as a change in the quadrupolar splitting in the ^{2}H NMR spectra[53] similar to what was observed for AMP Ovispirin when it interacted with liposomes composed of palmitoyloleoylphosphatidylcholine (POPC) perdeuterated in the acyl chains.[56] Conversely, if interaction with lipids occur in the deuterated acyl chain regions, changes in quadrupolar splitting can reflect changes in motional order parameter within the hydrophobic region.[53] So, alteration in the lipid order parameter can reveal information about disordering effects or even depth of insertion.

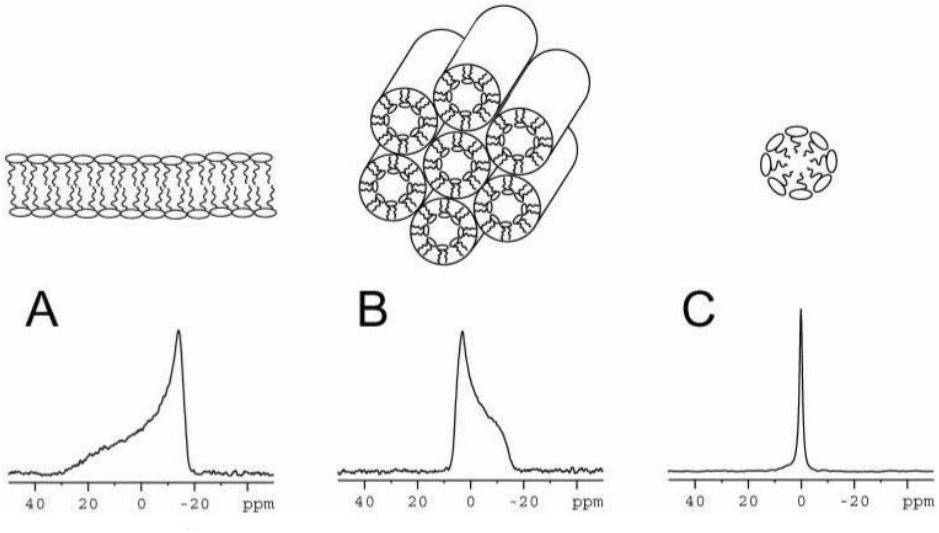

Figure 1-12. ^{31}P NMR line shapes characteristic of different lipid morphologies. (A) lamellar bilayer, (B) inverted hexagonal phase, (C) spherical micelle. Reprinted with permission from Figure 4 of *Concepts in Magnetic Resonance (Part A)*, **2004**, *23A (2)*, 89-120.[53] Copyright © (2004) Wiley Periodicals Inc.

Membrane interaction, binding, and structure of AMPs can also be examined through high resolution solution NMR techniques by using model membranes such as micelles or bicelles.[57,58] These membrane mimetics are used rather than bigger liposomes such as GUVs (giant unilamellar vesicles), LUVs (large unilamellar vesicles , SUVs (small unilamellar vesicles) and MLVs (multilamellar vesicles) because micelles or bicelles isotropically tumble in solution and have correlation times in the nanosecond range.[59] Micelles (SDS, DPC, or DHPC) have been widely used because it has the advantage of simplicity in sample preparation and usually gives high resolution spectra as exemplified in membrane binding and structural studies involving several AMPs.[57,60] However, the use of micelles as membrane models is controversial because of its small radius and high membrane curvature which lack a planar structure. On the other hand, bicelles have become a more accepted membrane mimic because it contains a better natural membrane planar bilayer structure.[61] Bicelles are generally composed of short- and long-acyl chain phospholipids (such as DHPC and DMPC, respectively), and their shape can be controlled by the ratio (q) of the long chain to short chain ones. Bicelles with $q<1$, which have disc-like structures with the

short chain lipids lining the rim and the long chain lipids lining the planar regions, are used because they possess fast tumbling and isotropic properties required for high-resolution solution NMR studies. At higher q values (q >2.5), bicelles are magnetically oriented and are suitable for solid-state NMR studies.

For studies probing the interaction (such as binding and localization) of soluble proteins with membranes, isotropic micelles or bicelles are usually used.[61,62] For instance, it was revealed that the antibacterial peptide Pexiganan (MSI-78) preferentially interacts with zwitterionic detergent (DPC) micelles more than anionic (SDS) ones.[63] Moreover, the use of paramagnetic quenchers to such as Mn^{2+} can be used to assess the depth of bound compounds in membrane models such as micelles and bicelles. Because the presence of a paramagnetic quencher such as Mn^{2+} in solution can increase the relaxation rates of nuclei in its proximity, it can be used to assess which segments of AMPs remain accessible to the aqueous solvent and which are not (signifying membrane insertion) upon interaction with the model membranes. Paramagnetic quenching measurements using bicelles were also carried out with cell-penetrating peptide penetratin to assess it position with respect to the phospholipids in the membrane.[64]

1.3.2 Examining Membrane Permeabilization by Fluorescence Spectroscopy and Microscopy Techniques

As discussed in the previous sections, disruption of membrane integrity by AMPs or membrane-active compounds can occur in various ways. However, regardless of the mechanism it transpired from, the ability of molecules to induce permeation or lysis can still be quantified by the percentage of leakage of specific fluorescent probes entrapped in a vesicle.[65] A commonly used method uses carboxyfluorescein incorporated inside LUVs, leading to the probe's self-quenching as a consequence of being highly concentrated.[65,66] When AMPs or membrane-active compounds induce membrane permeability, the probe leaks out and becomes diluted, leading to an increase in fluorescence proportional to percent leakage. After obtaining the fluorescence at 100% leakage by exposing the vesicles to Triton X-100 (positive control), it is possible to calculate for the leakage percentage using the standard equation, % Leakage = $(I-I_o)/(I_{positive\ control} - I_o)$.[65,66] Some AMPs such as Magainin 2[67], Protegrin[68], and Melittin[69] are known to act on the membrane bilayer by forming pores that allow ions such H^+, Na^+ and Ca^{2+} to pass through.[70] Numerous fluorescence based assays which utilizes a pH or membrane potential sensitive dyes can be used to detect such pore/ion channel formation.[71] For instance, K^+/H^+ flux induced by antifungal antibiotic amphotericin B to POPC liposomes containing ergosterol and ergosterol derivatives were monitored by entrapping a pH dependent fluorescent dye BCECF to the liposomes.[72,73] Attaching of a fluorescent moiety to the molecules being evaluated or to the lipid bilayer components can also be one way of examining membrane interactions and permeabilization. Fluorescent membrane lipid derivatives labeled with fluorescent moieties such as pyrene, NBD, lissamine rhodamine, BODIPY, and texas red, in the phospholipid headgroup or in the lipid acyl chain can also be incorporated to liposomes for real time imaging fluorescence microscopy experiments and examinations of selective partitioning in membrane phases (L_o/L_d) (Figure 1-13). For instance, by using fluorescent daptomycin and DOPC/DOPG GUVs with 1% fluorescent lipid Rh-PE (1,2-dioleoyl-sn-glycero-3-phosphoethanolamine-N-(lissamine rhodamine B sulfonyl) (ammonium salt), it was discovered that membrane interaction of the AMP induced formation of aggregates on the surface of the GUVs as viewed from confocal microscopy.[58] With

the aid of the fluorescent probes attached to both the lipid and AMP, the composition of the exuded aggregates could be identified to contain both daptomycin and lipid molecules. This lead the authors to propose that daptomycin might exhibit a lipid extracting effect and correlate it with the peptide's antibacterial activity.[19]

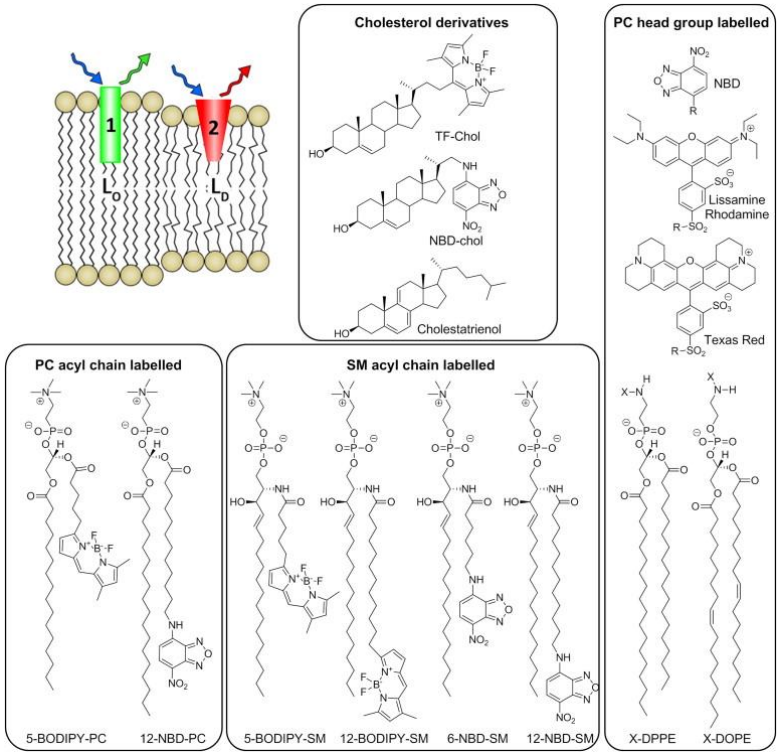

Figure 1-13. Examples of membrane lipid components with fluorescent moieties which can be used for membrane phase (L_o/L_d) partitioning studies.[74] Reprinted with permission from Figure 2 of *Chemistry & Biology*. **2014**, *21(1)*, 97-113. Copyright © (2014) Elsevier Ltd.

1.3.3 Other Methods for Examining Membrane Interaction and Permeabilization of Membrane-Active Compounds

Aside from NMR and fluorescence techniques, there are several other ways of obtaining experimental information regarding membrane permeabilization. Biophysical techniques such as circular dichroism, and isothermal titration calorimetry, can also be utilized to achieve this goal.[65] AMPs or other bioactive compounds that contain aromatic amino acid residues such as tyrosine, tryptophan, or phenylalanine or π-conjugated systems in their structures, can be examined by inspecting changes in their intrinsic fluorescence, as a consequence its heightened sensitivity to the hydrophobicity of its environment.[75] In a study to characterize the extent of membrane interaction of Novicidin with membranes composed of DMPC and DMPG membranes, Tyrosine fluorescence experiments were carried out. Results from this experiment aided in characterizing Novicidin's preferential biding of negatively charged phospholipids promoting its insertion to the bilayer.[76]

Thermodynamic characterization of peptide-membrane interactions can be carried out by isothermal titration calorimetry (ITC), a straight forward method to determine basic chemical details of binding interaction.[77] The principle of this method is based on the detection of the heat of reaction, an intrinsic property of almost all chemical reactions including peptide-lipid membrane interactions. In a study investigating the membrane interactions of mastoparan-X, the use of ITC, together with cryo-transmission electron microscopy (cryo-TEM), enabled the determination of the thermodynamic parameters of its pore formation process.[78] Moreover, in another study, ITC was also used to measure the affinity of integrin αIIbβ3 complex (a transmembrane protein) to model membranes in the form of phospholipid bicelles.[79]

Examining the changes and modifications to peptide characteristics upon interaction with biological membranes can also give relevant information towards the understanding of how AMPs elicit their biological activity. One method frequently employed is circular dichroism spectroscopy, a technique that can be used to estimate the overall secondary structure of peptides.[65] This technique is based on the absorbance characteristics of peptide bonds in the far UV region (240-180 nm). Since every secondary structure element has a distinguishing CD absorbance spectra, changes in the peptide structure as it interacts with lipid membranes can be monitored.[65] Magainin 2 (Mag2), an AMP isolated from the tree frog *Xenopus leavis*, is known to rely significantly on the formation amphipathic α-helical structures to elicit its biological action by inducing toroidal pores in the membrane.[80] In a study conducted for Mag2, the influence of membrane surface charge to Mag2 structure was examined by CD spectroscopy and results indicated that a negative charge on the membrane surface is important for helix formation.[81]

These among others are just a few examples of how membrane interaction and permeabilization of AMPs and other membrane active compounds can be examined. Combination of such techniques make it possible to obtain a more holistic understanding of how AMPs or other membrane-active compounds elicit their biological activity by interacting with the biological membranes.

1.4 Marine Sponge-derived Natural Products and their Bioactivities

1.4.1 Why Sponges?

Sponges are a large and diverse group of invertebrates under the phylum Porifera which are considered functionally important members of the marine benthic communities.[1–3] They are considered as simple yet highly-evolved multi-cellular organisms which live as sedentary filter feeders taking up nutrients, organic materials, and microorganisms from the sea water.[1–3] Sponges are characterized as having bodies full of pores (called *ostia*) and canals through which water passes at impressive rates (about thousands of liters per kg of sponge per day).[4–7] Most sponges thrive in waters 5-50 meters in depth but some can still grow at hundreds of meters below sea level, even under extreme environment conditions. Sponges are a dominant faunal component in tropical and temperate reefs while it can occupy up to 80% of the available surface in polar regions.[8,9] Although over 10,000 species of sponges are present, its identification remains challenging as it is solely based on the type, size, and distribution of its microscopic skeletal supports called spicules.[3,6]

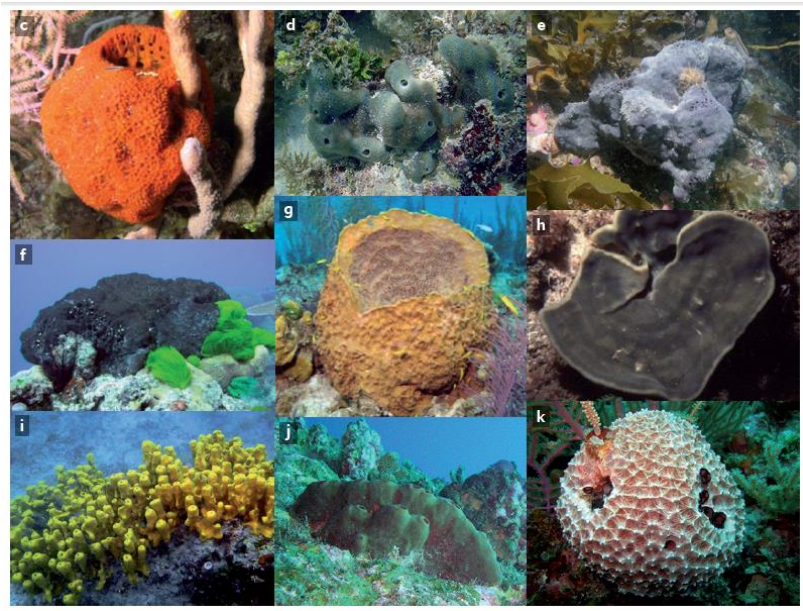

Figure 1-14. Underwater images of marine sponges. Reprinted with permission from Figure 1 of *Nature Reviews Microbiology*, **2012**, *10*, 641-654[2], *Open Mar. Biol. J.*, **2010**, *4*, 57-64[4], and *Environ. Microbiol.*, **2012**, *14*, 335-346[5]. Copyright © (2012) Macmillan Publishers Ltd., (2010) Bentham Science, and (2011) John Wiley & Sons

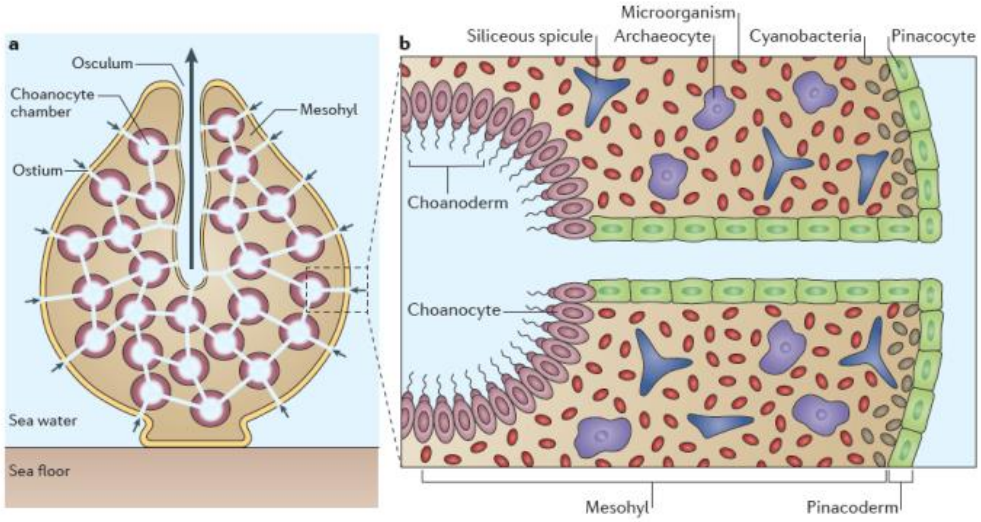

Figure 1-15. Schematic overview of a typical demosponge. Reprinted with permission from Figure 1 of *Nature Reviews Microbiology*, **2012**, *10*, 641-654.[2] Copyright © (2012) Macmillan Publishers Ltd.

Table 1-1. Natural Products suspected or known to be produced by bacterial symbionts of sponges.[2]

Natural Product	Suspected bacterial source	Host sponge
Brominated biphenylethers	*Oscillatoria spongeliae*	*Lamellodysidea* spp.
Chlorinated peptides	*Oscillatoria spongeliae*	*Lamellodysidea* spp.
Theopalauamide	'*Candidatus Entotheonella palauensis'*	*Theonella swinhoei*
Swinholide A	Unicellular bacterium	*Theonella swinhoei*
Onnamide A	Unidentified bacterium	*Theonella swinhoei*
Psymberin	Unidentified bacterium	*Psammocinia bulbosa*

Marine sponges have been an abundant source of diverse and highly potent bioactive compounds appealing as a target for isolation studies.[10–14] Aside from being recognized as the largest source of new marine natural products reported annually, sponges have been known to afford a multitude of compounds with pharmaceutical value since the 1950's.[12] Compounds isolated from sponges have interesting, novel, and unusual structures which may have been produced to serve as protective agents against predators.[2] These compounds may also be attributed to the occurrence of symbiotic microbes living within sponges.[5] Sponges provide lodging to organisms such as algae, dinoflagellates, annelid worms, and microbes to name a few.[2,11,15,16] Since microbes have been reported to contribute up to 40% to the tissue volume of sponges and that many of the isolated substances from sponges resemble typical products of microbial pathways such as polyketides and non-ribosomal peptides,[2,8] it is not implausible to think that some compounds isolated from sponges are actually produced by the symbiotic organisms that occupy it.[2,11]

The structural diversity of compounds isolated from marine sponges provide novel leads against bacterial, viral, fungal, parasitic and cancer diseases which prove to be difficult targets for current pharmaceuticals.[10] Bioactive metabolites isolated from sponges include terpenoids, alkaloids, macrolides, polyethers, nucleoside derivatives, and peptides to name a few.[10] For instance, Halichondrin B, a polyene macrolide first isolated from the marine sponge *Halichondria okadai* in 1986, exhibited exquisite anticancer activity against murine cancer cells *in vivo* and *in vitro*.[12,17,18] After its complete synthesis was achieved in 1992,[12] development of its structurally simplified pharmaceutical analog eribulin was realized. In 2010, eribulin received approval from the U.S. Food and Drug Administration and is being administered to patients with metastatic breast cancer.[19]

Another significant class of bioactive metabolites isolated from marine sponges comprise of linear and cyclic peptides. In 1985, the first bioactive peptide discodermin A, was isolated from the marine sponge *Discodermia kiiensis* by Matsunaga *et al* and was reported to posses antimicrobial activity against *Bacillus subtilis* and *Proteus mirabilis*.[20,21] Interestingly, discodermin A contains several unusual structural features which include having a rarely found *t*-Leu residue and several amino acids in the D-form leading the researchers to speculate that it may be a metabolite produced by the bacteria or algal symbionts living in the sponge.[20] Since then, three other discodermins have been isolated (discodermin B-D) with small structural variations occurring in its tetradecapeptide structures.[22] In addition, discodermins were discovered to be potent inhibitors of phospholipase A_2 and inhibited tumor promotion of okadaic acid in mice.[21,23]

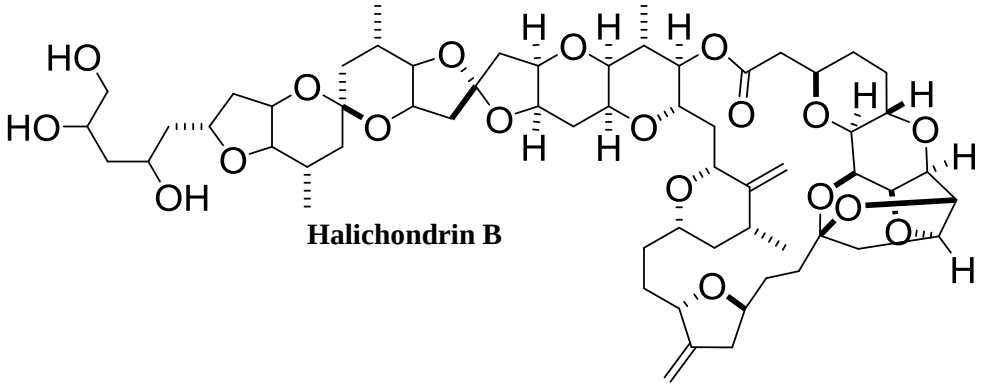

Halichondrin B

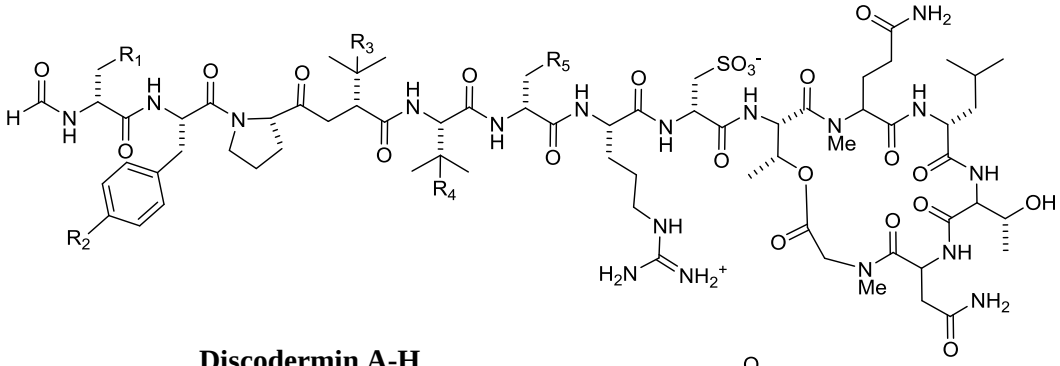

Discodermin A-H

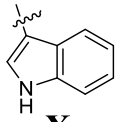

X

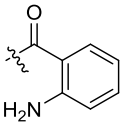

Y

A: R_1=R_2=H, R_3=R_4=Me, R_5=X
B: R_1=R_2= R_3=H, R_4=Me, R_5=X
C: R_1=R_2= R_4=H, R_3=Me, R_5=X
D: R_1=R_2= R_3= R_4=H, R_5=Y
E: R_1=R_2 =H, R_3= R_4=Me, R_5=Y
F: R_1=R_2=H, R_3= Me, R_4=Et, R_5=X
G: R_1=R_3= R_4=Me, R_2=H, R_5=X
H: R_1=H, R_2= OH, R_3=R_4=Me, R_5=X

1.4.2 Bioactive Compounds Isolated from *Lithistid* Sponges

After the isolation of discodermins, numerous peptides with interesting biological activities and structures have been discovered from various sponge species including those from order *Lithistida*. *Lithistid* sponges are a polyphyletic group of demosponges that occur in both shallow and deep-water environments. They are characterized by having an interlocking siliceous spicules skeleton material that gives its body a firm and hard-rock consistency.[12,21] Despite having a good physical protection against predators which should connote that there is less need for chemical defense, these sponges are still known to produce a diverse array of structurally complex and biologically active compounds which include polyketides, macrolides, alkaloids, pigments, lipids, sterols, and cyclic and linear peptides.[24]

Theonella sp. and *Theonella swinhoei*, also from *Lithistid* sponges, have also been prolific sources of linear and cyclic peptides with interesting biological activities.[27] These peptides are particularly rich in non-conventional amino acids including D-series and N-alkylated versions of the natural ones, which are thought to be responsible for their pronounced pharmacological activities. As a consequence, linear and cyclic peptides isolated from *Lithistid* sponges are speculated to be of non-ribosomal origin based on their structures which are reminiscent of products derived from mixed non-ribosomal peptide synthetase (NRPS) – polyketide synthase (PKS) pathways of microorganisms that reside in sponges.[28]

1.4.2.1 Cyclic Peptides Isolated from *Lithistid* Sponges *Theonella* sp. and *Theonella swinhoei*

Structure activity relationship studies have also highlighted the improved pharmacological activities of *Lithistid* sponge-derived metabolites having cyclic peptide structures, as demonstrated by koshikamides F and H. For instance, the lack of an N and C termini together with the presence of N-alkylated amino acids in the sequence of depsipeptides, are said to endow improved stability to its structure against enzymatic degradation and enhanced hydrophobicity leading to a more facile crossing of the biological membrane. In addition, cyclization reduces peptide conformational flexibility that may result in a higher receptor binding affinity and offer the possibility to determine their three dimensional structures.[35]

From a *Theonella* sp. sponge collected in Hachijo-jima island, cyclic peptides cyclotheonamide A and B were isolated.[36] Both are macrocyclic pentapeptides containing L-proline, D-phenylalanine, and 3 uncommon non-proteinogenic amino acid L-α-ketohomoarginine, L-β-aminoalanine, and vinylogous L-tyrosine. Cyclotheonamide A and B were reported to be inhibitors of serine proteases such as α- thrombin and trypsin.[36,37] Also, *Theonella* sp. obtained in Okinawa, another region of Japan, afforded five tridecapeptide lactones named theonellapeptolides la-le which are rich in *N*-methyl and D-amino acids.[21, 38] Theonellapeptolides lb-le possess moderate cytotoxicity against mouse lymphocytic leukemia cells (L1210) *in vitro* with IC_{50} values less than 2.5μg/mL and theonellapeptolide 1e was also reported to exhibit ion-transport activities for Na^+ and K^+ ions.[38]

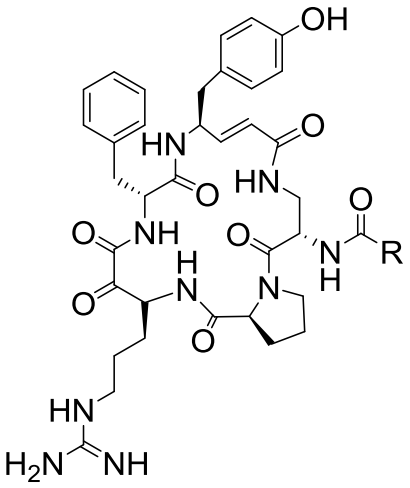

Cyclotheonamides A & B

A: R=H
B: R= CH_3

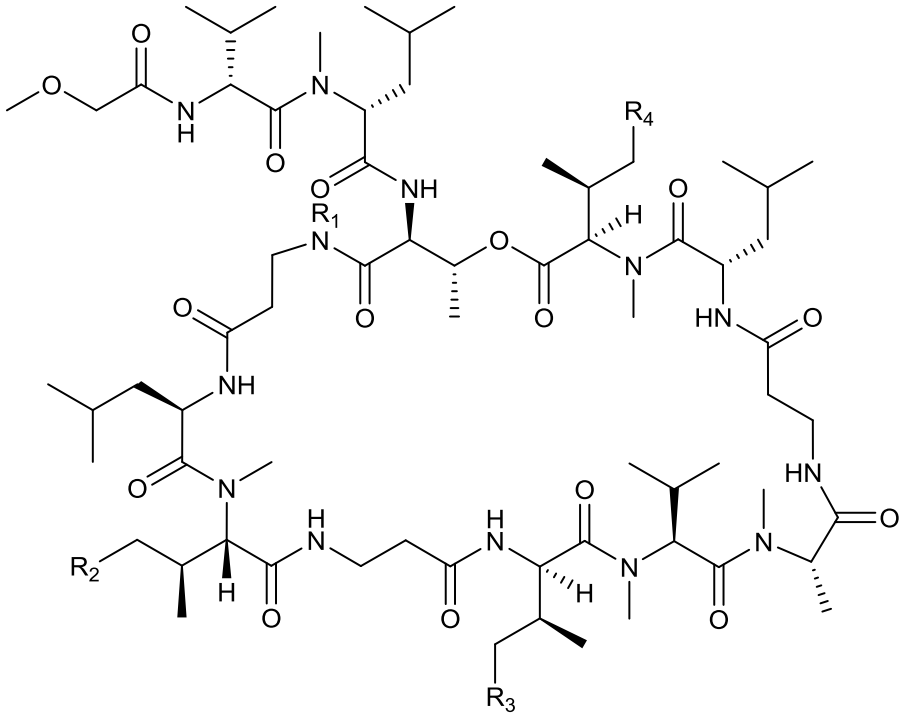

Theonellapeptolides 1a-1e

1a: R_1=H, R_2=CH_3, R_3=H, R_4=CH_3
1b: R_1=H, R_2=H, R_3= CH_3, R_4=CH_3
1c: R_1=H, R_2=CH_3, R_3= CH_3, R_4=H
1d: R_1=H, R_2=CH_3, R_3= CH_3, R_4=CH_3
1e R_1=CH_3, R_2=CH_3, R_3= CH_3, R_4=CH_3

Several studies were also conducted with *Theonella swinhoei* sponges obtained from different marine areas outside of Japan. For instance, an antifungal glycopeptide named Theonegramide was isolated from *Theonella swinhoei* obtained from Antolang, Negros island in the Philippines.[39] Its structure consists of an arabinose moiety attached to a bicyclic dodecapeptide, bridged by a rare histidinoalanine residue, and containing several unusual amino acids such as β-hydroxyaspargine and α-aminoadipic acid.[39] In addition, another bicyclic glycopeptide called Theopalauamide was also isolated from the same sponge obtained from Palau and Mozambique.[40] More importantly, it was discovered that this peptide was located in the filamentous eubacteria residing in the interior of the *T. swinhoei* sponge. Theopalauamide was reported to inhibit the growth of *Candida albicans* at 10 μg/disk based on the results of a standard paper disk assay.[40]

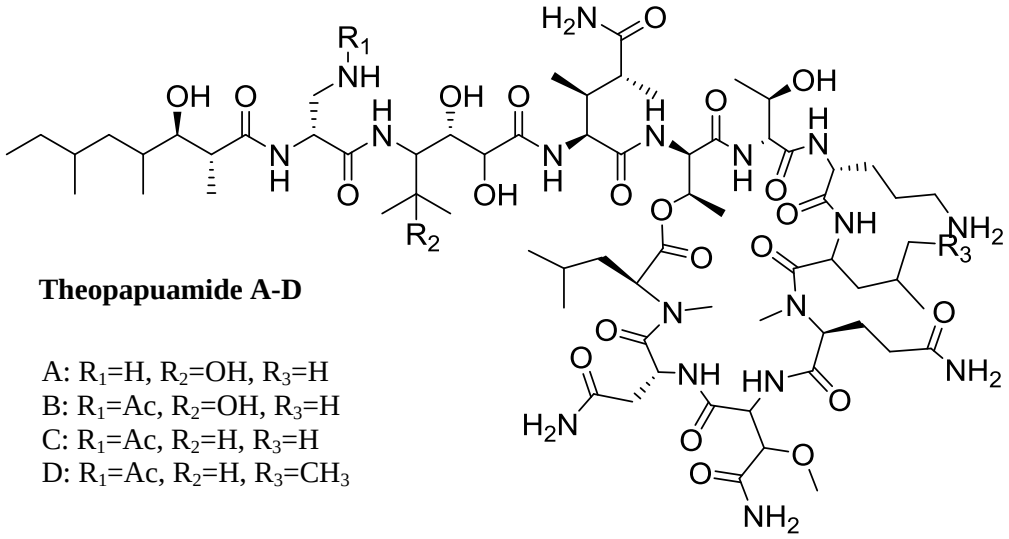

Theopapuamide A-D

A: R_1=H, R_2=OH, R_3=H
B: R_1=Ac, R_2=OH, R_3=H
C: R_1=Ac, R_2=H, R_3=H
D: R_1=Ac, R_2=H, R_3=CH_3

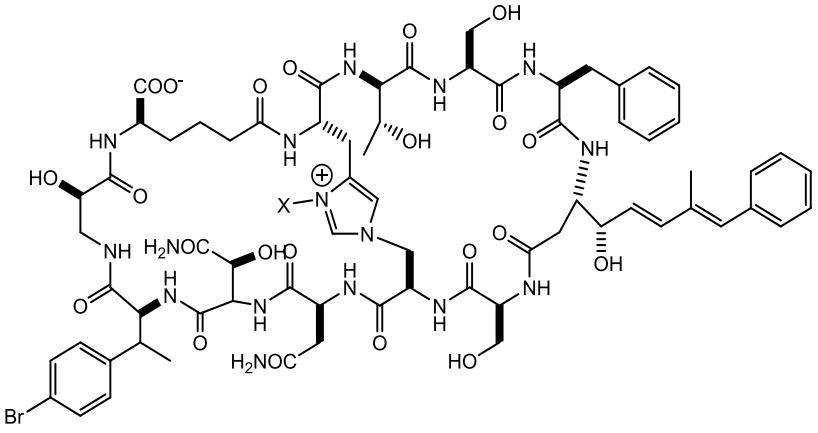

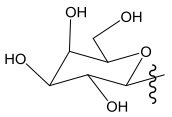

β-D-Gal

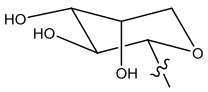

β-D-Ara

Theonegramide X = β-D-Ara
Theopalauamide X = β-D-Gal

1.4.3 Theonellamides and its bioactivities

Another variety of the *Theonella swinhoei* sponge, appearing to have a white interior, was also obtained from a Hachijo-jima island collection.[21] From the less polar fraction of the EtOH extract of this *T. swinhoei* sponge, cytotoxic macrodiolide bistheonellides A and B[21,41] were isolated while the polar fractions afforded Theonellamide F (TNM-F).[41] TNM-F, isolated in 1989 by Matsunaga *et al.*, is the first member of a family of antifungal and cytotoxic bicyclic dodecapeptides named Theonellamides (TNMs). TNMs (TNM-A to TNM-G) possess a unique structure characterized by a bis-macrocycle bridged by a τ-histidinoalanine (τ-HAL) residue and containing unusual amino acids (Figure 2-7)[41–43]. Some of the compounds from this group are further embellished by a monosaccharide covalently linked to the π-nitrogen of the τ-HAL residue. Structure-activity relationship studies indicate that bioactivities among this group are comparable regardless of the presence or absence of the sugar moiety, possibly underlining the role of the bicyclic framework of TNM in its biological action.[41–43] TNMs A-F were reported to inhibit growth of prototypical fungi (*Candida*, *Trichophyton*, and *Aspergillus*) with IC_{50} values of 2-7 μM and have cytotoxic activity against P388 mouse leukemia cells (IC_{50} 0.5-2.8 μM).[41–45]

Table 1-2 IC_{50} values of various TNMs.[42,43,44]

	IC_{50} (μg/mL)
Theonellamide A	5.0
Theonellamide B	1.7
Theonellamide C	2.5
Theonellamide D	1.7
Theonellamide E	0.9
Theonellamide F	2.7
Theonellamide G	2.0

Previous studies have indicated that TNM-F caused formation of acidic vacuoles around the nucleus of rat embryonic fibroblasts (Figure 2-3).[44] This effect of TNM-F on the cells was speculated to result from a disturbance of the cellular transport system. After comparing with Monesin, a Na^+ ionophore which also induces formation of vacuoles similar to that of TNM-F, data suggested that TNM-F has less-pronounced effects on cellular morphology or viability and greater effect on formation of vacuoles. Moreover, it was proposed that the acidic vacuole formation induced by TNM-F might be due to its inhibitory effect on the autophagic degradation of organelles and turnover of proteins.[44]

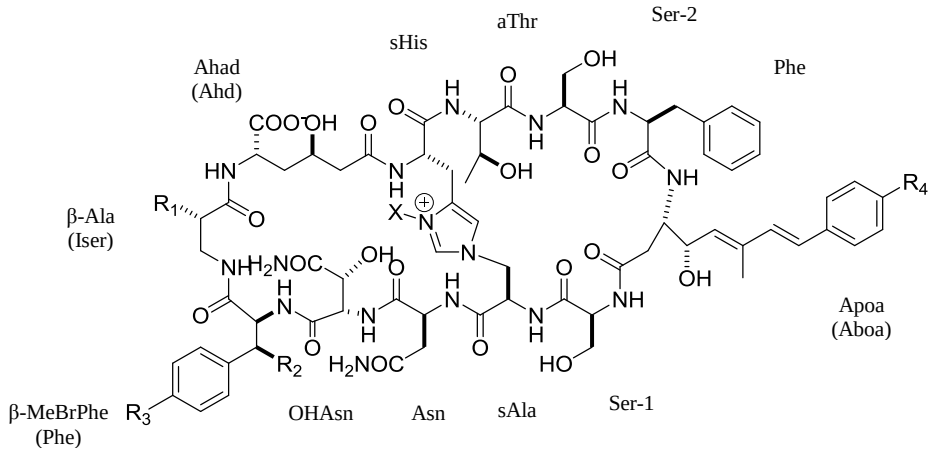

Theonellamides A-G

	R_1	R_2	R_3	R_4	X
Theonellamide A	OH	Me	Br	H	β-D-Gal
Theonellamide B	OH	Me	Br	Br	H
Theonellamide C	H	H	H	Br	H
Theonellamide D	H	H	Br	Br	β-D-Ara
Theonellamide E	H	H	Br	Br	β-D-Gal
Theonellamide F	H	H	Br	Br	H
Theonellamide G[a]	OH	H	Br	H	β-D-Gal

[a] 2-aminohexanedioic acid (Ahd) instead of α-amino-γ-hydroxyadipic acid (Ahad)

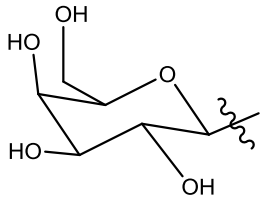

β-D-Gal

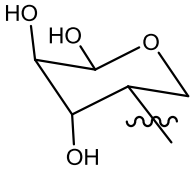

β-L-Ara

Apoa = (5E, 7E)-3-amino-4-hydroxy-6-methyl-8-phenyl-5,7-octadienoic acid
Aboa = (5E, 7E)-3-amino-4-hydroxy-6-methyl-8-(p-bromophenyl)-5,7-octadienoic acid
sAla = alanine portion of histidinoalanine
OHAsn = β-hydroxyaspargine
β-MeBrPhe = β-methyl-p-bromophenylalanine
Iser = isoserine
Ahad = α-amino-γ-hydroxyadipic acid
sHis = histidine portion of histidinoalanine
aThr = *allo*-threonine

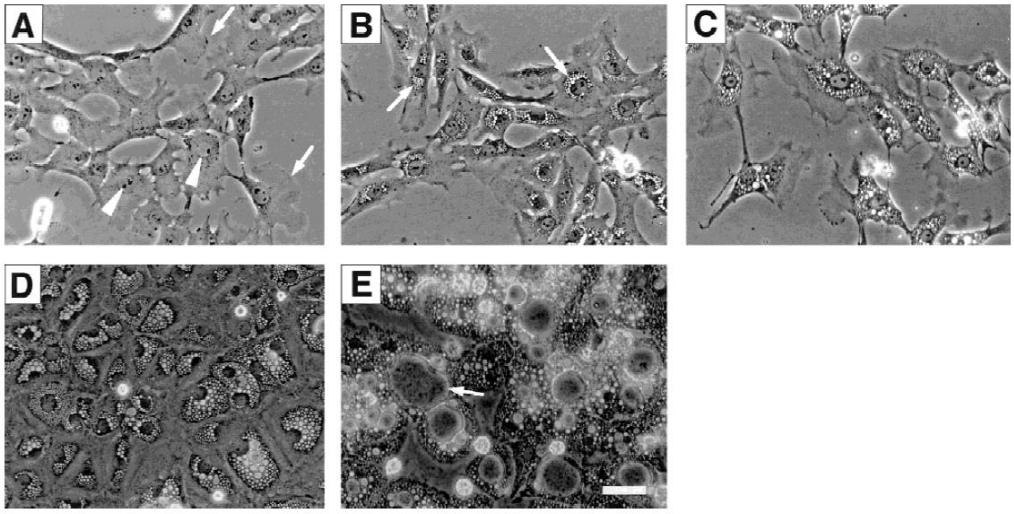

Figure 1-16. Formation of vacuoles in 3Y1 rat embryonic fibroblasts treated with Theonellamide F.(A) Cells treated with DMSO for 24 hours, (B)-(E) Cells treated with various concentrations of TNM-F with 24-120 h incubation.[43] Reprinted with permission from Figure 2 of *Mar. Biotechnol.*, **1999**, *1*, 337-341.[43] Copyright © (1999) Springer-Verlag.

In search of theonellamides' cellular targets, a binding assay was carried out using proteins from rabbit liver tissues and Theonellamide A attached to hydrazide-containing gel beads. After SDS-PAGE and amino acid sequence analyses of the bound proteins, results revealed that TNM-A bound to proteins homologous to mammalian 17β-hydroxysteroid dehydrogenase IV (80 kDa) and murine glutamate dehydrogenase (55 kDa) proteins.[44] While glutamate dehydrogenase's function is critical to cellular nitrogen and carbon metabolism, 17β-hydroxysteroid dehydrogenase IV functions to catalyze interconversion of steroid hormones, 2-enoyl-acyl-coenzyme A hydratase reaction, and intracellular transport of sterols and lipids. It is speculated that the possible effect of theonellamides on the intracellular transport of sterols and lipids may be one of the causes of its cytotoxicity.[44]

1.4.3.1 Sterol-dependent activities of Theonellamides

With the aid of chemical-genomic profiling and clustering analysis of yeast genes that confer altered sensitivity to TNMs, a mechanistic link between TNM and increased 1,3-β-D-glucan synthesis mediated by Rho1 signaling was revealed.[45] In the same study, results from subcellular localization and *in vitro* binding assays using a fluorescent-TNM derivative suggested that, TNM specifically binds to 3β-hydroxysterols such as cholesterol and ergosterol and cause membrane damage in *S. pombe* cells (Figure 2-4). Moreover, alleviation of this bioactivity in yeast cells that incurred genetic mutations in their ergosterol biosynthetic pathway further highlighted the role of the sterol not only in membrane binding, but also in eliciting TNMs effects on the cell wall.[45] Comparison of the yeast membrane morphological changes caused by the similar sterol-binding polyene antibiotic amphotericin B (enlargement of vacuoles) and TNM (highly fragmented vacuoles) and the fact that TNM exhibits time-dependent cytotoxicity versus AmB's acute cytotoxicity indicate that Theonellamides represent a new class of sterol-binding molecules.[45]

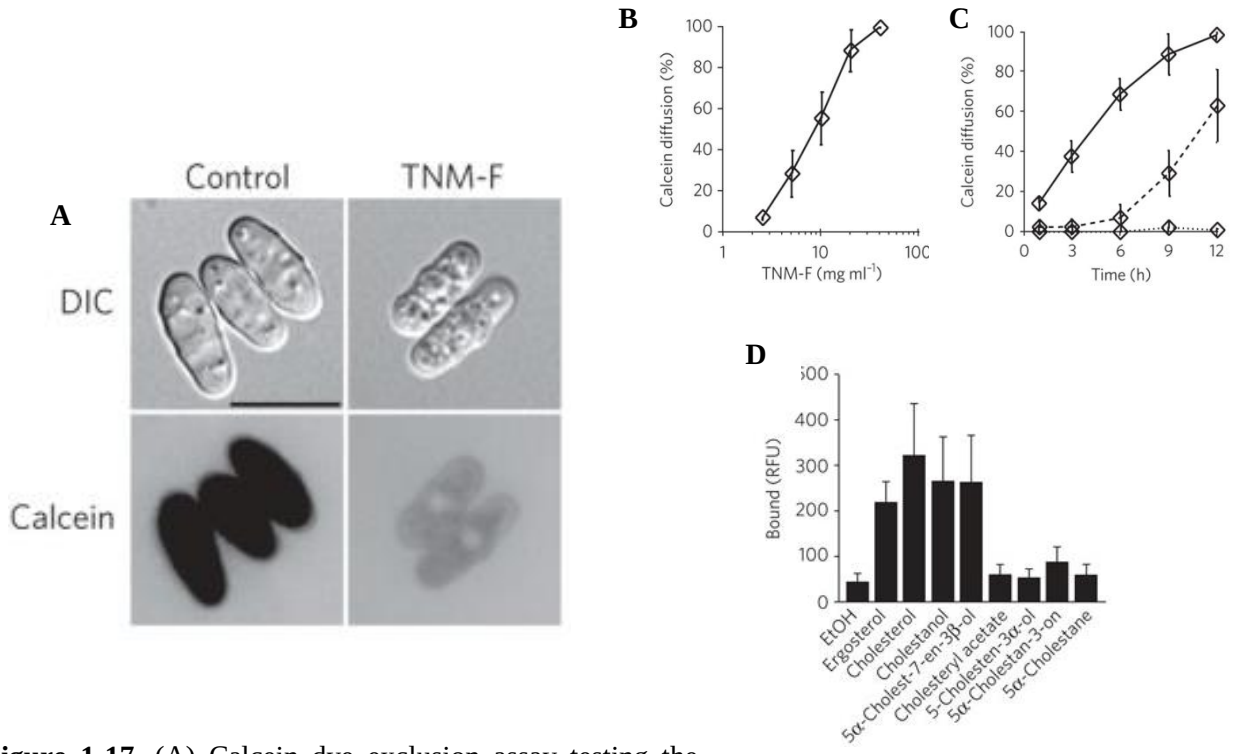

Figure 1-17. (A) Calcein dye exclusion assay testing the effect of TNM-F on the plasma membrane integrity of *S. pombe* cells. (B) and (C) Kinetics of Calcein diffusion induced by TNM-F. (D) Preferential binding of TNM-BF to 3β-hydroxysterols.[45] Reprinted with permission from Figure 3 and 5 of *Nature Chemical Biology*, **2010**, *6*, 519-526.[45] Copyright © (2010) Macmillan Publishers Ltd.

1.5 General Objective of this Research

As presented in previous sections, marine organisms such as sponges are important sources of bioactive metabolites with interesting activities, making them very good candidates for isolation studies. In this study, I focused on theonellamides (TNMs) specifically theonellamide A (TNM-A) which are a family of bicyclic dodecapeptides isolated from the marine sponge *Theonella sp.* Their moderate antifungal activities against prototypical fungi strains are very interesting to probe into because, similar to polyene antifungal Amphotericin B (AmB), preliminary studies suggested that TNMs also target membrane sterols' to elicit activity.

However, unlike AmB, which exhibit a more potent fungicidal effect, TNMs have a weaker time-dependent cytotoxicity suggesting that their mechanisms of membrane disruptions are dissimilar. Compared to antimicrobial peptides (AMPs), TNMs interaction with phospholipid membranes cannot occur through electrostatic interactions because of its neutrally charged structure's. Also, in contrast to TNMs sterol-dependent membrane activity, AMPs generally have weaker activities in cholesterol-

containing membranes. Finally, TNMs cyclic peptide structure, having no specific segregations in its hydrophilic and hydrophobic residues, seems less likely to insert to the membrane in the same way as AMPs given their amphipathic α-helical structures. These differences suggest TNMs uniqueness to other membrane disrupting compounds making it an interesting model compound to study a seemingly new type of membrane disrupting mechanism.

References:

1. S.J. Singer, Nicolson, G. Singer Nicolson FluidMosaicModel.pdf. *Science (80-.).* **175,** 720–731 (1972).

2. Lodish, H. *et al. Molecular Cell Biology*. (New York: W. H. Freeman, 2000).

3. Thompson, G. A. Membrane acclimation by unicellular organisms in response to temperature change. *J. Bioenerg. Biomembr.* **21,** 43–60 (1989).

4. Nenninger, A. *et al.* Independent mobility of proteins and lipids in the plasma membrane of Escherichia coli. *Mol. Microbiol.* **92,** 1142–1153 (2014).

5. Murata, M., Sugiyama, S., Matsuoka, S. & Matsumori, N. Bioactive Structure of Membrane Lipids and Natural Products Elucidated by a Chemistry-Based Approach. *Chem. Rec.* **15,** 675–690 (2015).

6. Corvera, E., Mouritsen, O. G., Singer, M. A. & Zuckermann, M. J. The permeability and the effect of acyl-chain length for phospholipid bilayers containing cholesterol: theory and experiment. *BBA - Biomembr.* **1107,** 261–270 (1992).

7. McMullen, T. P. W., Wong, B. C. M., Tham, E. L., Lewis, R. N. A. H. & McElhaney, R. N. Differential scanning calorimetric study of the interaction of cholesterol with the major lipids of the Acholeplasma laidlawii B membrane. *Biochemistry* **35,** 16789–16798 (1996).

8. Huang, J. & Feigenson, G. W. A microscopic interaction model of maximum solubility of cholesterol in lipid bilayers. *Biophys. J.* **76,** 2142–57 (1999).

9. Ikonen, E. Cellular cholesterol trafficking and compartmentalization. *Nat. Rev. Mol. Cell Biol.* **9,** 125–138 (2008).

10. Berg, J. M., Tymoczko, J. L. & Stryer, L. in *Biochemistry* (w. H. Freeman, 2002).

11. Lemmich, J. *et al.* The effect of cholesterol in small amounts on lipid bilayer softness in the region of the main phase transition. *Eur. Biophys. J. with Biophys. Lett.* **25,** 293–304 (1997).

12. Bastiaanse, E. M. L., Höld, K. M. & Van der Laarse, A. The effect of membrane cholesterol content on ion transport processes in plasma membranes. *Cardiovasc. Res.* **33,** 272–283 (1997).

13. Brogden, K. a. Antimicrobial peptides: pore formers or metabolic inhibitors in bacteria? *Nat. Rev. Microbiol.* **3,** 238–250 (2005).

14. Finlay, B. B. & Hancock, R. E. W. Can innate immunity be enhanced to treat microbial infections? *Nat. Rev. Microbiol.* **2,** 497–504 (2004).

15. Sato, H. & Feix, J. B. Peptide-membrane interactions and mechanisms of membrane destruction by amphipathic ??-helical antimicrobial peptides. *Biochim. Biophys. Acta - Biomembr.* **1758,** 1245–1256 (2006).

16. Baltz, R. H., Miao, V., Wrigley, S. K. & Miao, V. Natural products to drugs: daptomycin and relatied lipopeptide antibiotics. *Nat. Prod. Reports* **22,** 717–741 (2005).

17. Ball, L., Goult, C. M., Donarski, J. A., Mickle, J. & Ramesh, V. NMR structure determination and calcium binding e ff ects of lipopeptide antibiotic daptomycin. *Org. Biomol. Chem.* **2,** 1872–1878

(2004).

18. Hachmann, A. B. *et al.* Reduction in membrane phosphatidylglycerol content leads to daptomycin resistance in Bacillus subtilis. *Antimicrob. Agents Chemother.* **55,** 4326–4337 (2011).

19. Chen, Y. F., Sun, T. L., Sun, Y. & Huang, H. W. Interaction of daptomycin with lipid bilayers: A lipid extracting effect. *Biochemistry* **53,** 5384–5392 (2014).

20. Bush, K. Antimicrobial agents targeting bacterial cell walls and cell membranes. *Rev. Sci. Tech.* **31,** 43–56 (2012).

21. Yamamura, H. *et al.* Mimicking an antimicrobial peptide polymyxin B by use of cyclodextrin. *Chem. Commun.* **48,** 892 (2012).

22. Deris, Z. Z. *et al.* Probing the penetration of antimicrobial polymyxin lipopeptides into gram-negative bacteria. *Bioconjug. Chem.* **25,** 750–760 (2014).

23. Velkov, T., Roberts, K. D., Nation, R. L., Thompson, P. E. & Li, J. Pharmacology of polymyxins: new insights into an 'old' class of antibiotics. *Futur. Microbiol* **8,** 1–20 (2013).

24. Ofek, I. *et al.* Antibacterial synergism of polymyxin B nonapeptide and hydrophobic antibiotics in experimental gram-negative infections in mice. *Antimicrob. Agents Chemother.* **38,** 374–377 (1994).

25. Wang, G. Database-guided discovery of potent peptides to combat HIV-1 or superbugs. *Pharmaceuticals* **6,** 728–758 (2013).

26. Sanderson, J. M. Peptide-lipid interactions: insights and perspectives. *Org. Biomol. Chem.* **3,** 201–212 (2005).

27. Baumann, G. & Mueller, P. A Molecular Model of Membrane Excitability. *J. Supramol. Struct.* **557,** 538–557 (1974).

28. Yang, L., Harroun, T. a, Weiss, T. M., Ding, L. & Huang, H. W. Barrel-stave model or toroidal model? A case study on melittin pores. *Biophys. J.* **81,** 1475–1485 (2001).

29. Liu, L. P. & Deber, C. M. Guidelines for membrane protein engineering derived from de novo designed model peptides. *Biopolym. - Pept. Sci. Sect.* **47,** 41–62 (1998).

30. He, K., Ludtke, S. J., Worcester, D. L. & Huang, H. W. Neutron scattering in the plane of membranes: structure of alamethicin pores. *Biophys. J.* **70,** 2659–2666 (1996).

31. Cantor, R. S. Size distribution of barrel-stave aggregates of membrane peptides: influence of the bilayer lateral pressure profile. *Biophys. J.* **82,** 2520–2525 (2002).

32. Zhang, M., Zhao, J. & Zheng, J. Molecular understanding of a potential functional link between antimicrobial and amyloid peptides. *Soft Matter* **10,** 7425–51 (2014).

33. Palffy, R. & Gardlik, R. On the Physiology and Pathophysiology of Antimicrobial Peptides. *Mol. Med.* **15,** 1 (2008).

34. Ludtke, S., He, K. & Huang, H. Membrane Thinning Caused by Magainin 2+. *Biochemistry* **34,** 16764–16769 (1995).

35. Yamaguchi, S., Hong, T., Waring, A., Lehrer, R. I. & Hong, M. Solid-state NMR investigations of peptide-lipid interaction and orientation of a beta-sheet antimicrobial peptide, protegrin. *Biochemistry* **41,** 9852–9862 (2002).

36. Lee, M., Chen, F. & Huang, H. W. Energetics of Pore Formation Induced by Membrane Active Peptides †. *Biochemistry* **43,** 3590–3599 (2004).

37. Hallock, K. J., Lee, D.-K. & Ramamoorthy, A. MSI-78, an analogue of the magainin antimicrobial peptides, disrupts lipid bilayer structure via positive curvature strain. *Biophys. J.* **84,** 3052–60 (2003).

38. Wimley, W. C. Describing the Mechanism of Antimicrobial Peptide Action with the Interfacial Activity Model. *ACS Chem. Biol.* **5,** 905–917 (2010).

39. Krauson, A. J., He, J. & Wimley, W. C. Biochimica et Biophysica Acta Determining the mechanism of membrane permeabilizing peptides : Identi fi cation of potent , equilibrium pore-formers. *BBA - Biomembr.* **1818,** 1625–1632 (2012).

40. Steiner, H., Andreu, D. & Merrifield, R. B. Binding and action of cecropin and cecropin analogues : antibacterial peptides from insects. *Biochim. Biophys. Acta* **939,** 260–266 (1988).

41. Gazit, E., Boman, A., Boman, B. H. G. & J, Y. S. Interaction of the Mammalian Antibacterial Peptide Cecropin P 1 with Phospholipid Vesiclest. *Biochemistry* **34,** 11479–11488 (1995).

42. Pokorny, A., Birkbeck, T. H. & Almeida, P. F. F. Mechanism and Kinetics of δ -Lysin Interaction with Phospholipid Vesicles †. *Biochemistry* **41,** 11044–11056 (2002).

43. Pokorny, A. & Almeida, P. F. F. Kinetics of dye efflux and lipid flip-flop induced by ??-lysin in phosphatidylcholine vesicles and the mechanism of graded release by amphipathic, ??-helical peptides. *Biochemistry* **43,** 8846–8857 (2004).

44. Pokorny, A. & Almeida, P. F. F. Permeabilization of Raft-Containing Lipid Vesicles by δ -Lysin : A Mechanism for Cell Sensitivity to Cytotoxic Peptides †. *Biochemistry* **44,** 9538–9544 (2005).

45. Almeida, P. F. F., Yandek, L. E., Pokorny, A. & Flore, A. Mechanism of the Cell-Penetrating Peptide Transportan 10 Permeation of Lipid Bilayers. *Biophys. J.* **92,** 2434–2444 (2007).

46. Epand, R. M. *et al.* Biochimica et Biophysica Acta Lipid clustering by three homologous arginine-rich antimicrobial peptides is insensitive to amino acid arrangement and induced secondary structure. *BBA - Biomembr.* **1798,** 1272–1280 (2010).

47. Teixeira, V., Feio, M. J. & Bastos, M. Role of lipids in the interaction of antimicrobial peptides with membranes. *Prog. Lipid Res.* **51,** 149–177 (2012).

48. Ulrich, A. S. *et al.* Membrane-Active Peptides and the Clustering of Anionic Lipids. *Biophys. J.* **103,** 265–274 (2012).

49. Zhao, H. *et al.* Interaction of the antimicrobial peptide pheromone Plantaricin A with model membranes : Implications for a novel mechanism of action. *Biochim. Biophys. Acta* **1758,** 1461–1474 (2006).

50. Wiener, M. C. & White, S. H. Structure of a fluid dioleoylphosphatidylcholine bilayer determined by joint refinement of x-ray and neutron diffraction data Ill . Complete structure. *Biophys. J. Biophys. Soc.* **61,** 434–447 (1992).

51. Sengupta, D., Leontiadou, H., Mark, A. E. & Marrink, S. J. Toroidal pores formed by antimicrobial peptides show significant disorder. *Biochim. Biophys. Acta - Biomembr.* **1778,** 2308–2317 (2008).

52. Bhargava, K. & Feix, J. B. Membrane Binding , Structure , and Localization of Cecropin-Mellitin Hybrid Peptides : A Site-Directed Spin-Labeling Study. *Biophys. J.* **86,** 329–336 (2004).

53. Strandberg, E. & Ulrich, A. S. NMR Methods for Studying Antimicrobial Peptides. *Concepts Magn. Reson.* 89–120 (2004). doi:10.1002/cmr.a.20024

54. Seelig, J. 31P nuclear magnetic resonance and the head group structure of phospholipids in membranes. *Biochim. Biophys. Acta* **515,** 105–140 (1978).

55. Cullis, P. R. & de Kruijff, B. Lipid polymorphism and the funtional roles of lipids in biological membranes. *Biochim. Biophys. Acta* **559,** 399–420 (1979).

56. Yamaguchi, S. *et al.* Orientation and Dynamics of an Antimicrobial Peptide in the Lipid Bilayer by Solid-State NMR Spectroscopy. *Biophys. J.* **81,** 2203–2214 (2001).

57. Wang, G. Structure, dynamics and mapping of membrane-binding residues of micelle-bound antimicrobial peptides by natural abundance 13C NMR spectroscopy. *Biochim. Biophys. Acta - Biomembr.* **1798,** 114–121 (2010).

58. Shenkarev, Z. O. *et al.* Conformation and mode of membrane interaction in cyclotides: Spatial structure of kalata B1 bound to a dodecylphosphocholine micelle. *FEBS J.* **273,** 2658–2672 (2006).

59. Wong, T. C. Micelles and Bicelles as Membrane Mimics for Nuclear Magnetic Resonance Studies of Peptides and Proteins. 3809–3824 (2006). doi:10.1081/E-ESCS-120041048

60. Lauterwein, J., Bosch, C., Brown, L. R. & Wuthrich, K. Physiochemical studies of the protein-lipid interactions in melittin-containing micelles. *Biochim. Biophys. Acta* **556,** 244–264 (1979).

61. Matsumori, N., Morooka, A. & Murata, M. Conformation and location of membrane-bound salinomycin-sodium complex deduced from NMR in isotropic bicelles. *J. Am. Chem. Soc.* **129,** 14989–14995 (2007).

62. Durr, U. H. N., Gildenberg, M. & Ramamoorthy, A. The magic of bicelles lights up membrane protein structure. *Chem. Rev.* **112,** 6054–6074 (2012).

63. Lee, D. K. *et al.* Lipid composition-dependent membrane fragmentation and pore-forming mechanisms of membrane disruption by pexiganan (MSI-78). *Biochemistry* **52,** 3254–3263 (2013).

64. Lindberg, M., Biverståhl, H., Gräslund, A. & Mäler, L. Structure and positioning comparison of two variants of penetratin in two different membrane mimicking systems by NMR. *Eur. J. Biochem.* **270,** 3055–3063 (2003).

65. Torcato, I., Castanho, M. A. R. B. & Henriques, S. The Application of Biophysical Techniques to Study Antimicrobial Peptides. *J. Spectrosc.* **27,** 541–549 (2012).

66. Ambroggio, E. E., Separovic, F., Bowie, J. H., Fidelio, G. D. & Bagatolli, L. A. Direct visualization of membrane leakage induced by the antibiotic peptides: maculatin, citropin, and aurein. *Biophys. J.* **89,** 1874–1881 (2005).

67. Gallucci, E., Meleleo, D., Micelli, S. & Picciarelli, V. Magainin 2 channel formation in planar

lipid membranes: the role of lipid polar groups and ergosterol. *Eur. Biophys. J.* **32,** 22–32 (2003).

68. Capone, R. *et al.* Antimicrobial protegrin-1 forms ion channels: Molecular dynamic simulation, atomic force microscopy, and electrical conductance studies. *Biophys. J.* **98,** 2644–2652 (2010).

69. Tosteson, M. T. *et al.* Primary structure of peptides and ion channels. Role of amino acid side chains in voltage gating of melittin channels. *Biophys. J.* **58,** 1367–1375 (1990).

70. Sharma, S., Sahoo, N. & Bhunia, A. No TitleAntimicrobial PEptides and their Pore/Ion Channel Properties in Neutralization of Pathogenic Microbes. *Curr. Top. Med. Chem.* **16,** 46–53 (2016).

71. González, J. E., Oades, K., Leychkis, Y., Harootunian, A. & Negulescu, P. A. Cell-based assays and instrumentation for screening ion-channel targets. *Drug Discov. Today* **4,** 431–439 (1999).

72. Takano, T., Konoki, K., Matsumori, N. & Murata, M. Amphotericin B-induced ion flux is markedly attenuated in phosphatidylglycerol membrane as evidenced by a newly devised fluorometric method. *Bioorganic Med. Chem.* **17,** 6301–6304 (2009).

73. Nakagawa, Y. *et al.* Effect of sterol side chain on ion channel formation by amphotericin b in lipid bilayers. *Biochemistry* **53,** 3088–3094 (2014).

74. Klymchenko, A. S. & My Kreder, R. Chemistry & Biology Review Fluorescent Probes for Lipid Rafts: From Model Membranes to Living Cells. *Chem. Biol.* **21,** 97–113 (2014).

75. Yau, W., Wimley, W. C., Gawrisch, K. & White, S. H. The Preference of Tryptophan for Membrane Interfaces †. *Biochemistry* **37,** 14713–14718 (1998).

76. Gofman, Y. *et al.* Interaction of an Antimicrobial Peptide with Membranes : Experiments and Simulations with NKCS. *J. Phys. Chem. B* **114,** 4230–4237 (2010).

77. Freyer, M. W. & Lewis, E. A. in *Methods in Cell Biology* **84,** 79–113 (2008).

78. Henriksen, J. R. & Andresen, T. L. Thermodynamic profiling of peptide membrane interactions by isothermal titration calorimetry: A search for pores and micelles. *Biophys. J.* **101,** 100–109 (2011).

79. Situ, A. J., Schmidt, T., Mazumder, P. & Ulmer, T. S. Characterization of membrane protein interactions by isothermal titration calorimetry. *J. Mol. Biol.* **426,** 3670–3680 (2014).

80. Nguyen, K. T., Clair, V. Le, Ye, S. & Chen, Z. Molecular Interactions between Magainin 2 and Model Membranes in Situ. *J. Phys. Chem. B* **113,** 12358–12363 (2009).

81. Hall, K., Lee, T., Mechler, A. I., Swann, M. J. & Aguilar, M. Real-time Measurement of Membrane Conformational States Induced by Antimicrobial Peptides : Balance Between Recovery and Lysis. *Sci. Rep.* **4,** 1–9 (2014).

Chapter 2

Marine Sponge-derived Peptide Theonellamide A and its Affinity to 3β-hydroxysterols

2.1 Introduction – Marine Sponge-Derived Antifungal Compound Theonellamide A

As described in the previous chapter, Theonellamide-A (TNM-A, Figure 2-1), is a member of a group of marine sponge-derived bicyclic dodecapeptides (known as TNMs) first isolated from the *Lithistid* sponge *Theonella sp*. obtained in Hachijo-jima island, Japan.[1,2] This group of compounds possess several unusual amino acid residues and its structure is bridged by a very rare τ-histidinoalanine (τ-HAL) cross-linking residue.[1–3] Some members of the TNM group also contain a monosaccharide unit (β-D-Gal or β-L-Ara) covalently attached to the τ-HAL residue but structure activity relationship (SAR) experiments suggest comparable antifungal activities regardless of the presence or absence of the sugar moiety. Theonellamides possess antifungal activity against prototypical fungi (*Candida, Trichophyton,* and *Aspergillus*) at micromolar concentrations (2-7 μM) and have moderate cytotoxicity against P388 mouse leukemia cells (IC_{50} 0.5-2.8 μM).[1–4] However, its cytotoxicity against mammalian cells hinders its development as a potential antifungal pharmaceutical. Previous studies have indicated that TNMs bind to 3β-hydroxysterols in the membrane but its inability to distinguish between mammalian cell membrane sterol cholesterol from fungal cell membrane sterol ergosterol is speculated to be causing its cytotoxicity.[5,6]

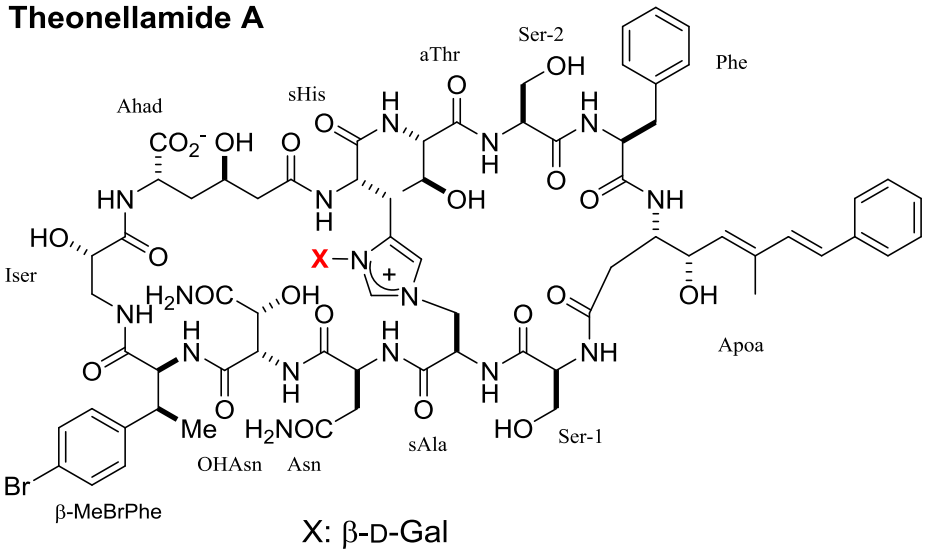

Figure 2-1 Structure of Theonellamide A

2.2 Previous Studies Conducted for Theonellamide-A

2.2.1 Surface Plasmon Resonance Studies

Previous results from our group revealed enhanced binding of TNM-A to 3β-hydroxysterol-containing liposomes, through surface plasmon resonance (SPR) experiments. The SPR sensograms (Figure 2-2) indicated that TNM-A had stronger affinity to 3β-hydroxysterol (ergosterol or cholesterol)-containing palmitoyloleoylphosphatidylcholine (POPC) liposomes as compared to 3α-hydroxysterol-containing or sterol-free liposomes.[7] In addition, kinetic evaluation of the SPR sensograms revealed that TNM-A-membrane binding occurs via a 2-step process with the first step being accelerated by the presence of 3β-hydroxysterols. The enhanced binding of TNM-A to 3β-hydroxysterol containing POPC liposomes could either be a consequence of sterol-induced changes in the physiochemical properties of the membrane promoting membrane binding of TNM-A or direct interaction of TNM-A with 3β-hydroxysterols. In order to confirm the reason for the peptide's enhanced binding, solid state ^{2}H NMR measurements were carried out using deuterated cholesterol, ergosterol, or epi-cholesterol containing POPC MLVs with a 1:18 sterol to lipid mole ratio.

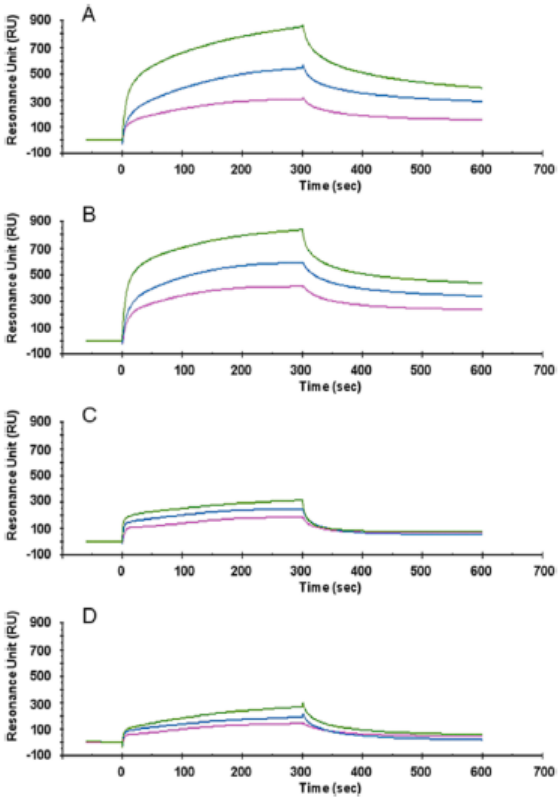

Figure 2-2 SPR Sensograms for binding of TNM-A to liposomes captured on a dodecylamine-modified CM5 sensor chip. (A) 10 mol % cholesterol-containing POPC liposomes, (B) 10 mol % ergosterol-containing POPC liposomes, (C) 10 mol % epicholesterol-containing POPC liposomes, and (D) pure POPC liposomes. Sensograms correspond to 20 (green), 15 (blue), and 10 μM TNM-A (violet).[7] Reprinted with permission from Figure 3 of *Biochemistry*, **2013**, *52*, 2410-2418.[7] Copyright © (2013) American Chemical Society.

2.2.2 Solid State Nuclear Magnetic Resonance Studies

Results of the ^{2}H NMR experiments suggested that the enhanced affinity of TNM-A to 3β-hydroxysterol containing liposomes is due to their direct interaction. This was evidenced by the stark attenuation of the deuterium quadrupolar splitting signal when TNM-A was incorporated to POPC liposomes containing d_1-cholesterol and d_1-ergosterol while that of d_1-epi-cholesterol containing liposomes remained unchanged (Figure 2-3).[7] Attenuation of the deuterium signal indicates that the fast rotational motion of the 3β-hydroxysterols cholesterol and ergosterol were inhibited in the presence of TNM-A. This results corroborate with SPR findings that show no enhancement of affinity for TNM-A to POPC liposomes containing 3α-hydroxysterols.[7]

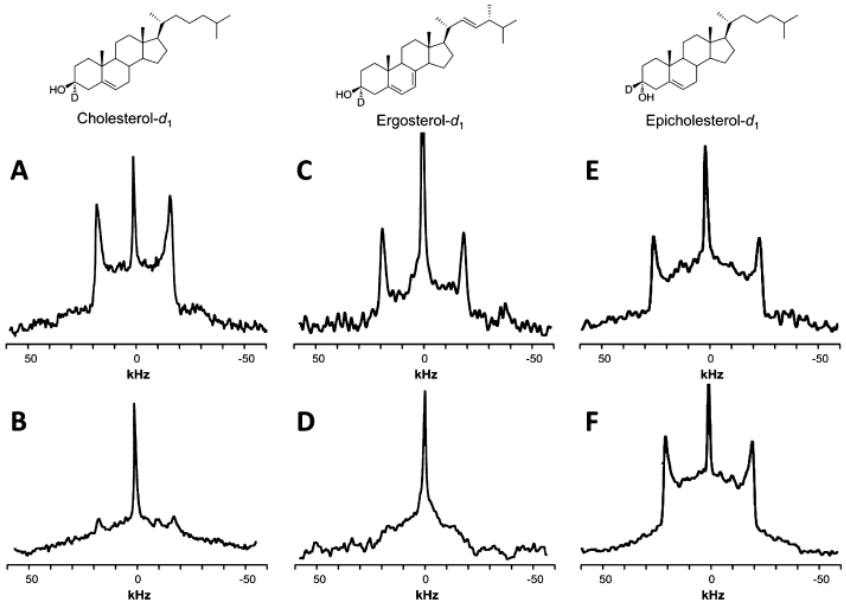

Figure 2-3 ^{2}H NMR spectra of 3-d_1-sterol incorporated into POPC bilayers in the absence (A, C, and E) and presence (B, D, and F) of TNM-A. Reprinted with permission from *Biochemistry*, **2013**, *52*, 2410-2418.[46] Copyright © (2013) American Chemical Society.

Interaction of TNM-A with sterol-containing liposomes were also examined by solid state ^{31}P NMR. MLVs composed of POPC and TNM-A (18:1 mole ratio) or POPC/cholesterol/TNM-A (18:1:1 mole ratio) were prepared with a final concentration of 50% (w/v) in H_2O. For pure POPC and POPC/sterol MLVs, a powder pattern spectra characteristic of a lamellar bilayer was observed for both samples (Figure 2-4, A & B).[8] When TNM-A was incorporated to the MLVs, isotropic peaks appeared for both sterol-free and sterol-containing liposomes (Figure 2-4, C & D).[8] Isotropic peaks usually arise due to the presence of small and fast-tumbling particles such as micelles or small unilamellar vesicles or it can signify molecular motion of ^{31}P species that result to regions of high membrane curvature.[9,10] However,

regardless of the reason, results clearly indicate that incorporation of TNM-A to both POPC or POPC/cholesterol MLVs causes disruption of the tight phospholipid packing which could lead to membrane perturbation or deformation. Changes in the chemical shift anisotropy (CSA), a parameter that is directly related to fluidity as well as structural and dynamic response of the polar head groups containing the phosphorus nuclei[11],were also examined for MLVs incorporated with TNM-A. Results indicate that no significant changes to CSA could be observed when TNM-A was incorporated to both sterol-free and sterol-containing MLV evidenced by the comparable spectral widths of all the four samples (Figure 2-4, A-D). This suggests that although the interaction of the peptide to the liposomes caused disruption of bilayer integrity, no changes in membrane fluidity were detected.

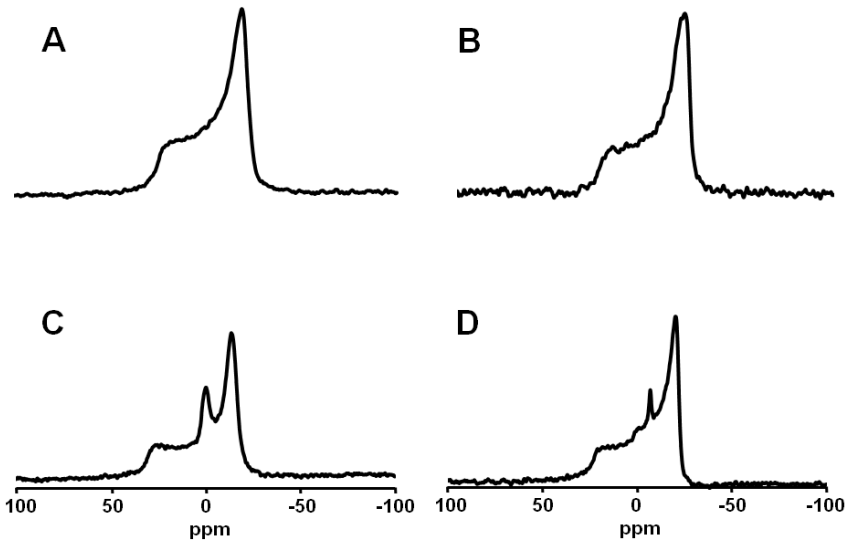

Figure 2-4 Solid state ^{31}P NMR spectra of pure POPC (A and C) and POPC:cholesterol (B and D) liposomes in the absence (A and B) and presence (C and D) of TNM-A at 30^{o}C.[8] Reprinted with permission from Figure 2 of *Biochim. Biophys. Acta - Biomembr.* **2016**, *1858***,** 1373.[8]

2.2.3 Microscopy Studies

Morphological changes in POPC or POPC/cholesterol liposomes induced by TNM-A were also examined by our group using microscopy techniques. Results obtained from differential interference microscopy indicated that addition of TNM-A to pure POPC or POPC/sterol GUVs resulted to membrane morphological changes such as elongation of vesicles and wrinkling of the membrane surface (Figure 2-5).[12] Morphological changes induced by TNM-A were concentration dependent, from as low as 1 μM TNM-A for POPC/chol GUVs. Although these changes were more evident and occur more frequently in sterol-containing liposomes, these results still suggest that TNM-A is capable of membrane deformation in both pure POPC and POPC/cholesterol GUVs.

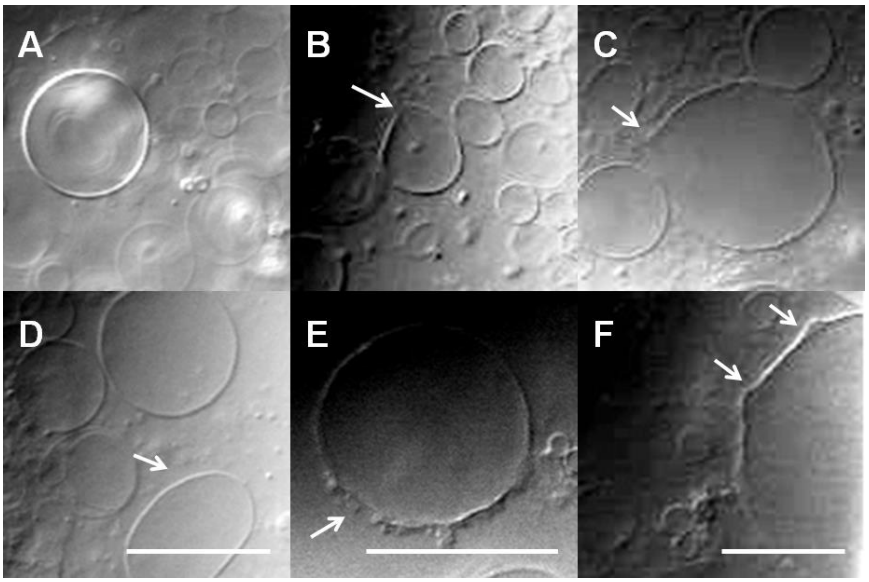

Figure 2-5 Differential interference micrographs of membrane deformations induced by TNM-A. Top (A-C) and bottom (D-E) correspond to cholesterol-free and cholesterol containing (5 mol%) POPC GUVs, respectively. Final concentrations of TNM-A were 1 μM (A, D), 10 μM (B, E), and 20 μM (C, F).[12]

2.3 Significance and Objectives of this Study

Theonellamides' sterol-dependent membrane activity makes it a promising novel antifungal pharmaceutic because a key to its action is a physiologically important membrane component that target organisms will have a difficult time to modify.[51] However, its development as a pharmaceutic has been hindered by its inability to specifically target fungal cells. TNMs also exhibit cytotoxicity to mammalian cells which is speculated to be influenced by its inability to distinguish fungal cell membrane sterol ergosterol from mammalian cell membrane sterol cholesterol. In order to harness TNMs potential as an antifungal agent, an advantageous tradeoff between its antifungal activity and cytotoxicity must be reached. Therefore, it is of utmost importance to gain a complete understanding of TNMs mechanism of action - how it acts on the membrane, how it recognizes 3β-hydroxysterols, and how it elicits its biological activity. However, despite the numerous studies carried out for TNMs as described in the previous sections, its mechanism of action still remains unclear.

Although characterizing TNMs interactions with biological and artificial membranes appear to be more important, experiments that probe TNM-A's behavior in the presence of 3β-hydroxysterols in must also be carried in order to find a way to circumvent the peptide's cytotoxicity. Since the direct interaction of TNM-A with Cho (and ergosterol) in POPC membranes was already confirmed using ^{2}H solid state NMR (ssNMR)[7]; we decided to perform peptide-sterol interaction studies more in detail using NMR-based techniques. Such methods have been proven to be suitable for examining interactions between natural products and sterols as seen for the amphotericin B-ergosterol interactions[13,14] in membranes and for the sterol recognition of amphidinol 3.[15,16] Unfortunately, solid state NMR techniques are not suitable for TNM-A studies because synthetic supply of ^{13}C and ^{19}F isotope-labelled peptide is unavailable due to the lack of suitable functionality used for introduction of the isotope tags together with the complexity of

the peptide structure. On the other hand, employing solution-state NMR measurements also prove to be challenging because high-resolution ^{1}H spectra are often difficult to obtain due to the insolubility of Chol in aqueous solvent systems containing more than 50% organic solvent. The use of membrane models such as micelles or bicelles were also unhelpful because the former cannot be incorporated with Chol while the latter can only contain 10% Chol and does not give rise to ^{1}H NMR signals as reported previously.[15,17,18] So in order to obtain ^{1}H NMR spectra of the sterol and TNM-A, both were dissolved in solution that somewhat mimics bilayer conditions.

The main objective of this study is to evaluate the 3β-hydroxysterol affinity of TNM-A to examine the molecular basis of interaction between the peptide and the 3β-hydroxy group of the sterol. Through this, we aimed to explore the applicability of solution ^{1}H NMR to examine the interaction between membrane-active small molecules and sterols in aqueous organic solvents. However, it should be noted that a more polar cholesterol derivative 25-hydroxycholesterol (hereon abbreviated as 25-HC, Figure 2-6) was used in most of the experiments due to the poor solubility of Chol in the NMR solvent used for TNM-A (4:1 DMSO-d_6 /H_2O). This sterol derivative contains the same sterol ring structure as Chol, only with an additional –OH moiety in its tail end giving it improved solubility in the NMR solvent of TNM-A. Prior to carrying out solution-state NMR measurements, the suitability of 25-HC as a Chol derivative was first evaluated. Through ^{2}H ssNMR, the direct interaction of TNM-A with 25-HC in POPC membranes was verified. In addition, the membrane disrupting activity of TNM-A in phospholipid membranes containing 25-HC as the sterol instead of cholesterol was also examined through ^{31}P ssNMR. ^{1}H NMR titration measurements were then carried out to evaluate TNM-A/3β-hydroxysterol affinity. The spectra obtained were also examined for chemical shift changes to deduce the possible sterol interaction site of TNM-A.

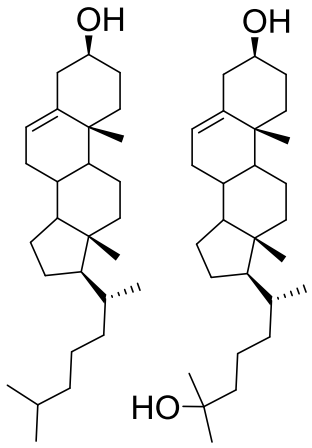

A. Cho **B. 25-HC**

Figure 2-6. Structure of (A) cholesterol and (B) 25-hydroxycholesterol

2.4 Results and Discussion

2.4.1 Evaluation of TNM-A/25-HC Interaction by ^{2}H Solid State NMR and TNM-A induced membrane perturbation by ^{31}P Solid State NMR

As described previously, a more polar Chol derivative was used in this study because native Chol has poor solubility in the NMR solvent of TNM-A (4:1 DMSO-d_6/H_2O). However, the use of 25-HC as a Chol derivative for TNM-A/3β-hydroxysterol studies warrants a confirmation of whether the peptide exhibits direct interaction with 25-HC as was observed for the native membrane sterol Chol. In a previous study, the direct interaction of TNM-A with 3-*d*-sterols (Figure 2-6)[7] was confirmed through solid state ^{2}H NMR as the pake doublet signals attributed to deuterated 3β-hydroxysterols incorporated in POPC liposomes were attenuated in the presence of the peptide. In this study, the same technique was carried out to observe direct interaction of TNM-A with the cholesterol derivative 25-HC.

The strategy for synthesizing 3*d*-25-HC is presented in Scheme 2-1. In the first step, pyridinuim chlorochromate (PCC) oxidation was performed with 25-hydroxycholesterol **1** as a substrate. The oxidation mechanism involves the attack of the oxygen from the secondary alcohol moiety of 25-HC to the chromium (VI) atom to form a Cr-O bond. After the proton from the positively charged secondary alcohol oxygen is transferred to one of the chromium oxygens, chromate ester is formed upon the displacement of the chlorine atom. Chlorine then acts as a base to abstract the proton attached to the secondary alcohol Cα (C-3 position), with the electrons from C-H bond forming the C-O bond leading to the oxidation of 25-HC **1** to a ketone 25-hydroxycholestenone **2**. The by-products of this reaction is the reduced chromium [Cr(IV)] in the form of $O{=}Cr(OH)_2$ and pyridinum chloride. Product **2** was purified from the crude product of the oxidation reaction by column chromatography using fluorosil as the stationary phase and eluting it with 10:1 Hexane/ethyl acetate. The second step of the reaction involves sodium borodeuteride ($NaBD_4$) reduction of purified **2** to introduce a deuterium atom to the C-3 position of **2** to obtain 3*d*-25-HC **3** (Scheme 2-1). 3*d*-cholesterol was synthesized in the same manner using cholesterol as the initial substrate.

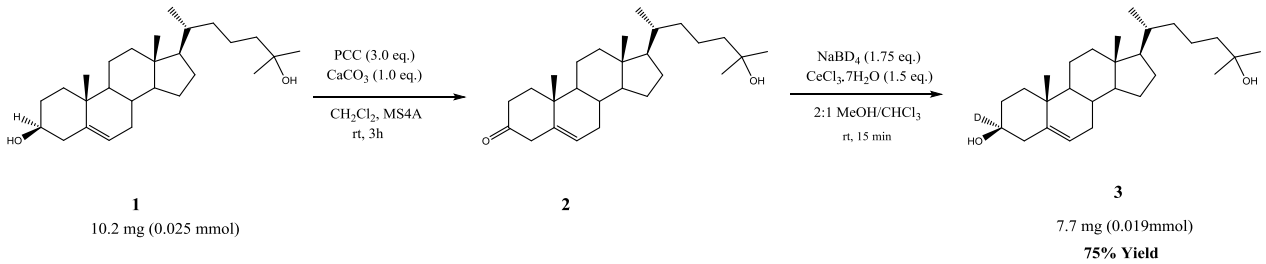

1
10.2 mg (0.025 mmol)

2

3
7.7 mg (0.019mmol)
75% Yield

Scheme 2-1. Synthesis of 3*d*-25-hydroxycholesterol

Sterol molecules in lipid membrane bilayers exhibit fast lateral diffusion in the absence of any external stimuli. Convincing evidence for TNM-A-sterol interactions can be obtained by detecting changes in sterol dynamics as a consequence of the presence of TNM-A, similar to what has been carried out to demonstrate AmB-ergosterol interactions.[19] By using deuterated-sterols, ^{2}H SSNMR measurements can characterize sterol motion in motionally restricted systems based on the "powder pattern" exhibited

by deuterium. Sterols incorporated in phospholipid bilayers undergo fast lateral diffusion which is observed in NMR as an axial rotation. This gives rise to a quadrupolar splitting ($\Delta\nu$) of the NMR absorption line which depends on the tilt angle of the C-^{2}H bond with respect to the axis of molecular averaging and the wobbling of the sterol.[20–23]

Results from Figure 2-7 shows the spectra of 3*d*-25-HC incorporated to POPC liposomes in an 18:1 mol ratio in the presence or absence of TNM-A. In the absence of TNM-A, results indicated that 3*d*-25-HC in POPC bilayers undergoes fast rotational motion evidenced by the appearance of a characteristic Pake doublet signal (quadrupolar splitting signal, $\Delta\nu$ = 31.1 kHz), in. However, when TNM-A was incorporated to the POPC: 3*d*-25-HC liposomes, stark attenuation of the quadrupolar splitting signal was observed (Figure 2-7B), indicating that the molecular rotation of the sterol decreased to intermediate motional speed[19], similar to what was observed when TNM-A was incorporated to POPC:3-*d*-cholesterol liposomes. These data not only confirm the direct interaction of TNM-A with the sterol derivative 25-HC, but also provide another evidence for TNM-broader specificity for 3β-hydroxysterols. Such results qualifies the use of the more polar cholesterol derivative 25-HC to carry out more detailed examination of TNM-A/3β-hydroxysterol interactions.

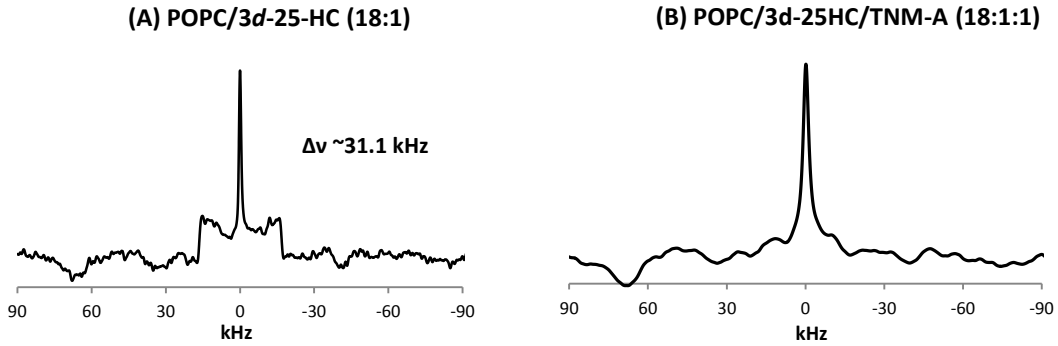

Figure 2-7. ^{2}H solid state NMR spectra of 3*d*-25HC incorporated to POPC liposomes in the absence (A) or presence (B) of TNM-A. Samples were prepared in ^{2}H-depleted H_2O solvent at 50% (w/v). The POPC: 3*d*-25HC:TNM-A mole ratio of (A) was 18:1:0 while (B) was 18:1:1.

Results obtained from previous ^{31}P solid-state NMR studies revealed that TNM-A can disrupt bilayer integrity of both Chol-free and Chol-containing phospholipid membranes.[8] In order to examine if TNM-A can also induce the same membrane disrupting effect in phospholipid bilayers containing 25-HC as compared with native Chol, similar ^{31}P SSNMR measurements were carried. The spectrum obtained for POPC/25-HC membranes (Figure 2-4B) exhibited line shapes that were characteristic of lamellar bilayer structures (Figure 2-8A). In addition, the membrane fluidity was not significantly changed when 25-HC was incorporated to phospholipid membranes as line width values of ~ 40.0 ppm, which is very similar to POPC/Chol membranes, was observed. More importantly, when TNM-A was incorporated to POPC/25-HC membranes (Figure 2-8B), a similar isotropic peak could also be observed indicating that TNM-A was also able to perturb 25-HC-containing membranes. The smaller

isotropic peak observed in the 25-HC containing membrane could indicate a weaker extent of membrane perturbation by the peptide but altogether, these data suggests that TNM-A exhibits a similar type of membrane disruption to both 25-HC and Chol-containing POPC bilayers.

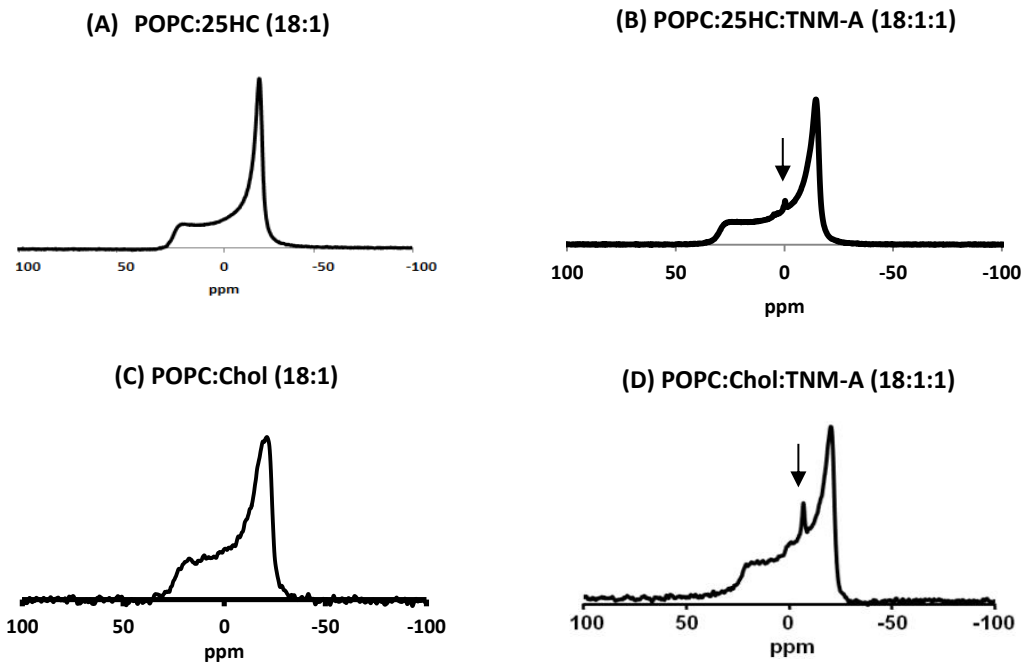

Figure 2-8. ^{31}P solid state NMR spectra of 25-HC (A & B) or Cholesterol (C & D)[8] incorporated to POPC liposomes in the absence (A or C) or presence (B or D) of TNM-A. Samples were prepared in ^{2}H-depleted H_2O solvent at 50% (w/v). The POPC:sterol:TNM-A mole ratio of (A) and (C) was 18:1:0 while (B) and (D) was 18:1:1. (C) and (D) are reprinted with permission from Figure 2 of *Biochim. Biophys. Acta - Biomembr.* **2016**, *1858***,** 1373.[8]

2.4.2 Affinity of TNM-A/25-HC Interactions

Despite having unequivocal evidence of TNM-A/25-HC interaction in POPC bilayers through ^{2}H SSNMR experiments, convincing data of the peptide/sterol interaction could not be obtained in solution state NMR measurements. In this study, quantitative evaluation of the affinity of TNM-A to 25-HC was carried out provide a useful platform for a more detailed examination of the molecular basis of interaction between TNM-A and the 3β-hydroxy group of sterol. Since it is essential for both 25-HC and TNM-A to be completely dissolved in solution during the entire procedure, measurements were carried out in an aqueous DMSO solution. The use of this solvent system can be justified by results from previous studies which indicated that TNM-A forms small aggregates in aqueous media but remains as monomers in aqueous DMSO solution. It also allows us to obtain high-resolution ^{1}H NMR spectra which is essential for monitoring chemical shift changes that could be incurred by TNM-A upon the addition of 25-HC.

Additionally, this type of solvent system could mimic the membrane surface environment to a certain extent due to the co-existence of hydrophobic methyl groups in DMSO and water molecules.

^{1}H NMR titration measurements were carried out by adding sterols to TNM-A while monitoring TNM-A proton chemical shift changes (Δδ, ppm). The strength of peptide-3βhydroxysterol interactions were evaluated using the obtained TNM-A/25-HC dissociation constants (K_d) values after the titration data was analyzed. A mathematical model for the 1:1 binding phenomena, described in detail in literature[24], was utilized to define the expected chemical shift changes during the titration experiment from two known ($[P]_t$ and $[L]_t$) and two unknown (K_d and $\delta_{\Delta PL}$) parameters. TNM-A proton chemical shift change (Δδ) as a consequence of sterol addition was plotted against [L]/[P] ratio to generate the titration curve. Non-linear curve fitting using the Excel® add-on program Solver was carried out using Equation 2-1 to find the best fit calculated binding curve to the experimental data points. Several titration curves were generated based on various peptide protons (Figure 2-9) but the K_d values for TNM-A/25-HC interactions were based only on the titration curves which had the best fitting to calculated binding curves (Phe βH and Ahad δH_l).

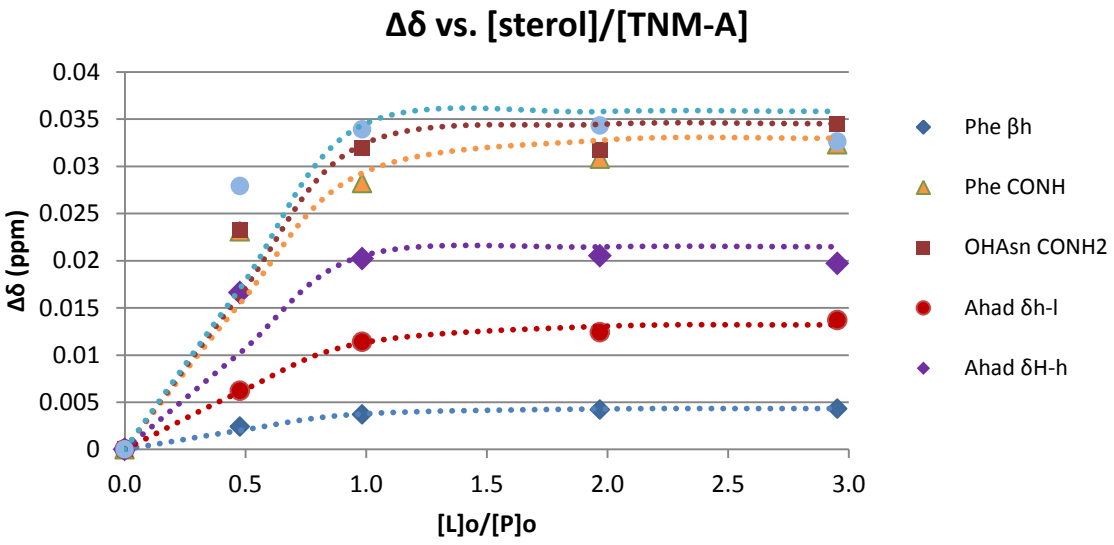

Figure 2-9 Generated Titration Curves for TNM-A/25-HC Interactions. All samples were in DMSO-d_6/H_2O (4:1) solvent and ^{1}H NMR measurements were all at 30°C.

Dissociation constants for TNM-A/25-HC interactions obtained from the titration curves with the best curve fitting (Figure 2-10) were in the 38 –49 μM range (Table 2-1) indicating a moderate affinity of the peptide to 25-HC. Based on SPR measurements, K_d values obtained for the interaction of TNM-A with 3β-hydroxysterols (cholesterol or ergosterol) incorporated in POPC MLVs were about 9 μM also indicating moderate affinity.[7] Although both methods gave K_d values in the low micro molar range, the slight disparity of the dissociation constants obtained may be a reflection of the differing experimental conditions employed in SPR and NMR titration methods. Since SPR measurements were carried out in aqueous conditions, there is a possibility that the sterol binding pocket of TNM-A is filled with water molecules which could promote entropy-driven interactions of with hydrophobic sterol molecules. In

contrast, NMR titration measurements were carried out in a less polar solvent (80% DMSO-d_6) which could have smaller entropic contributions to the binding free energy resulting to weaker affinities (larger K_d values) of TNM-A to the sterol. Nonetheless, on the basis of similar TNM-A affinities to both cholesterol and 25-HC, the use of the cholesterol derivative 25-HC for evaluating peptide/sterol interactions also is justifiable.

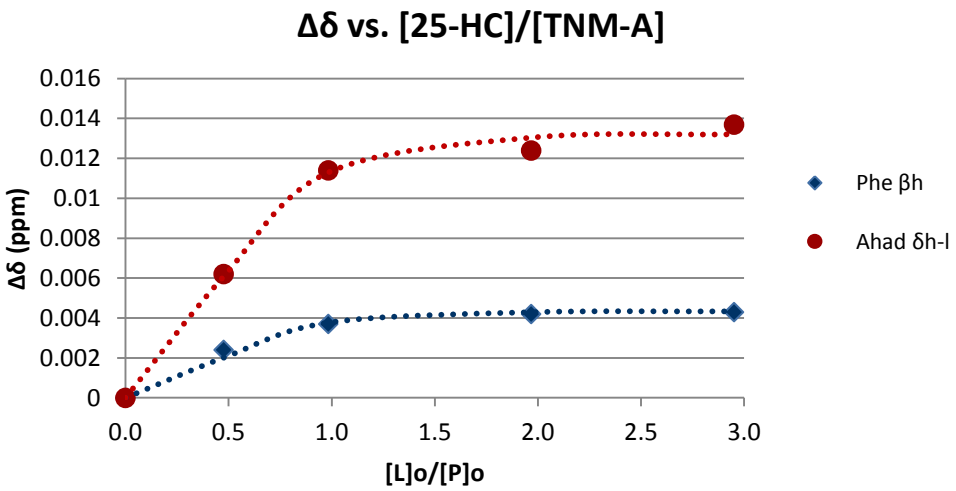

Figure 2-10. Titration Curve for TNM-A/25-HC interaction based on the chemical shift changes (Δδ) of Phe βH and Ahad δH_l of TNM-A.

$$\Delta\delta = \delta_{\Delta PL}\left[\frac{\left(K_D+[P]_t+[L]_t-\{(K_D+[P]_t+[L]_t)^2-(4*[P]_t*[L]_t)\}^{1/2}\right)}{2[P]_t}\right] \qquad \text{Equation 2-1}^{24}$$

Table 2-1. Calculated K_d values for TNM-A/25-HC interaction using the TNM-A protons indicated in Figure 2-14.

TNM-A/25-HC Titration	
TNM-A Proton #	K_d (μM)
Phe βH	37.5 μM
Ahad δH_l	48.6 μM
Average K_d	**43.1 μM**

2.4.3 Interaction of TNM-A with 25-HC assed by ^{1}H NMR titration and NOESY NMR

Despite having convincing proof of TNM-A/3β-hydroxysterol interactions in aqueous solutions, its possible sterol-interaction site still remains unclear. However, results from the titration NMR measurements can provide leads about the specific site of TNM-A which is responsible for its specific interaction with 3β-hydroxysterols. Analogous to chemical-shift mapping methods often carried out to identify ligand binding faces of proteins[25], TNM-A/25-HC interaction may also be monitored by identifying sterol-induced chemical shift changes in the peptide.

Results from ^{1}H NMR titration measurements indicated that the addition of 25-HC to TNM-A induced ^{1}H chemical shifts of several TNM-A protons to change (Figure 2-11A). However, most of the perturbed protons only incurred minimal chemical shift changes (Δδ) with the largest observed chemical shift change of about 0.035 ppm for TNM-A/25-HC (1:1 mole ratio). With the majority of perturbed protons only occurring very minor changes Δδ, it be suggesting that the electronic environment of the peptide's protons remained relatively unchanged during the peptide/sterol interaction. In addition, results obtained from NOESY NMR measurements with TNM-A/25-HC (1:1 mole ratio) suggested that no major conformational changes occurred in the peptide upon sterol addition as intramolecular NOEs of TNM-A incurred very minimal changes (Figure 2-11B). Interestingly, most of the TNM-A protons incurring the greatest Δδ after addition of 25-HC were part of the TNM-A's sequence involving several residues such as Iser, β-MeBrPhe, OHAsn, Asn, Apoa and sAla (Figure 2-12) instead of affecting a specific lone residue. These observations prompted speculations about the aforementioned region being involved in TNM-A-sterol interactions. If intermolecular NOEs between 25-HC and TNM-A protons belonging to this area of its structure can be detected, an important lead in the identification of the specific sterol interaction site of TNM-A could be obtained. However, no intermolecular NOEs between 25-HC and TNM-A protons in the speculated site of interaction, or in the entire peptide structure, was detected even at longer mixing times.

A possible underlying reason for the absence of TNM-A/25-HC intermolecular NOEs is that their interactions may be occurring in fast association and dissociation beyond the timescale of NOESY NMR detection limits. In NOESY measurements, motions other than isotropic molecular tumbling (e.g. association and dissociation) can greatly influence the detected NOE enhancements due to the fact that such motions affect correlation time τ_c and internuclear distance.[25] If TNM-A/25-HC interactions are undergoing fast exchange, detection of intermolecular NOEs would be difficult since the lifetime of the peptide-sterol complex is too short to allow magnetization transfers needed for NOEs to develop. If the peptide/sterol interaction affinity is strong, intermolecular NOEs between TNM-A and 25-HC could be detected, providing leads for TNM-A's site of sterol interaction comparable to what has been done to characterize the interaction and identify intermolecular protein-ligand NOEs between a small molecule ligand and the anti-apoptotic protein Bcl-xL.[26]

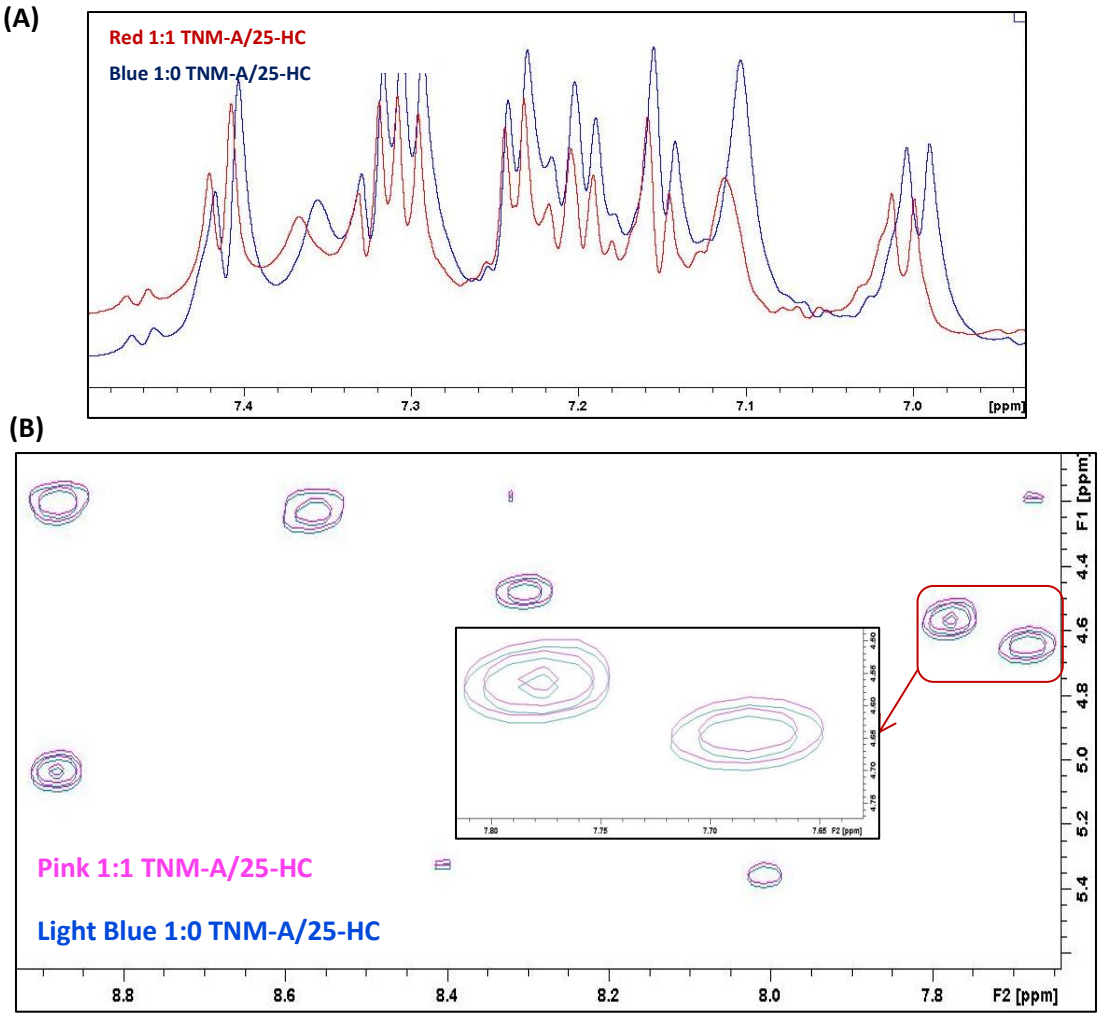

Figure 2-11. (A) Portion of the ^{1}H NMR spectral overlay of TNM-A (Blue) and TNM-A/25-HC (1:1) (Red) showing the chemical shift changes incurred by in TNM-a protons in the presence of 25-HC. (B) portion of the NOESY NMR spectral overlay of TNM-A (light blue) and TNM-A/25-HC (1:1) (pink). Inset of the bottom spectra shows the slight NOE peak shifts observed for TNM-A protons after 25-HC was added to the NMR sample. ^{1}H and NOESY NMR measurements were carried out at 30 ^{o}C with the peptide or peptide/sterol sample in DMSO-d_6/H_2O (4:1) solvent.

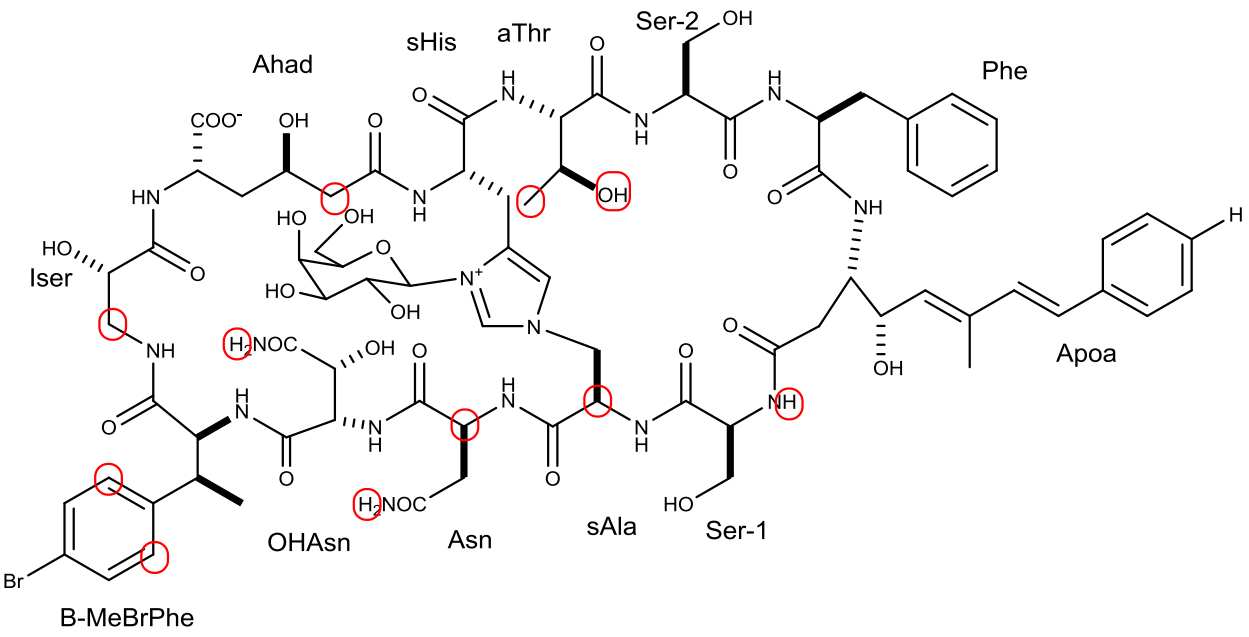

Figure 2-12. TNM-A structure with the protons incurring the greatest chemical shift changes after interaction with 25-HC encircled in red.

Table 2-2. TNM-A protons incurring the largest $\Delta\delta_{max}$ after titration with 25-HC.

TNM-A/25-HC Titration		
Residue[a]	Position	$\Delta\delta_{max}$ (rank[b])
Thr	γ	0.0343(2nd)
	OH	0.0209(7th)
Ser-2	CONH	0.0177(10th)
Ala	α	0.0327 (3rd)
Asn	α	0.0243 (5th)
	$CONH_2$	0.0317 (4th)
OHAsn	$CONH_2$	00197 (9th)
β-MeBrPhe	H-2,6	0.0351 (1st)
Iser	β	0.0224 (6th)
Ahad	δ	0.0205 (8th)

[a] Residues containing protons with significant $\Delta\delta_{max}$ values.
[b] Significant $\Delta\delta_{max}$ values ranked from highest to lowest.

2.3.5. Specific binding of TNM-A with 3β-hydroxysterols

Interaction with cholesterol-containing membranes is fundamental to the mechanism of action of numerous membrane-active peptide/proteins and toxins. However, determination of the structural basis for their recognition and binding to cholesterol-rich membranes is challenging and remains uncertain to most bioactive compounds. . In the case of cholesterol-dependent cytolysins (CDCs), its cholesterol binding motif was originally thought to comprise of an undecapeptide region which is highly conserved in CDCs[27] but recent studies have disproved this and indicated that its cholesterol-binding motif involves just a threonine-leucine pair in loop 1 at the base of domain 4.[28]

For TNM-A, the same information is being pursued because such data can aid in resolving the non-specific interactions of the peptide to both fungal and mammalian cell membranes, the latter of which is speculated to be the reason for its cytotoxicity. Ever since it was discovered that TNM-A preferentially binds to 3β-hydroxysterols more than to any other components of the plasma membrane[5], compelling evidence of its interaction with cholesterol (or ergosterol) in membrane bilayers or live-cell samples have surfaced.[67] As a matter of fact, fluorescent TNM derivatives have been recognized as valuable probes for the visualization of sterol-rich membrane domains both in live-cell samples and in liposomes.[6] Though examining the interaction of TNM-A with sterol-containing membranes is a very important step to carry out to determine the peptide's mechanism of action, it is also essential to understand the molecular basis of TNM-A's sterol interaction. In numerous instances, NMR techniques such as REDOR have been successful in characterizing interactions of natural products and sterols,[13,14,15,16] however such methods are not suitable for TNM-A mainly because of the lack of a stable source of isotope-labeled derivatives. Aside from the complex structure TNMs possess, they lack suitable functional groups to where isotope labels can be introduced.

Solution NMR measurements with TNM-A and cholesterol was problematic because of the insolubility of the sterol in the solvent used for high resolution NMR studies of the peptide (4:1 DMSO-d_6 /H_2O). But since both TNM-A and the 3β-hydroxysterol need to be completely dissolved in order to obtain high resolution NMR data, the use of a more polar Chol derivative became inevitable. Therefore, in this study, 25-HC was used to examine the interaction of TNM-A with 3β-hydroxysterols through ^{1}H NMR titration measurements, specifically to determine the peptide's affinity for sterols and locate the possible sterol interaction site. Through preliminary measurements, the use of 25-HC as a Chol derivative could be justified because results from ^{2}H SSNMR revealed that TNM-A also exhibits direct interaction with 25-HC when present in phospholipid membranes, similar to the peptide's interaction with Chol. Together with previous SPR data, these results not only emphasize the wide specificity of TNM-A's interaction with 3β-hydroxysterols but also reveal that the tail end moiety of the sterols do not dictate the peptide-sterol interactions.

Indications of the wide selectivity of TNM-A for 3β-hydroxysterols can also be observed from the results of ^{1}H NMR titration measurements. K_d values obtained from the curve fitting of the generated titration isotherms of TNM-A/25-HC in aqueous DMSO solvent were in between the 40-50 μM range. For comparison, the affinity of TNM-A to another cholesterol derivative, 17α-hydroxypregnenolone (Figure 2-13), was also examined by ^{1}H NMR titration and K_d values obtained were in the similar order to that with 25-HC at ~60-75 μM (Table 2-2). Here it should be noticed that the curve fitting is relatively

poor for 17α-HP, in particular at the [Lo]/[Po] ratio of 0.5. Interestingly, the half equivalence of 17α-HP gave 70% saturation of Δδmax, which appears inconsistent with the 1:1 complex formation and for this reason, this sterol was deemed inappropriate to be used as a cholesterol derivative for TNM-A/3β-hydroxysterol interaction studies. A possible explanation for this disparity is that 17α-HP may also interact with TNM-A through its tail end, which also has a hydroxyl moiety though in an α configuration, given its short and small structure. In the case of 25-HC, the possibility that TNM-A could also interact with the terminal hydroxyl moiety in its tail portion also cannot be discounted and may have influenced the lower affinity values obtained. Nevertheless, these findings emphasize the bigger role of the 3β-hydroxyl moiety of the sterol than the sterol tail group portion in its interaction with TNM-A.

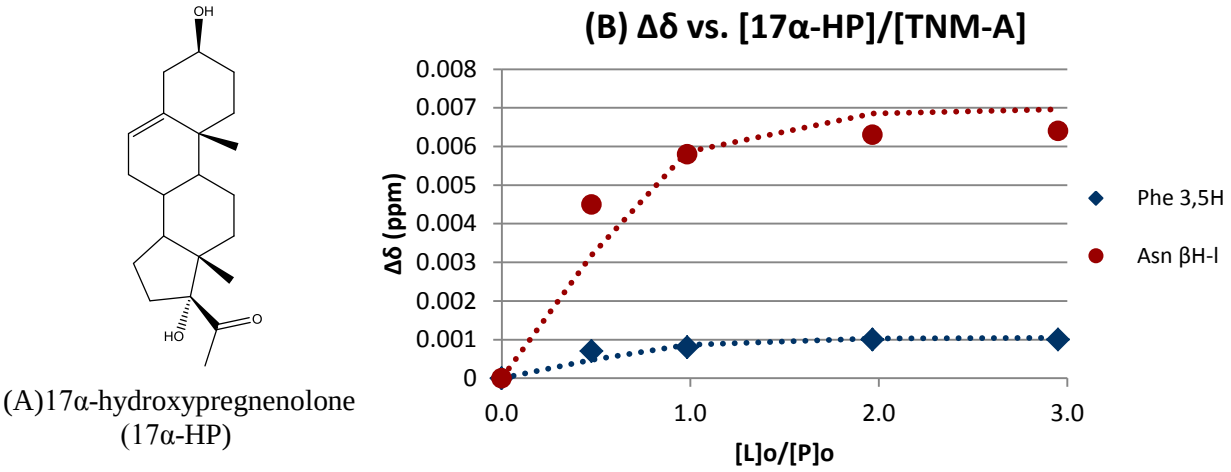

Figure 2-13. (A) Structure of another Chol derivative 17α-hydroxypregnenolone (17α-HP) used for the evaluation of TNM-A/3β-hydroxysterol affinity. (B) Titration Curve for TNM-A/17α-HP interaction based on the chemical shift changes (Δδ) of Phe 3,5H and Asn βH_l of TNM-A.

Table 2-3. Calculated K_d values for TNM-A/17α-HP interaction using the TNM-A protons indicated in Figure 2-10B.

TNM-A/17α-HP Titration	
TNM-A Proton #	K_d (μM)
Phe 3,5H	74.5 μM
Asn βH_l	60.9 μM
Average K_d	**67.7μM**

Based on SPR measurements, K_d values obtained for the interaction of TNM-A with POPC MLVs containing cholesterol was about 9 μM.[7] Although slightly higher K_d values (weaker affinity) were obtained through NMR titration measurements, all affinity constants were roughly in the same order being in the low micro molar range. As described in the previous sections, this slight disparity may be a reflection of the differing experimental conditions employed in SPR and NMR titrations (SPR in aqueous medium while NMR in more hydrophobic medium) that could have entropic influences to the free

binding energy of TNM-A/sterol interactions. Based on a preliminary TNM-A conformation study, one of possible 3D structures of TNM-A obtained show a bivalve-like structure with a cavity that is lined by the more hydrophobic side chains of Phe, Apoa, and β-MeBrPhe residues in one side and the more hydrophilic residues on the other side (Figure 2-14); In this conformational search carried out by Macromodel, differenct conformers in the main chain folding were observed depending on calculation conditions and initial structures. Thus, the 3D structure presented in Figure 2-14 could be one of possible conformers occurring in the NMR conditions but not likely to be the major conformer in an aqueous environment. In purely aqueous media such as that employed in SPR measurements, this cavity, which is speculated to be the sterol-binding site of TNM-A, can be filled with structured water molecules, and could promote entropy-driven interactions between the hydrophobic sterol molecules and the hydrophobic residue side chains of TNM-A. In NMR titration measurements, on the other hand, less polar solvent (80% DMSO-d_6) could have smaller entropic contributions to binding free energy. This is because the gain in stability of the peptide structure upon interaction with the sterol could be smaller since the cavity could be filled with the less polar DMSO molecules that could already interact with the hydrophobic side chain moieties of the residues of TNM-A lining the cavity resulting to lower affinities (larger K_d values) obtained from ^{1}H NMR titration experiments.

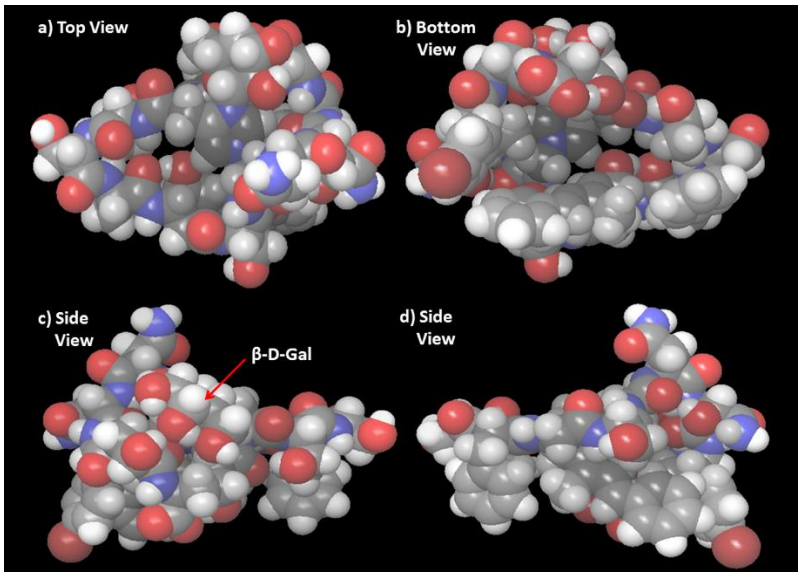

Figure 2-14. Space-filling model of the lowest potential energy conformation of TNM-A (-1772.83 kJ/mol) showing the top (a), (b) bottom, and side (c and d) views of the conformation. Probable 3D structures of TNM-A were obtained by conformational search using distance and dihedral angle constraints derived on the basis of NOEs and ^3J-coupling values obtained from NOESY and DQF-COSY experiments. Schrödinger Macromodel program (v9.4) was used for the simulation studies in an OPLS_2005 force field (in H_2O), and performed using the Monte Carlo Multiple Minimum (MCMM) method with a 50 kJ/mol energy cut-off to generate the lowest energy conformations.

The location of TNM-A protons incurring chemical shift changes when complexed with 25-HC was also assessed to locate the possible sterol interaction site of the peptide. Peptide/sterol NMR titration data indicated that the addition of 25-HC to TNM-A induced several ^{1}H signals of the peptide to change instead of affecting a specific single residue. Interestingly, several TNM-A protons which incurred significant chemical shift changes (*i.e.*, β-MeBrPhe H-2,6, Ahad H-β, sAla H-β, and αThr -OH and H-γ) were located inside the cavity or are part of the residues lining the cavity. These observations could be supporting the hypothesis that the peptide's site of sterol interaction involves the cavity observed from one of the lowest potential energy structures of TNM-A generated from Macromodel conformation search. Moreover, if the sterol inserts to the observed cavity in the TNM-A structure, the hydrophobic side chains of residues Apoa, Phe, and β-MeBrPhe can interact with the more hydrophobic regions of the sterol possibly endowing more stability to both peptide and sterol. However, since most of the chemical shift changes observed was minimal and intramolecular NOE intensities of TNM-A protons remained relatively unchanged upon addition of sterol, it is suggested that TNM-A conformation does not significantly change upon complexation with sterol. In addition, since no intermolecular NOEs between the peptide and 25-HC could be detected, the exact sterol binding site of TNM-A still remains unclear.

Results from this study revealed important details such as TNM-A's broad selectivity to 3β-hydroxysterols and its sterol affinity in aqueous solutions, which could lay the platform for more detailed research about TNM-A/sterol interactions. Moreover, results obtained from this study showed the applicability of solution ^{1}H NMR to examine the interaction between membrane-active small molecules and sterols in aqueous organic solvents. However, more detailed studies should be carried out to gain more convincing data about TNM-A's sterol binding site. In this manner, the molecular basis of the sterol-dependent membrane activity of TNM-A can be understood more clearly.

References:

1. Matsunaga, S., Fusetani, N., Hashimoto, K. & Walchli, M. Theonellamide F. A novel antifungal bicyclic peptide from a marine sponge Theonella sp. *J. Am. Chem. Soc.* **111,** 2582–2588 (1989).

2. Matsunaga, S. & Fusetani, N. Theonellamides A-E, cytotoxic bicyclic peptides, from a marine sponge Theonella sp. *J. Org. Chem.* **60,** 1177–1181 (1995).

3. Wada, S., Matsunaga, S., Fusetani, N. & Watabe, S. Theonellamide F, a Bicyclic Peptide Marine Toxin, Induces Formation of Vacuoles in 3Y1 Rat Embryonic Fibroblast. *Mar. Biotechnol. (NY).* **1,** 337–341 (1999).

4. Wada, S. I., Matsunaga, S., Fusetani, N. & Watabe, S. Interaction of cytotoxic bicyclic peptides, theonellamides A and F, with glutamate dehydrogenase and 17β-hydroxysteroid dehydrogenase IV. *Mar. Biotechnol.* **2,** 285–292 (2000).

5. Nishimura, S. *et al.* Marine antifungal theonellamides target 3beta-hydroxysterol to activate Rho1 signaling. *Nat. Chem. Biol.* **6,** 519–526 (2010).

6. Nishimura, S. *et al.* Visualization of sterol-rich membrane domains with fluorescently-labeled theonellamides. *PLoS One* **8,** 8–13 (2013).

7. Espiritu, R. A. *et al.* Interaction between the marine sponge cyclic peptide theonellamide a and sterols in lipid bilayers as viewed by surface plasmon resonance and solid-state 2H nuclear magnetic resonance. *Biochemistry* **52,** 2410–2418 (2013).

8. Espiritu, R. A. *et al.* Marine sponge cyclic peptide theonellamide A disrupts lipid bilayer integrity without forming distinct membrane pores. *Biochim. Biophys. Acta - Biomembr.* **1858,** 1373–1379 (2016).

9. Bechinger, B. & Salnikov, E. S. The membrane interactions of antimicrobial peptides revealed by solid-state NMR spectroscopy. *Chem. Phys. Lipids* **165,** 282–301 (2012).

10. Debouzy, J., Crouzier, D., Bourbon, F., Lahiani-skiba, M. & Skiba, M. Interaction Study of an Amorphous Solid Dispersion of Cyclosporin A in Poly-Alpha-Cyclodextrin with Model Membranes by 1 H- , 2 H- , 31 P-NMR and Electron Spin Resonance. **2014,** (2014).

11. Gray, K. C. *et al.* Amphotericin primarily kills yeast by simply binding ergosterol. *Proc. Natl. Acad. Sci. U. S. A.* **109,** 2234–9 (2012).

12. Espiritu, R. A. Mechanism of Action of Membrane-Active Marine Natural Products Theonellamide-A and Amphidinol 3. (Osaka University, 2013).

13. Nakagawa, Y. *et al.* The Structure of the Bimolecular Complex between Amphotericin B and Ergosterol in Membranes Is Stabilized by Face-to-Face van der Waals Interaction with Their Rigid Cyclic Cores. *Biochemistry* **55,** 3392–3402 (2016).

14. Nakagawa, Y. *et al.* Axial hydrogen at C7 position and bumpy tetracyclic core markedly reduce sterol's affinity to amphotericin B in membrane. *Biochemistry* **54,** 303–312 (2015).

15. Houdai, T., Matsumori, N. & Murata, M. Structure of membrane-bound amphidinol 3 in isotropic small bicelles. *Org. Lett.* **10,** 4191–4194 (2008).

16. Espiritu, R. A., Matsumori, N., Tsuda, M. & Murata, M. Direct and stereospecific interaction of

amphidinol 3 with sterol in lipid bilayers. *Biochemistry* **53,** 3287–3293 (2014).

17. Matsumori, N. & Murata, M. 3D structures of membrane-associated small molecules as determined in isotropic bicelles. *Nat. Prod. Rep.* **27,** 1480–1492 (2010).

18. Matsumori, N., Morooka, A. & Murata, M. Conformation and location of membrane-bound salinomycin-sodium complex deduced from NMR in isotropic bicelles. *J. Am. Chem. Soc.* **129,** 14989–14995 (2007).

19. Matsumori, N. *et al.* Direct interaction between amphotericin B and ergosterol in lipid bilayers as revealed by 2H NMR spectroscopy. *J. Am. Chem. Soc.* **131,** 11855–11860 (2009).

20. Dufourc, E. J. & Smith, I. A detailed analysis of the motions of cholesterol in lipid membranes by 2H-NMR relaxation. *Chem. Phys. Lipids* **41,** 123–135 (1986).

21. Murari, R., Murari, M. P. & Baumann, W. J. Sterol orientations in phosphatidylcholine liposomes as determined by deuterium NMR. *Biochemistry* **25,** 1062–1067 (1986).

22. Taylor, M. G., Akiyama, T., Saito, H. & Smith, I. C. P. Direct observation of the properties of cholesterol in membranes by deuterium NMR. *Chem. Phys. Lipids* **31,** 359–379 (1982).

23. Yeagle, P. L., Albert, a D., Boesze-Battaglia, K., Young, J. & Frye, J. Cholesterol dynamics in membranes. *Biophys. J.* **57,** 413–424 (1990).

24. Thordarson, P. Determining association constants from titration experiments in supramolecular chemistry. *Chem. Soc. Rev.* **40,** 1305–1323 (2011).

25. Rajagopal, P., Waygood, B., Reizer, J., Saier, M. & Klevit, R. Demonstration of protein-protein interaction specificity by. *Protein Sci.* **6,** 2624–2627 (1997).

26. Reibarkh, M., Malia, T. J., Hopkins, B. T. & Wagner, G. Identification of individual protein-ligand NOEs in the limit of intermediate exchange. *J. Biomol. NMR* **36,** 1–11 (2006).

27. Soltani, C. E., Hotze, E. M., Johnson, A. E. & Tweten, R. K. Structural elements of the cholesterol-dependent cytolysins that are responsible for their cholesterol-sensitive membrane interactions. *Proc. Natl. Acad. Sci. U. S. A.* **104,** 20226–31 (2007).

28. Farrand, A. J., LaChapelle, S., Hotze, E. M., Johnson, A. E. & Tweten, R. K. (12) Only two amino acids are essential for cytolytic toxin recognition of cholesterol at the membrane surface. *Proc. Natl. Acad. Sci. U. S. A.* **107,** 4341–6 (2010).

Chapter 3

Sterol-dependent Membrane Association of the Marine Sponge-Derived Bicyclic Peptide Theonellamide A

3.1 Introduction

Theonellamide-A (TNM-A, Figure 3-1), is a member of the theonellamide (TNM) family of bicyclic dodecapeptides isolated from the marine sponge *Theonella* sp.[1,2] TNMs exhibit antifungal activity against pathogenic fungi (*Candida, Trichophyton,* and *Aspergillus*) at micromolar concentrations (2-7 μM) and have moderate cytotoxicity against P388 mouse leukemia cells (IC_{50} 0.5-2.8 μM).[1–4] Recent findings indicated that TNMs represent a new class of sterol binding compounds having a different mechanism of action from the known sterol-binding polyene antibiotics such as amphotericin B.[5] TNMs can bind to 3β-hydroxysterols in the membranes but it fails to distinguish between cholesterol and ergosterol possibly leading to its cytotoxicity.[5,6]

Previous results from our group revealed direct and stereospecific interactions between TNM-A and 3β-hydroxysterol in lipid bilayers, through surface plasmon resonance (SPR) and solid-state ^{2}H NMR experiments.[7] In addition, the interaction of TNM-A with 3β-hydroxysterol-containing liposomes were also examined by ^{31}P solid state NMR (ssNMR) to assess its perturbing effects on the phospholipid bilayer packing of POPC MLVs. Results revealed that when TNM-A was incorporated to MLVs, isotropic peaks appeared for both sterol-free and sterol-containing liposomes but no significant changes to chemical shift anisotropy (CSA) were observed. Isotropic peaks usually arise due to the presence of small and fast-tumbling particles such as micelles or small unilamellar vesicles *or* it can signify molecular motion of ^{31}P species that result to regions of high membrane curvature.[8,9] Unlike the spectra of TNM-A, membrane disruption by the detergent-type mechanism of action usually leads to a large isotropic peak due to the formation of small and fast-tumbling particles such as micelles and very small vesicles.[9,10] Nonetheless, irrespective of the reason, results clearly indicate that incorporation of TNM-A to both POPC or POPC/cholesterol MLVs causes disruption of its tight phospholipid packing leading to membrane perturbation or deformation, but without altering membrane fluidity.[11]

Current findings suggest that the presence of Cho in the membrane is an important prerequisite for TNM-A to exhibit its membrane disrupting activity. However, a detailed mechanism to explain TNM-A's membrane action (and the influence of Cho) still remains elusive. In this study, the self-aggregating propensities of TNM-A in aqueous media was first assessed through NMR diffusion experiments and critical micelle concentration determination by Pyrene 1:3 ratio method[12] in order to understand its possible effects on the TNM-A/membrane binding process. Subsequently, the effect of TNM-A on the membrane integrity of artificial POPC or POPC/sterol liposomes were examined through confocal fluorescence microscopy to examine the effect of TNM-A interaction to phospholipid bilayers and reveal the role of 3β-hydroxysterols in the peptide's membrane perturbing/deforming activities. A fluorescent TNM derivative, TNM-DCCH (Figure 3-1) was added to native TNM-A samples at 10 mol% in order to simultaneously assess morphological changes and membrane localization of the peptide. The association process of TNM-A to model membranes was also evaluated using SDS-d_{25} micelles and both Cho-free and Cho-containing DMPC-d_{54}/DHPC-d_{22} bicelles (q=0.5). Finally, ^{1}H NMR paramagnetic quenching

experiments were carried to examine the insertion propensity and localization of TNM-A in the membrane upon interaction.

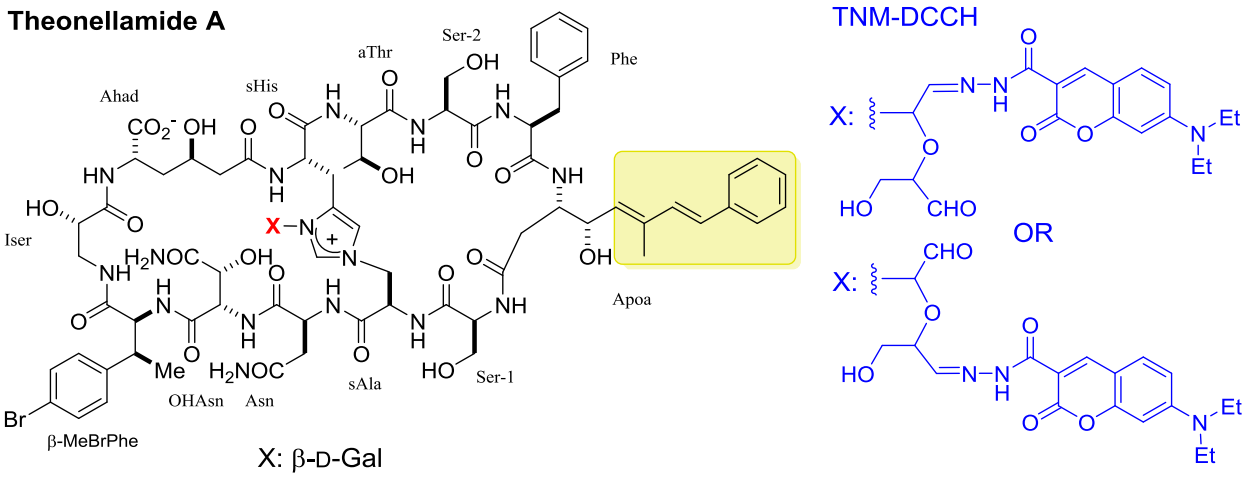

Figure 3-1. Structures of Theonellamide A and fluorescent derivative TNM-DCCH.

3.2 Results and Discussion

3.2.1 Behavior of TNM-A in solution

3.2.1.1 DOSY NMR measurements to assess self-aggregation propensities of TNM A in solution

Despite TNM-A's direct interaction with 3b-hydroxysterols previous SPR measurements indicate that membrane binding of TNM-A is highly dependent on the presence of 3β-hydroxysterols as evidenced by the significant disparity of K_d values obtained for the binding of the peptide to cholesterol-free liposomes (~420 μM) and cholesterol-containing liposomes (~9.2 μM). But despite the direct interaction of TNM-A to 3β-hydroxysterols, its affinity for such sterols are still weak. However, in order to have a better understanding of the membrane binding process of TNM-A, its properties in aqueous solution where it initially exists before association to the membrane should be considered. Previous studies indicate that self-aggregation of AMPs in aqueous solutions, where normal biological processes occur, can greatly influence membrane action.[13] For instance, experiments carried out with antibacterial compound dermaseptin and its derivatives suggest that less aggregated peptides recorded higher antibacterial potencies.[14] In another study which utilized an artificial neural approach to predict AMPs mechanism of action, results indicate that physiochemical properties including peptide aggregation can determine its action.[13]

Because of this, we carried out diffusion ordered spectroscopy (DOSY NMR) in order to assess the aggregation propensities of TNM-A in aqueous environment. In DOSY NMR, the diffusion coefficients (D) of particles in solution can be determined by applying a pulsed gradient field to the sample allowing the translational diffusion of molecules to be monitored. Due to molecule diffusion,

signal intensities of the protons from the molecule is attenuated and this signal decay is processed by curve fitting to obtain D. Through the Stokes-Einstein equation (Equation 3-1), the hydrodynamic radius (r_s) of particles in solution can be obtained given that the measurement temperature and solution viscosity are known.[15,16] In solution, the viscous drag of the solvent on the surface of the molecules results to a friction force that greatly influences the diffusion of the molecules contained in it.[17,18] In general, diffusion coefficient values can be related to the solvent accessible surface area of the molecules dissolved[17] so changes in D can be used to monitor changes in solute's oligomeric state.

$$D = \frac{k_b T}{6\pi\eta r_s} \qquad \text{Equation 3-1}$$

The diffusion coefficients obtained from the DOSY spectra indicate that TNM-A has the propensity to aggregate in an aqueous environment (Figure 3-2 and Table 3-1). In the organic solvent system DMSO-d_6/D_2O (4:1 v/v), which was also used for the structural studies of TNM-A, the peptide has a diffusion coefficient of 0.47–0.54 × 10^{-10} m^2/s at 1.2 mM and 0.55–0.68 × 10^{-10} m^2/s at 0.2 mM. In the aqueous system D_2O/H_2O (98:2 v/v), TNM-A showed diffusion coefficients of 0.91–0.93 × 10^{-10} m^2/s and 1.82–2.19 × 10^{-10} m^2/s for the higher and lower peptide concentrations, respectively. From these diffusion data and the viscosities of D_2O/H_2O (1.095 mPa•s)[19] and DMSO-d_6/D_2O 4:1 (3.861 mPa•s)[20], the calculated Stokes' radii for TNM-A in DMSO-d_6/D_2O (4:1 v/v) and D_2O/H_2O (98:2 v/v) were 1.05–1.21 nm and 2.14–2.18 nm, respectively, at the higher peptide content. This indicates that TNM-A occupies a larger volume in an aqueous environment and probably forms self-aggregates. The small difference of diffusion coefficients in the aqueous DMSO between the high and low TNM-A contents may be caused by a subtle difference in viscosity that is affected by the concentrations of solutes to a certain extent.

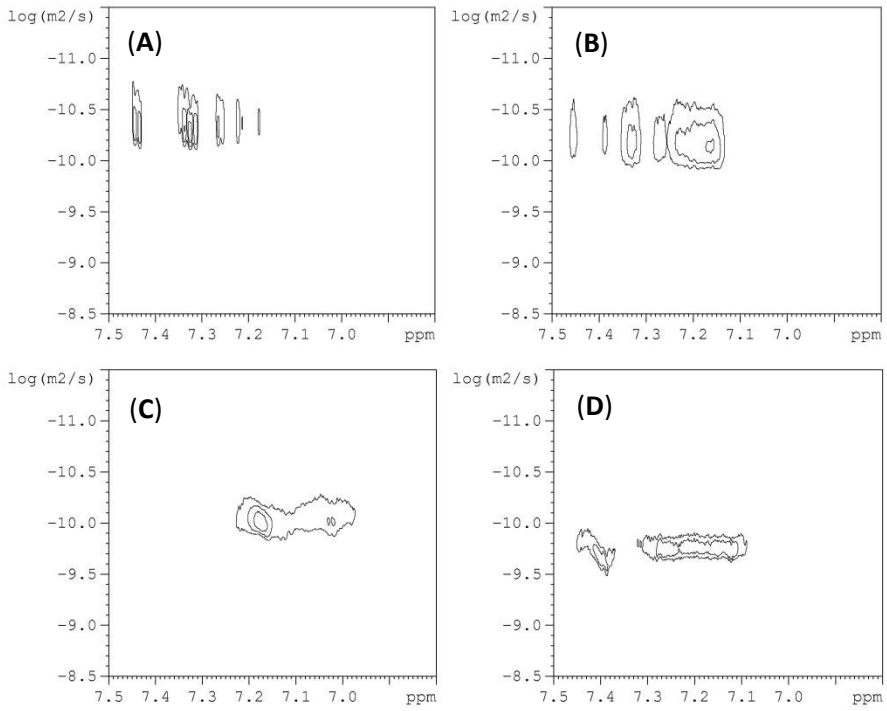

Figure 3-2. DOSY spectra of TNM-A in DMSO-d_6/D_2O (4:1 v/v) at 1.2 mM (A) and 0.2 mM (B) and in D_2O/H_2O (98:2 v/v) at 1.2 mM (C) and 0.2 mM (D). The diffusion coefficients were obtained from the midpoints of the peaks indicated in F1 axis. Judging from the apparent Stokes' radius and viscosity of the solvents, the TNM-A present in the aqueous medium forms oligomeric aggregates while occurring as monomers in DMSO-d_6/D_2O. Reprinted with permission from Figure 2 of *Bioorg. Med. Chem.*, **2016**, *24*, 5235-5242.[21] Copyright © (2016) Elsevier.

Table 3-1. Approximated diffusion coefficients (D) and calculated hydrodynamic radius (r_s) of TNM-A in two different solvents at 298 K. Reprinted with permission from Table 1 of *Bioorg. Med. Chem.*, **2016**, *24*, 5235-5242.[21] Copyright © (2016) Elsevier.

[TNM-A]	DMSO-d_6/D_2O (4:1 v/v)			D_2O/H_2O (98:2 v/v)		
	D ($\times 10^{-10}$ m^2/s)	r_s (nm)	V (nm^3)	D ($\times 10^{-10}$ m^2/s)	r_s (nm)	V (nm^3)
1.2 mM	0.47–0.54	1.05–1.21	4.85–7.42	0.91–0.93	2.14–2.18	41.05–43.40
0.2 mM	0.55–0.68	0.84–1.02	2.48–4.45	1.82–2.19	0.91–1.09	3.16–5.42

For comparison, a similar DOSY experiment was carried out using β-cyclodextrin which exists as monomers in aqueous media. From the obtained diffusion coefficient of β-cyclodextrin, its hydrodynamic radius was calculated to be very similar to reported values in literature. This result indicate that the viscosity values of D_2O/H_2O solvent mixtures reported in the literature.[20,22] are accurate enough for estimating the number of TNM-A molecules in oligomers (Figure 3-3 and Table 3-2).

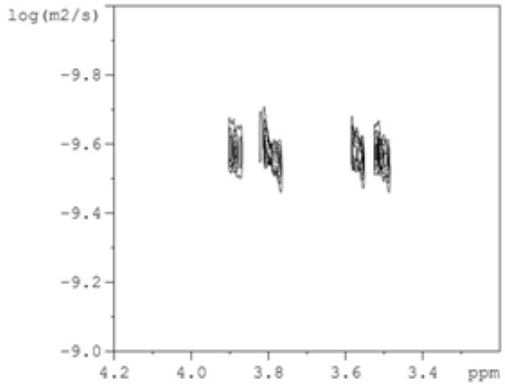

Figure 3-3. DOSY Spectrum of β-cyclodextrin in D_2O/H_2O (98:2) at 298 K. Reprinted with permission from the Supporting Information of *Bioorg. Med. Chem.*, **2016**, *24*, 5235-5242.[21] Copyright © (2016) Elsevier.

Table 3-2. Diffusion coefficients and related parameters obtained for b-cyclodextrin from DOSY experiments. Reprinted with permission from the Supporting Information of *Bioorg. Med. Chem.*, **2016**, *24*, 5235-5242.[21] Copyright © (2016) Elsevier.

	D from DOSY NMR in this study (m^2/s)	Reported *D* from literature (m^2/s)[23]	R_s from DOSY NMR in this study (nm)	R_s from literature (nm)[23]
β-cyclodextrin	2.63×10^{-10}	2.64×10^{-10}	0.76	0.71

Based on the volume values shown in Table 3-1, the number of TNM-A molecules in an oligomer was determined assuming that the peptide has a completely spherical form in both the solvent systems; for the high peptide content (1.2 mM) and low peptide content (0.2 mM), the average numbers of molecules per aggregate in aqueous media were approximately 9 and 2, respectively. This can be accounted for by the association–dissociation equilibrium between the monomers and oligomers that should be shifted to monomers in lower concentrations of the peptides. Considering TNM-A's amino acid composition, it is not unlikely that the peptide has the propensity to self-aggregate in aqueous environments because of the presence of several residues having highly hydrophobic side chains such as Apoa, Phe, and β-MeBrPhe. Exposure of such moieties in water could destabilize the peptide structure so it is likely that the peptide aggregates to keep its hydrophobic portions of TNM-A away from water. The occurrence of aggregates in aqueous phase was also reported for another membrane-active and antibacterial peptide trichogin GA

IV.[24] Although these values are only rough approximations, data clearly indicates that TNM-A has a propensity to form oligomers when existing in a purely aqueous environment.

3.2.1.2 Determination of the Critical Micelle Concentration of TNM-A alone in aqueous solutions or in the presence of 25-HC

Results from DOSY NMR measurements clearly revealed the propensity of TNM-A to form self-aggregates in purely aqueous solutions. The calculated aggregation number of TNM-A in H_2O were based on the assumption that TNM-A remains as monomers in DMSO/D_2O (4:1) solvent systems giving out peptide aggregation of about ~2 and ~9 for 200 μM and 1.2 mM concentrations in purely aqueous solutions, respectively. In order to verify the validity of such assumptions and to confirm the concentration at which TNM-A starts to aggregate in purely aqueous solutions, the peptide's critical micelle concentration was determined. This was carried out by using a standard CMC assay known as Pyrene 1:3 ratio method which relies on the solvent polarity-dependent fluorescence of pyrene in aqueous environments.[25,12]

Of Pyrene's 5 major vibrational peaks when in water, peaks at 373 nm (λ_1) and 384 nm (λ_3) are the most affected by solvent polarity changes.[26] So, the ratio of the fluorescence at λ_1 over λ_3 (I_1/I_3) can be used as an indicator of the local environment that pyrene is in. When pyrene is in the presence of a surfactant below its CMC, the I_1/I_3 ratio is high (usually above 1.0) indicating a highly polar environment. As the surfactant concentration is increased towards its CMC, pyrene starts to feel a change in its environment polarity because it starts to associate to the hydrophobic core of the surfactant micelles. At this point, the fluorescence at I_3 increases and the I_1/I_3 ratio decreases indicating a shift of pyrene to a more hydrophobic environment. When the surfactant concentration reaches its CMC, I_1/I_3 reaches a constant low value suggesting the complete incorporation of pyrene to the surfactant micelle core.[12] The result from this assay can be processed to determine CMC by first plotting I_1/I_3 vs. surfactant concentration to give a decreasing sigmoidal curve similar to that presented in Figure 3-4. There are 2 points in the curve χ_{cmc1} and χ_{cmc2} which can be used to approximate for a surfactant's critical micelle concentration. The generated decreasing sigmoidal curve is curve fit using Equation 3-2 to obtain fitting parameters x_o (equivalent to CMC_1) and Δx which will then be used to calculate for CMC_2 using Equation 3-3.

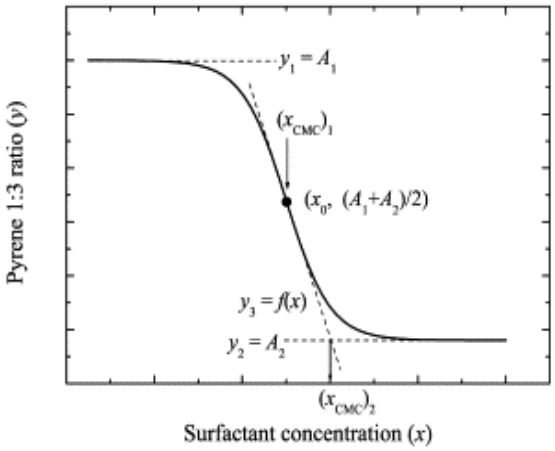

$$y = \frac{A_1 - A_2}{1 - e^{(x-x_o)/\Delta x}} \qquad \text{Equation 3-2}$$

$$(x_{CMC})_2 = x_o + 2\Delta x \qquad \text{Equation 3-3}^{12}$$

where
y = Pyrene I_1/I_3
x = total concentration of surfactant
A_1 and A_2 = upper and lower limits of sigmoid
Δx = concentration range where abrupt change in I_1/I_3 occurs
x_o = center of sigmoid $\approx \chi_{CMC1}$

Figure 3-4. A decreasing sigmoidal curve obtained by plotting the ratio of the pyrene fluorescence at λ_1 over λ_3 (I_1/I_3) vs. surfactant concentration. CMC_1 can be calculated after curve fitting the data to Equation 2-3 while CMC_2 can using calculated from Equation 2-4. Reprinted with permission from Figure 1 of the *Journal of Colloid and Interface Science*, **2003**, *258*, 116-122.[12] Copyright © (2003) Elsevier Science (USA).

The choice between χ_{cmc1} and χ_{cmc2} is based on the tendencies of pyrene to partition between the surfactant micelle core and the bulk solution.[12,27–29] For surfactants with high CMCs (>1 mM), χ_{cmc2} is a better approximate because this point reflects the highest concentration before surfactant completely turns into micelles indicated by the minimum I_1/I_3 value being reached. In such situations, the micelle formed by the surfactant above CMC is large enough to accommodate the pyrene molecule in its hydrophobic core so the lowest pyrene I_1/I_3 reflects the most hydrophobic environment pyrene can experience as it becomes complete associated inside the surfactant micelle. However, for surfactants with low CMCs (<1 mM), taking point χ_{cmc2} is said to give an over estimation of the CMC. This is because the formed micelles of such surfactants cannot fully accommodate pyrene due to its small size so it ends up partitioning between the bulk solvent and the micelle core. As a consequence, the pyrene I_1/I_3 ratio recorded is actually an average for pyrene in a highly polar and non-polar environment giving it a larger numerical value. For such surfactants with CMCs < 1mM, it is better to take χ_{cmc1} as the approximate critical micelle concentration.[12] The nature of the surfactant, whether ionic or non-ionic, can also aid in choosing the more accurate CMC value based on their $x_o/\Delta x$ ratio.[12] Results from previous studies indicated that for ionic surfactants, which often have a $x_o/\Delta x$ >10 or more, χ_{cmc2} values obtained are closer to the CMC obtained by conductance methods and others reported in literature. For anionic surfactants, which have $x_o/\Delta x$ ratio < 10, it would be more appropriate to take χ_{cmc1} as the surfactant CMC.[12]

Initially, pyrene fluorescence measurements were carried out to determine the CMC of TNM-A alone in aqueous solution. The decreasing sigmoidal curve obtained by plotting pyrene I_1/I_3 vs TNM-A concentration (in mM) is presented in Figure 3-5A. However, unlike most pyrene I_1/I_3 vs surfactant concentration plots, the decreasing sigmoidal pattern was not as distinct as the theoretical initial plateau region in Figure 3-4 where I_1/I_3 values should be stable seemed to be decreasing right away. Moreover, the slope of the sigmoidal curve was relatively shallow resulting to the range of TNM-A concentrations

where the decrease in pyrene I_1/I_3 was observed to be quite large. This shallow slope could reflect the cooperativity of the TNM-A micelle/aggregate formation and the partitioning of pyrene to formed TNM-A aggregates.[30] After the curve fitting procedure of the obtained data to Equation 3-2 the exact values for the fitting parameters x_o and Δx were obtained and both CMC_1 and CMC_2 values at 186 μM and 356 μM, respectively (Table 3-2, upper row) were found. Since both values are significantly less than 1 mM, it could be suggesting that the peptide aggregates may be too small to fully accommodate pyrene so the χ_{cmc1} at 186 μM was taken as the approximate CMC. Moreover, the $x_o/\Delta x$ ratio of the obtained data (~2.19), is well below 10 indicative of a non-ionic surfactant which indicates that the CMC also should be taken from point χ_{cmc1}. This χ_{cmc1} value also corroborates with the DOSY NMR data since at 200 μM concentration of the peptide in purely aqueous solutions, a change in the diffusion coefficient of TNM-A was already observed signifying a change in the peptide volume. At that point, aggregation number of TNM-A was calculated to be ~2.

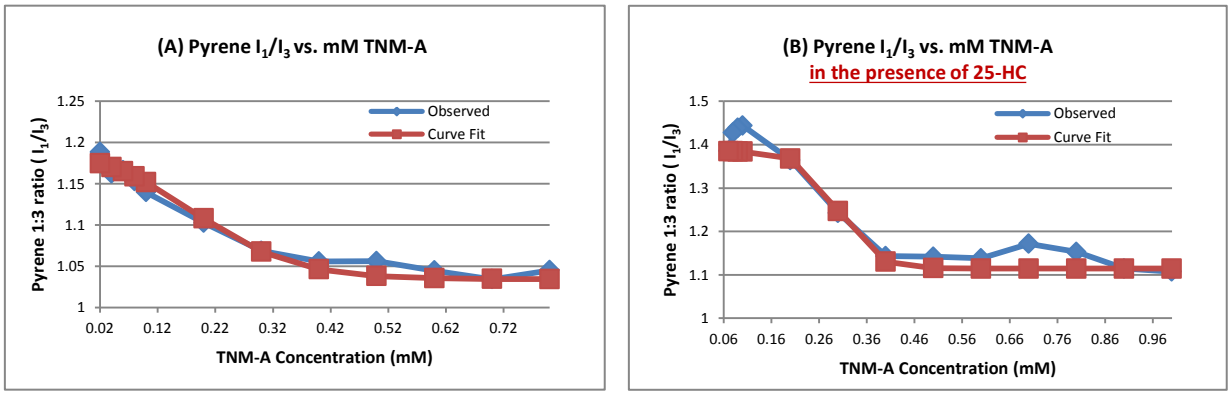

Figure 3-5. Plots of Pyrene I_1/I_3 versus TNM-A concentration when TNM-A is alone in solution (A) and in the presence of 25-HC (B).

Table 3-3. Obtained x_o and Δx from curve fitting and the calculated CMC_1 and CMC_2 values for TNM-A when alone in solution and when in the presence of the cholesterol derivative 25-HC.

	x_o	Δx	CMC_1	CMC_2	$x_o/\Delta x$
TNM-A alone	0.186	0.085	0.186 mM	0.356 mM	2.19
TNM-A in the presence of 25-HC	0.299	0.037	0.299 mM	0.372 mM	8.03

The CMC of TNM-A in the presence of 25-HC in aqueous solutions was also determined to evaluate the effect of TNM-A/3β-hydroxysterol interaction to the peptide's aggregation propensities. The decreasing sigmoidal curves generated by plotting pyrene I_1/I_3 vs. TNM-A concentration when in the presence of 25-HC are presented in 3-5B while the calculated CMC_1 and CMC_2 values are also presented in Table 3-3. Results indicated that when TNM-A is in solution together with 25-HC, the peptide's CMC increased to approximately twice its CMC when alone in solution from ~186 μM to ~299 μM. Since sterols cannot possibly form micelles by itself, the decrease in pyrene I_1/I_3 (pyrene shifting to a more hydrophobic environment) could not have come from being engulfed by 25-HC but certainly by the peptide. The increase in CMC for TNM-A when in the presence of 25-HC might be suggesting that the peptide could be binding more to 25-HC instead of other TNM-A molecules, delaying the formation of aggregates/micelles. In addition, these results not only confirm the interaction of TNM-A with 25-HC in solution but also the influence of 3β-hydroxysterols in the aggregation propensities of TNM-A.

However, it should be noted that these CMC values are just rough estimations because the pyrene 1:3 ratio method is may not be very suitable in determining CMC values of TNM-A because the aggregates it form contain a very discrete number of peptide molecules (~2 or 9 TNM-A molecules in an aggregate). In this situation, pyrene may be unable to effectively partition into the peptide aggregate especially when only dimers are formed. For this reason, it is highly probable that the CMC values of TNM-A are much lower than 186 μM. But overall, these results confirm that TNM-A forms aggregates in aqueous environments and that the presence of 25-HC increases TNM-A's CMC.

3.2.2 Interaction studies of TNM-A with Sterol-free and Sterol-containing Liposomes

3.2.2.1 Interaction studies of TNM-A with Sterol-free and Sterol-containing Liposomes using differential interference and confocal fluorescence microscopy

Previous results from ^{31}P ssNMR indicated that incorporation of TNM-A to both sterol-free and sterol-containing liposomes resulted in alteration of phospholipid packing suggested by the appearance of an isotropic peak. As mentioned earlier, isotropic peaks in ^{31}P ssNMR can indicate either the presence of fast-tumbling aggregates or an increase in membrane curvature. In order to assess how TNM-A disrupts the phospholipid bilayer, the interaction of TNM-A with sterol-free and sterol-containing liposomes were assessed by optical microscopic techniques such as differential interference microscopy and confocal fluorescence microscopy, using giant unilamellar vesicles (GUVs) as membrane mimics. Such experiments were carried to examine the time-course dependent morphological changes that can be induced by TNM-A to membrane bilayers upon interaction. Moreover, images obtained can be used to assess if membrane disruption by TNM-A results from an increase in membrane curvature. GUVs, which are typically several micrometers in size, have become a popular membrane model because it is large enough to be easily observable under optical microscopy unlike other unilamellar vesicles.[31]

3.2.2.2 Differential Interference Microscopy

In this experiment, pure POPC and POPC/cholesterol (19:1 mol ratio) GUVs were initially formed using the electroformation protocol[32,33] and then TNM-A was injected to the aqueous media containing the liposomes at a final concentration of 20 μM. The time-course peptide-induced morphological changes on the GUVs were monitored by viewing the liposomes through differential interference contrast, a natural contrast enhancement microscopy technique useful for unstained and transparent samples.[34] Figure 3-6 and 3-7 shows the time-course images of sterol-free and sterol-containing GUVs, respectively, before and after incubation with 20 μM TNM-A. Images in Figure 3-6 indicated that no significant morphological changes to sterol-free GUVs were detected during the entire 1 hour incubation period. Although some discrepancies in the number and position of GUVs captured in the images could be observed, these may just be a result of differing focal depth when the images were taken and the motion of GUVs as the liposomes are not fixed in the glass slides. On the other hand, when sterol-containing POPC GUVs were incubated with the same concentration of TNM-A, significant morphological changes to the liposomes became evident at about 40 mins after the peptide was added to GUVs (Figure 3-7, C). These morphological changes came in the form of membrane protrusions in the surface of sterol-containing GUVs, which also, surprisingly reverted back to some extent within the 1 hour incubation period (Figure 3-7, D).

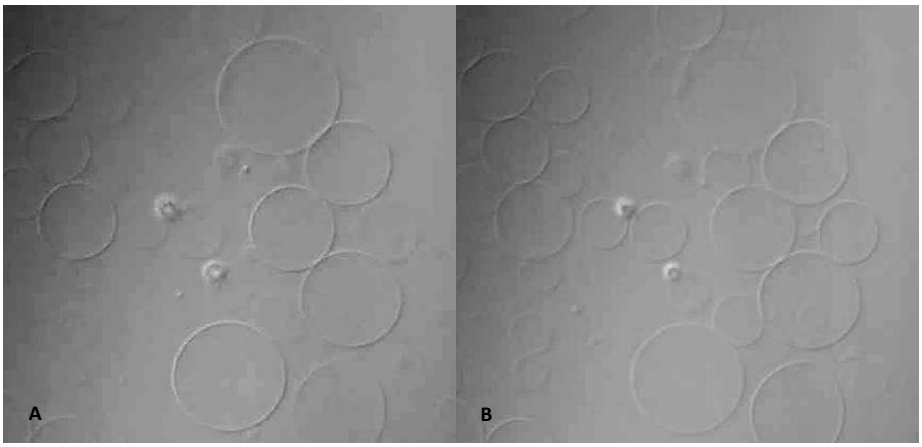

Figure 3-6. Sterol-free POPC GUVs (A) before and (B) after incubation with TNM-A (20 μM, 1 hour).

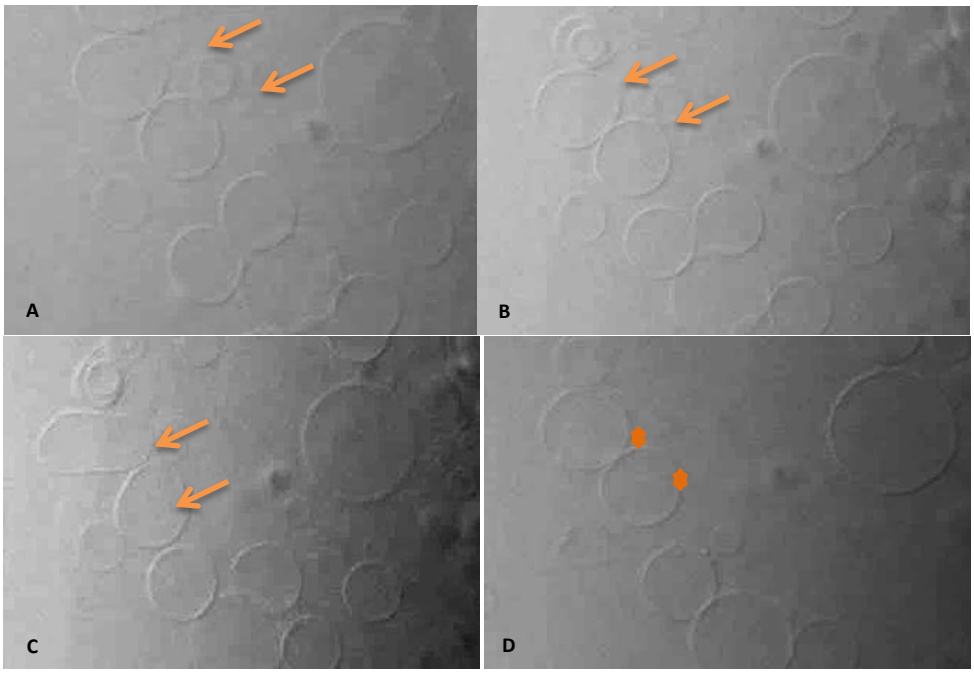

Figure 3-7. POPC/cholesterol (19:1 mole ratio) GUVs (A) before incubation with TNM-A and after (B) 25 min, (C) 40 min, and (D) 55 min incubation with TNM-A (20 μM)

These observations suggest that the interaction of TNM-A with membrane bilayers can induce morphological changes to liposomes only when containing cholesterol. At the same time, these data may be implying that TNM-A can disrupt membrane bilayer integrity of sterol-containing GUVs by increasing membrane curvature as can be seen in Figure 3-7 where GUVs appeared to have developed positive curvature.

3.2.2.3 Confocal Microscopy

Aside from examining the effect of TNM-A on membrane morphology of GUVs through natural contrast enhancement techniques (*i.e.,* differential interference microscopy), confocal microscopy was also carried out to have a more detailed examination of TNM-A/lipid interactions with the use of the fluorescent derivative TNM-DCCH.[6] The fluorescent derivative TNM-DCCH (Figure 3-1) contains a fluorescent 7-diethylcoumarin-3-carboxylic acid hydrazide (DCCH) moiety attached through a derivatized sugar moiety which is present in some TNM congeners since SAR experiments indicated that bioactivity of TNMs are comparable in the presence or absence the sugar moiety.[2,5] In this experiment, TNM-A containing TNM-DCCH (9:1 mol%) was incubated with preformed POPC or POPC/cholesterol GUVs[32,33] and time-course observations were made to examine the peptide's membrane binding, induction of membrane deformations, and the possibility of its internalization into the lumen of the GUVs.

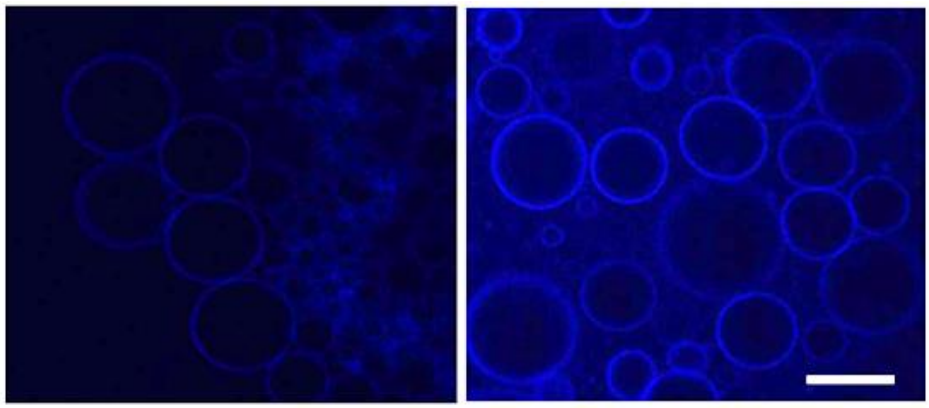

Figure 3-8. Confocal fluorescence microscopy images of sterol-free (left) and sterol-containing (right) POPC GUVs at 3 min after addition of 9:1 mol% TNM-A:TNM-DCCH to the total concentration of 20 μM. Scale bar = 25. Reprinted with permission from Figure 4 of *Biochimica et Bioophysica Acta*, **2016**, *1858*, 1373-1379.[35] Copyright © (2016) Elsevier.

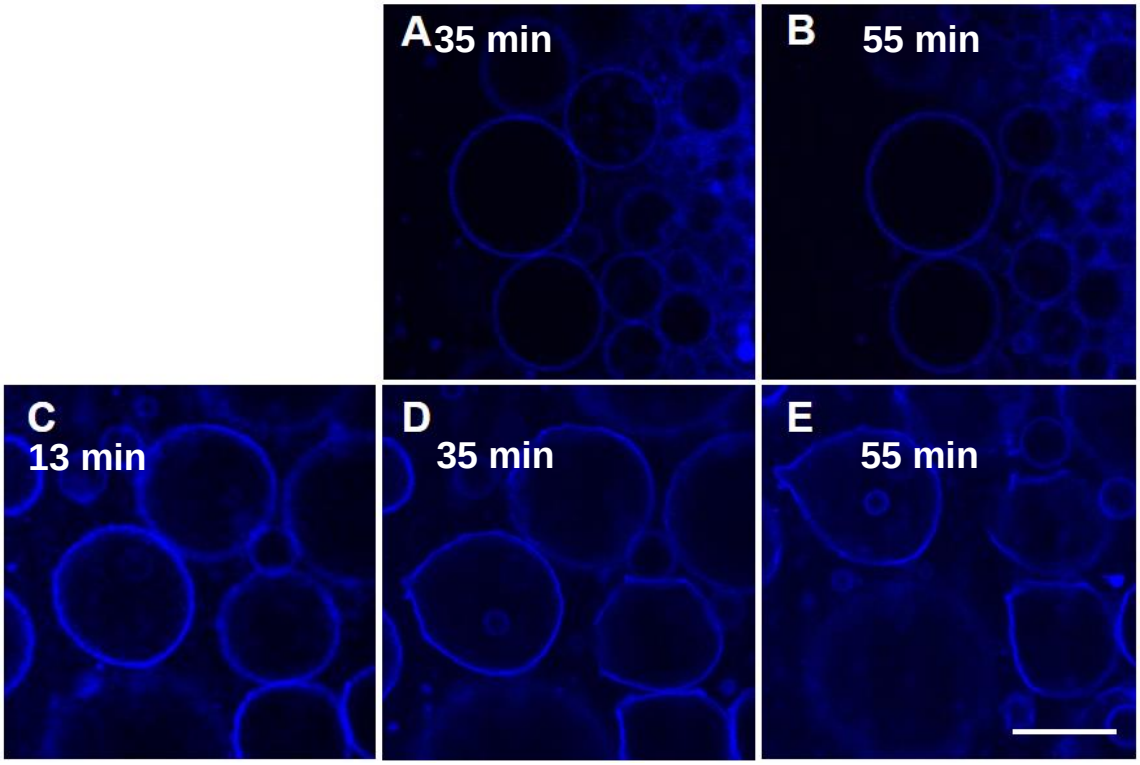

Figure 3-9. Time-lapse confocal microscopy images (A, B) of sterol-free POPC GUVs and (C, D and E) of sterol-containing POPC GUVs after addition of 9:1 mol% TNM-A:TNM-DCCH to a final concentration of 20 μM. Scale bar = 25 μm. Images of GUVs taken at a few minutes and even at 55 min (B) after the peptide addition were almost indistinguishable for sterol-free POPC GUVs. Reprinted with permission from Figure 4 of *Biochimica et Bioophysica Acta*, **2016**, *1858*, 1373-1379.[35] Copyright © (2016) Elsevier.

In terms of membrane binding, images taken early in the time course observations indicated that binding of TNM-A to the surface of liposomes occurs significantly slower in sterol-free GUVs than in cholesterol-containing GUVs as illustrated in Figure 3-8. At 3 minutes after TNM-A/TNM-DCCH (9:1 mol%) was added to the aqueous medium containing the liposomes, the boundaries of the sterol-containing GUVs were already very evident probably due to the increased binding of the peptide in the surface leading to higher fluorescence intensities in the membrane surface (Figure 3-8 [right]). In contrast, lower fluorescence intensities in the membrane surface of sterol-free GUVs were observed 3 minutes after the peptide was added to the media containing the liposomes perhaps due to the slower binding of TNM-A/TNM-DCCH (Figure 3-8 [left]).

These observations are corroborating with the kinetics of TNM-A-membrane interactions determined by SPR measurements.[7] The obtained rate constant values corresponding to the TNM-A/membrane binding step are ~40 times larger in cholesterol (or ergosterol)-containing liposomes than in sterol-free (or 3α-hydroxysterol-containing) liposomes, suggesting that TNM-A can bind to cholesterol-containing membranes faster than to pure phospholipid ones. Previously, it was reported that the faster binding kinetics of TNM-A to cholesterol-containing liposomes is due to the direct interaction of the

peptide to cholesterol based on ^{2}H ssNMR measurements[7], which again emphasizes the importance of the 3β-hydroxysterols in the membrane binding process of TNM-A.

The ability of TNM-A to induce morphological changes in sterol-containing POPC GUVs were observed once again in these experiments. Figure 3-9 shows the time-course images of sterol-free (A and B) and sterol-containing GUVs (C-E) before and after incubation with 20 μM TNM-A (9:1 mol % TNM-A/TNM-DCCH). Binding of TNM-A to the surface sterol-free and sterol-containing GUVs could be observed. However, as described previously, binding of TNM-A to sterol-free GUVs occurred slower so clear and defined GUV images could only be captured after a longer incubation time (~20 min). Observations from confocal microscopy were also similar to the differential interference microscopy results as no morphological changes were observed for sterol-free GUVs throughout the 1 hour incubation period with TNM-A (Figure 3-9, A and B) while distinct membrane deformations were observed in sterol-containing GUV as early as 35 mins after TNM-A addition (Figure 3-9, C-D).

From both differential interference and confocal fluorescence microscopy measurements, observations suggest that TNM-A can induce morphological changes only to sterol-containing liposomes by altering membrane curvature.

3.2.3 Assessing membrane association and localization of TNM-A by ^{1}H NMR paramagnetic quenching measurements

Results from confocal fluorescence microscopy prompted us to examine whether TNM-A interacts with the membrane by remaining in the surface and accumulating there or inserts into the bilayer because it is generally accepted that such interactions can result to membrane deformations. Numerous studies have acknowledged that the asymmetrical insertion of protein or peptide domains in the lipid bilayer can result to membrane protrusions (positive membrane curvature), as was observed for TNM-A in Cho-containing membranes.[36,37] Insertion of amphipathic compounds or proteins only to the outer leaflet of membranes could cause an area difference between leaflets which leads to the development of positive curvature to compensate for the area difference.[36] Moreover, TNM-A contains several residues having highly hydrophobic side chains (from Phe, β-MeBrPhe, and Apoa), which can possibly act as membrane anchors (highlighted in Figure 3-10A). It may also be possible that the crowding of peptides in the surface of membranes, which can result from peptide-peptide interactions, can lead to membrane disruptions by altering membrane curvature.[38,39]

So in order to assess the association and localization of TNM-A upon membrane interaction, ^{1}H NMR Mn^{2+} paramagnetic quenching measurements using model membranes SDS-d_{25} micelles and DMPC-d_{54}/DHPC-d_{22} bicelles were carried out. The use of paramagnetic probes for the investigation of proteins/peptides structure and orientation in membrane-mimetics using solution NMR have been widespread.[40] Paramagnetic quenchers work by increasing the relaxation rates of the nuclei in its proximity. Since paramagnetic quenchers such as Mn^{2+}, Cu^{2+}, and Co^{2+} are unable to penetrate to the hydrophobic core of model membranes and simply remains in solution,[41] such measurements can reveal if TNM-A binds to and interacts with the membrane through the surface (exposed to the solvent) or by inserting to the membrane. In this experiment, the extent of association of TNM-A to SDS-d_{25} micelles and DMPC-d_{54}/DHPC-d_{22} bicelles with or without cholesterol (Chol) were examined by observing the

effect of Mn^{2+} addition to the peptide's ^{1}H signal intensities and line broadening. If TNM-A remains surface-associated without inserting to the hydrophobic chains in the membrane interior upon interaction, its entire structure will remain exposed to the solvent and line broadening of its ^{1}H resonances could be observed. On the other hand, if Apoa or any part of TNM-A anchors into the membrane, these moieties will be affected to a smaller extent by the addition of a paramagnetic quencher (Figure 3-10B).

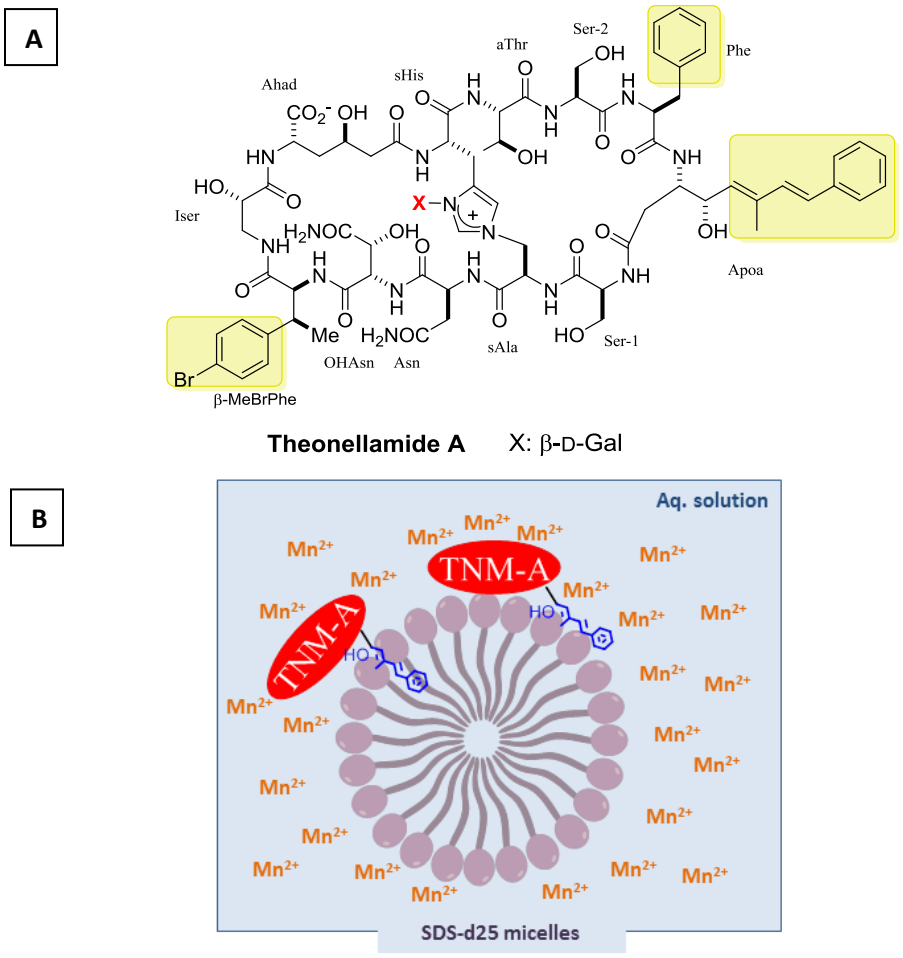

Figure 3-10. (A) Structure of TNM-A highlighting the hydrophobic side chains of TNM-A (B) 2 possible scenarios for the membrane localization of TNM-A (membrane inserted or surface-bound) examined by paramagnetic quenching experiments.

3.2.3.1 Assessing membrane binding of TNM-A using SDS-d_{25} micelles

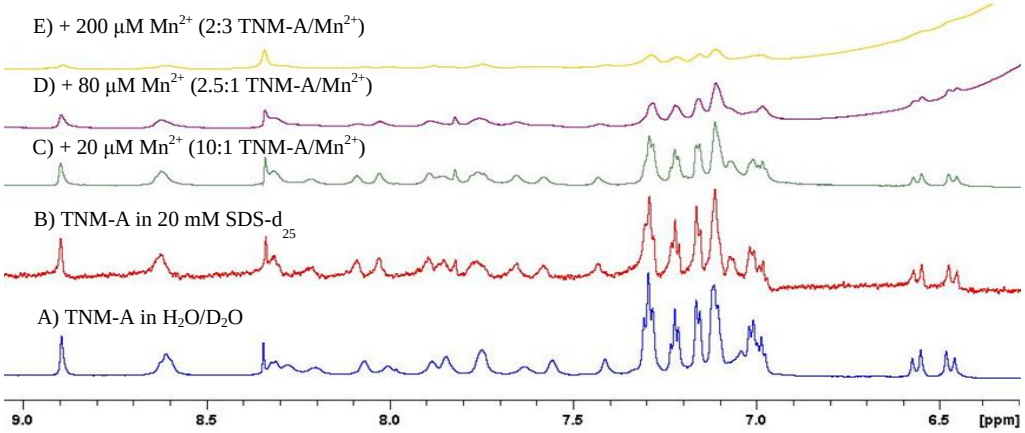

Figure 3-11. Overlay of the ^{1}H NMR spectra of TNM-A obtained from Mn^{2+} paramagnetic quenching measurements highlighting the olefinic and amide proton regions. Measurements were carried out at 25^{o}C with 512 scans and a 3s recycle delay. NMR samples contained 200 μM TNM-A in 20 mM SDS-d_{25} micelles [10 mM PBS buffer, 100 mM NaCl, (pH = 7.4)] with varying concentrations of $MnCl_2$. Reprinted with permission from Figure 7 of *Bioorg. Med. Chem.*, **2016**, *24*, 5235-5242.[21] Copyright © (2016) Elsevier.

Initially, the ^{1}H NMR spectrum of TNM-A in solution (Figure 3-11A) and in the presence of SDS-d_{25} micelles (Figure 3-11B) were obtained and comparison between the two were carried out. Results indicate that there were no significant differences in the spectra of TNM-A in solution and when in the presence of micelles with no notable line broadening observed. These observations could suggest that the mobility of TNM-A was not altered even in the presence of micelles possibly indicating that the peptide did not or just weakly associated with the model membrane surface.[42] Upon the addition of Mn^{2+} (Figure 3-11C & D) a simultaneous gradual increase in line broadening and decrease in signal intensities were observed for the olefinic protons and even in the entire spectra, suggesting that TNM-A remained accessible to Mn^{2+} (and the aqueous environment) upon interaction with the micelles. After 200μM Mn^{2+} was added, all signals in the upfield regions were greatly affected and some even became indistinguishable (Figure 3-11E). Broadening of signals even in the olefinic proton regions where the signals from the hydrophobic side chains of peptide residues thought to insert to the membrane are located, may be suggesting that the peptide is in a surface-bound rather than a membrane-inserted form.

A point of consideration could be that, the absence of cholesterol in the membrane model used in this experiment may be affecting the extent of interaction of TNM-A, leading to a surface-bound rather than a membrane inserted form of the peptide. It is not unreasonable to speculate this since SPR data suggests the stronger affinity of TNM-A to 3β-hydroxysterol containing liposomes over the sterol-free ones.[7] The influence of cholesterol in the membrane interaction of TNM-A appear to be an important prerequisite to its activity as evidenced by confocal fluorescence microscopy data. So, in order to have a better assessment of the membrane binding and localization of TNM-A, cho-containing model membranes must be used. Nevertheless, these data suggest that without cholesterol in the membrane, TNM-A are mostly freely existing in the aqueous media.

3.2.3.2 Assessing membrane binding and localization of TNM-A in Cho-free and Cho-containing DMPC-d_{54}/DHPC-d_{22} (q=0.5) bicelles

Instead of using SDS-d_{25} micelles, we replaced it with Cho-containing DMPC-d_{54}/DHPC-d_{22} bicelles to resolve the membrane affinity issue of TNM-A. In this experiment, DMPC-d_{54}/DHPC-d_{22} with a ratio (q) of long acyl-chain- to-short acyl chain phospholipids at ~0.5 were used because it also fulfills the fast-tumbling and isotropic property requirements desired for solution NMR measurements, similar to micelles. [13,14,43] More importantly, previous studies have shown that it can be incorporated with Cho.[40,44] Although TNM-A seem to stay unbound in the presence of Cho-free membranes, interaction of TNM-A with Cho-free bicelles were still examined to allow comparative analysis with the data obtained from Cho-containing bicelles.

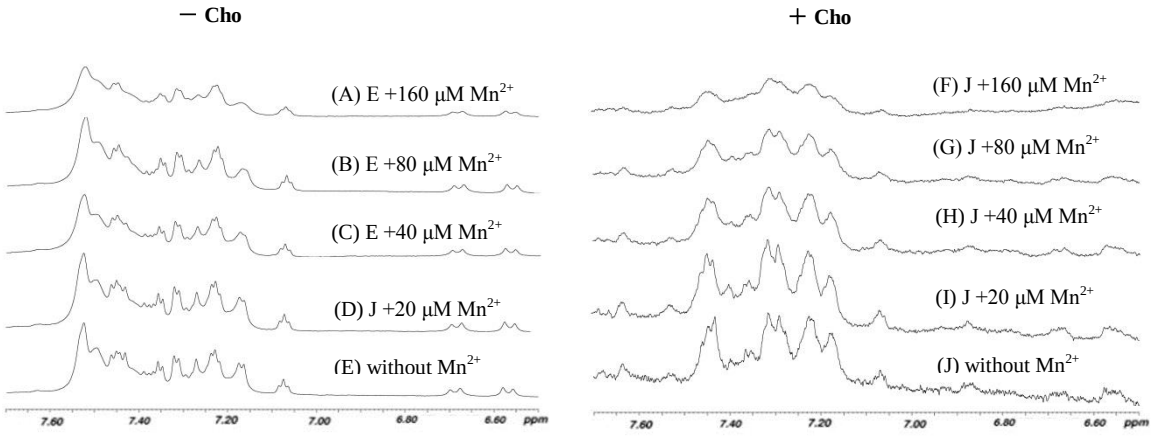

Figure 3-12. Overlay of the ^{1}H NMR Spectra of TNM-A incorporated in Cho-free (A-E) and Cho-containing (F-J) DMPC-d_{54}/DHPC-d_{22} bicelles (q=0.5) in a D_2O (100 mM NaCl) solvent without Mn^{2+} (E and J) and with increasing concentrations of Mn^{2+}(A-D and F-I). Mn^{2+}/TNM-A mol ratio: Blue trace 0:1, Red 10:1, Green 5:1, Violet 2.5:1, Yellow 1.25:1. The final concentrations of TNM-A and phospholipids are 200μM and 160 mM, respectively. (All spectra were taken with 512 scans at 310 K). Reprinted with permission from Figure 7 of *Bioorg. Med. Chem.*, **2016**, *24*, 5235-5242.[21] Copyright © (2016) Elsevier.

The upfield region of the spectra was not very useful in assessing the line broadening effects of Mn^{2+} addition to TNM-A protons because the weak peptide signals were highly overlapping with the DMPC-d_{54}, DHPC-d_{22}, and cholesterol signals. For TNM-A, the downfield region of the spectra provided more useful and unambiguous data because only the signals from the peptide were present in this region. The ^{1}H NMR spectra of TNM-A in Cho-free (Figure 3-12 A-E) and Cho-containing (Figure 3-12 F-J) DMPC-d_{54}/DHPC-d_{22} bicelles appeared different in two aspects. First, the olefinic proton signals in the 6.5-7.6 ppm range were more broadened when the peptide was incorporated to DMPC-d_{54}/DHPC-d_{22}/Cho bicelles than to when it is in Cho-free ones where peptide signals were relatively well-resolved. Second, the peptide signals in the 6.5-7.6 ppm region due to the conjugated diene moiety of the Apoa residue were

almost flattened out due to significant line broadening after the peptide was incorporated Cho-containing bicelles. While in Cho-free bicelles, these conjugated olefinic protons showed relatively sharp signals. These observations could suggest that mobility of TNM-A in DMPC-d_{54}/DHPC-d_{22}/Cho bicelles is more restricted, thus implying that the peptide bound more effectively to Cho-containing bicelles.

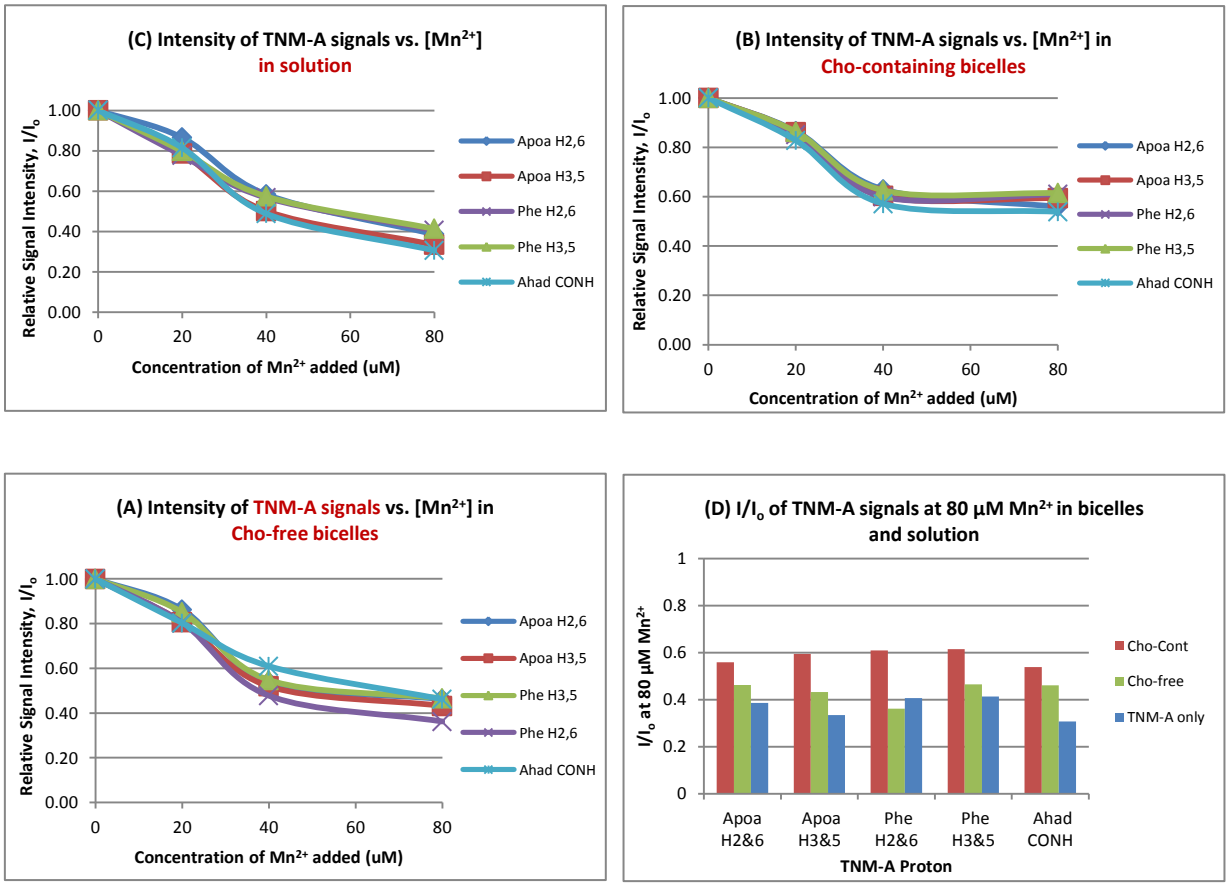

Figure 3-13. Relative signal intensities (I/I_o) of TNM-A protons when incorporated in (A) Cho-free and (B) Cho-containing bicelles and in the absence of bicelles (C) with increasing concentrations of Mn^{2+}. The difference in the effect of 80 µM Mn^{2+} on the I/I_o values of the TNM-A protons when incorporated to bicelles and in when in solution can be seen from (D). I/I_o values were calculated from the ratio of the peptide peak intensity in the presence of x µM of Mn^{2+} over the peak intensity in the absence of Mn^{2+}. The final concentrations of TNM-A and phospholipids are 200µM and 160 mM, respectively. (All spectra were taken with 512 scans at 310 K). Reprinted with permission from Figure 7 of *Bioorg. Med. Chem.*, **2016**, *24*, 5235-5242.[21] Copyright © (2016) Elsevier.

The effect of Mn^{2+} on the relative signal intensity (I/I_o) of TNM-A signals were evident when the peptide was incorporated to both Cho-free (Figure 3-13A) and Cho-containing bicelles (Figure 3-13B) based on the [Mn^2+]-dependent decrease in I/I_o observed. This means that the peptide was accessible to

the paramagnetic quencher regardless if it is in the presence of Cho-free or Cho-containing bicelles and could thus be an indication that TNM-A is bound to the surface of the bicelles and not inserted regardless of the presence or absence of Cho in the membrane. These observations may also indicate that although TNM-A binds more to Cho-containing bicelles (based on the more broadened peptide signals when TNM-A was incorporated to DMPC-d_{54}/DHPC-d_{22}/Cho bicelles), its structure still is accessible to the aqueous environment and is thus not inserted to the membrane.

When TNM-A was incorporated to sterol-free bicelles, the effect of Mn^{2+} to I/I_o of the same TNM-A protons were similar to that when TNM-A was purely in solution in the absence of bicelles (Figure 3-13C). But it may be important to note that the protons of TNM-A were slightly more resistant to addition of Mn^{2+} when incorporated to Cho-free bicelles as its I/I_o values at the highest [Mn^{2+}] appeared slightly higher (and thus, less affected) than when the peptide was purely in solution (Figure 3-13D, green bars) suggesting that peptide still bound to the surface. In addition, TNM-A signals also appeared less sensitive to Mn^{2+} addition when incorporated to Cho-containing bicelles as I/I_o were higher at the initial addition ([Mn^{2+}]=20 μM, I/I_o ~0.85) and at the highest concentration of Mn^{2+} ([Mn^{2+}]=80 μM, I/I_o ~0.54-0.61) compared to when the peptide was in the presence of Cho-free membranes. These data may indicate that although most of TNM-A molecules exist in solution, some peptides still associate to Cho-free membranes. Moreover, the higher I/I_o values of TNM-A signals when in Cho-containing membranes suggest that the peptide associates more to this type of membrane.

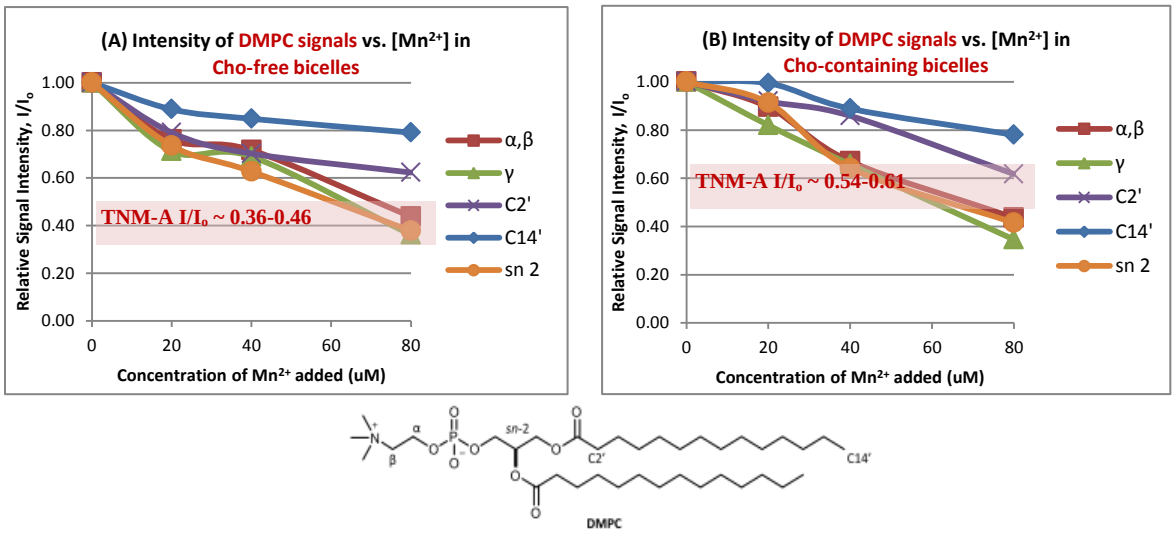

Figure 3-14. Relative signal intensities (I/I_o) of phospholipid (PL) protons in increasing concentrations of Mn^{2+}. I/I_o values were calculated from the ratio of the PL peak intensity in the presence of x μM of Mn^{2+} over the peak intensity in the absence of Mn^{2+}. The final concentrations of TNM-A and phospholipids are 200μM and 160 mM, respectively. (All spectra were taken with 512 scans at 310 K). Reprinted with permission from Figure 7 of *Bioorg. Med. Chem.*, **2016**, *24*, 5235-5242.[21] Copyright © (2016) Elsevier.

The localization of TNM-A upon binding to sterol-free and sterol-containing bicelles were assessed with respect to the depth of lipid molecule moieties by comparing the I/I_o of phospholipid (PL) protons (*i.e.*, γ, α, β, and *sn*-2 protons)[41] with that of the peptide's. The PL protons attached to the γ, α, β,

and *sn*-2 positions appeared greatly influenced by Mn^{2+} addition while protons in the C2' and C14' of the PL acyl chain were the least affected based on the obtained I/I_o values of the said protons (Figure 3-14 A&B). When incorporated to Cho-free bicelles and at highest [Mn^{2+}], I/I_o values of the peptide protons (~0.36-0.46) were similar to the I/I_o values of the fully hydrated protons of the PL such as α, β, γ, and *sn*-2 protons (~0.36-0.43). On the other hand, when incorporated to Cho-containing bicelles and at highest [Mn^{2+}], I/I_o values of the peptide protons (~0.54-0.61) were similar to the I/I_o values for the partially hydrated protons of the PL such as that attached to the C2' of the PL acyl chain (~0.61). Such observations imply that TNM-A interacts with Cho-free bicelles through the shallow region of the membrane near the polar headgroup zone while its interaction with Cho-containing bicelles occurs in a relatively deeper portion of the membrane surface closer to the boundary between the polar headgroup zone and hydrophobic core (lipid-water interface).

Altogether, results from ^{1}H NMR paramagnetic quenching measurements indicate that TNM-A binds more effectively to Cho-containing membranes than to Cho-free ones by associating in a deeper region of the membrane surface. Moreover, TNM-A stays surface-bound and does not insert itself into the membrane upon interaction regardless of the presence or absence of Cho so majority of the peptide structure remains exposed to the aqueous environment.

3.3 Possible Mechanism for membrane disruption by TNM-A

Little is known about the detailed mechanism of action of TNMs although it has been confirmed that TNM-A preferentially binds to 3β-hydroxysterol-containing membranes through its direct interaction with Cho and ergosterol based on SPR and ^{2}H NMR studies.[7] Moreover, ^{31}P NMR results suggested that incorporation of TNM-A to pure POPC or POPC/chol MLVs resulted in disruption of the planar bilayer structure as implied by the appearance of isotropic peaks.[11] However, the detailed mechanism on how it TNM-A can disrupt membrane integrity of Cho-containing bilayers is still unclear. In order to probe into the membrane disrupting mechanism of TNM-A, it was necessary to consider several aspects that influence the binding and interaction of the peptide with the membranes.

Self-aggregation and membrane association of membrane-active peptides are important aspects to understand in order to predict more accurately the processes it undergoes to elicit membrane permeabilization.[24] Our results from DOSY NMR clearly indicated that TNM-A has the tendency to form oligomeric structures in aqueous environment and it is highly probable that the presence of such structures could affect the actual binding of the peptide to the membranes. For instance, the antimicrobial peptide trichogin GA IV was shown to exist as monomers and small aggregates in water with the latter exhibiting reduced partition into the membrane phase.[24] In another study about dermaseptin-derived peptides, it was revealed that those with less aggregation propensities in aqueous media showed higher bioactivity. Aggregate formed by the said peptides probably leads to precipitation leading to container surface adhesion and thus could never revert back to its more active monomeric form.[14] In the case of TNM-A aggregation in aqueous environments, less TNM-A monomers will be available to effectively bind to Cho-containing membranes. Since the oligomeric form of the peptide may even have a weaker affinity to the membrane, progression of membrane deformation of TNM-A is slow.

A high surface density of peptide/protein domains inserted in the outer leaflet of the membrane compared to the inner leaflet (asymmetrical membrane binding) is known to be a contributory factor in the generation of high membrane curvatures.[36,37] Positive curvature, similar to the deformation induced by TNM-A in lipid membranes (Figure 3-9)[21], can be generated due to the difference in area between the inner and outer leaflets when amphipathic peptides or proteins interact only with the outer surface of membranes.[40] Examining the structure of TNM-A, it contains several residues (Phe, β-MeBrPhe, and Apoa) which possesses hydrophobic moieties that can potentially act as membrane anchors to the outer leaflets of bilayers. Fittingly, our results from ^{1}H NMR paramagnetic quenching experiments indicated that TNM-A had a slightly deeper membrane association to Chol-containing bicelles, although still mostly existing in the surface. This observation is also in agreement with membrane affinity data from SPR measurements wherein K_d values reveal that TNM-A has a stronger affinity to POPC/Chol membranes (K_d, ~9.2 μM) than to sterol-free ones (K_d, ~420 μM).[7] Association of the aggregated forms of TNM-A to the membrane still cannot be discounted but it should bind to the bilayer surface much weaker because its hydrophobic moieties are tucked inside the peptide aggregates. However the higher affinity of TNM-A to chol-containing membranes can probably lead to the release of more monomeric TNM-A from the aggregates to interact with the membrane surface and accumulate there causing an increase in membrane curvature. Such interactions can lead to an increase in the hydrophobicity of the possible peptide-sterol complex within the membrane allowing the dissociation of the peptide from the aggregates and its membrane association to be more favorable. Besides that, reports indicate that formation of positive curvature can be a result of a stress-relieving mechanism by the membrane when lateral pressure in the outer leaflet of the membrane is increased due to peptide binding.[45]

In summary, Figure 3-15 presents the hypothesized scenario to explain the membrane disrupting activity of TNM-A. Initially, TNM-A exists as aggregates in aqueous environments, probably to gain thermodynamic stability by keeping its hydrophobic moieties buried away from water. In the absence of 3β-sterols in the membrane (Figure 3-15A), affinity of TNM-A to the membrane is weak so the peptide aggregates will have less drive to dissociate into monomers and associate to the membrane. As a consequence, the number of peptide molecules binding to the membrane surface is low and no accumulation happens (Figure 3-15B). The TNM-A aggregates expose the hydrophilic face to the aqueous phase because its hydrophobic residues are mostly incorporated in the core of the oligomers. Thus, its weak hydrophobic interaction with the membrane destabilizes the membrane-bound form, thus retaining the aggregates mostly in water and no membrane deformation occurs (Figure 3-15C). In the presence of 3β-sterol in the membrane (Figure 3-15D), the ~40x higher affinity of TNM-A to the membrane[7] can drive significantly more peptide molecules to dissociate from the peptide aggregates and bind to the membrane surface. As TNM-A (monomers or aggregates) accumulate in the outer leaflet of Cho-containing bilayers, its surface coverage increases and the peptide also associates to a deeper region of the membrane in the lipid water interface (Figure 3-15F). The outer leaflet phospholipids are pushed aside to accommodate the peptides resulting to an increase in curvature strain and elastic energy in the membrane surface. Consequently, positive membrane curvature will develop to relieve membrane stress caused by peptide binding (Figure 3-15G). At this point, membrane deformations could lead to transient membrane defects that could sometimes allow diffusion of TNM-A molecules to the inner leaflet/compartment of liposomes or could progress even more, enough to destabilize the outer leaflet of the membrane and enhance membrane permeability.

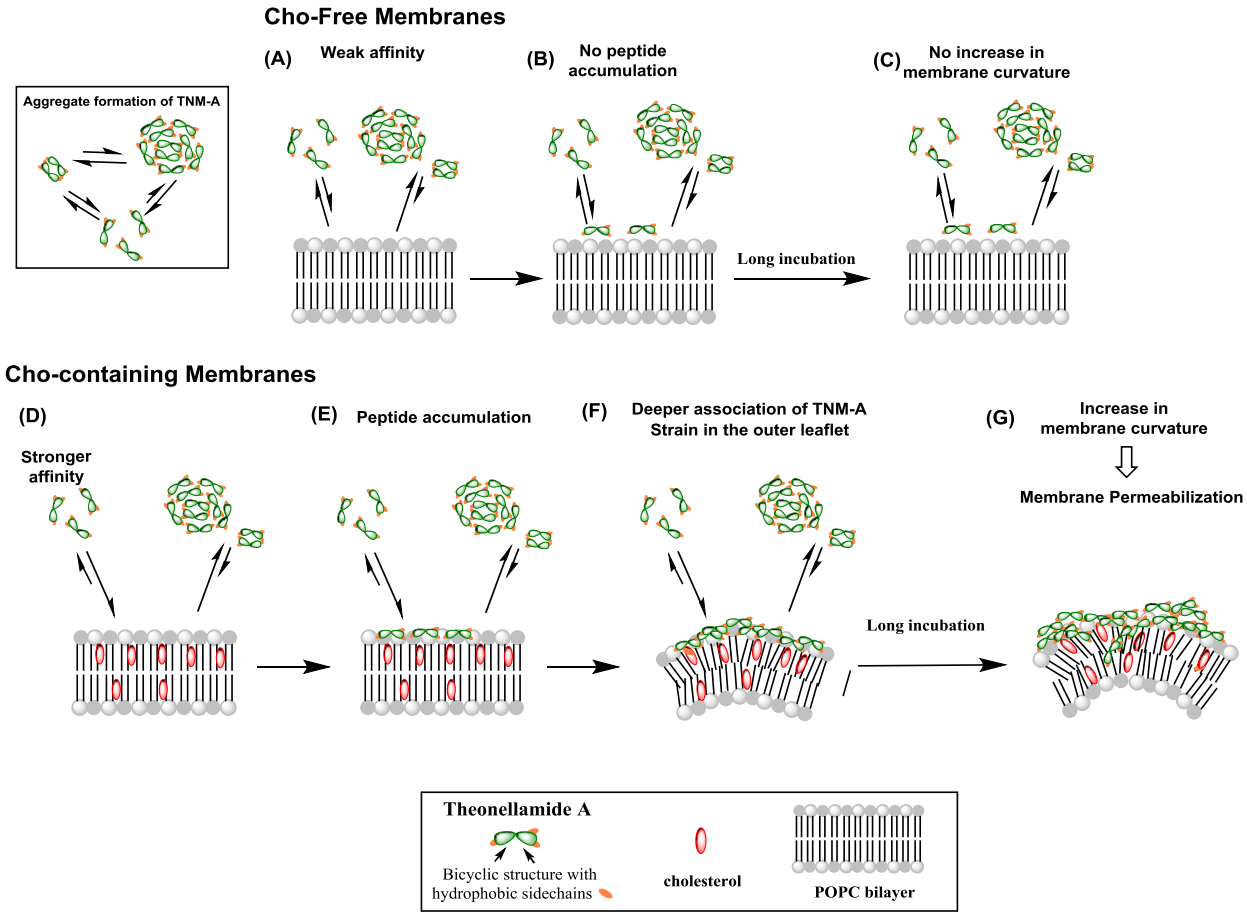

Figure 3-15. Hypothesized scenario to explain the membrane disrupting activity of TNM-A. Reprinted with permission from Figure 7 (Edited version) of *Bioorg. Med. Chem.*, **2016**, *24*, 5235-5242.[21] Copyright © (2016) Elsevier.

References:

1. Matsunaga, S., Fusetani, N., Hashimoto, K. & Walchli, M. Theonellamide F. A novel antifungal bicyclic peptide from a marine sponge Theonella sp. *J. Am. Chem. Soc.* **111,** 2582–2588 (1989).

2. Matsunaga, S. & Fusetani, N. Theonellamides A-E, cytotoxic bicyclic peptides, from a marine sponge Theonella sp. *J. Org. Chem.* **60,** 1177–1181 (1995).

3. Wada, S., Matsunaga, S., Fusetani, N. & Watabe, S. Theonellamide F, a Bicyclic Peptide Marine Toxin, Induces Formation of Vacuoles in 3Y1 Rat Embryonic Fibroblast. *Mar. Biotechnol. (NY).* **1,** 337–341 (1999).

4. Wada, S. I., Matsunaga, S., Fusetani, N. & Watabe, S. Interaction of cytotoxic bicyclic peptides, theonellamides A and F, with glutamate dehydrogenase and 17β-hydroxysteroid dehydrogenase IV. *Mar. Biotechnol.* **2,** 285–292 (2000).

5. Nishimura, S. *et al.* Marine antifungal theonellamides target 3beta-hydroxysterol to activate Rho1 signaling. *Nat. Chem. Biol.* **6,** 519–526 (2010).

6. Nishimura, S. *et al.* Visualization of sterol-rich membrane domains with fluorescently-labeled theonellamides. *PLoS One* **8,** 8–13 (2013).

7. Espiritu, R. A. *et al.* Interaction between the marine sponge cyclic peptide theonellamide a and sterols in lipid bilayers as viewed by surface plasmon resonance and solid-state 2H nuclear magnetic resonance. *Biochemistry* **52,** 2410–2418 (2013).

8. Bechinger, B. & Salnikov, E. S. The membrane interactions of antimicrobial peptides revealed by solid-state NMR spectroscopy. *Chem. Phys. Lipids* **165,** 282–301 (2012).

9. London, E. & Feigenson, G. W. Phosphorus NMR analysis of phospholipids in detergents. *J. Lipid Res.* **20,** 408–412 (1979).

10. Salnikov, E. S. & Bechinger, B. Lipid-controlled peptide topology and interactions in bilayers: Structural insights into the synergistic enhancement of the antimicrobial activities of pgla and magainin 2. *Biophys. J.* **100,** 1473–1480 (2011).

11. Espiritu, R. A. *et al.* Marine sponge cyclic peptide theonellamide A disrupts lipid bilayer integrity without forming distinct membrane pores. *Biochim. Biophys. Acta - Biomembr.* **1858,** 1373–1379 (2016).

12. Aguiar, J., Carpena, P., Molina-Bol??var, J. A. & Carnero Ruiz, C. On the determination of the critical micelle concentration by the pyrene 1:3 ratio method. *J. Colloid Interface Sci.* **258,** 116–122 (2003).

13. Torrent, M., Andreu, D., Nogues, V. M. & Boix, E. Connecting peptide physicochemical and antimicrobial properties by a rational prediction model. *PLoS One* **6,** 1–8 (2011).

14. Feder, R., Dagan, A. & Mor, A. Structure-activity relationship study of antimicrobial dermaseptin S4 showing the consequences of peptide oligomerization on selective cytotoxicity. *J. Biol. Chem.* **275,** 4230–4238 (2000).

15. Wang, C. K. *et al.* Translational Di ff usion of Cyclic Peptides Measured Using Pulsed- Field Gradient NMR. *J. Phys. Chem.* **118,** 11129–11136 (2014).

16. Johnson Jr., C. S. Diffusion ordered nuclear magnetic resonance spectroscopy: principles and applications. *Prog. Nucl. Magn. Reson. Spectrosc.* **34,** 203–256 (1999).

17. Krishnan, V. V & Cosman, M. An empirical relationship between rotational correlation time and solvent accessible surface area. *J. Biomol. NMR* **12,** 177–182 (1998).

18. Arold, S. *et al.* Characterization and molecular basis of the oligomeric structure of HIV-1 Nef protein. *Protein Sci.* **9,** 1137–1148 (2000).

19. Taylor, M. G., Akiyama, T., Saito, H. & Smith, I. C. P. Direct observation of the properties of cholesterol in membranes by deuterium NMR. *Chem. Phys. Lipids* **31,** 359–379 (1982).

20. Sacco, A. & Matteoli, E. Isotopic substitution effects on the volumetric and viscosimetric properties of water-dimethylsulfoxide mixtures at 25° C. *J. Solution Chem.* **26,** 527–535 (1997).

21. Cornelio, K. *et al.* Sterol-Dependent Membrane Association of the Marine Sponge-Derived Bicyclic Peptide Theonellamide A as Examined by 1H NMR. *Bioorg. Med. Chem.* **24,** 5235–5242 (2016).

22. Cho, C. H., Urquidi, J., Singh, S. & Robinson, G. W. Thermal Offset Viscosities of Liquid H2O, D2O, and T2O. *J. Phys. Chem. B* **103,** 1991–1994 (1999).

23. Cabaleiro-Lago, C., Nilsson, M. & Söderman, O. Self-diffusion NMR studies of the host-guest interaction between beta-cyclodextrin and alkyltrimethylammonium bromide surfactants. *Langmuir* **21,** 11637–11644 (2005).

24. Stella, L. *et al.* Aggregation and water-membrane partition as major determinants of the activity of the antibiotic peptide trichogin GA IV. *Biophys. J.* **86,** 936–45 (2004).

25. Dominguez, a, Fernandez, A., Gonzalez, N., Iglesias, E. & Montenegro, L. Determination of Critical Micelle Concentration of Some Surfactants by Three Techniques. *J.Chem.Educ.* **10,** 1227–1231 (1997).

26. J.K.thomas, K. kalyanasundara. Environmental effects on vibronic band intensities in pyrene monomer fluorescence and their application in studies of micellar systems. *J. Am. Chem. Soc.* **2039,** 2039–2044 (1977).

27. Zana, R., Lévy, H. & Kwetkat, K. Mixed Micellization of Dimeric (Gemini) Surfactants and Conventional Surfactants. I. Mixtures of an Anionic Dimeric Surfactant and of the Nonionic Surfactants C12E5 and C12E8. *J. Colloid Interface Sci.* **197,** 370–376 (1998).

28. Frindi, M., Michels, B. & Zana, R. Ultrasonic Absorption Studies Studies if Surfactant Exchange between Micelles and Bulk Phase in Aqueous Micellar Solutions of Nonionic Surfactants with a Short Alkyl Chain. *J. Phys. Chem.* **96,** 8137–8141 (1992).

29. Regev, O. & Zana, R. Aggregation Behavior of Tyloxapol, a Nonionic Surfactant Oligomer, in Aqueous Solution. *J. Colloid Interface Sci.* **210,** 8–17 (1999).

30. Henriksen, J. R., Etzerodt, T., Gjetting, T. & Andresen, T. L. Side chain hydrophobicity modulates therapeutic activity and membrane selectivity of antimicrobial peptide mastoparan-X. *PLoS One* **9,** 1–9 (2014).

31. Philippot, J. & Schuber, F. *Liposomes as Tools in Basic Research and Industry*. (CRC Press, Inc, 1995).

32. Meleard, P., Bagatolli, L. A. & Pott, T. Giant Unilamellar Vesicle Electroformation. From Lipid Mixtures to Native Membranes Under Physiological Conditions. *Methods Enzymol.* **465,** 161–176 (2009).

33. Angelova, M. & Dimitrov, D. No Title. *Faraday Discuss. Chem. Soc.* **81,** 303–311 (1986).

34. Alberts, B. *et al.* in *Molecular Biology of the Cell* (Garland Science, 2002).

35. Espiritu, R. A. *et al.* Marine sponge cyclic peptide theonellamide A disrupts lipid bilayer integrity without forming distinct membrane pores. *Biochim. Biophys. Acta - Biomembr.* **1858,** (2016).

36. Campelo, F., McMahon, H. T. & Kozlov, M. M. The Hydrophobic Insertion Mechanism of Membrane Curvature Generation by Proteins. *Biophys. J.* **95,** 2325–2339 (2008).

37. Zimmerberg, J. & Kozlov, M. M. How proteins produce cellular membrane curvature. *Nat. Rev. Mol. Cell Biol.* **7,** 9–19 (2006).

38. Stachowiak, J. C. *et al.* Membrane bending by protein–protein crowding. *Nat. Cell Biol.* **14,** 944–949 (2012).

39. Kirchhausen, T. Bending membranes. *Nat. Cell Biol.* **14,** 906–908 (2012).

40. Shapiro, R. A., Brindley, A. J. & Martin, R. W. Thermal stabilization of DMPC/DHPC bicelles by addition of cholesterol sulfate. *J. Am. Chem. Soc.* **132,** 11406–11407 (2010).

41. Moniz, T., de Castro, B., Rangel, M. & Ivanova, G. NMR study of the interaction of fluorescent 3-hydroxy-4-pyridinone chelators with DMPC liposomes. *Phys. Chem. Chem. Phys.* **18,** 5027–5033 (2016).

42. Lee, D. K. *et al.* Lipid composition-dependent membrane fragmentation and pore-forming mechanisms of membrane disruption by pexiganan (MSI-78). *Biochemistry* **52,** 3254–3263 (2013).

43. Draney, A., Smrt, S. & Lorieau, J. Use of Isotropically Tumbling Bicelles to Measure Curvature Induced by Membrane Components. *Langmuir* **30,** 11723–11733 (2014).

44. Cho, H. S., Dominick, J. L. & Spence, M. M. Lipid domains in bicelles containing unsaturated lipids and cholesterol. *J. Phys. Chem. B* **114,** 9238–9245 (2010).

45. Koller, D. & Lohner, K. The role of spontaneous lipid curvature in the interaction of interfacially active peptides with membranes. *Biochim. Biophys. Acta - Biomembr.* **1838,** 2250–2259 (2014).

Chapter 4

Conclusions

Theonellamide-A (TNM-A) is a member of the family of antifungal bicyclic dodecapeptides known as theonellamides, isolated from the marine sponge *Theonella* sp. TNMs mechanism of action have yet to be completely elucidated but it has already been established that this family of compounds are 3β-hydroxysterol-binding molecules and that the presence of the aforementioned sterols in the membrane is essential for these compounds to exhibit their membrane disrupting activity. Unfortunately, TNMs exhibit cytotoxic activity as it cannot distinguish between fungal cell membrane sterol ergosterol and mammalian cell membrane sterol cholesterol. In order for TNMs to gain therapeutic value worthy of drug development, its affinity and selectivity for fungal membranes be optimized. But in order to do this, its mechanism of action and sterol-recognition mechanism should first be established.

Based on the results of this study, the following conclusions can be made about TNM-A:

1. TNM-A exhibits non-specific interactions with 3β-hydroxysterols based on results from ^{2}H and ^{31}P ssNMR measurements. Based on the former, a similar attenuation of the pake doublet signals attributed to 3-*d*-25-hydroxycholesterol was observed in the presence of TNM-A compared to when 3-*d*-cholesterol or 3-*d*-ergosterol were incorporated to POPC MLVs. ^{31}P ssNMR results indicated that TNM-A exhibited a similar membrane disrupting effect to 25-HC-contianing phospholipid membranes compared to cholesterol-containing ones.

2. Based on ^{1}H NMR titration experiments, the K_d values characterizing the interaction of TNM-A with 3β-hydrosterols in solution were about ~37-49 μM.

3. The interaction of TNM-A with 3β-hydrosterols in solution does not induce significant conformational changes to the peptide based ^{1}H and NOESY NMR measurements. In addition, despite establishing the direct interaction of TNM-A with 3β-hydrosterols through ^{2}H ssNMR measurements, no intermolecular NOEs between the peptide and the sterol could be detected through NOESY NMR.
    a. It was speculated that a fast association/dissociation of TNM-A/3β-hydrosterols complex resulted to the absence of intermolecular NOEs between the peptide and sterol. The lifetime of the peptide-sterol complex could be too short to allow magnetization transfers needed for NOEs to develop.

4. DOSY NMR results indicated that TNM-A has the propensity to self-aggregate in aqueous environments and is dependent on peptide concentration. Aggregation number of

TNM-A in H_2O is approximately ~2 and 9 at 200 μM and 1.2 mM peptide concentrations, respectively.

5. The CMC of TNM-A in aqueous media was determined through the pyrene 1:3 method and was calculated to be ~ 186 μM. When in the presence of 3β-hydroxysterols, the CMC of TNM-A was increased to ~ 299 μM.

6. Results from differential interference and confocal fluorescence microscopy indicated that TNM-A does not alter the membrane morphology of Chol-free POPC GUVs. On the other hand, TNM-A can alter membrane curvature of Chol-containing POPC GUVs.

7. Based on ^{1}H NMR paramagnetic quenching measurements, results revealed that TNM-A stays surface-bound and does not insert itself into the membrane upon interaction regardless of the presence or absence of Chol, so majority of the peptide structure remains exposed to the aqueous environment.
    a. TNM-A inefficiently binds to Chol-free membranes and mainly remains in the aqueous media. When it does bind, it stays in the shallowest region of the membrane near the polar phospholipid headgroup. On the other hand, TNM-A binds more to Chol-containing membranes and tend to stay in a relatively deeper region of the membrane close to the lipid-water interface.

Chapter 5

Experimental Section

5.1 Materials

Reverse-phased column chromatography stationary phase ODS(C_{18})-AQ gel (12 nm S-50 μm) from YMC Co. Ltd. (Kyoto, Japan), glass plates covered with 60 F_{254} silica gel or RP-18 F_{254} for normal and reversed phase thin layer chromatography (TLC) isolation monitoring. NMR solvents DMSO-d_6 and D_2O were obtained from Euriso-top (Les Algorithmes, Saint-Aubin, France) and Cambridge Isotopes Laboratory (Andover, MA, USA), respectively. Deuterium-depleted water was purchased from Isotec Inc (St. Louis, MO, USA). Sodium dodecyl sulfate-d_{25} (SDS-d_{25}), 1,2-dimyristoyl-d_{54}-*sn*-glycero-3-phosphocholine (DMPC-d_{54}), 1,2-dimyristoyl-d_{54}-*sn*-glycero-3-phosphocholine (DMPC), and 1,2-dihexanoyl-d_{22}-*sn*-glycero-3-phosphocholine (DHPC-d_{22}) were purchased from Avanti Polar Lipids, Inc. 1-palmitoyl-2-oleoyl-sn-glycero-3-phosphocholine (POPC) was purchased from NOF Corporation (Tokyo, Japan). Paramagnetic Quencher Mn^{2+} was obtained in the form of an $MnCl_2$ salt purchased from Nacalai Tesque Inc. (Kyoto, Japan). Cholesterol (Cho) was purchased from Nacalai Tesque Inc. (Kyoto, Japan) and 25-hydroxycholesterol (25-HC) was purchased from Sigma Aldrich (St. Louis, MO, USA). Phospholipid C-test and Cholesterol E-test were purchased from Wako Pure Chemical Industries (Osaka, Japan). Chloroform, methanol (MeOH), n-propanol (PrOH), 2-propanol, dichloromethane (DCM), ethyl acetate, hexane, acetonitrile, disodium hydrogen phosphate (Na_2HPO_4), monosodium dihydrogen phosphate (NaH_2PO_4), tris(hydroxymethyl)aminoethane, Manganese (II) Chloride ($MnCl_2$), sodium chloride (NaCl), potassium chloride (KCl), pyridinum chlorochromate (PCC), calcium carbonate ($CaCO_3$), and cerium chloride heptahydrate ($CeCl_3 \bullet 7H_2O$) were purchase from Nacalai Tesque, Inc. (Kyoto, Japan). Molecular sieves 4Å beads was purchased from Sigma Aldrich (St. Louis, MO, USA). All the other chemicals used were analytical grade and used without further purification. Water used was purified using a Millipore Simpli Lab System (Millipore, Inc., Bedford, MA). TNM-DCCH, (DCCH, Molecular Probes) was a kind gift from Professor Nishimura of Kyoto University and was synthesized as reported. [1] 3-*d*-cholesterol and 3-*d*-25-hydroxycholesterol were synthesized as previously reported.[2]

5.2 Instruments

HPLC	Shimadzu SCL-10Avp
UV Spectrophotometer	Shimadzu UV-2500, Eppendorf BioSpectrometer
Mass Spectrometer	Thermo Scientific LTQ Orbitrap XL
Spectrofluorometer	JASCO FP-6500
NMR Spectrometer	Bruker AVANCE700, JEOL ECA400WB, ECS400, ECA500
Confocal Microscope	Olympus FluoView^{TM} FV1000-D
Lyophilizer	EYELA FDU-1200
Rotary Evaporator	EYELA COOL ACE CA-1111, NVC-2000
	Technosigma N-1000, Iwaki Thermo Bath
Analytical Balance	A&D GR-202, HF-3200
pH Meter	TOA HM-40S
	Horiba Twin Compact pH meter B-211
Water Purifying Apparatus	Millipore Elix-UV, Simpli Lab
Vortex Mixer	Scientific Industries VORTEX Genie-2
Sonicator	Yamato BRANSON 1510

5.3 Methods

5.3.1 Isolation of TNM-A

Theonellamide A (TNM-A) was isolated as reported previously.[3] Briefly, frozen sponge (Kind gift from Prof. Shigeki Matsunaga of the University of Tokyo) was ground using a blender and extracted with a mixture of *n*-ProH/H_2O (2:1 v/v) overnight. Celite was added to the mixture and mixed thoroughly. After which, the mixture was filtered using a Buchner funnel. The filtrate was combined with the washings from the residue in the funnel and the PrOH solvent was removed using a rotary evaporator.

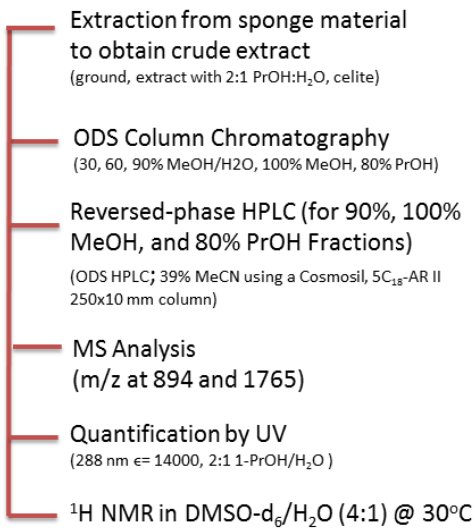

Scheme 5-1. Schematic diagram of TNM-A isolation from sponge.

5.3.1.1 TNM-A Purification through Reverse-Phase Liquid Chromatography and HPLC

After concentration of the combined extracts, the resulting crude material was subjected to ODS flash column chromatography with increasing concentrations of aqueous MeOH at 30%, 60%, 90%, followed by 100% MeOH. To completely wash out the column, it was eluted with 80% PrOH in water. The latter fractions (90% and 100% MeOH, 80% PrOH) were concentrated and then dissolved in MeOH before subjecting to further purification by HPLC.

One pre-packed column (Cosmosil, $5C_{18}$-AR-II, 250 x 10 mm) was connected to a Shimadzu HPLC instrument. 30-40 µL of crude extract of the fractions obtained from RPLC was injected per purification run. The elution solvent was 39% acetonitrile in H_2O (degassed for 30 minutes using a sonicator) with a flow rate of 2 mL/min. The fraction with retention time (t_r) of about 13-15 minutes was collected. After completely evaporating the solvent from the purified fractions, aliquot portions were dissolved in PrOH/H_2O (2:1 v/v) and quantified using the UV spectrophotometer based on the absorbance at λ = 288 nm. ^{1}H NMR measurements (4:1 DMSO-d_6/H_2O, 30°C) were also carried out with TNM-A to assess purity.

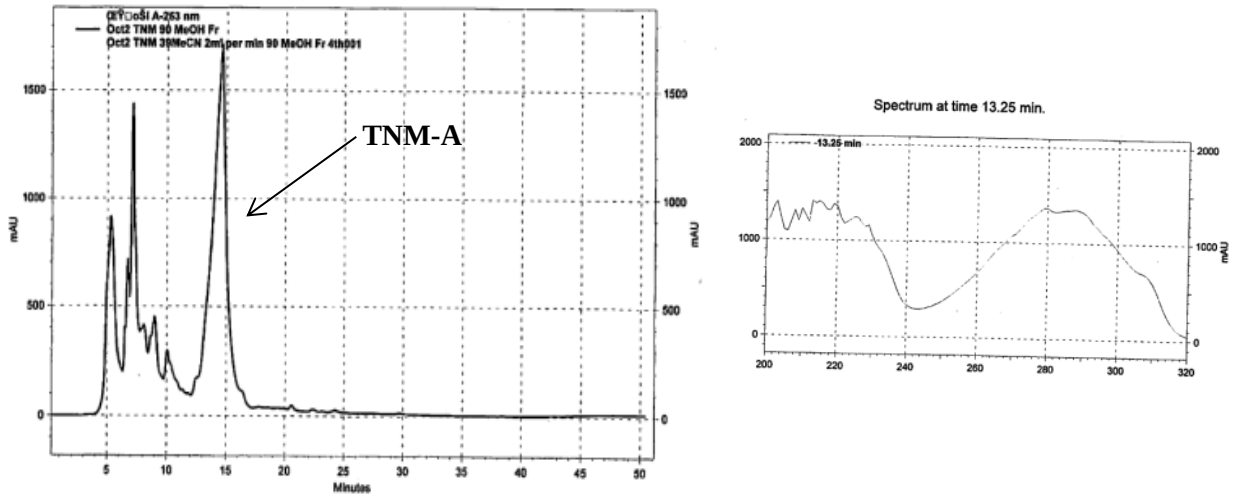

Figure 5-1. Sample chromatogram (left) and UV spectrum (right) of TNM-A isolation.

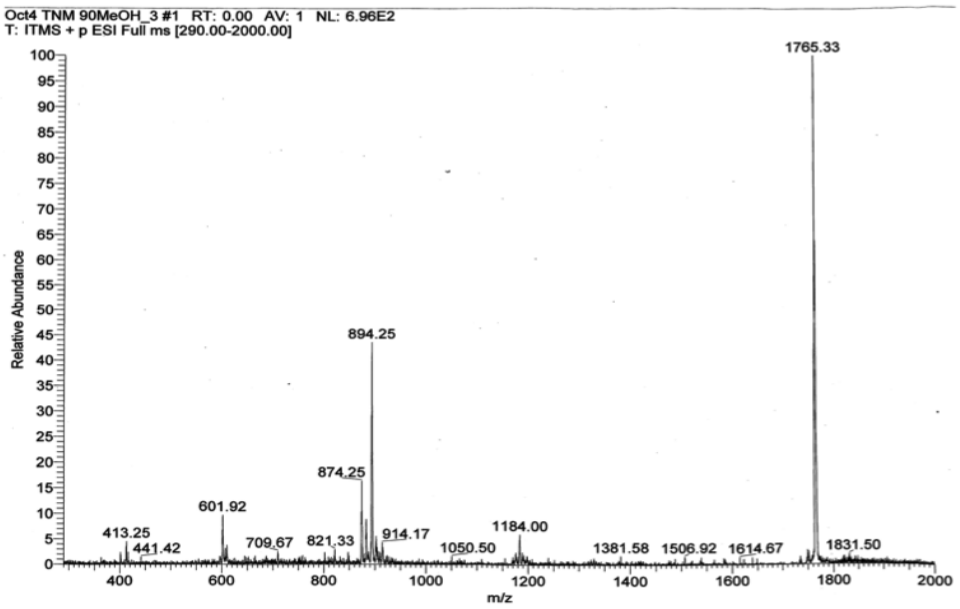

Figure 5-2. Mass Spectrum of TNM-A. Peaks at 894.25 m/z and 1765.33 m/z correspond to the half peak of $[TNM\text{-}A + Na]^{++}$ and $[TNM\text{-}A + H]^{+,}$ respectively.

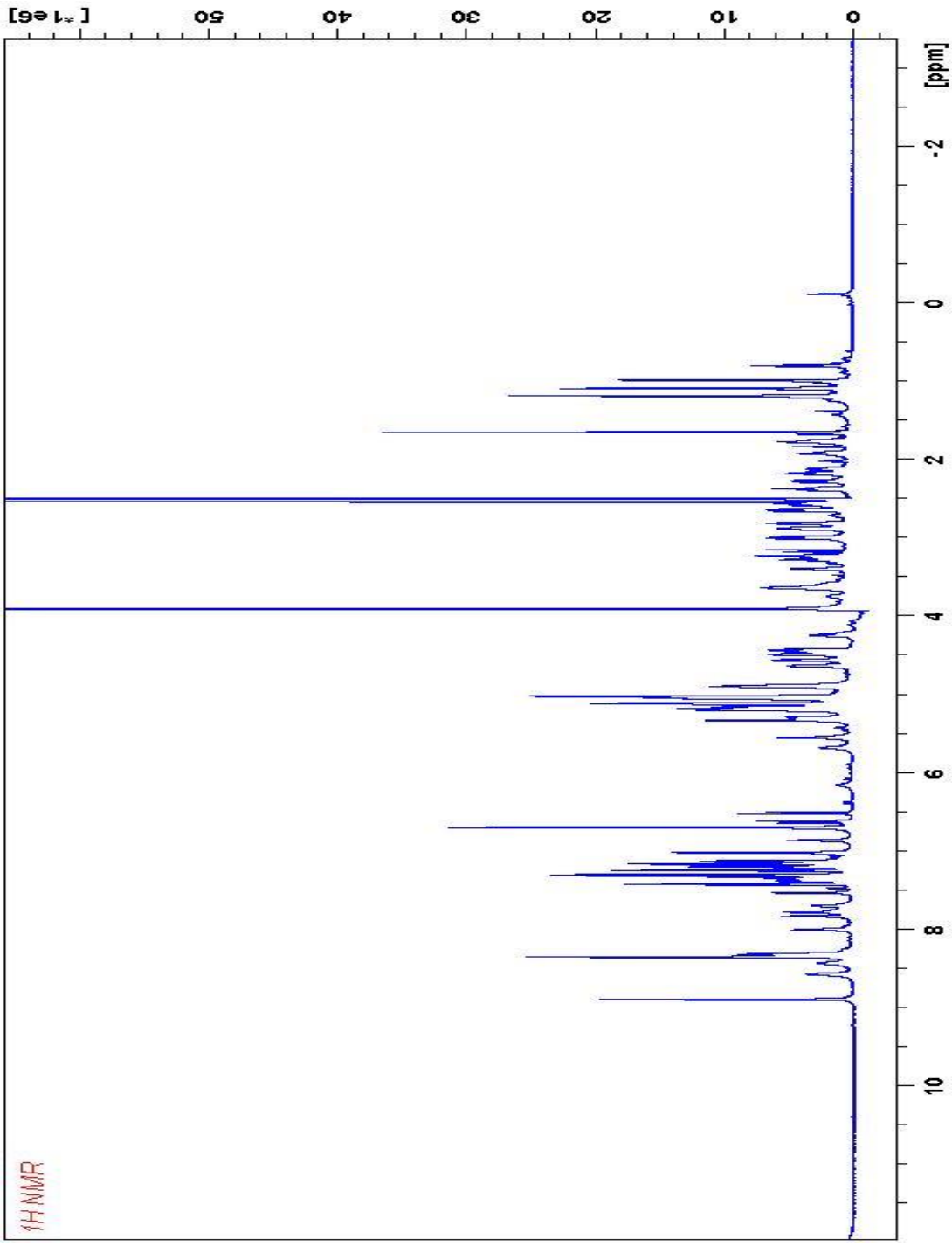

Figure 5-3. 700 MHz ^{1}H NMR spectra of TNM-A in DMSO-d_6/H_2O (4:1) obtained at 303 K.

5.3.2 1D and 2D Solution NMR Measurements for TNM-A/3β-hydroxysterol interaction studies

5.3.2.1 Sample Preparation

Samples for the NMR measurements were pure TNM-A or TNM-A/25-HC mixtures at various mole ratios. For the TNM-A/3β-hydroxysterol interactions, TNM-A and TNM-A/25-HC (1:1 mole ratio) were prepared in (4:1 v/v) DMSO-d_6/H_2O. Before transferring to a 5 mm NMR tube, the sample was degassed using a sonicator for about 15 minutes, and sealed with the NMR tube cover and parafilm afterwards. Samples for the ^{1}H NMR titration measurements were pure TNM-A (1:0 mole ratio) and TNM-A/25-HC at 1:0.5, 1:1, 1:2, and 1:3 mole ratios, prepared similarly as stated above. The final concentration of TNM-A in all samples were 1.13 mM and all NMR samples have a sample volume of 500 μL.

5.3.2.2 NMR Measurements and Data Processing

The ^{1}H NMR measurements were carried out using the Bruker AVANCE700 NMR instrument using the standard *p3919gp* water suppression pulse sequence at 298 K. For 2D NOESY NMR measurements, the *noesyesgpph* pulse sequence was used with varying mixing times at 30 ms, 50 ms, and 100 ms at 303 K. Obtained spectra were processed using the Bruker TOPSPIN ver. 3.1 program.

For the processing of ^{1}H NMR titration data, the chemical shift changes (Δδ) incurred by several TNM-A protons upon titration with increasing mole ratios of 25-HC were recorded. The dissociation constant for a dynamic peptide-ligand complex is given by

$$PL \rightleftarrows P + L$$

$$K_d = \frac{[P][L]}{[PL]} \qquad \textbf{Equation 5-1}$$

where [P], [L], and [PL] are the equilibrium peptide, ligand, and complex concentrations. A mathematical model for the 1:1 binding phenomena, described in detail in literature[4], was utilized to define the expected chemical shift changes during the titration experiment from two known ($[P]_t$ and $[L]_t$) and two unknown (K_d and $\delta_{\Delta PL}$) parameters. The TNM-A protons' chemical shift change (Δδ) as a consequence of sterol addition was plotted against [L]/[P] ratio to generate the titration curve. Non-linear curve fitting using the Excel® add-on program Solver was carried out using Equation 5-2 to find the best fit calculated binding curve to the experimental data points and obtain the K_d values for TNM-A/25-HC interaction.

$$\Delta\delta = \delta_{\Delta PL}\left[\frac{\left(K_D+[P]_t+[L]_t-\{(K_D+[P]_t+[L]_t)^2-(4*[P]_t*[L]_t)\}^{1/2}\right)}{2[P]_t}\right] \qquad \textbf{Equation 5-2}[4]$$

5.3.3 ^{2}H solid state NMR Measurements to verify TNM-A/25-HC direct interaction in membranes

5.3.3.1 Synthesis of 3*d*-25-hydroxycholesterol and 3*d*-cholesterol

Pyridinuim chlorochromate (PCC) oxidation was performed with 25-hydroxycholesterol **1** as the substrate converting it to 25-hydroxycholestenone **2**. Product **2** was purified from the crude product of the oxidation reaction by column chromatography using fluorosil as the stationary phase and eluting it with 10:1 Hexane/ethyl acetate. Sodium borodeuteride ($NaBD_4$) reduction of **2** was then carried out to introduce a deuterium atom to the C-3 position of 25-HC to obtain 3*d*-25-HC **3** (Scheme 1). 3*d*-cholesterol was synthesized in the same manner using cholesterol as the initial substrate.

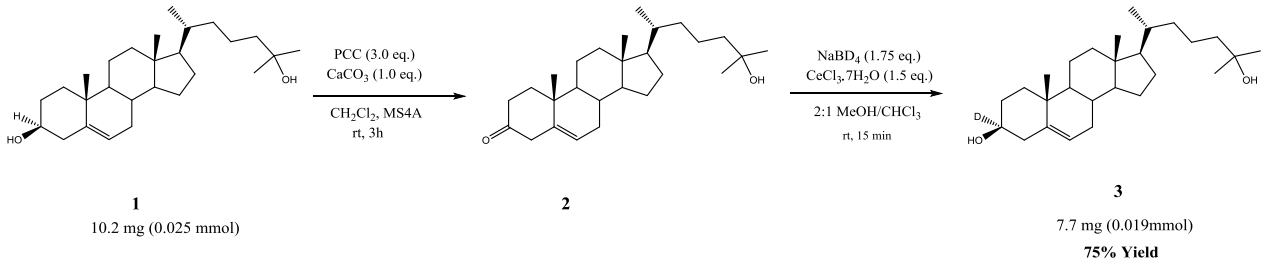

Scheme 5-2. Synthesis of 3*d*-25-hydroxycholesterol

5.3.3.2 ^{2}H and ^{31}P solid state NMR sample preparation

POPC/3*d*-25-HC (18:1 mole ratio) and POPC/3*d*-25-HC/TNM-A (18:1:1 mole ratio) samples were prepared by dissolving 35 mg POPC (0.05 mmol), 0.996 mg 3*d*-25-HC (2.57 μmol), and 0 or 4.5 mg TNM-A (2.57 μmol) in two separate 20 mL round bottom flasks with ~ 10 mL (2:1 v/v) $CHCl_3$/MeOH solvent. Lipid mixtures were vortex-mixed for a few seconds and the solvents were completely removed by rotary evaporator and vacuum drying in overnight. The resulting lipid films obtained after complete solvent drying was rehydrated with 1 mL of MilliQ H2O and sonicated to completely remove the lipids from the flask walls and were subjected to three cycles of freeze(-80^{o}C)-thaw (40^{o}C). After, lipid samples were transferred to an Eppendorf tube and lyophilized overnight to completely remove H_2O. The samples were again rehydrated with deuterium-depleted H_2O to obtain a sample concentration of 50% (w/v). After the samples were homogenized, it was transferred to a 5 mm glass tube (Wilmad) and sealed with epoxy glue. These same set of samples were used in the ^{31}P solid state NMR measurements.

5.3.3.3 Solid State NMR Measurements and Data Processing

^{2}H NMR measurements were recorded using a JEOL 400 MHz ECA400 NMR (Tokyo, Japan) spectrometer. Spectra was collected using a 5 mm ^{2}H static probe (Doty Scientific Inc., Columbia, SC) following a quadrupolar echo sequence.[2] The 90^{o} pulse width was 2 μs, interpulse delay was 30 μs, and

the repetition rate was 0.5 s. The sweep width was 200 kHz, with a scan number of about 400000. All measurements were carried out at 303K. The same NMR instrument was used for the ^{31}P NMR measurements. Spectra were collected using 7 mm CP-MAS probe (Doty Scientific Inc., Columbia, SC) without rotation. A single pulse sequence with proton decoupling was carried out with parameters: 18 ms acquisition time, 7.2 μs 90^{o} pulse width, 2 s relaxation delay, with a total number of scans of 15000. All obtained spectra were processed using the JEOL Delta ver. 5.0.4 program.

5.3.4 Diffusion Ordered Spectroscopy (DOSY NMR) for TNM-A self-aggregation studies

To estimate the self-aggregation propensities of TNM-A in aqueous environments, its diffusion coefficient in 2 solvent systems were obtained through DOSY NMR measurements. TNM-A samples were prepared in either DMSO-d_6/D_2O (4:1) or D_2O/ H_2O (98:2) solvents to obtain a final concentration of 1.2 mM. A stimulated echo sequence with bipolar gradient pulses for diffusion (stebpgp1s19) was used. Spectra were recorded at 25^{o}C with 8 scans for each of the 32 gradient steps which had the gradient strength logarithmically increased from 2% to 98% of the maximum strength (50 G/cm). The diffusion time (Δ) was set to 0.12 s and the length of the square diffusion encoding gradient pulses (δ) was set to 3 ms. To obtain a 2D DOSY spectra, the ^{1}H NMR 32 array data sets were processed using the *dosy2d* command in the Bruker TOPSPIN ver.3.1 program. The quality of the spectra were improved by adjusting the values of the noise sensitivity factor (NC=2), spike suppression factor (SpiSup=4), and the line width factor (LWF=4) and leaving the other parameters set as the default values. The diffusion coefficients *D* (m^2/s) were determined from the DOSY spectra based on the $\log_{10}$D values corresponding to the midpoint of the observed peaks. The hydrodynamic radius of TNM-A was estimated as previously reported,[5] using the obtained diffusion coefficient values through the Stoke-Einstein equation (Equation 5-3) given below,

$$r_s = \frac{k_b T}{6\pi\eta \mathrm{D}} \qquad \textbf{Equation 5-3}$$

where r_s is the hydrodynamic radius, k_b is the Boltzmann constant, T is the absolute temperature, η is the solvent viscosity, and D is the diffusion coefficient. The solvent viscosities of DMSO-d_6/D_2O (4:1) [η=0.003861 Pa•s] and D_2O/H_2O (98:2) [η=0.001095 Pa•s at 25^{o}C and η=0.0008274 Pa•s at 37^{o}C] were estimated based on reported values.[6,7]

5.3.5 Determination of Critical Micelle Concentration by Pyrene 1:3 Ratio Method

Samples containing various concentrations of TNM-A and pyrene (constant at 200 μM) were prepared in H_2O (100 mM NaCl). Then, the fluorescence emission spectra of pyrene in the samples were obtained using a JASCO FP-6500 spectrofluorometer with an excitation wavelength of 335 nm. The emission of pyrene at 374 nm (λ_1) over the emission at 383 nm (λ_3) was plotted against TNM-A concentration. This generated a decreasing sigmoidal graph similar to that shown in Figure 5-3. For the blank sample, a separate solution containing only 200 μM pyrene in H_2O (100 mM NaCl) was used. For

samples containing 25-HC, equimolar concentrations of the sterol was combined with TNM-A at various concentrations and pyrene at a constant concentration of 200 μM. All the florescence measurements were carried out at 25°C. For the data processing, the fitting parameters x_o, which is equivalent to CMC_1, and Δx were obtained by fitting the decreasing sigmoidal curve generated from the pyrene I_1/I_3 vs. TNM-A concentration or I_1/I_3 vs. log (TNM-A concentration) plots to the equation 5-4. CMC_2 was calculated by substituting the fitting parameters to equation 5-5.

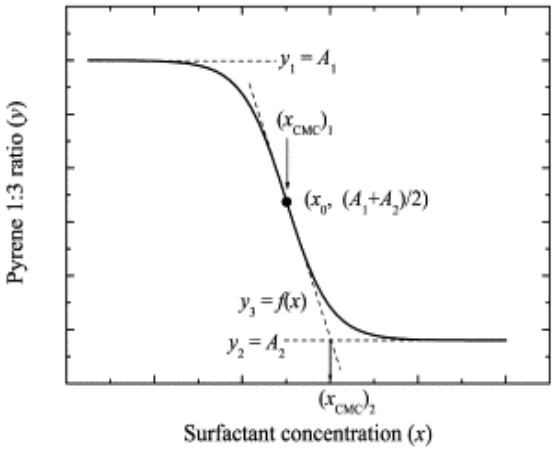

where
y = Pyrene I_1/I_3
x = total concentration of surfactant
A_1 and A_2 = upper and lower limits of sigmoid
Δx = concentration range where abrupt change in I_1/I_3 occurs
x_o = center of sigmoid ≈ χ_{CMC1}

$$y = \frac{A_1 - A_2}{1 - e^{(x - x_o)/\Delta x}} \qquad \textbf{Equation 5-4}$$

$$(x_{CMC})_2 = x_o + 2\Delta x \qquad \textbf{Equation 5-5}$$

Figure 5-4. Example of a decreasing sigmoidal curve generated from plotting pyrene I_1/I_3 vs. surfactant concentration.[8] Reprinted with permission from Figure 1 of the *Journal of Colloid and Interface Science*, **2003**, *258*, 116-122.[8] Copyright © (2003) Elsevier Science (USA).

5.3.6 Differential Interference and Confocal Microscopy Measurements

GUVs used for differential interference or confocal microscopy measurements were either pure POPC or POPC/chol at a 9:1 mole ratio. GUVs were formed through the electroformation method previously reported.[9] Briefly, specific amounts of POPC or POPC/chol were mixed in $CHCl_3$ or $CHCl_3$/MeOH (4:1 v/v) to make a final phospholipid concentration of 1mg/mL. 15-20 μL aliquots were deposited to parallel-aligned Pt electrodes mounted to a 1 mm thick 24x60 mm glass side. After drying the solvent under vacuum overnight, a silicon space filler was added in between the slide holding the electrodes and a sealer glass slide. MilliQ H_2O (300-500 μL) was injected through the fill port to completely immerse the electrodes and the slide was kept in a thermostated objective plate (Tokai Hit ThermoPlate, Tokai Hit Co., Ltd.) at 40°C with an applied alternating current (10 V, 10 Hz) for 1 hour to form the GUVs (Arbitrary Waveform Generator 33220A, Agilent Technologies). Pure TNM-A or TNM-A with 10 mol% of fluorescent TNM-DCCH dissolved in MilliQ H_2O was injected to the formed GUVs through the fill port to obtain a final concentration of 20 μM. Time-course observations were carried out at 27°C for 1 hour using the FluoView™ FV1000-D scanning unit with an IX81 inverted microscope (Olympus Corp.). A LUCPLFLN 60x universal semi-apochromat objective with an NA of 0.70 (Olympus Corp.) was used for the observations. Acquisition speed was 8 μs/pixel and images were visualized using the FV10-ASW-3.0 software. Contrast was edited using Adobe Photoshop CS6 to provide clear confocal

images. TNM-DCCH has an excitation wavelength of λ_{ex} = 415 nm and an emission wavelength of λ_{em} = 480 nm.

5.3.7 ^{1}H NMR Paramagnetic Quenching Measurements

5.3.7.1 Sample Preparation

Paramagnetic quenching of TNM-A ^{1}H resonances by Mn^{2+} was carried out to assess the membrane localization of TNM-A in SDS-d_{25} micelles or DMPC-d_{54}/DHPC-d_{22} bicelles (q=0.5) free or containing cholesterol. For TNM-A samples containing micelles, SDS-d_{25} micellar solution was mixed with TNM-A in 500 µL of 10 mM PBS buffer (100 mM NaCl, pH=7.4) to obtain a final detergent and peptide concentration of 20 mM and 0.2 mM, respectively. The TNM-A samples containing bicelles were prepared by dissolving 10 mg DHPC-d_{22} (21.06 µmol), 7.7 mg DMPC-d_{54} (10.50 µmol), 0 or 0.406 mg cholesterol (1.05 µmol), and 0.175 mg TNM-A (0.1 µmol) in 3 mL $CHCl_3$/MeOH (1:1 v/v) in a round bottom flask. After mixing the components thoroughly, the solvents was evaporated and completely dried in vacuum for over 8 hours. The obtained lipid film was rehydrated with 200 µL of 100 mM NaCl in D_2O and occasionally vortex mixed at room temperature for 1 hour to form the bicelles.

5.3.7.2 NMR Measurements

The ^{1}H NMR spectra of 0.2 mM TNM-A in the absence or presence of 20 mM deuterated SDS-d_{25} micelles [10 mM PBS buffer, 100 mM NaCl, (pH = 7.4)] or Cho-free and Cho-containing DMPC-d_{54}/DHPC-d_{22} bicelles [(q=0.5) 160 mM total phospholipid concentration in 100 mM NaCl in D_2O] were first acquired at 310 K with 512 scans and a recycle delay of 3 s using a Bruker 700 MHz NMR. After, increasing concentrations of $MnCl_2$ (20 µM, 40 µM, 80 µM, 160µM were added to the samples and ^{1}H NMR spectra were again acquired after each titration step using the same NMR measurement parameters. The ^{1}H NMR spectra of pure TNM-A in the absence of any model membranes but with the same increasing concentrations of $MnCl_2$ were also acquired to assess the effect of the paramagnetic quencher to the resonances of the peptide alone.

References:

1. Nishimura, S. *et al.* Visualization of sterol-rich membrane domains with fluorescently-labeled theonellamides. *PLoS One* **8,** 8–13 (2013).

2. Matsumori, N. *et al.* Direct interaction between amphotericin B and ergosterol in lipid bilayers as revealed by 2H NMR spectroscopy. *J. Am. Chem. Soc.* **131,** 11855–11860 (2009).

3. Matsunaga, S. & Fusetani, N. Theonellamides A-E, cytotoxic bicyclic peptides, from a marine sponge Theonella sp. *J. Org. Chem.* **60,** 1177–1181 (1995).

4. Thordarson, P. Determining association constants from titration experiments in supramolecular chemistry. *Chem. Soc. Rev.* **40,** 1305–1323 (2011).

5. Wang, C. K. *et al.* Translational Di ff usion of Cyclic Peptides Measured Using Pulsed- Field Gradient NMR. *J. Phys. Chem.* **118,** 11129–11136 (2014).

6. Sacco, A. & Matteoli, E. Isotopic substitution effects on the volumetric and viscosimetric properties of water-dimethylsulfoxide mixtures at 25° C. *J. Solution Chem.* **26,** 527–535 (1997).

7. Cho, C. H., Urquidi, J., Singh, S. & Robinson, G. W. Thermal Offset Viscosities of Liquid H2O, D2O, and T2O. *J. Phys. Chem. B* **103,** 1991–1994 (1999).

8. Aguiar, J., Carpena, P., Molina-Bol??var, J. A. & Carnero Ruiz, C. On the determination of the critical micelle concentration by the pyrene 1:3 ratio method. *J. Colloid Interface Sci.* **258,** 116–122 (2003).

9. Angelova, M. & Dimitrov, D. No Title. *Faraday Discuss. Chem. Soc.* **81,** 303–311 (1986).

Acknowledgments

First of all, I would like to thank God Almighty for leading me to where I am today. I am always grateful for all the blessings that he has given me, just like this opportunity to further my studies abroad. Because of him, I have the strength and persistence to endure all the difficult times I encountered, not only in my academic career but also in my personal life.

I would like to thank my mother Vida, sister Jennifer, and the rest of my immediate and extended family. Their constant reassurance especially when I am very frustrated with work helps me to keep moving forward and feel better - that everything will turn out right, as how the Lord planned it to be. Mama, thank you very much for visiting me in Osaka when you can. My apartment feels so much like home when you are present. Thank you for always checking on me, every day. Thank you for everything! To the special person in my life, Enzo. Thank you for all the support and encouragement. Thank you for staying beside me especially when things get tough. Papa, thank you so much! I know you are looking after me from the heavens.

I would like to extend my deepest gratitude to Professor Michio Murata for giving me the chance to study in Osaka University and accepting me in his laboratory. I am very thankful for all his guidance, advice, and concern during my entire stay in his laboratory. If not for him, I wouldn't have made it to Osaka University. I would also like to thank Professor Nobuaki Matsumori, Professor Shinya Hanashima, and Professor Hiroshi Tsuchikawa for all their valuable advice and guidance.

I would also like to express my gratitude to Professor Gerardo Janairo for encouraging me to pursue graduate studies abroad and introducing me to Professor Murata. Thank you for your advice and guidance. To all my teachers and co-faculty members from De La Salle University Chemistry department, thank you for all the very enjoyable and comforting conversations. Even though I am no longer teaching, I feel that I am still part of the family.

To my labmates, thank you for making my stay in Murata laboratory very memorable. There are so many memories that I have with all of you. To my tutor, Haruka Saiki, thank you for all your help in everything. I appreciate how you made me feel very acquainted to the laboratory life and to life in Japan in general. To Dian Kurniati and Huey Huang, although we only stayed together in the lab for a few semester, thank you for helping me adjust to the researcher life in Japan especially in my first few months in the laboratory. Thank you for being my constant companions for lunch and dinner. To Misaki Yofu, I am sincerely indebted to you for all the help you've given me. Thank you for always deciding what's best for me and my lab mates. Thank you for taking care of me during my entire stay in Japan. To Kaori Oshima, thank you for all your advice and assistance whenever I have problems with experiments. Thank you for all your concern and help. Thank you to everyone for the friendship.

Finally, to my friends in Osaka, especially to Milli and Raymond, thank you very much for making Japan feel like home. Thank you for helping me de-stress. Thank you for all the very enjoyable trips, sleepovers, Karaoke nights, parties, movie/eating marathons. To my friend Frem, thank you for everything! Although you're in Australia, thank you for all the constant reminders that everything will be fine. Thank you for all the concern and for always cheering me up. To all my blockmates in college and my teammates in DLSU, thank you for all the encouragement!

Appendix I

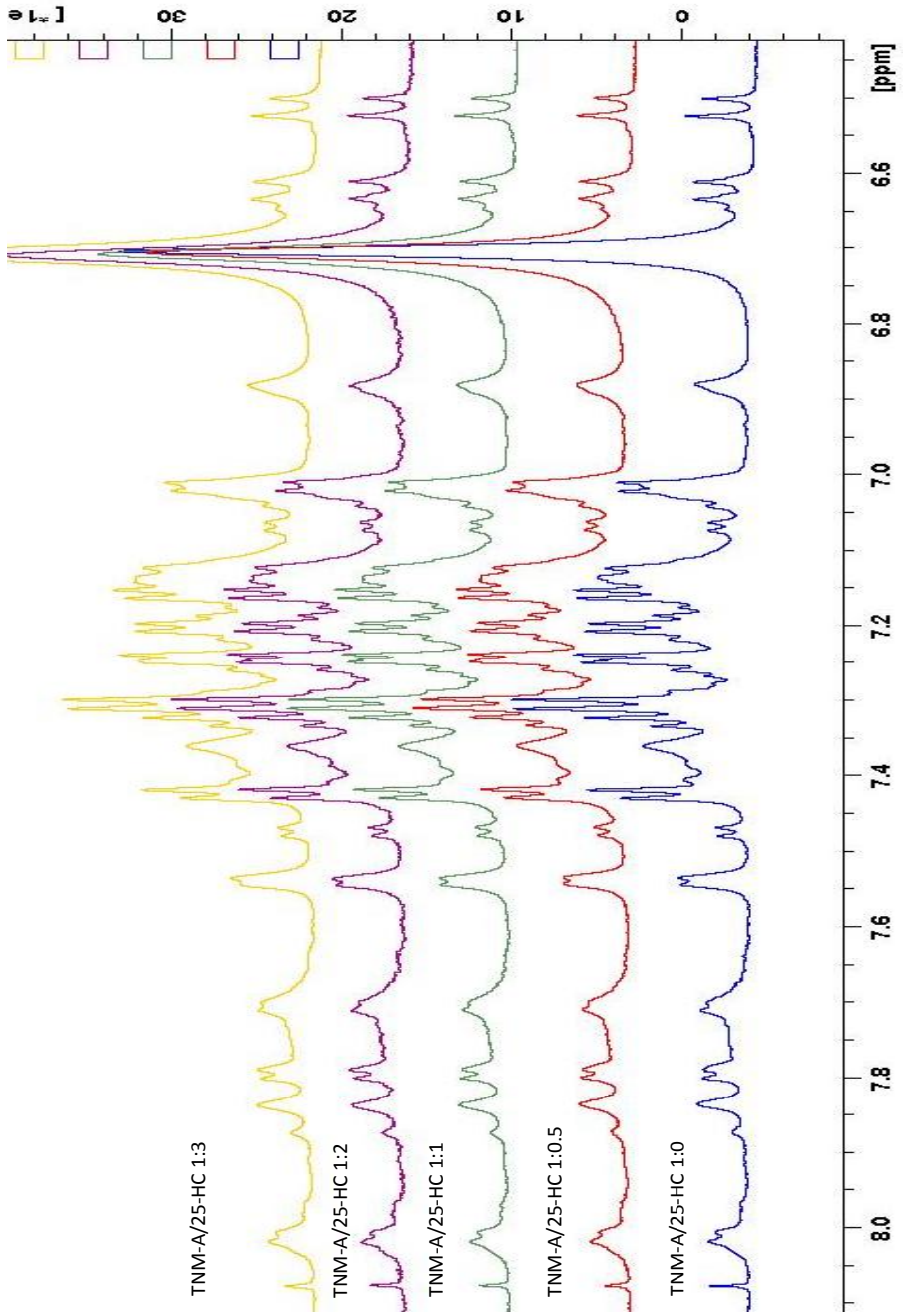

Figure A1. Overlay of a portion of the 700 MHz ^{1}H NMR Spectra of TNM-A and TNM-A/25-HC at different mole ratios obtained from ^{1}H NMR titration measurements. All samples were in DMSO-d_6/H_2O (4:1) solvent and ^{1}H NMR measurements were all at 30^{o}C.

Appendix II

Reprint Permissions

JOHN WILEY AND SONS LICENSE TERMS AND CONDITIONS

Jun 05, 2016

This Agreement between Kimberly B Cornelio ("You") and John Wiley and Sons ("John Wiley and Sons") consists of your license details and the terms and conditions provided by John Wiley and Sons and Copyright Clearance Center.

License Number	3882800397892
License date	Jun 05, 2016
Licensed Content Publisher	John Wiley and Sons
Licensed Content Publication	The Chemical Record
Licensed Content Title	Bioactive Structure of Membrane Lipids and Natural Products Elucidated by a Chemistry-Based Approach
Licensed Content Author	Michio Murata,Shigeru Sugiyama,Shigeru Matsuoka,Nobuaki Matsumori
Licensed Content Date	Jun 30, 2015
Licensed Content Pages	16
Type of use	Dissertation/Thesis
Requestor type	University/Academic
Format	Print and electronic
Portion	Figure/table
Number of figures/tables	1
Original Wiley figure/table number(s)	Figure 1
Will you be translating?	No
Title of your thesis / dissertation	Mechanism of action of the marine sponge derived bicyclic peptide Theonellamide A
Expected completion date	Aug 2016
Expected size (number of pages)	100
Requestor Location	Kimberly B Cornelio Laboratory for Biomolecular Chemistry 1-1 Machikaneyama, Toyonaka Osaka, 560-0043 Japan Attn: Kimberly B Cornelio
Publisher Tax ID	EU826007151
Billing Type	Invoice
Billing Address	Kimberly B Cornelio Laboratory for Biomolecular Chemistry 1-1 Machikaneyama, Toyonaka

Figure A2-1. Reprint permission for Figure 1-1 of thesis from *Chem. Rec.* **2015,** *00*, 1-16.

NATURE PUBLISHING GROUP LICENSE TERMS AND CONDITIONS

Jun 06, 2016

This Agreement between Kimberly B Cornelio ("You") and Nature Publishing Group ("Nature Publishing Group") consists of your license details and the terms and conditions provided by Nature Publishing Group and Copyright Clearance Center.

License Number	3883360571466
License date	Jun 06, 2016
Licensed Content Publisher	Nature Publishing Group
Licensed Content Publication	Nature Reviews Molecular Cell Biology
Licensed Content Title	Cellular cholesterol trafficking and compartmentalization
Licensed Content Author	Elina Ikonen
Licensed Content Date	Feb 1, 2008
Licensed Content Volume Number	9
Licensed Content Issue Number	2
Type of Use	reuse in a dissertation / thesis
Requestor type	academic/educational
Format	print and electronic
Portion	figures/tables/illustrations
Number of figures/tables/illustrations	1
High-res required	no
Figures	Box 1 Cellular cholesterol trafficking and compartmentalization
Author of this NPG article	no
Your reference number	
Title of your thesis / dissertation	Mechanism of action of the marine sponge derived bicyclic peptide Theonellamide A
Expected completion date	Aug 2016
Estimated size (number of pages)	100
Requestor Location	Kimberly B Cornelio Laboratory for Biomolecular Chemistry 1-1 Machikaneyama, Toyonaka Osaka, 560-0043 Japan Attn: Kimberly B Cornelio
Billing Type	Invoice
Billing Address	Kimberly B Cornelio

Figure A2-2. Reprint permission for Figure 1-2 of thesis from *Nat. Rev. Mol. Cell Biol.* **2008,** *9*, 125-138.

ROYAL SOCIETY OF CHEMISTRY LICENSE TERMS AND CONDITIONS

Jun 06, 2016

This Agreement between Kimberly B Cornelio ("You") and Royal Society of Chemistry ("Royal Society of Chemistry") consists of your license details and the terms and conditions provided by Royal Society of Chemistry and Copyright Clearance Center.

License Number	3883361095466
License date	Jun 06, 2016
Licensed Content Publisher	Royal Society of Chemistry
Licensed Content Publication	Organic & Biomolecular Chemistry
Licensed Content Title	NMR structure determination and calcium binding effects of lipopeptide antibiotic daptomycin
Licensed Content Author	Lee-Jon Ball,Catherine M. Goult,James A. Donarski,Jason Micklefield,Vasudevan Ramesh
Licensed Content Date	Jun 15, 2004
Licensed Content Volume Number	2
Licensed Content Issue Number	13
Type of Use	Thesis/Dissertation
Requestor type	academic/educational
Portion	figures/tables/images
Number of figures/tables/images	1
Format	print and electronic
Distribution quantity	10
Will you be translating?	no
Order reference number	
Title of the thesis/dissertation	Mechanism of action of the marine sponge derived bicyclic peptide Theonellamide A
Expected completion date	Aug 2016
Estimated size	100
Requestor Location	Kimberly B Cornelio Laboratory for Biomolecular Chemistry 1-1 Machikaneyama, Toyonaka Osaka, 560-0043 Japan Attn: Kimberly B Cornelio
Billing Type	Invoice
Billing Address	Kimberly B Cornelio

Figure A2-3. Reprint permission for Figure 1-3 of thesis from *Org. Biomol. Chem*. **2004**, *2*, 1872-1878.

RightsLink®

Home | Account Info | Help | Live Chat

Title:	Antimicrobial peptides: pore formers or metabolic inhibitors in bacteria?
Author:	Kim A. Brogden
Publication:	Nature Reviews Microbiology
Publisher:	Nature Publishing Group
Date:	Mar 1, 2005

Logged in as:
Kimberly Cornelio
Account #:
3001034647
LOGOUT

Order Completed

Thank you for your order.

This Agreement between Kimberly B Cornelio ("You") and Nature Publishing Group ("Nature Publishing Group") consists of your license details and the terms and conditions provided by Nature Publishing Group and Copyright Clearance Center.

Your confirmation email will contain your order number for future reference.

Get the printable license.

License Number	3883370205011
License date	Jun 06, 2016
Licensed Content Publisher	Nature Publishing Group
Licensed Content Publication	Nature Reviews Microbiology
Licensed Content Title	Antimicrobial peptides: pore formers or metabolic inhibitors in bacteria?
Licensed Content Author	Kim A. Brogden
Licensed Content Date	Mar 1, 2005
Licensed Content Volume	3
Licensed Content Issue	3
Type of Use	reuse in a dissertation / thesis
Requestor type	academic/educational
Format	print and electronic
Portion	figures/tables/illustrations
Number of figures/tables/illustrations	3
High-res required	no
Figures	Figure 3, 4, and 5
Author of this NPG article	no
Your reference number	
Title of your thesis / dissertation	Mechanism of action of the marine sponge derived bicyclic peptide Theonellamide A
Expected completion date	Aug 2016
Estimated size (number of pages)	100
Requestor Location	Kimberly B Cornelio Laboratory for Biomolecular Chemistry 1-1 Machikaneyama, Toyonaka Osaka, 560-0043 Japan Attn: Kimberly B Cornelio
Billing Type	Invoice
Billing address	Kimberly B Cornelio

Figure A2-4. Reprint permission for Figure 1-5 to 1-7 of thesis from *Nat. Rev. Microbiol.*, **2005**, *3*, 238-250.

JOHN WILEY AND SONS LICENSE TERMS AND CONDITIONS

Jun 06, 2016

This Agreement between Kimberly B Cornelio ("You") and John Wiley and Sons ("John Wiley and Sons") consists of your license details and the terms and conditions provided by John Wiley and Sons and Copyright Clearance Center.

License Number	3883370676153
License date	Jun 06, 2016
Licensed Content Publisher	John Wiley and Sons
Licensed Content Publication	Biopolymers
Licensed Content Title	Mode of action of linear amphipathic α-helical antimicrobial peptides
Licensed Content Author	Ziv Oren,Yechiel Shai
Licensed Content Date	May 6, 1999
Licensed Content Pages	13
Type of use	Dissertation/Thesis
Requestor type	University/Academic
Format	Print and electronic
Portion	Figure/table
Number of figures/tables	1
Original Wiley figure/table number(s)	Figure 1
Will you be translating?	No
Title of your thesis / dissertation	Mechanism of action of the marine sponge derived bicyclic peptide Theonellamide A
Expected completion date	Aug 2016
Expected size (number of pages)	100
Requestor Location	Kimberly B Cornelio Laboratory for Biomolecular Chemistry 1-1 Machikaneyama, Toyonaka Osaka, 560-0043 Japan Attn: Kimberly B Cornelio
Publisher Tax ID	EU826007151
Billing Type	Invoice
Billing Address	Kimberly B Cornelio Laboratory for Biomolecular Chemistry 1-1 Machikaneyama, Toyonaka Osaka, Japan 560-0043 Attn: Kimberly B Cornelio

Figure A2-5. Reprint permission for Figure 1-5 to 1-7 of thesis from *Biopolymers*, **1998**, *47*, 451-463.

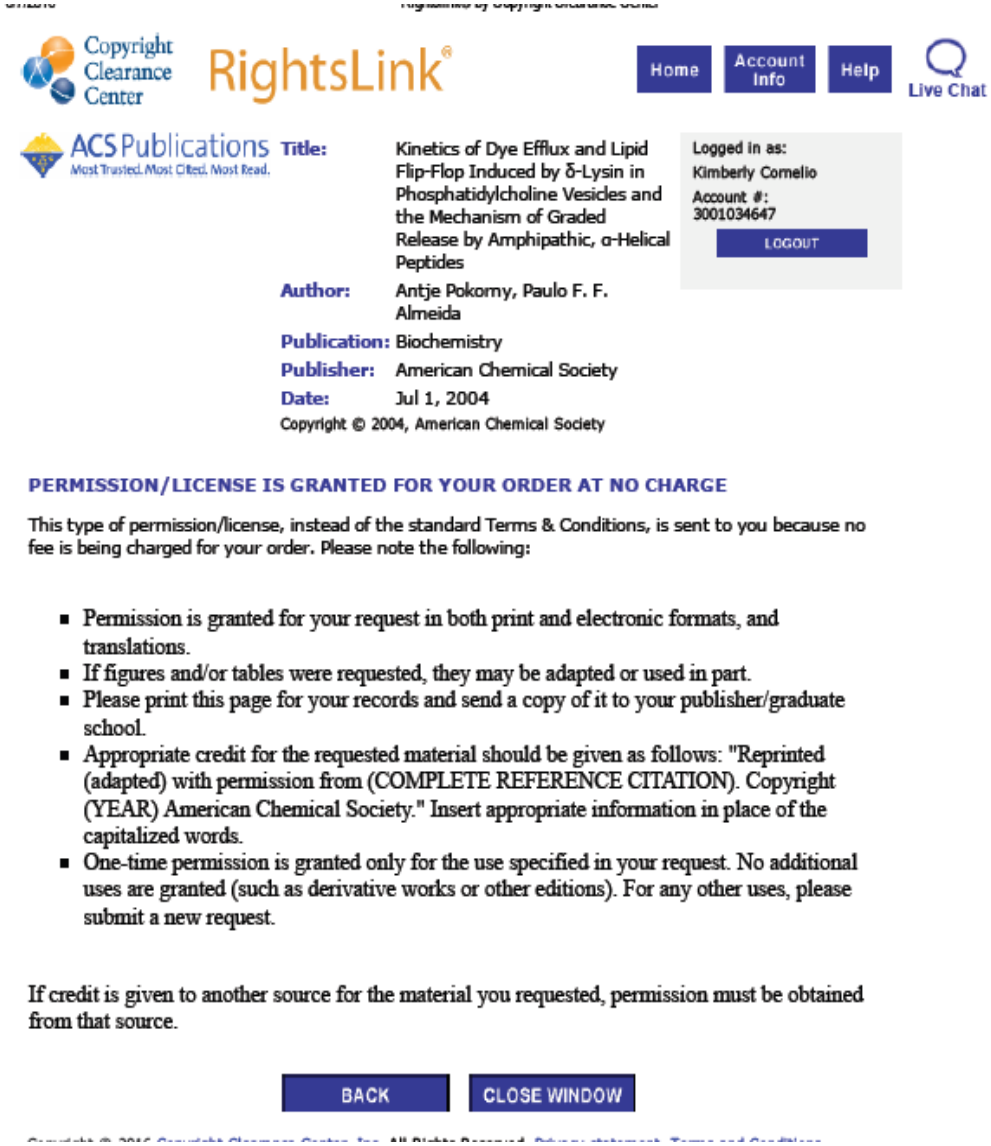

Copyright Clearance Center RightsLink®

Home | Account Info | Help | Live Chat

ACS Publications
Most Trusted. Most Cited. Most Read.

Title: Kinetics of Dye Efflux and Lipid Flip-Flop Induced by δ-Lysin in Phosphatidylcholine Vesicles and the Mechanism of Graded Release by Amphipathic, α-Helical Peptides

Author: Antje Pokorny, Paulo F. F. Almeida

Publication: Biochemistry

Publisher: American Chemical Society

Date: Jul 1, 2004

Copyright © 2004, American Chemical Society

Logged in as:
Kimberly Cornelio
Account #:
3001034647
LOGOUT

PERMISSION/LICENSE IS GRANTED FOR YOUR ORDER AT NO CHARGE

This type of permission/license, instead of the standard Terms & Conditions, is sent to you because no fee is being charged for your order. Please note the following:

- Permission is granted for your request in both print and electronic formats, and translations.
- If figures and/or tables were requested, they may be adapted or used in part.
- Please print this page for your records and send a copy of it to your publisher/graduate school.
- Appropriate credit for the requested material should be given as follows: "Reprinted (adapted) with permission from (COMPLETE REFERENCE CITATION). Copyright (YEAR) American Chemical Society." Insert appropriate information in place of the capitalized words.
- One-time permission is granted only for the use specified in your request. No additional uses are granted (such as derivative works or other editions). For any other uses, please submit a new request.

If credit is given to another source for the material you requested, permission must be obtained from that source.

BACK | CLOSE WINDOW

Figure A2-6. Reprint permission for Figure 1-8 of thesis from *Biochemistry*, **2004**, *43*, 8846-8857.

6/7/2016 Rightslink® by Copyright Clearance Center

Copyright Clearance Center RightsLink®

Home | Account Info | Help | Live Chat

ACS Publications Most Trusted. Most Cited. Most Read.

Title: Permeabilization of Raft-Containing Lipid Vesicles by δ-Lysin: A Mechanism for Cell Sensitivity to Cytotoxic Peptides

Author: Antje Pokorny, Paulo F. F. Almeida

Publication: Biochemistry

Publisher: American Chemical Society

Date: Jul 1, 2005

Copyright © 2005, American Chemical Society

Logged in as: Kimberly Cornelio
Account #: 3001034647
LOGOUT

PERMISSION/LICENSE IS GRANTED FOR YOUR ORDER AT NO CHARGE

This type of permission/license, instead of the standard Terms & Conditions, is sent to you because no fee is being charged for your order. Please note the following:

- Permission is granted for your request in both print and electronic formats, and translations.
- If figures and/or tables were requested, they may be adapted or used in part.
- Please print this page for your records and send a copy of it to your publisher/graduate school.
- Appropriate credit for the requested material should be given as follows: "Reprinted (adapted) with permission from (COMPLETE REFERENCE CITATION). Copyright (YEAR) American Chemical Society." Insert appropriate information in place of the capitalized words.
- One-time permission is granted only for the use specified in your request. No additional uses are granted (such as derivative works or other editions). For any other uses, please submit a new request.

If credit is given to another source for the material you requested, permission must be obtained from that source.

BACK | CLOSE WINDOW

Copyright © 2016 Copyright Clearance Center, Inc. All Rights Reserved. Privacy statement. Terms and Conditions.
Comments? We would like to hear from you. E-mail us at customercare@copyright.com

Figure A2-7. Reprint permission for Figure 1-8 of thesis from *Biochemistry*, **2005**, *44*, 9538-9544.

ELSEVIER LICENSE
TERMS AND CONDITIONS

Jan 22, 2017

This Agreement between Kimberly B Cornelio ("You") and Elsevier ("Elsevier") consists of your license details and the terms and conditions provided by Elsevier and Copyright Clearance Center.

License Number	4034560928084
License date	Jan 22, 2017
Licensed Content Publisher	Elsevier
Licensed Content Publication	Progress in Lipid Research
Licensed Content Title	Role of lipids in the interaction of antimicrobial peptides with membranes
Licensed Content Author	Vitor Teixeira,Maria J. Feio,Margarida Bastos
Licensed Content Date	April 2012
Licensed Content Volume Number	51
Licensed Content Issue Number	2
Licensed Content Pages	29
Start Page	149
End Page	177
Type of Use	reuse in a thesis/dissertation
Portion	figures/tables/illustrations
Number of figures/tables/illustrations	1
Format	both print and electronic
Are you the author of this Elsevier article?	No
Will you be translating?	No
Order reference number	
Original figure numbers	3
Title of your thesis/dissertation	Mechanism of action of the marine sponge derived bicyclic peptide Theonellamide A
Expected completion date	Aug 2016
Estimated size (number of pages)	100
Elsevier VAT number	GB 494 6272 12
Requestor Location	Kimberly B Cornelio Laboratory for Biomolecular Chemistry 1-1 Machikaneyama, Toyonaka Osaka, 560-0043 Japan Attn: Kimberly B Cornelio
Total	0 JPY
Terms and Conditions	

Figure A2-8. Reprint permission for Figure 1-9 of thesis from *Prog. Lipid Res.*, **2012**, *51*, 149-177.

ELSEVIER LICENSE
TERMS AND CONDITIONS

Jun 06, 2016

This Agreement between Kimberly B Cornelio ("You") and Elsevier ("Elsevier") consists of your license details and the terms and conditions provided by Elsevier and Copyright Clearance Center.

License Number	3883380972370
License date	Jun 06, 2016
Licensed Content Publisher	Elsevier
Licensed Content Publication	Biochimica et Biophysica Acta (BBA) - Biomembranes
Licensed Content Title	Interaction of the antimicrobial peptide pheromone Plantaricin A with model membranes: Implications for a novel mechanism of action
Licensed Content Author	Hongxia Zhao,Rohit Sood,Arimatti Jutila,Shambhunath Bose,Gunnar Fimland,Jon Nissen-Meyer,Paavo K.J. Kinnunen
Licensed Content Date	September 2006
Licensed Content Volume Number	1758
Licensed Content Issue Number	9
Licensed Content Pages	14
Start Page	1461
End Page	1474
Type of Use	reuse in a thesis/dissertation
Intended publisher of new work	other
Portion	figures/tables/illustrations
Number of figures/tables/illustrations	1
Format	both print and electronic
Are you the author of this Elsevier article?	No
Will you be translating?	No
Order reference number	
Original figure numbers	Figure 13
Title of your thesis/dissertation	Mechanism of action of the marine sponge derived bicyclic peptide Theonellamide A
Expected completion date	Aug 2016
Estimated size (number of pages)	100
Elsevier VAT number	GB 494 6272 12

Figure A2-9. Reprint permission for Figure 1-10 of thesis from *Biochimica et Biophysica Acta*, **2006**, *1758*, 1461–1474.

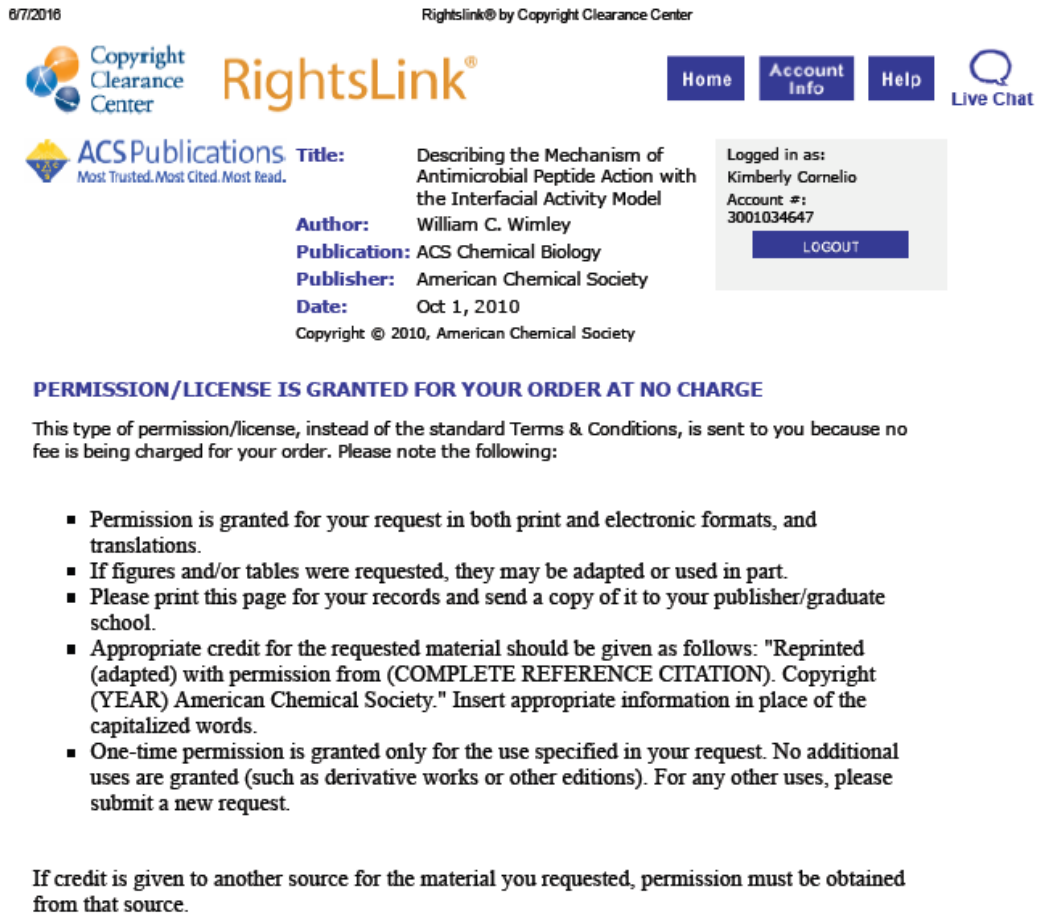

Figure A2-10. Reprint permission for Figure 1-11 of thesis from *ACS Chem. Biol.*, **2010**, *5*, 905-917.

ELSEVIER LICENSE
TERMS AND CONDITIONS

Jun 06, 2016

This Agreement between Kimberly B Cornelio ("You") and Elsevier ("Elsevier") consists of your license details and the terms and conditions provided by Elsevier and Copyright Clearance Center.

License Number	3883381508706
License date	Jun 06, 2016
Licensed Content Publisher	Elsevier
Licensed Content Publication	Biochimica et Biophysica Acta (BBA) - Biomembranes
Licensed Content Title	Toroidal pores formed by antimicrobial peptides show significant disorder
Licensed Content Author	Durba Sengupta,Hari Leontiadou,Alan E. Mark,Siewert-Jan Marrink
Licensed Content Date	October 2008
Licensed Content Volume Number	1778
Licensed Content Issue Number	10
Licensed Content Pages	10
Start Page	2308
End Page	2317
Type of Use	reuse in a thesis/dissertation
Portion	figures/tables/illustrations
Number of figures/tables/illustrations	1
Format	both print and electronic
Are you the author of this Elsevier article?	No
Will you be translating?	No
Order reference number	
Original figure numbers	Figure 2
Title of your thesis/dissertation	Mechanism of action of the marine sponge derived bicyclic peptide Theonellamide A
Expected completion date	Aug 2016
Estimated size (number of pages)	100
Elsevier VAT number	GB 494 6272 12
Requestor Location	Kimberly B Cornelio Laboratory for Biomolecular Chemistry 1-1 Machikaneyama, Toyonaka

Figure A2-11. Reprint permission for Figure 1-11 of thesis from *Biochim. Biophys. Acta*, ***2008***, *1778*, 2308-2317.

JOHN WILEY AND SONS LICENSE TERMS AND CONDITIONS

Jun 06, 2016

This Agreement between Kimberly B Cornelio ("You") and John Wiley and Sons ("John Wiley and Sons") consists of your license details and the terms and conditions provided by John Wiley and Sons and Copyright Clearance Center.

License Number	3883390325636
License date	Jun 06, 2016
Licensed Content Publisher	John Wiley and Sons
Licensed Content Publication	Concepts in Magnetic Resonance: Part A, Bridging Education and Research
Licensed Content Title	NMR methods for studying membrane-active antimicrobial peptides
Licensed Content Author	Erik Strandberg,Anne S. Ulrich
Licensed Content Date	Nov 9, 2004
Licensed Content Pages	32
Type of use	Dissertation/Thesis
Requestor type	University/Academic
Format	Print and electronic
Portion	Figure/table
Number of figures/tables	1
Original Wiley figure/table number(s)	Figure 4
Will you be translating?	No
Title of your thesis / dissertation	Mechanism of action of the marine sponge derived bicyclic peptide Theonellamide A
Expected completion date	Aug 2016
Expected size (number of pages)	100
Requestor Location	Kimberly B Cornelio Laboratory for Biomolecular Chemistry 1-1 Machikaneyama, Toyonaka Osaka, 560-0043 Japan Attn: Kimberly B Cornelio
Publisher Tax ID	EU826007151
Billing Type	Invoice
Billing Address	Kimberly B Cornelio Laboratory for Biomolecular Chemistry 1-1 Machikaneyama, Toyonaka Osaka, Japan 560-0043

Figure A2-12. Reprint permission for Figure 1-12 of thesis from *Concepts in Magnetic Resonance (Part A)*, **2004**, *23A (2)*, 89-120.

ELSEVIER LICENSE
TERMS AND CONDITIONS

Jun 06, 2016

This Agreement between Kimberly B Cornelio ("You") and Elsevier ("Elsevier") consists of your license details and the terms and conditions provided by Elsevier and Copyright Clearance Center.

License Number	3882900089656
License date	Jun 06, 2016
Licensed Content Publisher	Elsevier
Licensed Content Publication	Chemistry & Biology
Licensed Content Title	Fluorescent Probes for Lipid Rafts: From Model Membranes to Living Cells
Licensed Content Author	Andrey S. Klymchenko,Rémy Kreder
Licensed Content Date	16 January 2014
Licensed Content Volume Number	21
Licensed Content Issue Number	1
Licensed Content Pages	17
Start Page	97
End Page	113
Type of Use	reuse in a thesis/dissertation
Portion	figures/tables/illustrations
Number of figures/tables/illustrations	1
Format	both print and electronic
Are you the author of this Elsevier article?	No
Will you be translating?	No
Order reference number	
Original figure numbers	Figure 3
Title of your thesis/dissertation	Mechanism of action of the marine sponge derived bicyclic peptide Theonellamide A
Expected completion date	Aug 2016
Estimated size (number of pages)	100
Elsevier VAT number	GB 494 6272 12
Requestor Location	Kimberly B Cornelio Laboratory for Biomolecular Chemistry 1-1 Machikaneyama, Toyonaka

Figure A2-13. Reprint permission for Figure 1-13 of thesis from *Chemistry & Biology*. **2014**, *21(1)*, 97-113.

NATURE PUBLISHING GROUP LICENSE TERMS AND CONDITIONS

Jun 08, 2016

This Agreement between Kimberly B Cornelio ("You") and Nature Publishing Group ("Nature Publishing Group") consists of your license details and the terms and conditions provided by Nature Publishing Group and Copyright Clearance Center.

License Number	3884140086292
License date	Jun 08, 2016
Licensed Content Publisher	Nature Publishing Group
Licensed Content Publication	Nature Reviews Microbiology
Licensed Content Title	Genomic insights into the marine sponge microbiome
Licensed Content Author	Ute Hentschel, Jörn Piel, Sandie M. Degnan and Michael W. Taylor
Licensed Content Date	Sep 1, 2012
Licensed Content Volume Number	10
Licensed Content Issue Number	9
Type of Use	reuse in a dissertation / thesis
Requestor type	academic/educational
Format	print and electronic
Portion	figures/tables/illustrations
Number of figures/tables/illustrations	1
High-res required	no
Figures	Figure 1
Author of this NPG article	no
Your reference number	
Title of your thesis / dissertation	Mechanism of action of the marine sponge derived bicyclic peptide Theonellamide A
Expected completion date	Aug 2016
Estimated size (number of pages)	100
Requestor Location	Kimberly B Cornelio Laboratory for Biomolecular Chemistry 1-1 Machikaneyama, Toyonaka Osaka, 560-0043 Japan Attn: Kimberly B Cornelio
Billing Type	Invoice
Billing Address	Kimberly B Cornelio

Figure A2-14. Reprint permission for Figure 1-14 and 1-15 of thesis from *Nature Reviews Microbiology*, **2012**, *10*, 641-654.

JOHN WILEY AND SONS LICENSE TERMS AND CONDITIONS

Jun 08, 2016

This Agreement between Kimberly B Cornelio ("You") and John Wiley and Sons ("John Wiley and Sons") consists of your license details and the terms and conditions provided by John Wiley and Sons and Copyright Clearance Center.

License Number	3884140627120
License date	Jun 08, 2016
Licensed Content Publisher	John Wiley and Sons
Licensed Content Publication	Environmental Microbiology
Licensed Content Title	Marine sponges and their microbial symbionts: love and other relationships
Licensed Content Author	Nicole S. Webster,Michael W. Taylor
Licensed Content Date	Mar 28, 2011
Licensed Content Pages	12
Type of use	Dissertation/Thesis
Requestor type	University/Academic
Format	Print and electronic
Portion	Figure/table
Number of figures/tables	1
Original Wiley figure/table number(s)	Figure 3
Will you be translating?	No
Title of your thesis / dissertation	Mechanism of action of the marine sponge derived bicyclic peptide Theonellamide A
Expected completion date	Aug 2016
Expected size (number of pages)	100
Requestor Location	Kimberly B Cornelio Laboratory for Biomolecular Chemistry 1-1 Machikaneyama, Toyonaka Osaka, 560-0043 Japan Attn: Kimberly B Cornelio
Publisher Tax ID	EU826007151
Billing Type	Invoice
Billing Address	Kimberly B Cornelio Laboratory for Biomolecular Chemistry 1-1 Machikaneyama, Toyonaka Osaka, Japan 560-0043

Figure A2-15. Reprint permission for Figure 1-14 of thesis from *Environ. Microbiol.*, **2012**, *14*, 335-346.

SPRINGER LICENSE
TERMS AND CONDITIONS

Jun 08, 2016

This Agreement between Kimberly B Cornelio ("You") and Springer ("Springer") consists of your license details and the terms and conditions provided by Springer and Copyright Clearance Center.

License Number	3884140911293
License date	Jun 08, 2016
Licensed Content Publisher	Springer
Licensed Content Publication	Marine Biotechnology
Licensed Content Title	Theonellamide F, a Bicyclic Peptide Marine Toxin, Induces Formation of Vacuoles in 3Y1 Rat Embryonic Fibroblast
Licensed Content Author	Shun-ichi Wada
Licensed Content Date	Dec 31, 1969
Licensed Content Volume Number	1
Licensed Content Issue Number	4
Type of Use	Thesis/Dissertation
Portion	Figures/tables/illustrations
Number of figures/tables/illustrations	1
Author of this Springer article	No
Order reference number	
Original figure numbers	Figure 2
Title of your thesis / dissertation	Mechanism of action of the marine sponge derived bicyclic peptide Theonellamide A
Expected completion date	Aug 2016
Estimated size(pages)	100
Requestor Location	Kimberly B Cornelio Laboratory for Biomolecular Chemistry 1-1 Machikaneyama, Toyonaka Osaka, 560-0043 Japan Attn: Kimberly B Cornelio
Billing Type	Invoice
Billing Address	Kimberly B Cornelio Laboratory for Biomolecular Chemistry 1-1 Machikaneyama, Toyonaka Osaka, Japan 560-0043 Attn: Kimberly B Cornelio

Figure A2-16. Reprint permission for Figure 1-16 of thesis from *Mar. Biotechnol.*, **1999**, *1*, 337-341.

NATURE PUBLISHING GROUP LICENSE TERMS AND CONDITIONS

Jun 08, 2016

This Agreement between Kimberly B Cornelio ("You") and Nature Publishing Group ("Nature Publishing Group") consists of your license details and the terms and conditions provided by Nature Publishing Group and Copyright Clearance Center.

License Number	3884141129867
License date	Jun 08, 2016
Licensed Content Publisher	Nature Publishing Group
Licensed Content Publication	Nature Chemical Biology
Licensed Content Title	Marine antifungal theonellamides target 3β-hydroxysterol to activate Rho1 signaling
Licensed Content Author	Shinichi Nishimura, Yuko Arita, Miyuki Honda, Kunihiko Iwamoto, Akihisa Matsuyama, Atsuko Shirai
Licensed Content Date	Jun 13, 2010
Licensed Content Volume Number	6
Licensed Content Issue Number	7
Type of Use	reuse in a dissertation / thesis
Requestor type	academic/educational
Format	print and electronic
Portion	figures/tables/illustrations
Number of figures/tables/illustrations	2
High-res required	no
Figures	Figure 3, Figure 5
Author of this NPG article	no
Your reference number	
Title of your thesis / dissertation	Mechanism of action of the marine sponge derived bicyclic peptide Theonellamide A
Expected completion date	Aug 2016
Estimated size (number of pages)	100
Requestor Location	Kimberly B Cornelio Laboratory for Biomolecular Chemistry 1-1 Machikaneyama, Toyonaka Osaka, 560-0043 Japan Attn: Kimberly B Cornelio

Figure A2-17. Reprint permission for Figure 1-17 of thesis from *Nature Chemical Biology*, **2010**, *6*, 519-526.

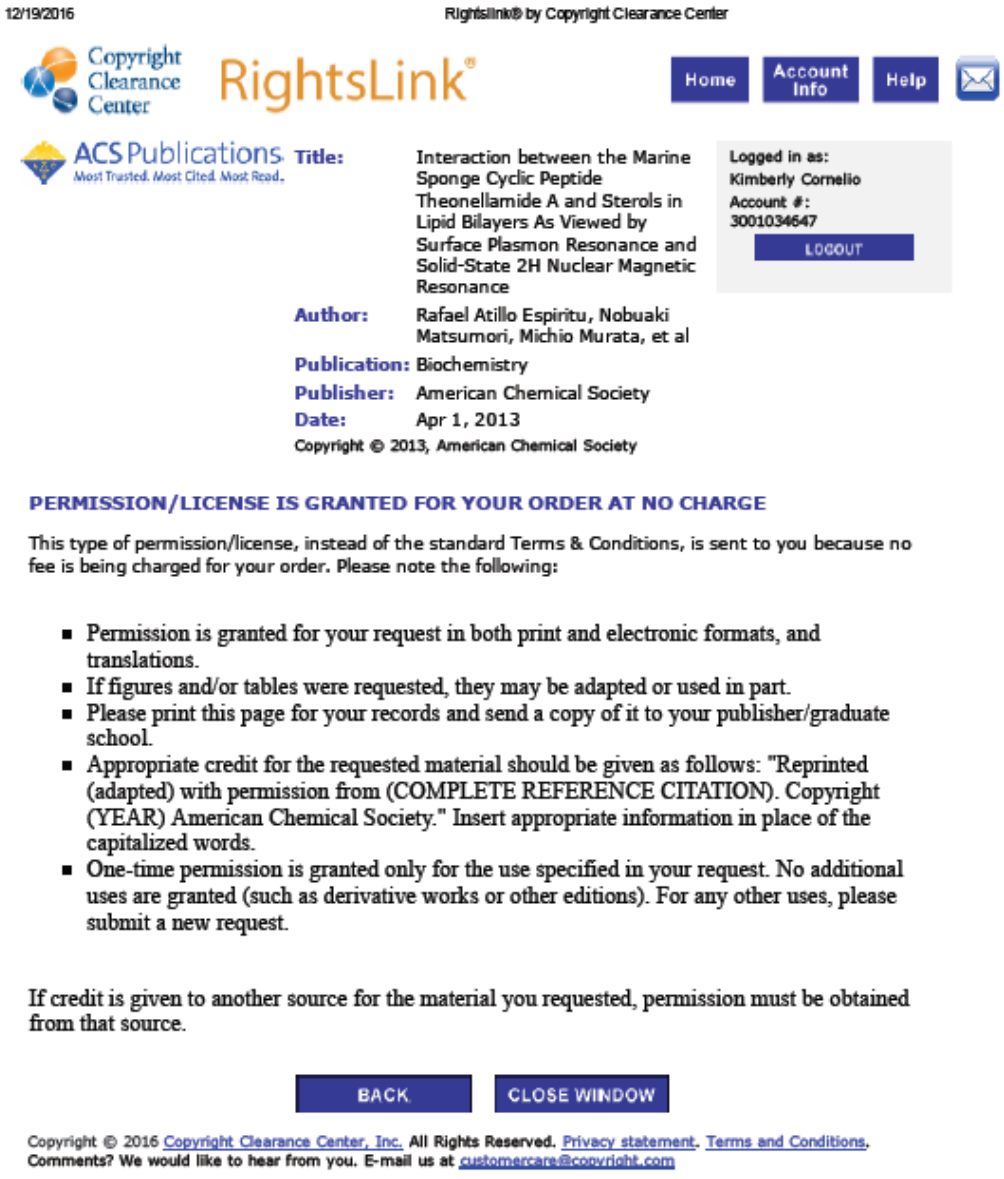

12/19/2016 Rightslink® by Copyright Clearance Center

Copyright Clearance Center RightsLink®

Home | Account Info | Help

ACS Publications Most Trusted. Most Cited. Most Read.

Title: Interaction between the Marine Sponge Cyclic Peptide Theonellamide A and Sterols in Lipid Bilayers As Viewed by Surface Plasmon Resonance and Solid-State 2H Nuclear Magnetic Resonance

Author: Rafael Atillo Espiritu, Nobuaki Matsumori, Michio Murata, et al

Publication: Biochemistry

Publisher: American Chemical Society

Date: Apr 1, 2013

Copyright © 2013, American Chemical Society

Logged in as: Kimberly Cornelio
Account #: 3001034647
LOGOUT

PERMISSION/LICENSE IS GRANTED FOR YOUR ORDER AT NO CHARGE

This type of permission/license, instead of the standard Terms & Conditions, is sent to you because no fee is being charged for your order. Please note the following:

- Permission is granted for your request in both print and electronic formats, and translations.
- If figures and/or tables were requested, they may be adapted or used in part.
- Please print this page for your records and send a copy of it to your publisher/graduate school.
- Appropriate credit for the requested material should be given as follows: "Reprinted (adapted) with permission from (COMPLETE REFERENCE CITATION). Copyright (YEAR) American Chemical Society." Insert appropriate information in place of the capitalized words.
- One-time permission is granted only for the use specified in your request. No additional uses are granted (such as derivative works or other editions). For any other uses, please submit a new request.

If credit is given to another source for the material you requested, permission must be obtained from that source.

BACK CLOSE WINDOW

Copyright © 2016 Copyright Clearance Center, Inc. All Rights Reserved. Privacy statement. Terms and Conditions.
Comments? We would like to hear from you. E-mail us at customercare@copyright.com

Figure A2-18. Reprint permission for Figure 2-2 and 2-3 of thesis from *Biochemistry*, **2013**, *52*, 2410-2418.

Copyright Clearance Center RightsLink®

Home | Account Info | Help

Title: Marine sponge cyclic peptide theonellamide A disrupts lipid bilayer integrity without forming distinct membrane pores

Author: Rafael Atillo Espiritu,Kimberly Cornello,Masanao Kinoshita,Nobuaki Matsumori,Michio Murata,Shinichi Nishimura,Hideaki Kakeya,Minoru Yoshida,Shigeki Matsunaga

Publication: Biochimica et Biophysica Acta (BBA) - Biomembranes

Publisher: Elsevier

Date: June 2016

Logged in as:
Kimberly Cornello
Account #:
3001034647
LOGOUT

Order Completed

Thank you for your order.

This Agreement between Kimberly B Cornello ("You") and Elsevier ("Elsevier") consists of your license details and the terms and conditions provided by Elsevier and Copyright Clearance Center.

Your confirmation email will contain your order number for future reference.

Printable details.

License Number	4010080486727
License date	Dec 15, 2016
Licensed Content Publisher	Elsevier
Licensed Content Publication	Biochimica et Biophysica Acta (BBA) - Biomembranes
Licensed Content Title	Marine sponge cyclic peptide theonellamide A disrupts lipid bilayer integrity without forming distinct membrane pores
Licensed Content Author	Rafael Atillo Espiritu,Kimberly Cornello,Masanao Kinoshita,Nobuaki Matsumori,Michio Murata,Shinichi Nishimura,Hideaki Kakeya,Minoru Yoshida,Shigeki Matsunaga
Licensed Content Date	June 2016
Licensed Content Volume	1858
Licensed Content Issue	6
Licensed Content Pages	7
Type of Use	reuse in a thesis/dissertation
Portion	figures/tables/illustrations
Number of figures/tables/illustrations	1
Format	both print and electronic
Are you the author of this Elsevier article?	Yes
Will you be translating?	No
Order reference number	
Original figure numbers	Figure 4
Title of your thesis/dissertation	Mechanism of action of the marine sponge derived bicyclic peptide Theonellamide A
Expected completion date	Aug 2016
Estimated size (number of pages)	100
Elsevier VAT number	GB 494 6272 12

https://s100.copyright.com/AppDispatchServlet

Figure A2-19. Reprint permission for Figure 2-4, Figure 2-8 C and D, Figure 3-6 and Figure 3-7 of thesis from *Biochim. Biophys. Acta - Biomembr*. **2016**, *1858***,** 1373.

12/15/2016 RightsLink by Copyright Clearance Center

Copyright Clearance Center RightsLink®

Home | Account Info | Help

Title: On the determination of the critical micelle concentration by the pyrene 1:3 ratio method
Author: J. Aguiar,P. Carpena,J.A. Molina-Bolívar,C. Carnero Ruiz
Publication: Journal of Colloid and Interface Science
Publisher: Elsevier
Date: 1 February 2003
Copyright © 2003 Elsevier Science (USA). All rights reserved.

Logged in as:
Kimberly Cornelio
Account #:
3001034647
LOGOUT

Order Completed

Thank you for your order.

This Agreement between Kimberly B Cornelio ("You") and Elsevier ("Elsevier") consists of your license details and the terms and conditions provided by Elsevier and Copyright Clearance Center.

Your confirmation email will contain your order number for future reference.

Printable details.

License Number	4010071398075
License date	Dec 15, 2016
Licensed Content Publisher	Elsevier
Licensed Content Publication	Journal of Colloid and Interface Science
Licensed Content Title	On the determination of the critical micelle concentration by the pyrene 1:3 ratio method
Licensed Content Author	J. Aguiar,P. Carpena,J.A. Molina-Bolívar,C. Carnero Ruiz
Licensed Content Date	1 February 2003
Licensed Content Volume	258
Licensed Content Issue	1
Licensed Content Pages	7
Type of Use	reuse in a thesis/dissertation
Portion	figures/tables/illustrations
Number of figures/tables/illustrations	1
Format	both print and electronic
Are you the author of this Elsevier article?	No
Will you be translating?	No
Order reference number	
Original figure numbers	1
Title of your thesis/dissertation	Mechanism of action of the marine sponge derived bicyclic peptide Theonellamide A
Expected completion date	Aug 2016
Estimated size (number of pages)	100
Elsevier VAT number	GB 494 6272 12
Requestor Location	Kimberly B Cornelio Laboratory for Biomolecular Chemistry 1-1 Machikaneyama, Toyonaka Osaka, 560-0043 Japan Attn: Kimberly B Cornelio
Total	0 JPY

https://s100.copyright.com/AppDispatchServlet 1/2

Figure A2-20. Reprint permission for Figures 2-12 of thesis from *Journal of Colloid and Interface Science*, **2003**, *258*, 116-122.

Title: Sterol-dependent membrane association of the marine sponge-derived bicyclic peptide Theonellamide A as examined by 1H NMR

Author: Kimberly Cornello,Rafael Atillo Espiritu,Yasuto Todokoro,Shinya Hanashima,Masanao Kinoshita,Nobuaki Matsumori,Michio Murata,Shinichi Nishimura,Hideaki Kakeya,Minoru Yoshida,Shigeki Matsunaga

Publication: Bioorganic & Medicinal Chemistry

Publisher: Elsevier

Date: 1 November 2016

Logged in as: Kimberly Cornello
Account #: 3001034647
LOGOUT

Order Completed

Thank you for your order.

This Agreement between Kimberly B Cornello ("You") and Elsevier ("Elsevier") consists of your license details and the terms and conditions provided by Elsevier and Copyright Clearance Center.

Your confirmation email will contain your order number for future reference.

Printable details.

License Number	4010080296478
License date	Dec 15, 2016
Licensed Content Publisher	Elsevier
Licensed Content Publication	Bioorganic & Medicinal Chemistry
Licensed Content Title	Sterol-dependent membrane association of the marine sponge-derived bicyclic peptide Theonellamide A as examined by 1H NMR
Licensed Content Author	Kimberly Cornello,Rafael Atillo Espiritu,Yasuto Todokoro,Shinya Hanashima,Masanao Kinoshita,Nobuaki Matsumori,Michio Murata,Shinichi Nishimura,Hideaki Kakeya,Minoru Yoshida,Shigeki Matsunaga
Licensed Content Date	1 November 2016
Licensed Content Volume	24
Licensed Content Issue	21
Licensed Content Pages	8
Type of Use	reuse in a thesis/dissertation
Portion	figures/tables/illustrations
Number of figures/tables/illustrations	6
Format	both print and electronic
Are you the author of this Elsevier article?	Yes
Will you be translating?	No
Order reference number	
Original figure numbers	Figure 2,3,4,5,6,7 and Table 1
Title of your thesis/dissertation	Mechanism of action of the marine sponge derived bicyclic peptide Theonellamide A
Expected completion date	Aug 2016
Estimated size (number of pages)	100

Figure A2-21. Reprint permission for Figures 3-2, 3-3, 3-9 to 3-13, Tables 3-1 and 3-2 of thesis from *Bioorg. Med. Chem.*, **2016**, *24*, 5235-5242

ELSEVIER LICENSE
TERMS AND CONDITIONS

Jan 23, 2017

This Agreement between Kimberly B Cornelio ("You") and Elsevier ("Elsevier") consists of your license details and the terms and conditions provided by Elsevier and Copyright Clearance Center.

License Number	4034570326547
License date	Jan 23, 2017
Licensed Content Publisher	Elsevier
Licensed Content Publication	Journal of Colloid and Interface Science
Licensed Content Title	On the determination of the critical micelle concentration by the pyrene 1:3 ratio method
Licensed Content Author	J. Aguiar,P. Carpena,J.A. Molina-Bolívar,C. Carnero Ruiz
Licensed Content Date	1 February 2003
Licensed Content Volume Number	258
Licensed Content Issue Number	1
Licensed Content Pages	7
Start Page	116
End Page	122
Type of Use	reuse in a thesis/dissertation
Intended publisher of new work	other
Portion	figures/tables/illustrations
Number of figures/tables/illustrations	1
Format	both print and electronic
Are you the author of this Elsevier article?	No
Will you be translating?	No
Order reference number	
Original figure numbers	1
Title of your thesis/dissertation	Mechanism of action of the marine sponge derived bicyclic peptide Theonellamide A
Expected completion date	Aug 2016
Estimated size (number of pages)	100
Elsevier VAT number	GB 494 6272 12
Requestor Location	Kimberly B Cornelio Laboratory for Biomolecular Chemistry 1-1 Machikaneyama, Toyonaka Osaka, 560-0043 Japan Attn: Kimberly B Cornelio

Figure A2-22. Reprint permission for Figures 3-4 of thesis from *Journal of Colloid and Interface Science*, **2003**, *258*, 116-122.

Publications Related to this Thesis

1. Sterol-dependent membrane association of the marine sponge-derived bicyclic peptide Theonellamide A as examined by 1H NMR. *Bioorganic & Medicinal Chemistry* **2016** ***24*** (21), 5235-5242.
2. Marine sponge cyclic peptide theonellamide A disrupts lipid bilayer integrity without forming distinct membrane pores. *Biochim. Biophys. Acta - Biomembr.* **1858,** 1373–1379 (2016).

Bioorganic & Medicinal Chemistry 24 (2016) 5235–5242

Contents lists available at ScienceDirect

Bioorganic & Medicinal Chemistry

journal homepage: www.elsevier.com/locate/bmc

Sterol-dependent membrane association of the marine sponge-derived bicyclic peptide Theonellamide A as examined by ^{1}H NMR

Kimberly Cornelio [a,b], Rafael Atillo Espiritu [a,†], Yasuto Todokoro [a], Shinya Hanashima [a], Masanao Kinoshita [b,c], Nobuaki Matsumori [a,c,*], Michio Murata [a,b,*], Shinichi Nishimura [d], Hideaki Kakeya [d], Minoru Yoshida [e], Shigeki Matsunaga [f]

[a] Department of Chemistry, Graduate School of Science, Osaka University, Osaka 563-0043, Japan
[b] Lipid Active Structure Project, ERATO, Japan Science and Technology Agency, Osaka 560-0043, Japan
[c] Department of Chemistry, Graduate School of Sciences, Kyushu University, Fukuoka 819-0395, Japan
[d] Division of Bioinformatics and Chemical Genomics, Graduate School of Pharmaceutical Sciences, Kyoto University, Kyoto 606-8501, Japan
[e] Advanced Science Institute, RIKEN Center for Sustainable Resource Science, Saitama 351-0198, Japan
[f] Graduate School of Agricultural and Life Sciences, The University of Tokyo, Tokyo 113-8657, Japan

ARTICLE INFO

Article history:
Received 30 July 2016
Revised 22 August 2016
Accepted 23 August 2016
Available online 24 August 2016

Keywords:
Marine sponge
Cyclic peptide
Cholesterol
Membrane curvature

ABSTRACT

Theonellamide A (TNM-A) is an antifungal bicyclic dodecapeptide isolated from a marine sponge *Theonella* sp. Previous studies have shown that TNM-A preferentially binds to 3β-hydroxysterol-containing membranes and disrupts membrane integrity. In this study, several ^{1}H NMR-based experiments were performed to investigate the interaction mode of TNM-A with model membranes. First, the aggregation propensities of TNM-A were examined using diffusion ordered spectroscopy; the results indicate that TNM-A tends to form oligomeric aggregates of 2–9 molecules (depending on peptide concentration) in an aqueous environment, and this aggregation potentially influences the membrane-disrupting activity of the peptide. Subsequently, we measured the ^{1}H NMR spectra of TNM-A with sodium dodecyl sulfate-d_{25} (SDS-d_{25}) micelles and small dimyristoylphosphatidylcholine (DMPC)-d_{54}/dihexanoylphosphatidylcholine (DHPC)-d_{22} bicelles in the presence of a paramagnetic quencher Mn^{2+}. These spectra indicate that TNM-A poorly binds to these membrane mimics without sterol and mostly remains in the aqueous media. In contrast, broader ^{1}H signals of TNM-A were observed in 10 mol % cholesterol-containing bicelles, indicating that the peptide efficiently binds to sterol-containing bilayers. The addition of Mn^{2+} to these bicelles also led to a decrease in the relative intensity and further line-broadening of TNM-A signals, indicating that the peptide stays near the surface of the bilayers. A comparison of the relative signal intensities with those of phospholipids showed that TNM-A resides in the lipid–water interface (close to the C2′ portion of the phospholipid acyl chain). This shallow penetration of TNM-A to lipid bilayers induces an uneven membrane curvature and eventually disrupts membrane integrity. These results shed light on the atomistic mechanism accounting for the membrane-disrupting activity of TNM-A and the important role of cholesterol in its mechanism of action.

1. Introduction

Marine sponges are an abundant source of diverse and highly potent biologically active compounds.[1] The *Lithistid* sponges of genus *Theonella* have provided several bioactive secondary metabolites with interesting therapeutic activities such as theonellapeptolides (cytotoxicity and K^+ and Na^+ transport activity),[2] theonelladines A–D (antineoplastic),[3] misakinolide A (antitumor),[4,5] and swinholide A (antifungal).[6] Another group of compounds named theonellamides (TNMs) were isolated from the same family of sponges collected off Hachijo-jima island as reported by Matsunaga et al.[7]

TNM's unique structure is characterized by a bismacrocycle skeleton bridged by a τ-histidinoalanine (τ-HAL) residue, contains several unusual amino acids, and occasionally has a sugar moiety.[7,8] TNMs A–F inhibit the growth of prototypical fungi (*Candida*,

Abbreviations: DOSY, diffusion ordered spectroscopy; 3β-OH, 3β-hydroxysterol; GUV, Giant unilamellar vesicle; MLV, multilamellar vesicle.

* Corresponding authors.
† Current address: Department of Chemistry, De La Salle University, Manila 0922, Philippines.

http://dx.doi.org/10.1016/j.bmc.2016.08.043
0968-0896/

Trichophyton, and *Aspergillus*) with IC_{50} values of 2–7 μM and exhibit cytotoxic activity against P388 mouse leukemia cells (IC_{50} 0.5–2.8 μM).[9–11] The detailed mechanism of action of TNMs are still unknown although new findings have been brought about from the studies of a subcellular localization and in vitro binding assays.[10,12,13] These studies have shown that TNMs specifically bind to 3β-hydroxysterols such as cholesterol (Chol) and ergosterol; the latter may be responsible for its antifungal potency. Moreover, the alleviation of the membrane-binding activity of TNM for yeast cells with impaired ergosterol biosynthesis further highlighted the possible role of sterols in its mechanism of action.[10] Among other sterol-dependent membrane permeabilizers such as polyene macrolides and polyols, TNM is particularly unique in exhibiting antifungal activity without forming distinct pores across the cell membranes.[12] Recently, NMR-based techniques have been successfully applied to investigate amphotericin B-ergosterol interactions in membranes[14,15] and sterol recognition by amphidinol 3.[16,17] In these experiments, the NMR signals of natural products were directly detected, leading to the elucidation of detailed interaction mode of these natural products with membrane sterols.[14,17] Regarding amphotericin B, we established an efficient synthetic route to facilitate the labeling of the molecule with ^{13}C and ^{19}F nuclei, which is essential for elucidating the complex structure in membranes based on the interatomic distances between the labeled atoms using solid-state NMR.[14] On the other hand, the direct observation of NMR signals of TNM in a membrane-associated form has not yet been achieved, mainly because its large complex structure containing several unusual amino acid residues hampers the synthetic supply of the labeled analogue.

We have previously observed the ^{2}H and ^{31}P NMR signals of membrane lipids in the presence of TNM; solid-state ^{2}H NMR spectra and surface plasmon resonance (SPR) experiments indicated that TNM-A preferentially binds to 3β-hydroxysterols in POPC liposomes.[12,18] ^{31}P NMR spectra also showed that the incorporation of TNM-A to Cho-containing POPC liposomes disrupted the phospholipid bilayers without significantly altering the membrane fluidity and integrity.[19] Unlike the spectra of TNM-A, membrane disruption by the detergent-type mechanism of action usually leads to a large isotropic peak due to the formation of small and fast-tumbling particles such as micelles and very small vesicles.[20,21]

Recently, it has been deduced that the accumulation of TNM-A in Cho-containing POPC liposomes resulted in alteration of membrane curvature, causing the permeabilization of the vesicles.[19] To generate the curvature, the hydrophobic side chains of TNM-A probably penetrate the shallow region of an outer leaflet, thus expanding the bilayer surface and modifying the curvature of the membrane.[19] Changes in membrane curvature cause dynamic morphological changes in liposomes and lead to the destabilization and permeabilization of the bilayer structure.[22,23] To more precisely elucidate the mechanism of TNM-A activity derived from its unique structure, the membrane binding process in the aqueous phase and the depth of the membrane penetration should be investigated. In this study, therefore, we aimed to obtain the precise interaction mode of TNM-A with membrane lipids by NMR spectroscopy. To achieve this goal, we focused on the direct observation of the ^{1}H NMR signals of TNM-A in an aqueous environment and in a membrane-associated form. First, the self-aggregation propensities of TNM-A in water were examined; this is an important facet to understand membrane binding. To estimate the number of molecules in an aggregate, diffusion-ordered ^{1}H NMR spectroscopy (DOSY) experiments were conducted. Next, the association process of TNM-A to lipid layers was investigated using SDS-d_{25} micelles and DMPC-d_{54}/DHPC-d_{22} bicelles ($q = 0.5$). ^{1}H NMR paramagnetic quenching experiments using Mn^{2+} were also performed to assess the insertion and localization of TNM-A in the bilayer portion of bicelles.

2. Methods and materials

2.1. Materials

TNM-A was isolated as reported previously.[8] Briefly, the frozen sponge was extracted several times with *n*-PrOH/H_2O (2:1 v/v). After the concentration of the combined extracts, the resulting crude material was subjected to ODS flash column chromatography and eluted with increasing concentrations of MeOH in an aqueous solution. The final purification of the more polar fractions on a C_{18} reversed-phase HPLC column afforded TNM-A (Fig. 1). Cho was purchased from Nacalai Tesque Inc. (Kyoto, Japan). Sodium dodecyl sulfate (SDS-d_{25}), 1,2-dimyristoyl-d_{54}-*sn*-glycero-3-phosphocholine (DMPC-d_{54}), 1,2-dimyristoyl-*sn*-glycero-3-phosphocholine (DMPC), and 1,2-dihexanoyl-d_{22}-*sn*-glycero-3-phosph ocholine (DHPC-d_{22}) were purchased from Avanti Polar Lipids. Paramagnetic quencher Mn^{2+} in the form of $MnCl_2$ salt and β-cyclodextrin were purchased from Nacalai Tesque Inc. (Kyoto, Japan). NMR solvents DMSO-d_6 and D_2O were obtained from Eur-iso-top (Les Algorithmes, Saint-Aubin, France) and Cambridge Isotopes Laboratory (Andover, MA, USA), respectively. All other chemicals were standard and analytical quality reagents.

2.2. NMR sample preparations

To assess the membrane binding and localization of TNM-A, mixed micelles and Chol-containing bicelles were prepared and titrated with increasing concentrations of paramagnetic quenching ion Mn^{2+}. To incorporate the TNM-A samples in micelles, the SDS-d_{25} micellar solution in 500 μL of 10 mM PBS buffer (100 mM NaCl, pH = 7.4) was mixed with TNM-A to obtain the final SDS-d_{25} and peptide concentrations of 20 mM and 0.2 mM, respectively. The TNM-A samples were incorporated in bicelles ($q = 0.5$) by dissolving 10 mg DHPC-d_{22} (21.06 μmol), 7.7 mg DMPC-d_{54} (10.50 μmol), 0.406 mg Chol (1.05 μmol), and 0.175 mg TNM-A (0.1 μmol) in 3 mL $CHCl_3$/MeOH (1:1 v/v) in a round-bottom flask. After mixing the components thoroughly, the solvent was evaporated and dried in vacuum for 8 h. The dry lipid film was rehydrated with 200 μL of 100 mM NaCl in D_2O and occasionally vortexed at room temperature for 1 h, affording the bicelle samples incorporated with TNM-A. The Chol-free bicelles were prepared by the same method without adding Chol in the lipid mixture. For the DOSY measurements to evaluate peptide aggregation, TNM-A solutions were prepared in either DMSO-d_6/D_2O (4:1 v/v) or D_2O/H_2O (98:2 v/v) solvent mixture to obtain a final concentration of 0.2 mM or 1.2 mM.

2.3. ^{1}H NMR DOSY

To estimate the self-aggregation propensities of TNM-A in aqueous environments, its diffusion coefficient in two solvent systems was obtained through DOSY NMR measurements. A stimulated echo sequence with bipolar gradient pulses for diffusion (stebpgp1s19) was used. The spectra were recorded at 298 K with eight scans for each of the 32 gradient steps where the gradient strength logarithmically increased from 2% to 98% of the maximum strength (56.7 G/cm). The diffusion time (Δ) was set to 0.12 s, and the length of the square diffusion encoding gradient pulses (δ) was set to 3 ms. To obtain a 2D DOSY spectra, 32 array datasets were processed using the *dosy2d* command in the Bruker TOPSPIN ver. 3.1 program. The quality of the spectra was improved by adjusting the values of the noise sensitivity factor (PC = 2), spike suppression factor (SpiSup = 4), and linewidth factor (LWF = 4) while leaving the other parameters set as the default values. The diffusion coefficients D (m^2/s) were determined from the DOSY spectra based on the $\log_{10}D$ values corresponding to the midpoints of the observed

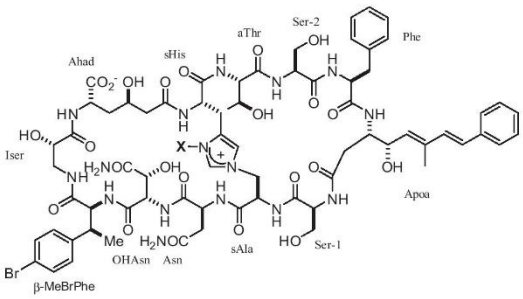

Figure 1. Structure of Theonellamide-A (TNM-A).

peaks. The hydrodynamic radius of TNM-A was estimated as previously reported[24] using the obtained diffusion coefficient values through the Stokes–Einstein equation.

2.4. ^{1}H NMR paramagnetic quenching measurements

The ^{1}H NMR spectra of 0.2 mM TNM-A in the absence or presence of 20 mM deuterated SDS-d_{25} micelles [10 mM PBS buffer, 100 mM NaCl, (pH = 7.4)] or Chol-free and Chol-containing DMPC-d_{54}/DHPC-d_{22} bicelles [(q = 0.5) with 160 mM total phospholipid concentration in 100 mM NaCl in D_2O] were first acquired. Then, increasing concentrations of $MnCl_2$ (20 μM, 40 μM, 80 μM, and 160 μM) were added to the samples, and the ^{1}H NMR spectra were again acquired after each titration step using the same NMR measurement parameters. The ^{1}H NMR spectra of pure TNM-A in the absence of any model membrane, but with the same increasing concentrations of $MnCl_2$ were also acquired to evaluate the effects of the paramagnetic quencher on the resonances of the peptide alone.

3. Results

3.1. DOSY NMR measurements to evaluate the aggregation propensities of TNM-A

The binding affinity of TNM-A to phospholipid bilayers has been shown to be enhanced by 3β-hydroxysterols based on the K_d values obtained from the SPR measurements.[12] Moreover, a propensity to form aggregates in aqueous media could be another factor affecting the membrane affinity of TNM-A. Therefore, DOSY experiments were carried out to evaluate the aggregation state of TNM-A in an aqueous environment. DOSY is often used to determine the diffusion coefficient (D) of particles in a solution; the hydrodynamic radius (r_s) of the particles could be obtained from the Stokes–Einstein equation.[24,25]

The diffusion coefficients obtained from the DOSY spectra indicate that TNM-A has the propensity to aggregate in an aqueous environment (Fig. 2). In the organic solvent system DMSO-d_6/D_2O (4:1 v/v), which was also used for the structural studies of TNM-A, the peptide has a diffusion coefficient of 0.47–0.54 × 10^{-10} m^2/s at 1.2 mM and 0.55–0.68 × 10^{-10} m^2/s at 0.2 mM. In the aqueous system D_2O/H_2O (98:2 v/v), TNM-A showed diffusion coefficients of 0.91–0.93 × 10^{-10} m^2/s and 1.82–2.19 × 10^{-10} m^2/s for the higher and lower peptide concentrations, respectively. From these diffusion data and the viscosities of D_2O/H_2O (1.095 mPa·s)[26] and DMSO-d_6/D_2O 4:1 (3.861 mPa·s)[27], the calculated Stokes' radii for TNM-A in DMSO-d_6/D_2O (4:1 v/v) and D_2O/H_2O (98:2 v/v) were 1.05–1.21 nm and 2.14–2.18 nm, respectively, at the higher peptide content. This indicates that TNM-A occupies a larger volume in an aqueous environment and probably forms self-aggregates. The small difference of diffusion coefficients in the aqueous DMSO between the high and low TNM-A contents may be caused by a subtle difference in viscosity that is affected by the concentrations of solutes to a certain extent.

For comparison with TNM-A, a similar DOSY experiment was carried out using β-cyclodextrin that resides as monomers in aqueous media. The results indicate that the viscosity values of D_2O/H_2O solvent mixtures reported in the literature[26,27] are accurate enough for estimating the number of TNM-A molecules in oligomers (Fig. S1). Based on the volume values shown in Table 1, the number of TNM-A molecules in an oligomer was determined assuming that the peptide has a completely spherical form in both the solvent systems; for the high peptide content (1.2 mM) and low peptide content (0.2 mM), the average numbers of molecules per aggregate in aqueous media were approximately 9 and 2, respectively. This can be accounted for by the association–dissociation equilibrium between the monomers and oligomers that should be shifted to monomers in lower concentrations of the peptides (Fig. 7). The self-aggregation is quite possible because TNM-A contains highly hydrophobic residues such as Apoa, Phe, and β-MeBrPhe; these can be embedded deep inside the peptide oligomer and stay away from the aqueous environment. The occurrence of aggregates in aqueous phase was also reported for another membrane-active and antibacterial peptide trichogin GA IV.[28]

3.2. Evaluation of the membrane association of TNM-A by ^{1}H NMR spectra of micelles and bicelles in the presence and absence of Chol

The fluorescence microscopic images in our previous study showed that TNM-A binds to Cho-containing POPC GUVs faster than sterol-free GUVs and induces a positive curvature in the former membrane much more efficiently.[19] Therefore, NMR experiments were conducted to clarify whether TNM-A accumulates near the surface of the membrane or penetrates the interior. For this purpose, ^{1}H NMR paramagnetic quenching experiments were conducted using SDS-d_{25} micelles and DMPC-d_{54}/DHPC-d_{22} bicelles; Mn^{2+} was used as the paramagnetic quencher that exclusively stays in the aqueous phase and significantly enhances the relaxation rates of ^{1}H nuclei in its proximity, resulting in the broadening or even disappearance of the ^{1}H signals near the surface of the membrane or in the aqueous phase. If TNM-A remains surface-associated without penetrating the membrane interior, its entire structure would be exposed to the solvent, and significant line-broadening of its ^{1}H resonances would be observed. On the other hand, if Apoa or any part of TNM-A anchors into the membrane interior, these moieties would be affected to a smaller extent by Mn^{2+}.[29,30]

The ^{1}H NMR spectra of TNM-A in the presence and absence of SDS-d_{25} micelles (the bottom two spectra in Fig. 3) are very similar, indicating none or very weak association of TNM-A with SDS micelles.[30] Moreover, the incremental addition of Mn^{2+} caused significant line-broadening and loss of signal intensity of the entire ^{1}H NMR resonances of TNM-A. These observations indicate that the peptide may remain unbound to the micelles or interact with the surface of micelles because of the absence of Chol in the micelles; our previous study showed that the affinity of TNM-A to sterol-free membranes is low (K_d ~ 420 μM) based on SPR measurements.[12]

To evaluate the binding affinity of TNM-A to a phospholipid bilayer, Chol-containing DMPC-d_{54}/DHPC-d_{22} bicelles possessing a small bilayer-based planer portion unlike spherical micelles were used. The q value is the ratio of long acyl-DMPC and short acyl-DHPC. The bicelles with q = 0.5 were adopted since sizes of the

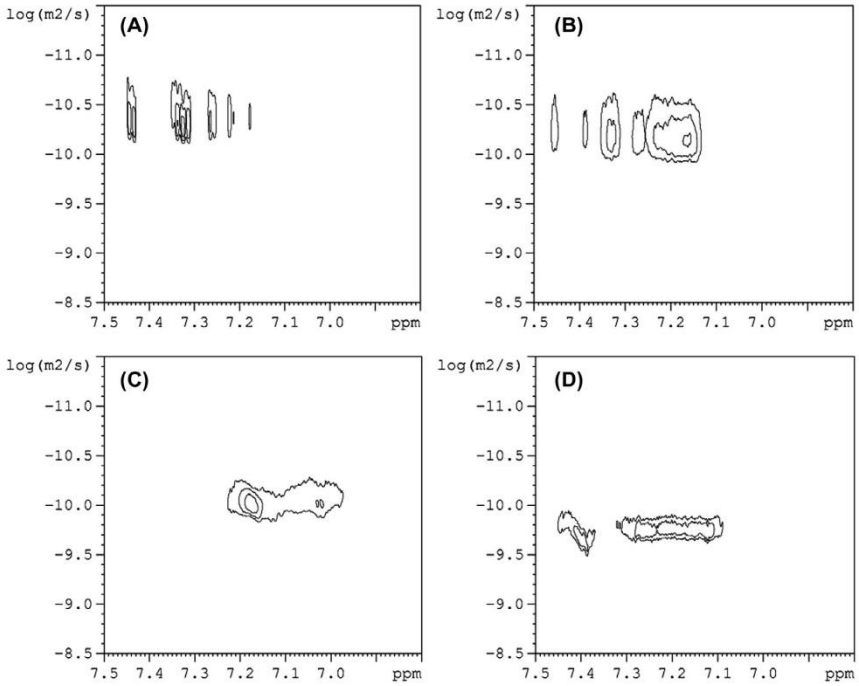

Figure 2. DOSY spectra of TNM-A in DMSO-d_6/D_2O (4:1 v/v) at 1.2 mM (A) and 0.2 mM (B) and in D_2O/H_2O (98:2 v/v) at 1.2 mM (C) and 0.2 mM (D). The diffusion coefficients were obtained from the midpoints of the peaks indicated in F1 axis. Judging from the apparent Stokes' radius and viscosity of the solvents, the TNM-A present in the aqueous medium forms oligomeric aggregates while occurring as monomers in DMSO-d_6/D_2O.

Table 1
Approximated diffusion coefficients (D) and calculated hydrodynamic radius (r_s) of TNM-A in two different solvents at 298 K

[TNM-A]	DMSO-d_6/D_2O (4:1 v/v)			D_2O/H_2O (98:2 v/v)		
	D ($\times 10^{-10}$ m^2/s)	r_s (nm)	V (nm^3)	D ($\times 10^{-10}$ m^2/s)	r_s (nm)	V (nm^3)
1.2 mM	0.47–0.54	1.05–1.21	4.85–7.42	0.91–0.93	2.14–2.18	41.05–43.40
0.2 mM	0.55–0.68	0.84–1.02	2.48–4.45	1.82–2.19	0.91–1.09	3.16–5.42

bicelles are small enough to allow the fast-tumbling. This was necessary for detecting the ^1H NMR signals using a solution NMR instrument.[31–33] More importantly, the bicelles are known to incorporate Chol up to ~10 mol %.[34,35]

The ^1H NMR spectra of TNM-A in Chol-free (Fig. 4A–E) and Chol-containing (Fig. 4F–J) bicelles are different. The 6.5–7.6 ppm range in Figure 4 shows the aromatic/olefinic signals, which were more broadened with Chol-containing bicelles than with Chol-free bicelles; in particular, the two doublet signals in 6.5–6.7 ppm region due to the conjugated diene moiety of the Apoa residue almost flattened out due to significant line-broadening in the Chol-containing bicelles. Thus, the mobility of the side chain is more restricted in the Chol-containing bicelles, indicating that the peptide binds more efficiently to Chol-containing membranes. The spectra of TNM-A in the presence of SDS-d_{25} micelles and those in the presence of Chol-free bicelles were quite different, even though the interaction of the peptide to both the sterol-free membranes should be weak. The difference in the isotope contents of the solvents used for the preparations of micelles (15% D_2O) and bicelles (100% D_2O) may contribute to the spectral changes observed for TNM-A, where the amide protons disappeared in the bicelle spectra. Another possible reason is that the aromatic residues shown in Figure 4 containing highly hydrophobic side chains of the peptide may have some weak interactions with the bicelles surface, but not with micelle surface, thus changing their chemical shifts. The cationic trimethylammonium moiety of the phosphocholine headgroup may drive the weak association of TNM-A aromatic residues to the surface of DMPC bicelles through cation–π interactions,[36,37] which in the case of micelles could be unfavorable as it has a negative sulfate headgroup. In general, membrane-interacting peptides show significant changes in the ^1H NMR signals in the presence of detergents, particularly for their aromatic residues.[38]

3.3. Membrane penetration of TNM-A examined by ^1H NMR paramagnetic quenching experiments

The effects of Mn^{2+} on the signal intensity and linewidths were evident when the peptide was incorporated in both Chol-free and Chol-containing bicelles (Figs. 4A–D, 4F–I, and S1). The relative signal intensities (I/I_o) between the Chol-free (Fig. 5A) and Chol-containing bicelles (Fig. 5B) indicate that TNM-A resides

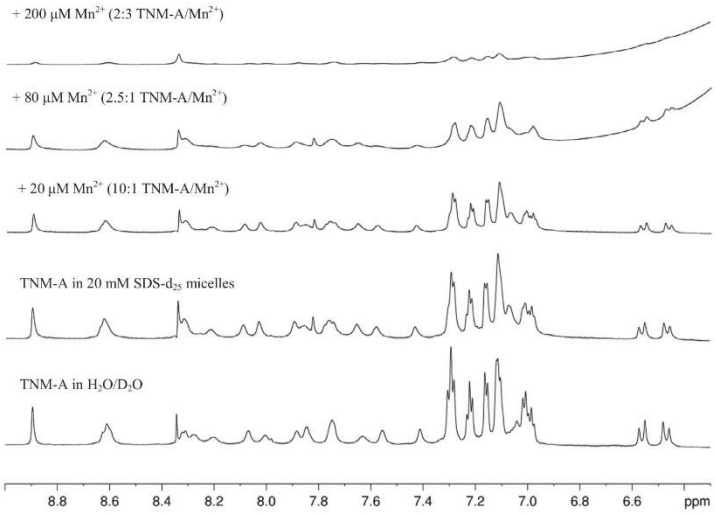

Figure 3. ^{1}H NMR spectra of the olefinic and amide proton region of TNM-A with increasing concentrations of Mn^{2+}. Measurements were carried out at 25 °C in H_2O/D_2O containing 200 μM TNM-A and 0 mM (bottom) and in 20 mM SDS-d_{25} micelles in 10 mM PBS buffer containing 100 mM NaCl (pH = 7.4) with varying concentrations of $MnCl_2$. The bottom two spectra were measured without Mn^{2+}.

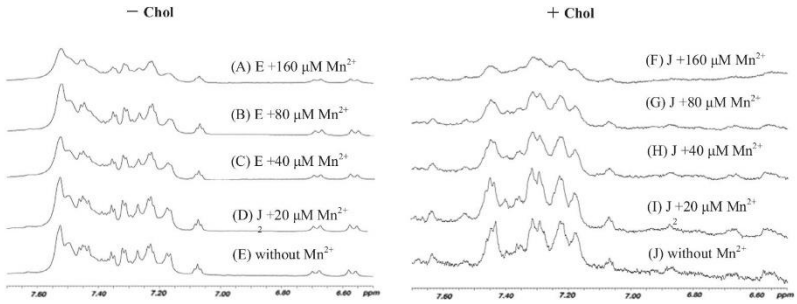

Figure 4. ^{1}H NMR Spectra of TNM-A incorporated in Chol-free (A–E) and Chol-containing (F–J) DMPC-d_{54}/DHPC-d_{22} bicelles (q = 0.5) in D_2O (100 mM NaCl) without Mn^{2+} (E and J) and with increasing concentrations of Mn^{2+} (A–D and F–I). The amount of Chol added to bicelles was 10 mol % of DMPC-d_{54}. Mn^{2+}/TNM-A mol ratios: from the bottom to the top, 0:10, 1:10, 2:10, 4:10, and 8:10. The final concentrations of TNM-A and phospholipids (DMPC+DHPC) were 200 μM and 160 mM, respectively. All the spectra were recorded with 512 scans at 310 K.

close to Mn^{2+} in the aqueous phase regardless of the presence or absence of Chol in the membranes. The results reveal that its structure is accessible to the aqueous environment and mostly stay in the surface and/or shallower portion of the membrane even though TNM-A binds more efficiently to Chol-containing bicelles.

On the other hand, the I/I_o values of some TNM-A signals such as the Phe residue were similar for the Chol-free bicelles and bicelle-free solutions (Fig. 5C). More importantly, the signal intensity in the Chol-containing bicelles was less sensitive to Mn^{2+} concentrations, because the I/I_o values were significantly higher at the initial addition ([Mn^{2+}] = 20 μM, $I/I_o \sim 0.85$) and also at the highest concentration of Mn^{2+} ([Mn^{2+}] = 80 μM, $I/I_o \sim 0.54$–0.61) compared to those in the Chol-free membranes (Fig. 5A and B). These data indicate that although TNM-A molecules mostly reside in the aqueous phase, the peptide partly associates with Chol-free membranes.

To evaluate the localization of TNM-A in the membrane upon binding, the relative signal intensities of the DMPC protons[39] (I/I_o values) were measured in the presence of Chol-free and Chol-containing bicelles. The lipid protons attached to the γ, α, β, and *sn*-2 positions were significantly influenced by Mn^{2+}, whereas those in the C-2′ and C-14′ of the acyl chain were the least affected (Fig. 6A and B). When incorporated to Chol-free bicelles at 80 μM Mn^{2+}, the I/I_o values of the peptide protons (∼0.36–0.46) were similar to those of the protons of DMPC at the α, β, and *sn*-2 positions (∼0.36–0.43). On the other hand, when incorporated to Chol-containing bicelles at 80 μM Mn^{2+}, their I/I_o values (∼0.54–0.61) were similar to those of the C-2 position in DMPC acyl chains (∼0.61). These results indicate that TNM-A interacts with Chol-free bicelles in the shallower region of the membrane near the headgroup zone, whereas its interaction with Chol-containing bicelles occurs in a slightly deeper portion of the membrane body near the boundary between the headgroup and hydrophobic core.

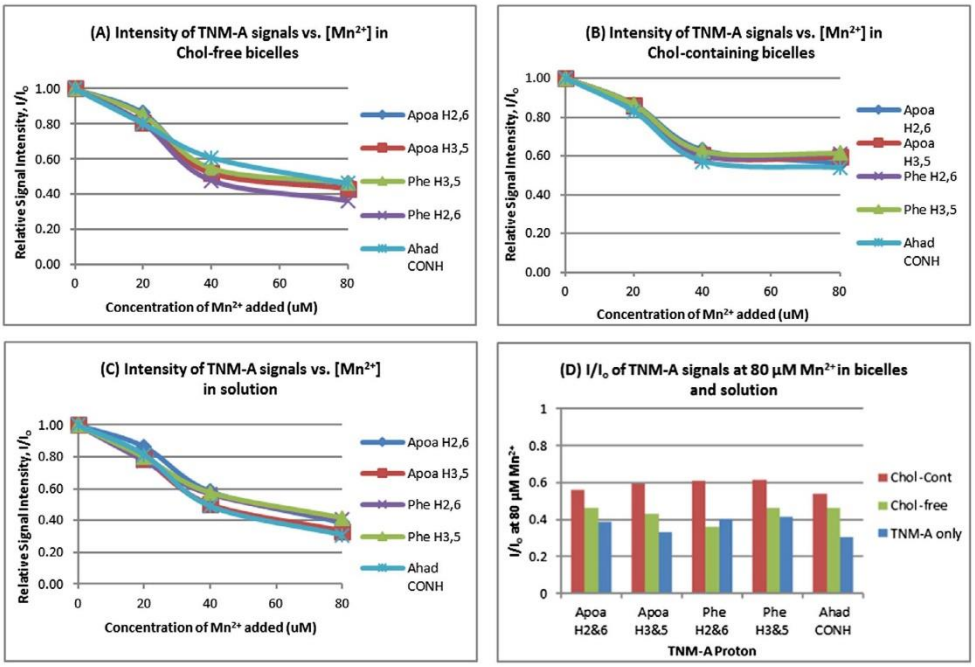

Figure 5. Relative intensities (I/I_o) of the ^{1}H signals of TNM-A incorporated in Chol-free (A) and Chol-containing (B) bicelles and in the absence of bicelles (C) with increasing concentrations of Mn^{2+}. The I/I_o values of the TNM-A protons with 80 µM Mn^{2+} (D). The I/I_o values were calculated from the ratio of the ^{1}H peak intensity in the presence and absence of Mn^{2+} at the indicated amino acid residue of TNM-A. The concentrations of TNM-A and phospholipids (DMPC+DHPC) were 200 µM and 160 mM, respectively.

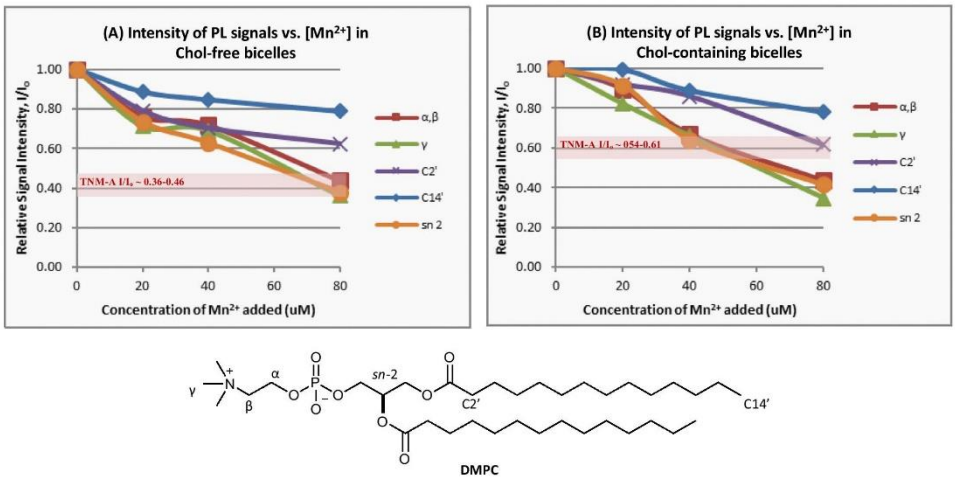

Figure 6. Relative signal intensities (I/I_o) of DMPC protons in increasing concentrations of Mn^{2+}. The I/I_o values were calculated from the ratio of the DMPC peak intensity in the presence of Mn^{2+} and that in the absence of Mn^{2+}. The final concentrations of TNM-A and phospholipids were 200 µM and 160 mM, respectively. All the spectra were measured with 512 scans at 310 K.

4. Discussion

We have previously revealed that TNM-A preferentially binds to 3β-hydroxysterol-containing membranes through its direct interaction with Chol and ergosterol based on the SPR and solid-state NMR studies.[12] More recently, confocal fluorescence microscopy has disclosed that TNM-A permeabilizes the membrane by altering the membrane morphology; this effect significantly occurs only in

Chol-containing liposomes.[18] However, it remains unclear how the interaction of TNM-A with membranes leads to the uneven membrane curvature, and what role Chol plays in such a process. To investigate the detailed mechanism underlying the membrane deformation by TNM-A, it was necessary to consider several aspects that influence the binding and interaction of the peptide with membranes.

Self-aggregation and membrane association of bioactive peptides are fundamental factors that define their specific mechanism of action leading to membrane permeabilization.[28] The results of the DOSY experiments clearly indicate that TNM-A has a tendency to form oligomeric aggregates in an aqueous environment; this affects the association/dissociation equilibrium of the peptide in the membrane. For instance, the antimicrobial peptide trichogin GA IV exists in water as monomers and small aggregates, the latter shows reduced partition into the membrane phase.[28] Another study on dermaseptin-derived peptides indicated that peptides with less aggregation propensity in aqueous media have a higher potency.[31,32] Once large aggregates are formed, they tend to be precipitate and adhere to the surface of the container and never return to the monomeric state. On the other hand, the DOSY experiments showed that TNM-A forms very small aggregates or oligomers in water. The formation of oligomers that cannot be converted to a monomeric form in aqueous phase provides TNM-A another characteristic feature. As shown in Figure 7, the monomers of TNM-A efficiently bound to Chol-containing membrane similar to the peptides described above,[31] but their concentration was relatively low because of the biased equilibrium between monomers and oligomers with a large excess of oligomers. This low concentration of the monomers and weak affinity of the oligomers to membrane probably contribute to a very slow progress in membrane deformation by TNM-A.[19]

In biological membranes, the generation of a curvature is often attributed to the high surface density of protein domains asymmetrically inserted into the lipid bilayer.[40,41] The interaction of amphipathic proteins and peptides only with the surface of membranes could cause an areal difference between the inner and outer leaflets, leading to the development of a positive curvature;[40] a similar deformation of liposomes could be seen for TNM-A (Fig. S3).[19] In the structure of TNM-A, some hydrophobic residues such Phe, β-MeBrPhe, and Apoa potentially act as membrane anchors and preferentially interact with the outer leaflets of bilayers. In the Chol-containing bicelles, a slightly deeper penetration of TNM-A, albeit still residing in the shallow area, was observed in the ^{1}H NMR paramagnetic quenching experiments. This is consistent with the stronger affinity of TNM-A to POPC-Chol membranes (K_d, ~9.2 μM) than to sterol-free membranes (K_d, ~420 μM).[12] The high affinity of monomeric TNM-A to Chol-containing membranes led to the release of more monomeric peptides from the oligomeric aggregates and allowed them to attach to the membrane surface. Moreover, the increased lateral pressure in the outer leaflet due to the peptide binding caused the membrane strain that can be relieved by the formation of a positive curvature.[42]

Based on these and previous findings.[10,12,19] we propose a hypothetical scenario to explain the membrane-disrupting activity of TNM-A (Fig. 7). Initially, TNM-A forms oligomeric aggregates in the aqueous phase because of its amphiphilic nature. In the case of a Chol-free membrane (Fig. 7A), the affinity of TNM-A is so weak that the peptide aggregates have less tendency to dissociate into monomers and associate with the membrane to a smaller extent (Fig. 7B). The TNM-A aggregates expose the hydrophilic face to the aqueous phase because its hydrophobic residues are mostly incorporated in the core of the oligomers. Thus, its weak hydrophobic interaction with the membrane destabilizes the membrane-

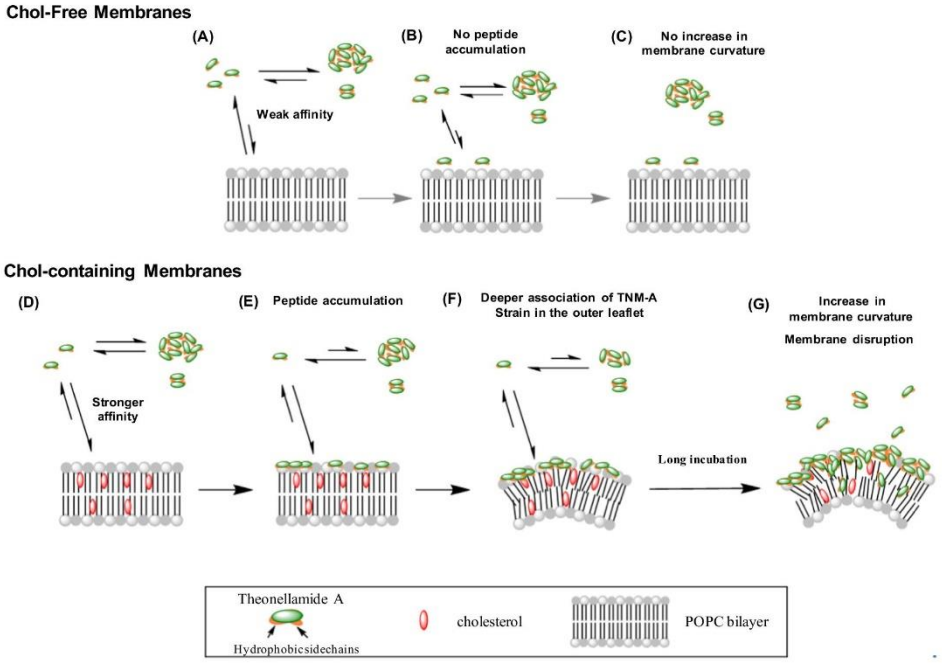

Figure 7. Hypothesized scenario accounting for the membrane-disrupting activity of TNM-A.

bound form, thus retaining the aggregates mostly in water. In the case of a Chol-containing membrane (Fig. 7D), the 20 times higher affinity of TNM-A to the membrane[12] can induce the dissociation of significantly more peptide molecules from the aggregates; these molecules bind efficiently to the membrane surface. As TNM-A accumulates in the outer leaflet of Chol-containing bilayers, its surface coverage increases, and the peptide also penetrates a slightly deeper region of the membrane in the lipid–water interface (Fig. 7F). The outer leaflet of phospholipids is pushed aside to accommodate the peptides, increasing the strain of the outer leaflet (Fig. 7G). At this point, membrane deformations lead to transient membrane defects, sufficient to disrupt the membrane integrity and enhance the membrane permeability. A more detailed atomistic study is underway to confirm the hypothesis.

5. Conclusion

In this study, ^{1}H NMR spectroscopic techniques were successfully applied to elucidate the mechanism underlying the membrane-disrupting activity of TNM-A. The DOSY measurements indicate that TNM-A has a propensity to form oligomers (aggregation number: ~2 and 9 peptide molecules) in an aqueous environment; this probably affects the membrane association and disrupting activity of the peptide, because the formation of stable oligomers facilitates the slow binding of the peptide to the membrane surface. In the presence of Chol-free membranes, TNM-A does not efficiently bind to the surface, while a small fraction of the peptide interacts shallowly with the polar region of the bilayer membranes. In contrast, in the presence of Chol-containing membranes, TNM-A binds more efficiently and tends to penetrate slightly deeper to the bilayer, where the peptide-induced positive curvature leads to membrane disruption.

Acknowledgments

We are grateful to Dr. N. Inazumi (Osaka University) for his advice and help with the NMR measurements. This work was supported by Grants-in-Aid for Scientific Research KAKENHI (S) (grant No. 16H06315), (B) (15H03121), (A) (25242073), and for Challenging Exploratory Research (16K13100) as well as in part by JST, ERATO Lipid Active Structure Project. K. C. expresses her special thanks to MEXT, Japan, and Osaka University for providing a Ph. D. scholarship.

A. Supplementary data

Supplementary data associated with this article can be found, in the online version, at http://dx.doi.org/10.1016/j.bmc.2016.08.043.

References and notes

1. Faulkner, J. *Nat. Prod. Rep.* **1997**, *14*, 259.
2. Kobayashi, M.; Lee, N.; Shibuya, H.; Momose, T.; Kitagawa, I. *Chem. Pharm. Bull.* **1991**, *39*, 1177.
3. Kobayashi, J.; Murayama, T.; Ohizumi, Y.; Sasaki, T.; Ohta, T.; Nozoe, S. *Tetrahedron Lett.* **1989**, *30*, 4833.
4. Sakai, R.; Higa, T.; Kashman, Y. *Chem. Lett.* **1986**, 1499.
5. Kato, Y.; Fusetani, N.; Matsunaga, S.; Hashimoto, K.; Sakai, R.; Higa, T.; Kashman, Y. *Tetrahedron Lett.* **1987**, *28*, 6225.
6. Carmely, S.; Kashman, Y. *Tetrahedron Lett.* **1985**, *26*, 511.
7. Matsunaga, S.; Fusetani, N.; Hashimoto, K.; Walchli, M. *J. Am. Chem. Soc.* **1989**, *111*, 2582.
8. Matsunaga, S.; Fusetani, N. *J. Org. Chem.* **1995**, *60*, 1177.
9. Wada, S.; Matsunaga, S.; Fusetani, N.; Watabe, S. *Mar. Biotechnol. (NY)* **1999**, *1*, 337.
10. Nishimura, S.; Arita, Y.; Honda, M.; Iwamoto, K.; Matsuyama, A.; Shirai, A.; Kawasaki, H.; Kakeya, H.; Kobayashi, T.; Matsunaga, S.; Yoshida, M. *Nat. Chem. Biol.* **2010**, *6*, 519.
11. Youssef, D. T. A.; Shaala, L. A.; Mohamed, G. A.; Badr, J. M.; Bamanie, F. H.; Ibrahim, S. R. M. *Mar. Drugs* **2014**, *12*, 1911.
12. Espiritu, R. A.; Matsumori, N.; Murata, M.; Nishimura, S.; Kakeya, H.; Matsunaga, S.; Yoshida, M. *Biochemistry* **2013**, *52*, 2410.
13. Arita, Y.; Nishimura, S.; Ishitsuka, R.; Kishimoto, T.; Ikenouchi, J.; Ishii, K.; Umeda, M.; Matsunaga, S.; Kobayashi, T.; Yoshida, M. *Chem. Biol.* **2015**, *22*, 604.
14. Nakagawa, Y.; Umegawa, Y.; Matsushita, N.; Yamamoto, T.; Tsuchikawa, H.; Hanashima, S.; Oishi, T.; Matsumori, N.; Murata, M. *Biochemistry* **2016**, *55*, 3392.
15. Matsumori, N.; Tahara, K.; Yamamoto, H.; Morooka, A.; Doi, M.; Oishi, T.; Murata, M. *J. Am. Chem. Soc.* **2009**, *131*, 11855.
16. Espiritu, R. A.; Matsumori, N.; Tsuda, M.; Murata, M. *Biochemistry* **2014**, *53*, 3287.
17. Houdai, T.; Matsumori, N.; Murata, M. *Org. Lett.* **2008**, *10*, 4191.
18. Murata, M.; Sugiyama, S.; Matsuoka, S.; Matsumori, N. *Chem. Rec.* **2015**, *15*, 675.
19. Espiritu, R. A.; Cornelio, K.; Kinoshita, M.; Matsumori, N.; Murata, M.; Nishimura, S.; Kakeya, H.; Yoshida, M.; Matsunaga, S. *Biochim. Biophys. Acta—Biomembr.* **2016**, *1858*, 1373.
20. Salnikov, E. S.; Bechinger, B. *Biophys. J.* **2011**, *100*, 1473.
21. London, E.; Feigenson, G. W. *J. Lipid Res.* **1979**, *20*, 408.
22. Boucrot, E.; Pick, A.; Çamdere, G.; Liska, N.; Evergren, E.; McMahon, H. T.; Kozlov, M. M. *Cell* **2012**, *149*, 124.
23. Shnyrova, A. V.; Bashkirov, P. V.; Akimov, S. a.; Pucadyil, T. J.; Zimmerberg, J.; Schmid, S. L.; Frolov, V. A. *Science* **2013**, *339*, 1433.
24. Wang, C. K.; North, S. E.; Swedberg, J. E.; Harvey, P. J.; Mathiowetz, A. M.; Price, D. A.; Liras, S.; Craik, D. J. *J. Phys. Chem.* **2014**, *118*, 11129.
25. Johnson, C. S., Jr. *Prog. Nucl. Magn. Reson. Spectrosc.* **1999**, *34*, 203.
26. Cho, C. H.; Urquidi, J.; Singh, S.; Robinson, G. W. *J. Phys. Chem. B* **1999**, *103*, 1991.
27. Sacco, A.; Matteoli, E. *J. Solution Chem.* **1997**, *26*, 527.
28. Stella, L.; Mazzuca, C.; Venanzi, M.; Palleschi, A.; Didonè, M.; Formaggio, F.; Toniolo, C.; Pispisa, B.; Didone, M. *Biophys. J.* **2004**, *86*, 936.
29. Xiao, S.; Yang, L.; Li, F. *J. Pept. Sci.* **2012**, *18*, 45.
30. Lee, D. K.; Brender, J. R.; Sciacca, M. F. M.; Krishnamoorthy, J.; Yu, C.; Ramamoorthy, A. *Biochemistry* **2013**, *52*, 3254.
31. Feder, R.; Dagan, A.; Mor, A. *J. Biol. Chem.* **2000**, *275*, 4230.
32. Torrent, M.; Andreu, D.; Nogues, V. M.; Boix, E. *PLoS One* **2011**, *6*, 1.
33. Draney, A.; Smrt, S.; Lorieau, J. *Langmuir* **2014**, *30*, 11723.
34. Cho, H. S.; Dominick, J. L.; Spence, M. M. *J. Phys. Chem. B* **2010**, *114*, 9238.
35. Shapiro, R. A.; Brindley, A. J.; Martin, R. W. *J. Am. Chem. Soc.* **2010**, *132*, 11406.
36. Petersen, F. N. R.; Jensen, M. Ø.; Nielsen, C. H. *Biophys. J.* **2005**, *89*, 3985.
37. Grauffel, C.; Yang, B.; He, T.; Roberts, M. F.; Gershenson, A.; Reuter, N. *J. Am. Chem. Soc.* **2013**, *135*, 5740.
38. Zetta, L.; Kaptein, R. *Eur. J. Biochem.* **1984**, *145*, 181.
39. Moniz, T.; de Castro, B.; Rangel, M.; Ivanova, G. *Phys. Chem. Chem. Phys.* **2016**, *18*, 5027.
40. Campelo, F.; McMahon, H. T.; Kozlov, M. M. *Biophys. J.* **2008**, *95*, 2325.
41. Zimmerberg, J.; Kozlov, M. M. *Nat. Rev. Mol. Cell Biol.* **2006**, *7*, 9.
42. Koller, D.; Lohner, K. *Biochim. Biophys. Acta—Biomembr.* **2014**, *1838*, 2250.

Biochimica et Biophysica Acta 1858 (2016) 1373–1379

Contents lists available at ScienceDirect

Biochimica et Biophysica Acta

journal homepage: www.elsevier.com/locate/bbamem

Marine sponge cyclic peptide theonellamide A disrupts lipid bilayer integrity without forming distinct membrane pores

Rafael Atillo Espiritu [a,1], Kimberly Cornelio [a,b], Masanao Kinoshita [b,2], Nobuaki Matsumori [a,2,*], Michio Murata [a,b], Shinichi Nishimura [c], Hideaki Kakeya [c], Minoru Yoshida [d], Shigeki Matsunaga [e]

[a] Department of Chemistry, Graduate School of Science, Osaka University, Osaka 560-0043, Japan
[b] JST ERATO, Lipid Active Structure Project, Osaka 560-0043, Japan
[c] Division of Bioinformatics and Chemical Genomics, Graduate School of Pharmaceutical Sciences, Kyoto University, Kyoto 606-8501, Japan
[d] Chemical Genomics Research Group, RIKEN Center for Sustainable Resource Science, Saitama 351-0198, Japan
[e] Graduate School of Agricultural and Life Sciences, The University of Tokyo, Tokyo 113-8657, Japan

ARTICLE INFO

Article history:
Received 19 October 2015
Received in revised form 12 March 2016
Accepted 17 March 2016
Available online 18 March 2016

Keywords:
Theonellamide A
Liposomes
Mechanism of action
Solid state nuclear magnetic resonance
Confocal microscopy

ABSTRACT

Theonellamides (TNMs) are antifungal and cytotoxic bicyclic dodecapeptides derived from the marine sponge *Theonella* sp. These peptides specifically bind to 3β-hydroxysterols, resulting in 1,3-β-D-glucan overproduction and membrane damage in yeasts. The inclusion of cholesterol or ergosterol in phosphatidylcholine membranes significantly enhanced the membrane affinity of theonellamide A (TNM-A) because of its direct interaction with 3β-hydroxyl groups of sterols. To better understand TNM-induced membrane alterations, we investigated the effects of TNM-A on liposome morphology. ^{31}P nuclear magnetic resonance (NMR) and dynamic light scattering (DLS) measurements revealed that the premixing of TNM-A with lipids induced smaller vesicle formation. When giant unilamellar vesicles were incubated with exogenously added TNM-A, confocal micrographs showed dynamic changes in membrane morphology, which were more frequently observed in cholesterol-containing than sterol-free liposomes. In conjunction with our previous data, these results suggest that the membrane action of TNM-A proceeds in two steps: 1) TNM-A binds to the membrane surface through direct interaction with sterols and 2) accumulated TNM-A modifies the local membrane curvature in a concentration-dependent manner, resulting in dramatic membrane morphological changes and membrane disruption.

1. Introduction

Species of marine sponges that belong to the genera *Theonella* have proven to be a rich source of natural products [1] with therapeutic potential. Such products include antifungals [2–6], cytotoxins [7–9], pregnane-X-receptor agonist [10], and HIV-1 entry inhibitor [11] and other compounds with anti-inflammatory [12], antipsoriatic [13], and actin polymerization inhibitor [14] activities. Theonellamides (TNMs), as exemplified by TNM-A shown in Fig. 1, are a series of unique bicyclic dodecapeptides derived from the marine sponge *Theonella* sp. [5,6]. These peptides contain some unusual amino acids, including a histidinoalanine residue that bridges their bis-macrocyclic structure. Some homologs contain a sugar moiety that is not critical for their cytotoxic or antifungal activities [5,6]. Recent biochemical and molecular genetics studies have provided considerable insight into the mechanism of action of TNMs and the related compound theopalauamide [5,6]. Using molecular bar-coded ORF libraries, theopalauamide activity was shown to be attenuated in yeast cells with impaired ergosterol biosynthesis [15]. Another study revealed a mechanistic link between TNM and enhanced 1,3-β-D-glucan synthesis that is mediated by the Rho1 signaling pathway [16]. A fluorescent-labeled TNM derivative was also shown to specifically bind *in vitro* to 3β-hydroxysterols, such as cholesterol and ergosterol, resulting in a loss of membrane integrity [16]. In the same experiment, TNM-treated yeast cells developed fragmented vacuoles, whereas treatment with the standard antifungal drug amphotericin B, which also binds to membrane sterols, resulted in vacuolar enlargement. Based on these apparent phenotypic differences, coupled with the comparatively slow progression of TNM-induced toxicity, TNMs are considered a novel class of sterol-binding molecules with a

Abbreviations: MeCN, acetonitrile; DCCH, 7-diethylaminocoumarin-3-carboxylic acid hydrazide; DLS, dynamic light scattering; ESI-Q-TOF, electrospray ionization quadrupole time-of-flight; GUV, giant unilamellar vesicle; Hepes, 4-(2-Hydroxyethyl)piperazine-1-ethanesulfonic acid; LUV, large unilamellar vesicle; MLV, multilamellar vesicle; NMR, nuclear magnetic resonance; POPC, 1-palmitoyl-2-oleoyl-sn-glycero-3-phosphocholine; SPR, surface plasmon resonane; TNMs, theonellamides; TNM-A, theonellamide A; UV, ultraviolet.

* Corresponding author at: Department of Chemistry, Kyushu University, Fukuoka 819-0395, Japan.
E-mail address: matsmori@chem.kyushu-univ.jp (N. Matsumori).
[1] Current address: Department of Chemistry, De La Salle University, Manila 0922, Philippines.
[2] Current address: Department of Chemistry, Kyushu University, Fukuoka 819–0395, Japan.

http://dx.doi.org/10.1016/j.bbamem.2016.03.019
0005-2736/

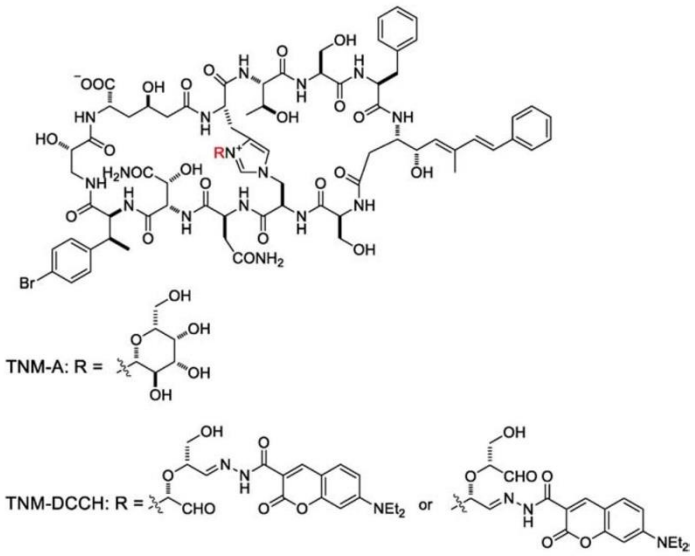

Fig. 1. Structures of theonellamide A (TNM-A) and a fluorescent probe, TNM-DCCH.

unique mechanism of action, distinct from that of known antifungal agents. This assumption is further corroborated by a recent finding that living cells treated with TNM undergo a cholesterol-, cytoskeleton-, and energy-dependent shrinkage that is not usually observed with other sterol-binding or membrane-targeting agents [17]. Furthermore, the same study demonstrated that the peptides were able to recognize sterols in the liquid-disordered domain and to cause phase separation in artificial membranes. These results point to the potential use of TNMs for studying sterol dynamics in membranes. In fact, we have demonstrated in a previous study how a fluorescent-labeled TNM can act as an alternative probe for sterol, both in fixed and living cells [18].

To understand the mechanisms whereby TNMs recognize sterols in lipid bilayers, further detailed investigations of their bimolecular interactions are required. We have recently demonstrated through surface plasmon resonance (SPR) and solid state ^{2}H NMR that TNM-A (Fig. 1) stereospecifically interacts with 3β-hydroxysterols, such as cholesterol and ergosterol, in lipid bilayers [19]. The SPR experiments revealed that incorporation of cholesterol or ergosterol into palmitoyl-oleolyphosphatidylcholine (POPC) liposomes significantly enhances the affinity of the peptide over that of epicholesterol (3α-hydroxysterol)-containing or sterol-free bilayers. Kinetic analysis of the SPR sensorgrams further suggested that the membrane-binding of TNM-A occurs in 2 steps: TNM-A binds to the membrane surface in the first step and exerts an influence on the membrane in the second step. The SPR results suggest that 3β-hydroxysterol is mainly responsible for the first step. The enhanced affinity for sterol-containing liposomes is because of the direct intermolecular interactions between TNM-A and 3β-hydroxysterols, as determined by solid state ^{2}H NMR of deuterated sterols, which revealed that TNM-A recognizes a 3β-OH group upon membrane binding and leads to the peptide accumulation in the shallow region of the membrane [19]. Kinetic analysis by SPR also suggests that sterol does not play a major role in promoting the second step.

Thus, we hypothesized that, unlike amphotericin B, TNM-A does not form distinct pores in the second step after membrane binding; however, its accumulation on the membrane surface may lead to morphological changes in the membrane. In this study, we investigate the effects of TNM-A on the morphology of artificial membranes both in the presence and absence of cholesterol, using solid state ^{31}P nuclear magnetic resonance (NMR), dynamic light scattering (DLS), and fluorescence microscopy with fluorescently labeled TNM-A (TNM-DCCH, Fig. 1).

2. Materials and methods

2.1. Materials

Theonellamide A (TNM-A) was isolated as described previously [6]. 1-Palmitoyl-2-oleoyl-*sn*-glycero-3-phosphocholine (POPC) was purchased from NOF Corporation (Tokyo, Japan). Cholesterol was purchased from Nacalai Tesque (Kyoto, Japan). Deuterium oxide was purchased from Euriso-Top (Saclay, France). All other chemicals were standard and analytical quality reagents.

2.2. Preparation of fluorescent TNM probe

TNM-DCCH was prepared in a similar manner as other fluorescent derivatives [15,18], while 7-diethylaminocoumarin-3-carboxylic acid hydrazide (DCCH, Molecular Probes) was used as a fluorophore. TNM-DCCH: UV (60% MeCN) λmax (ε) 430 (43,200), 278 (28,000) nm; ESI-Q-TOF (positive) *m/z* 1014.8508 (calculated for $C_{89/2}H_{113/2}Br_{1/2}N_{19/2}Na_{1/2}O_{15}$ 1014.8485).

2.3. Sample preparation for ^{31}P NMR

For ^{31}P NMR spectrum measurements of POPC membranes in the presence or absence of TNM-A, a round-bottom flask containing POPC (7.2 μmol), cholesterol (0 or 0.4 μmol), and TNM-A (0 or 0.4 μmol) dissolved in a solution of $CHCl_3$–MeOH (2:1 v/v) was prepared. The solvent was removed *in vacuo* and dried further for overnight. The lipid film was subsequently rehydrated in 1 mL of Milli-Q water (Merck Millipore). After vortexing for a few minutes, the lipid suspension was subjected to 3 cycles of freezing (−80 °C) and thawing (40 °C) to make multilamellar vesicles (MLVs). This vesicle suspension was lyophilized for overnight, rehydrated with deuterium oxide (50% w/w), homogenized by vortexing, freezing, and thawing and subsequently transferred to a 7-mm Teflon tube.

2.4. Solid state ^{31}P NMR measurements

All ^{31}P NMR spectra were recorded on a 400 MHz ECA400 (JEOL, Tokyo, Japan) at 30 °C using a 7-mm CP-MAS probe (Doty Scientific Inc., Columbia, South Carolina, USA)) without rotation. A single pulse sequence with proton decoupling was employed along with the following parameters: acquisition time, 18 ms; 90° pulse width, 5.6 μs; relaxation delay, 2 s; and total number of scans, approximately 25,000.

2.5. Liposome preparation and dynamic light scattering measurements

For DLS measurements of POPC membranes in the presence or absence of TNM-A, a round-bottom flask containing POPC, cholesterol, and TNM-A (molar ratios; 20:0:0, 19:0:1, 18:0:2, 19:1:0, 18:1:1, 17:1:2, 18:2:0, 17:2:1, or 16:2:2) dissolved in a solution of $CHCl_3$–MeOH (2:1 v/v) was prepared. For all the samples, the amount of POPC was 0.55 mg (0.72 μmol). The solvent was removed *in vacuo* and dried further for overnight. The lipid film was subsequently rehydrated in 1 mL of Milli-Q water (Merck Millipore). After intermittent vortexing at 40 °C, the lipid suspension was subjected to 3 cycles of freezing (−40 °C) and thawing (40 °C) to make multilamellar vesicles (MLVs). The suspension was then transferred into a cuvette, incubated for 1 h at room temperature, and the size distribution of the vesicles was measured with a dynamic light scattering particle size analyzer LB-550 (HORIBA, Ltd., Kyoto, Japan) at 25 °C. DLS measurements were repeated five times for each sample and the average values were plotted in Fig. 3. Those values were fitted by the Gauss function using Origin Ver. 7 to define the peak top, as indicated by the solid curves in Fig. 3.

For DLS experiments by the exogenous addition of TNM-A to MLVs, the 165 μL of 560 μM TNM-A dissolved in water were exogenously added to the 835 μL of TNM-A-free MLV suspensions prepared as above. The final concentration of TNM-A in cuvette was 92.4 μM. The particle sizes were measured before and 0.1, 1, and 12 h after the exogenous addition with the incubation at 25 °C.

2.6. GUV preparation

Giant unilamellar vesicles (GUVs) were obtained by electroformation as described by Angelova and Dimitrov [20]. In brief, POPC solutions (with or without 10 mol% cholesterol) were prepared in $CHCl_3$ or $CHCl_3$–MeOH (4:1v/v) to a final phospholipid concentration of 1 mg/mL. Aliquots (15 μL) were subsequently deposited on parallel aligned electrodes (Pt wires, $\varphi = 100$ μm) attached to glass slides, after which the solvent was evaporated under vacuum overnight. Milli-Q water (300–400 μL, Simplicity UV) was then added to completely immerse the electrodes, which were then sealed with another glass slide using a rubber spacer with a small fill port for drug injection. This slide was maintained at 40 °C on a temperature controlled objective plate (Tokai Hit ThermoPlate, Tokai Hit Co., Ltd., Shizuoka, Japan), and an alternating current (10 V, 10 Hz) was applied (Arbitrary Waveform Generator 33220A; Agilent Technologies, Santa Clara, CA, USA) for 1 h to form GUVs.

2.7. Confocal fluorescence microscopy

After GUV formation, TNM-A (9:1 molar ratio of TNM-A:TNM-DCCH) dissolved in Milli-Q water was gently added to the sample through the fill port with a micropipette to a final TNM-A concentration of 20 μM. TNM-A-induced morphological changes of GUVs were observed using a FluoView™ FV1000-D scanning unit with an IX81 inverted microscope (Olympus Corp., Tokyo, Japan). A LUCPLFLN ×60 universal semi-apochromat objective with an NA of 0.70 (Olympus Corp.) was used to observe fluorescence. The acquisition speed was 8 μs/pixel and images were visualized using the FV10-ASW-3.0 software. Contrast was altered using Adobe Photoshop CS6 to provide clear confocal images. Observations were carried out over 1 h with the sample temperature maintained at 27 °C using a temperature-controlled objective plate. Excitation and emission wavelengths were 405 nm and 430–530 nm, respectively.

3. Results

3.1. Effects of premixed TNM-A on phospholipid bilayers

Solid state ^{31}P NMR is used to study changes in membrane morphology and phospholipid dynamics induced by antimicrobial peptides [21,22]. We first examined changes in phospholipid headgroup regions caused by the incorporation of TNM-A in cholesterol-containing and sterol-free POPC liposomes using ^{31}P NMR. Since TNM-A was shown to directly interact with membrane sterol at 5 or 10 mol% of all lipids [19], it is considered that physiological content of cholesterol (20 mol% or higher) is not always necessary to exert the membrane effect of TNM-A. Thus, the cholesterol content in the measurements was set to 5 mol% in POPC membranes in order to be consistent with our previous report on ^{2}H NMR and SPR [19]. In the absence of TNM-A, spectral shapes typical of lamellar bilayer structures were observed for both cholesterol-containing and sterol-free POPC liposomes (Fig. 2A, B). However, by premixing 5 mol% TNM-A, isotropic and/or narrow anisotropic signals appeared in both lipid systems, as indicated by the arrows in Fig. 2C, D. The appearance of isotropic and/or narrow anisotropic signals can be explained in two different ways; one possibility is the emergence of membrane domains exhibiting high curvatures, and the other is the formation of small, rapidly-tumbling structures such as micelles, bicelles, or small unilamellar vesicles [22].

Then, to distinguish between these possibilities, we conducted DLS measurements to determine the size distribution profiles of multilamellar vesicles (MLVs) premixed with TNM-A. Results showed that incorporation of the peptide into the MLVs did cause the formation of much smaller vesicles in both sterol-free and cholesterol-containing POPC liposomes, as seen in Fig. 3. The results further demonstrated that the MLV size becomes smaller with the increasing molar ratio of TNM-A, irrespective of the presence and absence of cholesterol, while the MLVs with the highest cholesterol content had the least change in terms of size (Fig. 3C). Although the effect of cholesterol on the size reduction of MLVs will be discussed later, the significant reduction in MLV size should give rise to the isotropic and/or narrow anisotropic signals in ^{31}P NMR (Fig. 2C, D).

Here it is to be noted that Figs. 2 and 3 are not always consistent; DLS experiments suggest a single distribution of the MLV size, whereas ^{31}P NMR spectra indicated the coexistence of large and small MLVs. The major difference in the sample preparations between DLS and ^{31}P NMR experiments was the extent of hydration; the ^{31}P NMR samples were hydrated by 50% (wt/wt) deuterium water to gain sensitivity, and therefore are about 2000 times denser than the DLS samples. It may be possible to assume that, although TNM-A catalyzes smaller vesicle formation, the high lipid concentration converts the smaller vesicles to the larger ones probably through membrane fusion, which may be also catalyzed by TNM-A. In other words, in a diluted lipid suspension, the smaller vesicle formation proceeds completely by the inclusion of TNM-A, while, at much higher lipid concentration, the smaller vesicle formation does not proceed completely due to a back reaction such as membrane fusion. In any case, it was convinced that TNM-A promotes smaller vesicle formation in both experiments.

3.2. Effects of exogenous addition of TNM-A on membrane morphology

Next, to investigate morphological changes in membrane induced by the exogenous addition of TNM-A, we used confocal microscopy with a fluorescent derivative of TNM-A (TNM-DCCH, Fig. 1) for visualizing giant unilamellar vesicles (GUVs). With diameters of approximately 100 μm, GUVs have been regarded as a suitable model for microscopic observations of the structural details of membrane organization at submicrometer sizes [23,24]. Before using TNM-DCCH, we confirmed

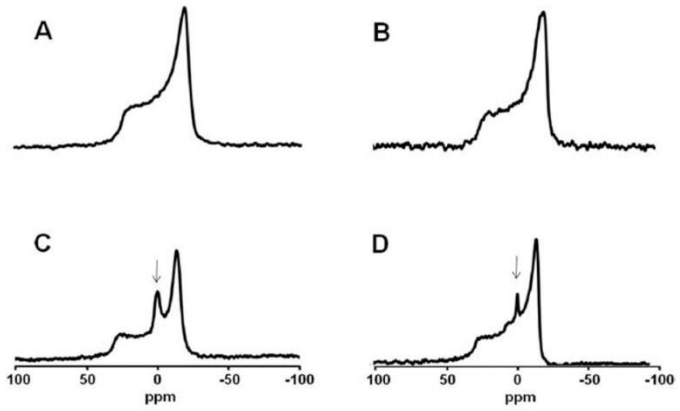

Fig. 2. Solid State ^{31}P NMR spectra of pure POPC (A and C) and POPC:cholesterol (B and D) liposomes in the absence (A and B) and presence (C and D) of TNM-A at 30°C. Molar ratios of TNM-A:cholesterol:POPC were 0:0:18 (A), 0:1:18 (B), 1:0:18 (C) and 1:1:18 (D).

that this probe retains the ability of TNM-A to bind specifically to cholesterol (Supplementary Fig. S1).

Confocal images of sterol-free POPC GUVs at various time intervals show very few, minimal membrane deformations; images of GUVs taken at several minutes and up to 55 min after exogenous addition of the peptide (final concentration 20 μM) are almost indistinguishable (Fig. 4). In contrast, sterol-containing membranes showed clear morphological changes at 13 min after TNM-A addition (Fig. 4), these changes increased in intensity over time. A semi-qualitative observation an hour after TNM-A addition shows that about two-thirds of GUVs were deformed in the presence of sterol (Supplementary Fig. S2), while deformed GUVs were not detected in the absence of cholesterol.

To further observe the cholesterol-dependent morphological change of vesicles, we performed the DLS experiments by exogenously adding TNM-A to MLV suspensions. The addition of TNM-A lessened the size of MLVs in a time-dependent manner, which is more prompt and prominent in cholesterol-containing MLVs (Fig. 5).

4. Discussion

We previously reported that a fluorescent derivative of TNM-A was specifically bound to 3β-hydroxysterols such as cholesterol and ergosterol, *in vitro*, and that sterol was required for peptide-induced aberrations and toxicity in yeast cells [16]. In a more recent report [19], we used SPR and solid state ^{2}H NMR to provide insight into the mechanisms underlying sterol recognition by TNM-A in the membrane microenvironment; TNM-A interacts directly with sterols embedded in lipid bilayers, leading to its accumulation in the shallow region of the membrane. Based on the moderate activity of TNM-A in dye leakage experiments with sterol-containing and sterol-free POPC liposomes, we hypothesized that the accumulation of TNM-A resulted in perturbations of membrane integrity rather than the formation of distinct pores [19]. To further investigate this hypothesis, this study employed solid state ^{31}P NMR measurements and microscopic observations. Our results indicate that TNM-A induces characteristic morphological changes in POPC liposomes and significant reduction of vesicle size.

Our previous kinetic evaluations of the interactions between TNM-A and liposomes using SPR revealed that the binding of TNM-A to bilayers consisted of 2 steps [19]. The first step was its binding to the membrane surface, which was greatly enhanced by the presence of 3β-hydroxysterols through direct bimolecular recognition. The second step, presumed to involve membrane deformation, proceeded regardless of the presence or absence of sterols and was not significantly accelerated by sterols [19]. In other words, the second step depended largely on the concentration of TNM-A that had accumulated on the membrane surface during the first step. In the present study, micrographs of GUVs revealed dynamic changes in membrane morphology induced by TNM-A; such changes were more frequently observed in cholesterol-containing membranes (Fig. 4 and Supplementary Fig. S2). The greater frequency of membrane morphological changes in cholesterol-containing membranes likely stems from increased TNM-A binding to the membrane surface, which is promoted by its direct interaction with cholesterol during the first binding step. These findings support our assumption that the second step of TNM-A membrane-binding corresponds to membrane morphological changes that occur when the peptide reaches a threshold concentration in a region of the membrane. In fact, the ^{31}P NMR and DLS results (Figs. 2 and 3) demonstrate the small vesicle

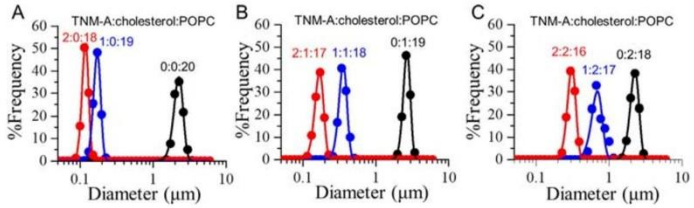

Fig. 3. Size distribution of TNM-A-free (black line) and TNM-A-containing (blue and red lines) POPC MLVs. Components were pre-mixed before hydration. The cholesterol contents were 0 (A), 5 (B), and 10 mol% (C).

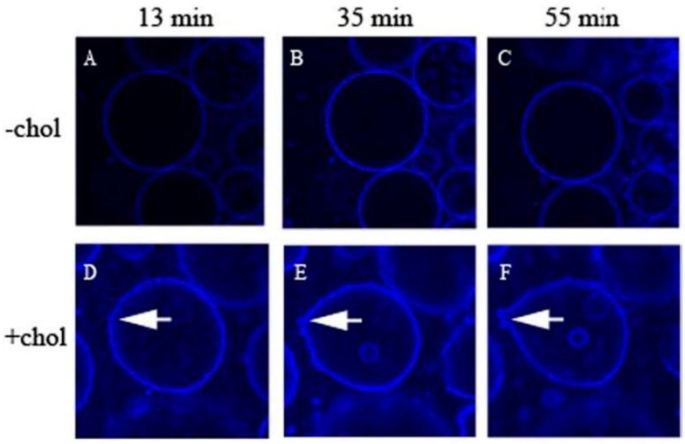

Fig. 4. Time-lapse confocal fluorescent microscopy images of sterol-free POPC GUVs (A – C) and sterol-containing POPC GUVs (D – F) after addition of 9:1 mol% TNM-A:TNM-DCCH to a final concentration of 20 μM. Images of GUVs taken at 13 min (A) and 55 min (C) after peptide addition were almost indistinguishable for sterol-free POPC GUVs. The arrows in the bottom images indicate the membrane protrusion induced by the peptide.

formation by TNM-A, regardless of the presence and absence of cholesterol, which would result from that the concentration of the premixed peptide exceeds the threshold.

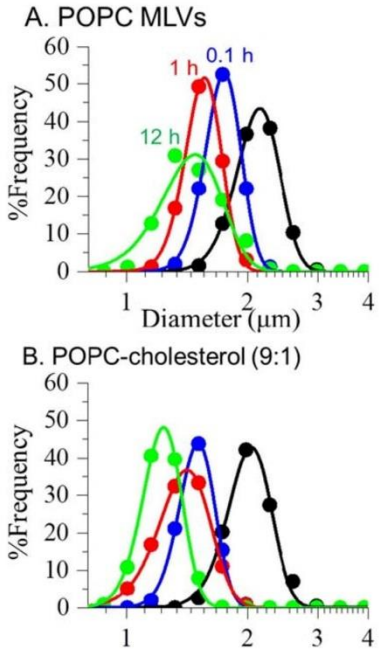

Fig. 5. Time course of DLS profiles for POPC (A) and POPC/cholesterol (9:1 by moles, B) MLVs before and after exogenous addition of TNM-A. The black, blue, red and green plots show the particle-size distribution of the MLVs before and 0.1, 1, and 12 h after the exogenous addition of TNM-A, respectively. The final concentration of TNM-A was 92.4 μM. The DLS data were fitted to a Gauss function to determine the average particle size (peak top). The average particle sizes of MLVs were 2.13 μm (black), 1.75 μm (blue), 1.56 μm (red) and 1.47 μm (green) for panel (A), and 2.04 μm (black), 1.50 μm (blue), 1.42 μm (red), and 1.04 μm (green) for panel (B).

Based on the above discussion, current data can be interpreted as follows. In the case of MLVs premixed with TNM-A (Figs. 2 and 3), the peptide in the membranes already reaches a threshold concentration to induce the morphological change of membrane, regardless of cholesterol contents. The morphological change would further destabilize the membrane structure, leading to the reduction in MLV size (Fig. 3) and the appearance of isotropic and narrow anisotropic signals in the ^{31}P NMR spectra (Fig. 2). Interestingly, the MLVs with the highest cholesterol content had the least change in terms of size (Fig. 3). One possible explanation for this is that cholesterol resisted the effect of TNM-A by stabilizing and rigidifying fluid phase of the vesicles. On the other hand, in the case of exogenous addition of TNM-A (Figs. 4 and 5), exertion of the TNM-A effect on membrane morphology requires the initial membrane-binding process of the peptide, which was known to be promoted by membrane cholesterol [19]. Thus, the TNM-A-induced morphological change of GUV and reduction in MLV size were observed more promptly and prominently on cholesterol-containing vesicles.

As described above, TNM-A induces local convex membrane curvature, likely resulting from asymmetric constraints generated on the lipid bilayer by the binding of TNM-A to the outer leaflet. In fact, the induction of both positive and negative membrane curvature by antimicrobial peptides is reported to be critical in their membrane destabilization activity [25]. For example, certain amphiphatic helical peptides have been shown to sense membrane curvature and subsequently induce dynamic processes such as membrane fission [26]. For such peptides, insertion of hydrophobic residues in the shallow region of the membrane generated changes in membrane curvature that were sufficient to drive these processes [27,28]. In this context, the hydrophobic phenyl sidechains of TNM-A (Fig. 1) are likely anchored in the shallow region of a membrane's outer leaflet, expanding the bilayer surface and thereby modifying the curvature of the membrane. Changes in membrane curvature cause dynamic morphological changes in the membrane, leading to membrane damage or destabilization [27,28].

In our previous paper [19], we demonstrated from SPR data that the incorporation of 10 mol % sterol into POPC membranes significantly (*ca.* 50 times) enhances the affinity of the peptide for the membrane, most of which is attributed to the initial binding to the membrane surface (*ca.* 20 times), while the second process is not significantly accelerated by sterol. By combining our previous and current data, we propose one of the possible mechanisms for membrane destabilization by TNM-A summarized in Fig. 6. In the absence of cholesterol or ergosterol, the

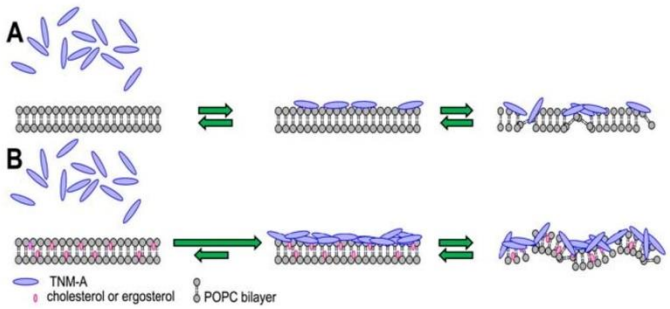

Fig. 6. Proposed mechanism for membrane disruption by TNM-A on sterol-free (A) and sterol-containing (B) POPC liposomes. A two-state reaction model was proposed for TNM-A binding to membranes in our previous report [19], in which the rate constants were evaluated by SPR analysis. Arrow lengths qualitatively indicate the amplitude of rate constants. For the exact rate constants, refer to [19].

amount of TNM-A bound to the membrane surface is lower (Fig. 6A); thus, a higher concentration of this peptide is required to reach its threshold. In contrast, a 3β-hydroxysterol (Fig. 6B) significantly accelerates peptide accumulation on the membrane surface through the direct interaction between TNM-A and the hydroxy moiety of the sterol, inducing modifications in the local membrane curvature and resulting in more pronounced and frequent appearance of membrane morphological changes. In this scenario, TNM-A mainly disrupts the membrane integrity in the shallow area and increases the membrane's local curvature, leading to the morphological defects observed in this study. Although the induction of membrane curvature upon TNM-A binding appears reminiscent of the toroidal pore model or the more recent interfacial activity model for the actions of partially amphiphatic antimicrobial peptides [29], even a high TNM-A concentration does not lead to formation of distinct membrane pores [19]. In addition, these morphological changes in membranes have seldom been reported for antimicrobial peptides, although they often promote liposome fusion [29]. In this context, the molecular mechanism that links TNM-A membrane binding and membrane disruption is unique and distinct from those of amphiphatic antimicrobial peptides.

5. Conclusions

Using confocal microscopy of GUVs with a fluorescent derivative of TNM-A, we verified that TNM-A dynamically induces distinct morphological changes (Fig. 4), which destabilize the membrane structures, resulting in the small vesicle formation (Figs. 3 and 5) and the appearance of isotropic and small anisotropic signals in the ^{31}P NMR spectra (Fig. 2). The higher frequency of these phenomena in cholesterol-containing membranes is caused by greater accumulation of TNM-A because of its direct interaction with cholesterol [19]. TNM-A binds to the membrane via shallow insertion, which subsequently modifies the local membrane curvature and results in disruption of the bilayer integrity as reported previously [16,19]. The observed morphological changes might be related to TNM-induced vacuolar fragmentation in yeasts [16]. However, additional experiments on this unique natural product are necessary to acquire a better understanding of the atomistic mechanism underlying the morphological changes revealed by the present study and the specific mode of 3β-hydroxysterol recognition.

Transparency document

The Transparency document associated with this article can be found, in online version.

Acknowledgements

This work was supported by Grants-in-Aid for Scientific Research (B) (15H03121), (S) (18101010) and (A) (25242073) and in part by JST, ERATO Lipid Active Structure Project. R.A.E. expresses his special thanks to MEXT, Japan, for providing a Ph.D. scholarship. We are grateful to Dr. Yuichi Umegawa and Dr. Naoya Inazumi, Osaka University, for their help in NMR measurements. We are also grateful to the RIKEN Brain Science Institute's Research Resource Center for mass spectrometry.

Appendix A. Supplementary data

Supplementary data to this article can be found online at http://dx.doi.org/10.1016/j.bbamem.2016.03.019.

References

[1] P.L. Winder, S.A. Pomponi, A.E. Wright, Natural products from the Lithistida: a review of the literature since 2000, Mar. Drugs 9 (2011) 2643–2682.
[2] R.F. Angawi, G. Bavestrello, B. Calcinai, H.A. Dien, G. Donnarumma, M.A. Tufano, I. Paoletti, E. Grimaldi, G. Chianese, E. Fattorusso, O. Taglialatela-Scafati, Aurantoside J: a new tetramic acid glycoside from *Theonella swinhoei*. Insights into the antifungal potential of aurantosides, Mar. Drugs 9 (2011) 2809–2817.
[3] E.W. Schmidt, C.A. Bewley, D.J. Faulkner, Theopalauamide, a bicyclic glycopeptide from filamentous bacterial symbionts of the lithistid sponge *Theonella swinhoei* from Palau and Mozambique, J. Org. Chem. 63 (1998) 1254–1258.
[4] C.A. Bewley, D.J. Faulkner, Theonegramide, an antifungal glycopeptide from the Philippine lithistid sponge *Theonella swinhoei*, J. Org. Chem. 59 (1994) 4849–4852.
[5] S. Matsunaga, N. Fusetani, K. Hashimoto, M. Wälchli, Theonellamide F. A novel antifungal bicyclic peptide from a marine sponge *Theonella* sp. J. Am. Chem. Soc. 111 (1989) 2582–2588.
[6] S. Matsunaga, N. Fusetani, Theonellamides A–E, cytotoxic bicyclic peptides, from a marine sponge Theonella sp. J. Org. Chem. 60 (1995) 1177–1181.
[7] T. Hamada, S. Matsunaga, G. Yano, N. Fusetani, Polytheonamides A and B, highly cytotoxic, linear polypeptides with unprecedented structural features, from the marine sponge, *Theonella swinhoei*, J. Am. Chem. Soc. 127 (2005) 110–118.
[8] A.S. Ratnayake, T.S. Bugni, X. Feng, M.K. Harper, J.J. Skalicky, K.A. Mohammed, C.D. Andjelic, L.R. Barrows, C.M. Ireland, Theopapuamide, a cyclic depsipeptide from a Papua New Guinea lithistid sponge *Theonella swinhoei*, J. Nat. Prod. 69 (2006) 1582–1586.
[9] S. De Marino, C. Festa, M.V. D'Auria, T. Cresteil, C. Debitus, A. Zampella, Swinholide J, a potent cytotoxin from the marine sponge *Theonella swinhoei*, Mar. Drugs 9 (2011) 1133–1141.
[10] C. Festa, S. De Marino, M.V. D'Auria, G. Bifulco, B. Renga, S. Fiorucci, S. Petek, A. Zampella, Solomonsterols A and B from *Theonella swinhoei*. The first example of C-24 and C-23 sulfated sterols from a marine source endowed with a PXR agonistic activity, J. Med. Chem. 54 (2011) 401–405.
[11] A. Plaza, G. Bifulco, M. Masullo, J.R. Lloyd, J.L. Keffer, P.L. Colin, J.N.A. Hooper, L.J. Bell, C.A. Bewley, Mutremdamide A and koshikamides C–H, peptide inhibitors of HIV-1 entry from different *Theonella* species, J. Org. Chem. 75 (2010) 4344–4355.
[12] C. Festa, S. De Marino, V. Sepe, M.V. D'Auria, G. Bifulco, C. Debitus, M. Bucci, V. Vellecco, A. Zampella, Solomonamides A and B, new anti-inflammatory peptides from *Theonella swinhoei*, Org. Lett. 13 (2011) 1532–1535.
[13] C. Festa, S. De Marino, V. Sepe, M.V. D'Auria, G. Bifulco, R. Andrés, M.C. Terencio, M. Payá, C. Debitus, A. Zampella, Perthamides C–F, potent human antipsoriatic cyclopeptides, Tetrahedron 67 (2011) 7780–7786.

[14] T. Oda, J. Xu, A. Fujita, M. Mochizuki, M. Namikoshi, Effects of bistheonellide A, an actin-polymerization inhibitor, on Chinese hamster V79 cells and on IL-8 production in PMA-stimulated HL-60 cells, Mar. Drugs 3 (2005) 22–27.
[15] C.H. Ho, L. Magtanong, S.L. Barker, D. Gresham, S. Nishimura, P. Natarajan, J.L.Y. Koh, J. Porter, C.A. Gray, R.J. Andersen, G. Giaever, C. Nislow, B. Andrews, D. Botstein, T.R. Graham, M. Yoshida, C. Boone, A molecular barcoded yeast ORF library enables mode-of-action analysis of bioactive compounds, Nat. Biotechnol. 27 (2009) 369–377.
[16] S. Nishimura, Y. Arita, M. Honda, K. Iwamoto, A. Matsuyama, A. Shirai, H. Kawasaki, H. Kakeya, T. Kobayashi, S. Matsunaga, M. Yoshida, Marine antifungal theonellamides target 3β-hydroxysterol to activate Rho1 signaling, Nat. Chem. Biol. 6 (2010) 519–526.
[17] Y. Arita, S. Nishimura, R. Ishitsuka, T. Kishimoto, J. Ikenouchi, K. Ishii, M. Umeda, S. Matsunaga, T. Kobayashi, M. Yoshida, Targeting cholesterol in a liquid-disordered environment by theonellamides modulates cell membrane order and cell shape, Chem. Biol. 22 (2015) 1–7.
[18] S. Nishimura, K. Ishii, K. Iwamoto, Y. Arita, S. Matsunaga, Y. Ohno-Iwashita, S.B. Sato, H. Kakeya, T. Kobayashi, M. Yoshida, Visualization of sterol-rich membrane domains with fluorescently-labeled theonellamides, PLoS One 8 (2013), e83716.
[19] R.A. Espiritu, N. Matsumori, M. Murata, S. Nishimura, H. Kakeya, S. Matsunaga, M. Yoshida, Interaction between the marine sponge cyclic peptide theonellamide A and sterols in lipid bilayers as viewed by surface plasmon resonance and solid-state ^{2}H nuclear magnetic resonance, Biochemistry 52 (2013) 2410–2418.
[20] M.I. Angelova, D.S. Dimitrov, Liposome electroformation, Faraday Discuss. Chem. Soc. 81 (1986) 303–311.
[21] E. Strandgerg, A.S. Ulrich, NMR methods for studying membrane-active antimicrobial peptide, Concepts Magn. Reson. A 23 (2004) 89–120.
[22] B. Bechinger, E.S. Salnikov, The membrane interactions of antimicrobial peptides revealed by solid-state NMR spectroscopy, Chem. Phys. Lipids 165 (2012) 282–301.
[23] L.A. Bagatolli, Membranes and fluorescence microscopy, in: C.D. Geddes (Ed.), Reviews in Fluorescence, Springer, New York 2009, pp. 33–51.
[24] O. Wesołowska, K. Michalak, J. Maniewska, A.B. Hendrich, Giant unilamellar vesicles – a perfect tool to visualize phase separation and lipid rafts in model systems, Acta Biochim. Pol. 56 (2009) 33–39.
[25] N.W. Schmidt, G.C.L. Wong, Antimicrobial peptides and induced membrane curvature: geometry, coordination chemistry, and molecular engineering, Curr. Opin. Solid State Mater. Sci. 17 (2013) 151–163.
[26] G. Drin, B. Antonny, Amphipathic helices and membrane curvature, FEBS Lett. 584 (2010) 1840–1847.
[27] E. Boucrot, A. Pick, G. Çamdere, N. Liska, E. Evergren, H.T. McMahon, M.M. Kozlov, Membrane fission is promoted by insertion of amphipathic helices and is restricted by crescent BAR domains, Cell 149 (2012) 124–136.
[28] A.V. Shnyrova, P.V. Bashkirov, S.A. Akimov, T.J. Pucadyil, J. Zimmerberg, S.L. Schmid, V.A. Frolov, Geometric catalysis of membrane fission driven by flexible dynamin rings, Science 339 (2013) 1433–1436.
[29] W.C. Wimley, Describing the mechanism of antimicrobial peptide action with the interfacial activity model, ACS Chem. Biol. 5 (2010) 905–917.